

SECONDARY DISPERSION OF TRANSITION  
METALS THROUGH A  
COPPER-RICH BOG IN THE  
CASCADE MOUNTAINS, BRITISH COLUMBIA

by

RAYMOND ERNEST WINGROVE LETT  
B.Sc., University of London. 1968  
M.Sc., University of Leicester. 1970

A THESIS SUBMITTED IN PARTIAL FULFILLMENT OF  
THE REQUIREMENTS FOR THE DEGREE OF  
DOCTOR OF PHILOSOPHY

in

THE FACULTY OF GRADUATE STUDIES  
(Department of Geological Sciences)

We accept this thesis as conforming  
to the required standard

THE UNIVERSITY OF BRITISH COLUMBIA  
October, 1978

© Raymond Ernest Wingrove Lett, 1978

In presenting this thesis in partial fulfilment of the requirements for an advanced degree at the University of British Columbia, I agree that the Library shall make it freely available for reference and study.

I further agree that permission for extensive copying of this thesis for scholarly purposes may be granted by the Head of my Department or by his representatives. It is understood that copying or publication of this thesis for financial gain shall not be allowed without my written permission.

Department of Geological Sciences

The University of British Columbia  
2075 Wesbrook Place  
Vancouver, Canada  
V6T 1W5

Date December 28th, 1978

## ABSTRACT

Horizontal and vertical variations of copper, cobalt, iron, manganese, molybdenum, nickel, zinc, organic carbon and pH were studied in a small bog close to a known copper-mineral occurrence in the foothills of the Cascade Mountains, British Columbia. This bog consists of up to 3 m thickness of moderately decomposed, water saturated, fetid organic material underlain by glacial till that almost completely covers the contact between copper-mineralized Nicola Group volcanic rocks and porphyry dykes.

Soils with more than 16% organic carbon and 0.1% HI-reducible sulphur are enriched in copper, cobalt, nickel, zinc and molybdenum. Sympathetic relationships between nickel and zinc and between cobalt and copper are demonstrated by correlation analysis of metal data. Metals generally increase down organic soil profiles, but fall sharply in the till except at the western end of the bog where small areas of concealed till have up to 0.5% copper and 100 ppm molybdenum. Iron and manganese are generally higher in the till than in organic soil although these metals are locally very abundant in near surface fibrous organic material.

Reducing, subsurface bog waters generally have higher dissolved iron, manganese and organic carbon, but lower copper contents than do surface waters. However, several subsurface water samples from the area underlain by copper-rich till contain up to 1 ppm copper. Copper is also very abundant in spring water flowing from a probable fault zone west of the bog; in seepages draining humic gleysolic soils surrounding the west side of the bog and in acid, semi-stagnant surface water.

Small, irregularly shaped grains of pyrite, chalcopyrite, covellite, native copper and framboidal pyrite are scattered throughout the organic soils. Copper sulphide and native copper grains are restricted to two areas at the eastern and western ends of the bog occurring between 1 and 3 m depth. Framboidal pyrite, however, has a wider spatial distribution in organic soils than the copper and copper-iron sulphide mineral grains.

Copper and iron are principally derived through oxidation of sulphides, disseminated in the underlying volcanic rocks, by circulating ground water which then discharges into the bog along concealed fault zones. Ground water, percolating through reduced till beneath organic soils and through humic gleysolic soils, dissolves cobalt, nickel, zinc, manganese, iron and molybdenum which then migrate through the bog as simple ions, complex ions or soluble metal-fulvate complexes. A major proportion of the dissolved copper, cobalt, nickel and zinc is probably immobilized by adsorption and complexing to solid humic and fulvic acid fractions in the soil. Authigenic copper and iron sulphides also form through reaction of metals with sulphide ions produced from biogenic sulphate reduction. Stability relationships between copper and iron minerals indicate that the grain textures reflect changes in Eh, pH, sulphide ion activity, metal ion activity and possibly dissolved organic carbon abundance.

Hydrous oxides of iron and possibly manganese form close to the bog surface where metal-rich solutions discharge into the oxidizing environment. Molybdenum is also concentrated in the acid fibrous organic layer due to immobility of the acid molybdenate ion. Abundant copper may be adsorbed from the metal-

rich surface water by plants and is then bound to proteins forming the cell-wall membrane. This form of copper is relatively stable and the metal will only be released from the association during advanced organic diagenesis.

## TABLE OF CONTENTS

	<u>Page</u>
ABSTRACT	ii
TABLE OF CONTENTS	v
LIST OF TABLES	viii
LIST OF FIGURES	x
LIST OF PLATES	xiii
ACKNOWLEDGEMENTS	xvi
CHAPTER 1: INTRODUCTION	1
1-1 Statement of the problem	1
1-2 Formation and classification of bogs	2
1-3 Bog sedimentation and formation of humic substances	4
1-4 Interaction of metals with humic substances in bogs	8
1-5 Diagenesis in bogs	14
1-6 Studies of trace metal distribution in bogs	17
1-7 Summary	22
CHAPTER 2: DESCRIPTION OF THE STUDY AREA	24
2-1 Location and access	24
2-2 Physiography, drainage and climate	24
2-3 Effects of glaciation and Pleistocene deposits	29
2-4 Geology of the study area	31
2-5 Mineral exploration history and previous geochemical investigations	37
2-6 Pedology and flora of the study area	38
CHAPTER 3: SAMPLING AND ANALYTICAL TECHNIQUES	48
3-1 Sampling methods and field observations	48
3-2 Analysis of samples for trace metals	52
3-3 Analysis of water samples for 2-2 biquinoline extractable copper	56
3-4 Organic carbon analysis	56
3-5 Sulphur analysis	59
3-6 Preparation of polished mounts from heavy mineral separates and organic soil fragments	60

	<u>Page</u>
3-7 Scanning electron microprobe and electron microscope studies	60
3-8 Analytical precision	61
CHAPTER 4: GEOCHEMICAL RESULTS	64
4-1 Trace and minor element abundances and pH in soils and till	64
4-2 Statistical treatment of the data	80
4-3 Statistical correlation between metals, organic carbon and pH in soils	87
4-4 Trace metals in volcanic ash	95
4-5 Trace metals in bog vegetation	97
4-6 Trace elements in ground and surface bog waters	97
4-7 HI reducible sulphur contents of soil and till	106
CHAPTER 5: SULPHIDE MINERALS IN ORGANIC SOILS AND TILL	109
5-1 Introduction	109
5-2 Composition and textures of sulphide mineral grains	109
5-3 Distribution of copper and iron mineral grains	121
5-4 Results of microprobe analyses of organic soil fragments	126
CHAPTER 6: DISCUSSION	137
6-1 Summary of results	137
6-2 Development of the bog and organic diagenesis	140
6-3 Accumulation of metals in organic soils	143
6-4 Bog water chemistry	151
6-5 Theoretical models for water chemistry and prediction of mineral solubilities	153
6-6 Stability of copper and iron minerals in organic soils	166
6-7 A conceptual model for metal dispersion	176
6-8 Applications to mineral exploration	179
CHAPTER 7: CONCLUSIONS	183
BIBLIOGRAPHY	185

Page

## APPENDICES

Appendix A:	Tabulated results for Co, Cu, Fe, Mn, Ni, Zn, organic carbon, pH and Mo in soils and till; Cu, Fe, Mn, Zn, organic carbon, SO <sub>4</sub> , Ca and pH in waters.	195
Appendix B:	B-1: Organic carbon by wet oxidation	202
	B-2: Organic carbon by Leco total carbon analyser	203
	B-3: Sulphate in water	204
	B-4: Biquinoline extractable copper in water	205
	B-5: Determination of sulphate in soil by HI reduction and bismuth colorimetry	207
Appendix C:	Probability graphs for metals, organic carbon and pH in soils and till	211
Appendix D:	Example of DIAG program output for water sample 74-RL-1429 and distribution of aqueous species in water samples 74-RL-1428, 1439, 1442, 1443 and 1444.	230

	<u>LIST OF TABLES</u>	<u>PAGE</u>
Table 3-1:	Instrumental operating conditions for atomic absorption spectrophotometers.	54
Table 3-2:	Analytical precision.	62
Table 4-1:	Geometric mean (X), mean $\pm$ 2 standard deviation, mean $\pm$ 1 standard deviation and Log standard deviation (S) of populations representing 89 soil samples.	82
Table 4-2:	Geometric mean (X), mean $\pm$ 2 standard deviation, mean $\pm$ 1 standard deviation and Log standard deviation (S) of populations representing 96 till samples.	83
Table 4-3:	Correlation matrix for soil samples with organic carbon content greater than 5%; (n = 63; r = 0.25 significant at 95% confidence level).	88
Table 4-4:	Correlation matrix for soil samples with organic carbon content greater than 16%; (n = 33; r = 0.35 significant at 95% confidence level).	88
Table 4-5:	Metal contents of volcanic ash samples. Cu, Co, Mn, Ni and Zn are in ppm; Fe is in %.	96
Table 4-6:	Metal contents in ppm of vegetation samples.	96
Table 4-7:	Arithmetic means (X), standard deviations (S) and ranges (R) for elements in water. Cu, Fe, Mn and Zn in ppb; C and Ca in ppm. P = % values detection limit.	98

Table 4-8:	Surface and subsurface water samples analysed by atomic adsorption spectrophotometry and by 2-2 biquinoline colorimetry.	103
Table 4-9:	Element contents in surface and subsurface bog water samples.	105
Table 4-10:	Hydriodic acid reducible sulphur and organic carbon contents of samples from four profiles.	107
Table 5-1:	Metals and organic carbon in soil samples used for microprobe analysis.	127
Table 6-1:	Distribution of aqueous species in water sample 74-RL-1429 at Log oxygen activity of -66.5.	156
Table 6-2:	Distribution of aqueous species in water sample 74-RL-1429 at Log oxygen activity of -66.0	157
Table 6-3:	Distribution of aqueous species in water sample 74-RL-1429 at Log oxygen activity of -65.5.	158
Table 6-4:	Equilibrium constants and reaction quotients for water sample 74-RL-1429 at Log oxygen activities of -66.5, -66.0 and -65.5 and at 25°C in the presence of solid chalcopyrite and pyrite	159
Table 6-5:	Equilibrium constants, reaction quotients and relative degree of mineral saturation in central bog subsurface water samples at Log oxygen activity of -66.5.	162
Table 6-6:	Proportion of metals theoretically bound to the fulvic acid fraction in subsurface bog water samples.	165

## LIST OF FIGURES

	<u>Page</u>
Figure 1-1: Fulvic acid structure proposed by Gamble and Schnitzer (1973).	7
Figure 1-2: Schematic diagram for trace metal interactions in organic soils.	7
Figure 1-3: Reactions between copper and fulvic acid fraction.	11
Figure 2-1: Location of study area.	27
Figure 2-2: Outline of the mineral property and location of bogs.	28
Figure 2-3: Geology of the study area (after Mustard 1968).	32
Figure 2-4: Geological cross section A - A' shown on figure 2-3.	36
Figure 2-5: Soil catena through the study area.	40
Figure 2-5a: Profile A.	41
Figure 2-5b: Profile B.	42
Figure 2-5c: Profile C.	43
Figure 2-6: Central bog drainage, soils and flora.	45
Figure 3-1: Location of soil and till profiles.	49
Figure 3-2: Soil and till sample locations.	51
Figure 3-3: Water sample locations.	53
Figure 3-4: Comparison of organic carbon analyses of 15 samples by wet oxidation, Leco method and loss on ignition at 550°C.	58
Figure 4-1: Organic carbon in soils and till.	65
Figure 4-2: Variation of metals, organic carbon and sulphur on a fibric mesisol profile.	66

	<u>Page</u>
Figure 4-3: Variation of metals, organic carbon and sulphur on a humic mesisol profile.	67
Figure 4-4: Copper in soils and till.	69
Figure 4-5: Variation of metals and pH on an orthic dystric brunisol profile.	71
Figure 4-6: Cobalt in soils and till.	73
Figure 4-7: Manganese in soils and till.	74
Figure 4-8: Iron in soils and till.	75
Figure 4-9: Nickel in soils and till.	76
Figure 4-10: Zinc in soils and till.	77
Figure 4-11: Molybdenum in soils and till.	78
Figure 4-12: pH in soils and till	79
Figure 4-13: Scatter diagram for $\text{Log}_{10}\text{Cu}$ against organic carbon.	90
Figure 4-14: Scatter diagram for $\text{Log}_{10}\text{Co}$ against $\text{Log}_{10}\text{Mn}$ .	91
Figure 4-15: Scatter diagram for $\text{Log}_{10}\text{Zn}$ against $\text{Log}_{10}\text{Ni}$ .	92
Figure 4-16: Scatter diagram for $\text{Log}_{10}\text{Zn}$ against $\text{Log}_{10}\text{Ni}$ ( 33 samples ).	94
Figure 4-17: Cu (ppb) in surface water samples.	100
Figure 4-18: Cu (ppb) in subsurface water samples.	101
Figure 5-1: Distribution of mineral grains in organic soils and till.	122
Figure 5-2: Distribution of framboidal pyrite.	123
Figure 5-3: Distribution of covellite, covellite-chalcopyrite and native copper grains.	124

Page

Figure 6-1:	Simplified Eh-pH diagram for mineral relationships in the Cu-Fe-S-O-H system at 25°C and 1 atmosphere pressure.	168
Figure 6-2a:	Stability relationships between copper minerals in water at 25°C and 1 atmosphere pressure as a function of Log oxygen activity, sulphate activity and pH.	171
Figure 6-2b:	Stability relationships between iron minerals in water at 25°C and 1 atmosphere pressure as a function of Log oxygen activity, sulphate activity and pH	172
Figure 6-3:	Conceptual model for dispersion of metals in the bog.	177

## LIST OF PLATES

	<u>Page</u>
Plate 2-1: A west looking view of the west end of the central bog.	25
Plate 5-1: Electron micrograph of a framboidal pyrite cluster in a polished mount made from a heavy mineral separate of soil sample 74-RL-1119.	110
Plate 5-2: Electron micrograph of an individual pyrite framboid ('A') from the cluster shown in plate 5-1.	111
Plate 5-3: Electron micrograph of pyrite framboids from sample 74-RL-1119.	112
Plate 5-4: Photomicrograph of the framboid cluster shown in plate 5-1.	114
Plate 5-5: Photomicrograph of a polished mount from sample 74-RL-1127 collected at station G 1.5 at 2.5 m depth.	114
Plate 5-6: Photomicrograph of a polished mount from sample 74-RL-1117 collected at station G 1.0 at 1.5 m depth.	116
Plate 5-7: Photomicrograph of a chalcopyrite-covellite grain from sample 74-RL-1119.	117
Plate 5-8: Photomicrograph of a grain from sample 74-RL-1113.	117
Plate 5-9: Photomicrograph from sample 74-RL-1119 showing chalcopyrite intergrown with covellite.	119
Plate 5-10: Photomicrograph from sample 74-RL-1119 showing covellite (Cv) forming discontinuous, roughly concentric layers in chalcopyrite (Cp).	119

	<u>Page</u>
Plate 5-11: Photomicrograph of a grain from sample 74-RL-1127.	120
Plate 5-12: Photomicrograph of a polished mount made from sample 73-RL-340.	120
Plate 5-13: Intensity pattern of $\text{CuK}\alpha$ X-radiation in sample 73-RL-340.	129
Plate 5-14: Intensity pattern of $\text{SK}\alpha$ X-radiation in sample 73-RL-340.	129
Plate 5-15: Intensity pattern of $\text{FeK}\alpha$ X-radiation in sample 73-RL-340.	129
Plate 5-16: Photomicrograph of a polished mount from sample 73-RL-323.	130
Plate 5-17: Intensity pattern of $\text{CuK}\alpha$ X-radiation in sample 73-RL-323.	131
Plate 5-18: Intensity pattern of $\text{SK}\alpha$ X-radiation in sample 73-RL-323.	131
Plate 5-19: Intensity pattern of $\text{FeK}\alpha$ X-radiation in sample 73-RL-323.	131
Plate 5-20: Photomicrograph of a polished mount from sample 73-RL-340.	132
Plate 5-21: Intensity pattern of $\text{CuK}\alpha$ X-radiation in sample 73-RL-340.	133
Plate 5-22: Intensity pattern of $\text{SK}\alpha$ X-radiation in sample 73-RL-340.	133
Plate 5-23: Intensity pattern of $\text{FeK}\alpha$ X-radiation in sample 73-RL-340.	133
Plate 5-24: Photomicrograph of a polished mount made from sample 73-RL-338.	135
Plate 5-25: Intensity pattern of $\text{CuK}\alpha$ X-radiation in sample 73-RL-338.	136

	<u>Page</u>
Plate 5-26: Intensity pattern of $SK\alpha$ X-radiation in sample 73-RL-338.	136
Plate 5-27: Intensity pattern of $FeK\alpha$ X-radiation in sample 73-RL-338.	136

## ACKNOWLEDGEMENTS

The author is sincerely grateful for the assistance provided by the following people during this study and especially to Dr. W. K. Fletcher who supervised the project. Drs. M. A. Barnes, W. C. Barnes, A. J. Sinclair and L. E. Lowe provided continuous advice, encouragement and critically reviewed this manuscript. Additional advice was offered by Dr. V. C. Brink on plant identification, by Dr. T. H. Brown on thermodynamics, by Dr. C. H. Cross on organic geochemistry, by Dr. L. M. Lavkulich on soil classification, by Dr. A. E. Soregaroli on economic geology and by Dr. H. V. Warren on biogeochemistry. Colleagues in the Department of Geological Sciences and Mining Industry who materially contributed to the project by their helpful discussion include Dr. G. Ashley, Mr. M. Bustin, Mr. I. Duncan, Dr. P. J. Doyle, Dr. S. J. Hoffman, Mr. J. M. Morganti and Mr. D. Wilton. Mr. E. Perkins advised on computer programming.

Mr. A. Dhillon, Mrs. A. Waskett-Myers, Mr. M. Waskett-Myers, Mr. G. Geogakopoulos, Mr. A. Lascis and Miss. L. McDonald assisted in sample analyses. Mr. I. Cameron and Mr. M. Waskett-Myers assisted in field studies and sample collection. Mrs. D. Coleman, Mr. A. McGregor and Mrs. Y. Michie provided drafting and typing services. Accommodation provided by Mr. H. Huff of Princeton, B.C., is gratefully appreciated.

The author is indebted to Mr. C. D. Bates (BP Canada Ltd.), Dr. P. E. Fox (Fox Geological Consultants), Dr. C. J. Hodgson (Amax Exploration Inc.), Dr. R. F. Horsnail (Amax Exploration Inc.), Mr. T. N. Macauley (Newmont Mining Corp. of Canada Ltd.)

and Mr. D. K. Mustard (BP Canada Ltd.) for releasing information relating to the geology of the project area and for helpful discussion.

Financial assistance during 1973 and 1974 was provided from Energy Mines and Resources research agreement number 65-1674 and by the Ernestine A. M. E. Kania Memorial Scholarship. Later support for the project was provided from the L-M mutual fund.

Finally I should like to thank my wife for her unfailing encouragement during the completion of this thesis.

## CHAPTER 1

## INTRODUCTION

## 1-1 STATEMENT OF THE PROBLEM

Conventional geochemical exploration techniques are often unsuccessful in glaciated areas where thick transported overburden may bury potentially economic base-metal deposits. Metals can, however, under favourable hydrologic conditions be transported into the secondary environment by deeply circulating ground water. Enhanced metal concentrations in bogs are generally the result of metal accumulation from dilute ground water solutions by organic matter. Interpretation of geochemical anomalies in bogs can be a problem especially in discriminating between metals concentrated from weakly mineralized ground water or surface water that has moved some distance laterally and those metals introduced from concealed sources beneath the bog. Important factors that must be considered when interpreting such anomalies are complex interactions of metals with organic substances and reactions between metals and such ligands as sulphide and carbonate. Both organic and inorganic associations will tend to immobilize metals in bogs. Trace and minor element distribution patterns have been studied in a small copper-rich bog close to a known copper mineral occurrence. Results of the investigations are described in this thesis and models are proposed to explain the spatial distribution patterns and the forms of copper present in the bog.

## 1-2 FORMATION AND CLASSIFICATION OF BOGS

The high content of natural organic complexing agents in bogs has been observed to strongly influence trace metal dispersion. The nature of these organic substances will reflect processes of bog sedimentation, which can vary under different hydrological and climatic conditions. Formation of different bog types will therefore have a significant effect on trace metal interactions.

Bogs can be defined as peat covered or filled landforms where, although the water table is close to the surface, there is usually little standing water (Tarnocai 1970). Peat which consists of mixed undecomposed plant fragments, products of their decomposition, microorganisms, minerals, and water, may be classified as an organic soil. Normal soil formation is characterised by a balance between the rate of organic debris accumulation and rate of total biological decomposition. The environment of peat formation, however, represents a break in the carbon cycle where rates of organic accumulation are far greater than the total destruction of materials (Given and Dickinson 1975).

Physical land forms which impede surface water movement to levels where sediment can deposit are potential bog sites (Moore and Bellamy 1974). Extent of peat formation in these areas will depend on the balance between plant residue accumulation, rate of decomposition and removal of the products from the system (Romanov 1961). High organic accumulation rates will raise the land surface and limit upward pore water move-

ment to plant roots. As the vegetation is unable to draw nutrients from the mineral soil beneath the organic material it is therefore forced to obtain elements from the developing host peat. Trace metals become depleted in the organic material unless continuously supplied by lateral influx of ground water.

Bogs where trace element nutrients are dominantly supplied through ground water movement have been classified, by Tarnocai (1970), as mineralotrophic or termed lower bogs by Manaskaya and Drozdova (1968). When nutrient flow to plant roots is decreased the monocotyledon flora, typical in mineralotrophic bogs, may be replaced by mosses which can thrive at very low trace element concentrations. Necessary nutrients will be adequately supplied by surface precipitation. Moss growth also tends to lower pH of the surface layers suppressing microorganism activity responsible for plant decomposition. Higher growth rates result in convex bog morphologies where organic material is largely fibrous sphagnum peat. Bogs of this type are classified as ombotrophic (Tarnocai 1970) or raised bogs (Manaskaya and Drozdova (1968). Where features characteristic of both main classes can be observed bogs are termed transitional.

Vegetation may play an important role in both organic matter accumulation and trace metal concentration. Transition metals, carbon, nitrogen and sulphur are essential for plant metabolism. Metals catalyse various enzyme systems which provide energy and form amino acids, proteins and vitamins (Nason and McElroy 1963). Large apparently non toxic metal accumulations can form in the tissues of certain plants espec-

ially species growing in bog environments. Fraser (1961), for example, observed that the moss, Pohlia nutrans, from the area of copper rich ground water seepages in a New Brunswick bog, contained up to 3.8% copper. Concentrations of 0.3% copper, 0.6% zinc and 0.06% lead were also found by Salmi (1967) in twig ash of the bog shrub Ledum Palustra. Location of these metal accumulations in plant tissues is uncertain although copper and zinc may be immobilized in leaf cell wall membranes thereby preventing toxic levels forming at metabolic sites (Turner (1969)). Metal release during decomposition could be important in formation of different organic products.

### 1-3 BOG SEDIMENTATION AND FORMATION OF HUMIC SUBSTANCES

Organic sediments in bogs are formed by microbial breakdown of plant material and the accumulation of dark, high molecular weight decomposition products. Rates at which these activities proceed depend on such factors as surface water flow, supply of nutrients to microorganisms e.g. nitrogen, and type of vegetation (Flaig 1972). Sedimentation rates in transitional bogs have been estimated by Grosse et al. (1964) and range from 0.1 to 1.6mm/year. Most intensive plant decomposition by the action of fungii, actinomyces and aerobic bacteria has been observed to occur in surface layers (Kuznetsov 1963; Flaig 1968; Given and Dickinson 1975). Different plant tissues will be attacked by specific microorganisms. Moore (1969), for example, established that the fungus Merulius Lacrymans digested cellulose and hemicellulose, but would not break down lignin.

Certain microorganisms may be restricted to different environments. Abundant fungi e.g. Fusarium are found in surface layers of mineralotrophic bogs. Smaller populations of the groups Peniillium and Clodosporium are, however, more common in ombotrophic environments. Fungial populations decrease in size with progressive depth in bog sediments due to lower oxygen concentrations (Waksman and Stevens 1929). Activity also depends on the humidity of the peat and has been observed, by Koronova (1961), to reach a maximum at 30°C with a water content of 60-80%.

Products formed as a result of advanced decomposition of plant materials include low molecular weight inorganic molecules such as methane, carbon dioxide, hydrogen, ammonia and hydrogen sulphide. These are formed mainly through the biogenic reduction of nitrates, small organic molecules such as carbohydrates and sulphate. Organic components such as humic substances, fulvic substances, amines and polysaccharides can also form although, however, the precise mechanism through which these substances are developed is uncertain. Humic and fulvic substances occur widely in natural environments including bogs, lake sediments and marine sediments. Various mechanisms for the formation of humic substances have been extensively reviewed by Felbeck (1971) and range from reaction paths dominated by microbial activity to reaction parths involving chemical polymerization of small organic molecules. Both microbial activity and polymerization reactions are probably involved at different stages in the genesis of humic and fulvic substances.

Products of plant decomposition which could interact with trace metals in bogs include soluble amino acids, simple organic acids, carbohydrates and humic polymer molecules. Humic substances have been studied in considerable detail and their properties will be only briefly described in this thesis. Stevenson and Butler (1969) define humic substances as a series of acidic, yellow-to black coloured, moderately high molecular weight polymers which have characteristics dissimilar to any other organic compounds occurring in living organisms. Arbitrary division of humic substances into the two main humic and fulvic acid fractions is based on solubility in alkaline or mineral acid solvents. Both humic and fulvic acid fractions are soluble in dilute sodium hydroxide, a medium generally used to extract humic substances from soil. Amorphous humic acid will be precipitated when the dark coloured alkaline, organic extracts are acidified with HCl. The yellow coloured solution which remains after separation of the humic acid is known as the fulvic acid fraction.

Fulvic acid fractions have lower molecular weights, greater solubility in aqueous solutions and larger carbon-hydrogen ratios than humic acid fractions (Manaskaya and Drozdova 1968). Variations in the properties of the acid fractions may reflect different types of organic matter from which they were extracted. Several workers have employed X-ray diffraction to investigate humic and fulvic acid structures. Results suggest that the basic units could be polymerized carbon lattices (Schnitzer and Khan 1972). Three dimensional 'cage' structures have also been proposed for the acids by Pauli (1968). Various side chains

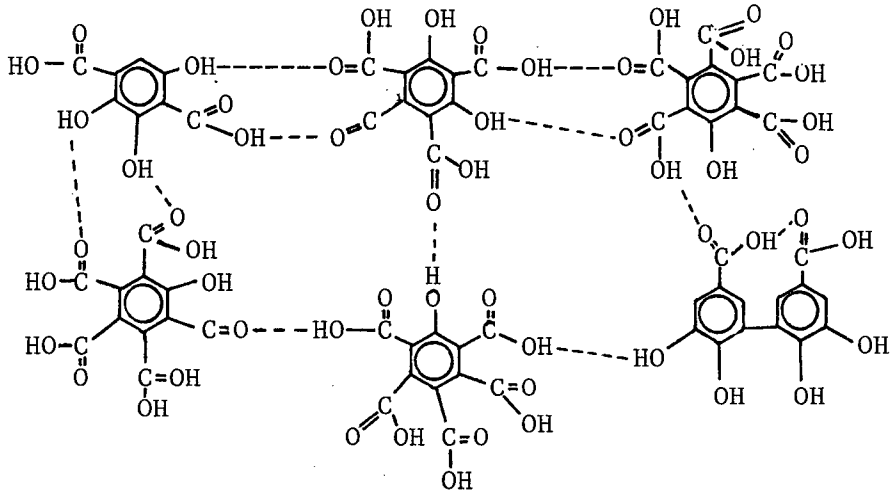


Figure 1-1: Fulvic acid structure proposed by Gamble and Schnitzer (1973).

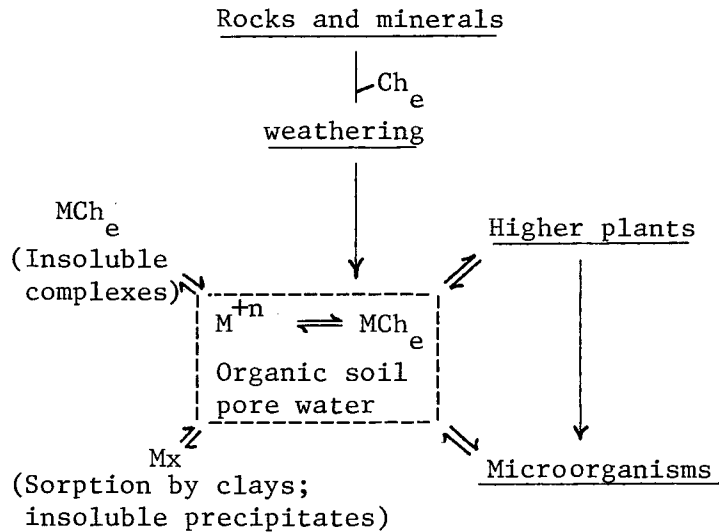


Figure 1-2: Schematic diagram for trace metal interactions in organic soils (adapted from Lindsay, 1972).

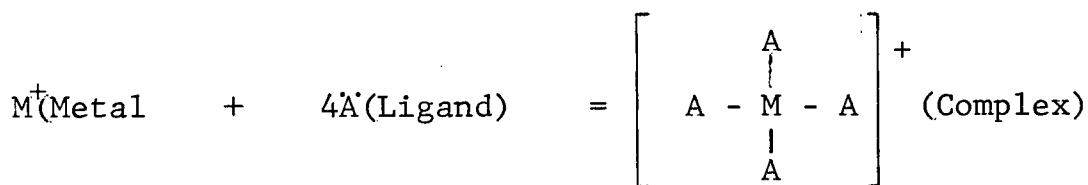
attached to the nucleus may carry carboxyl, phenolic hydroxyl, carbonyl and alcoholic functional groups. Ionization of carboxyl and phenolic groups is responsible for the weakly acidic and metal complexing properties of humic and fulvic acid fractions. Gamble and Schnitzer (1973) have proposed one structure for the fulvic acid fraction which is shown in Fig. 1-1.

#### 1-4 INTERACTION OF METALS WITH HUMIC SUBSTANCES IN BOGS

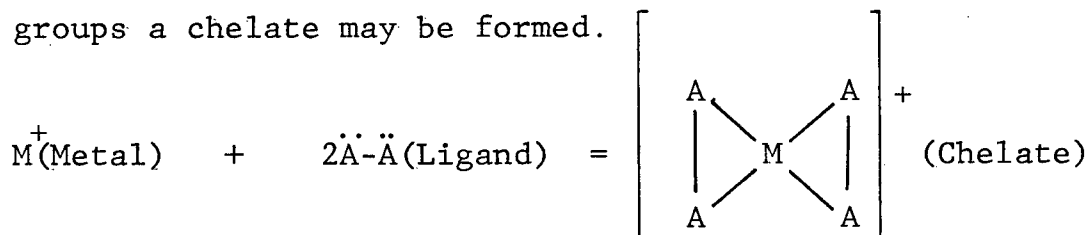
Partitioning of metals between the different solid and aqueous phases that are possible in bogs is illustrated in Fig. 1-2. Reactions in organic soils are dynamic (Lindsay 1972) since although they may approach equilibrium this state is rarely maintained. Metal interactions change in response to plant nutrient uptake from water, adsorption of metals to clays, sesquioxides and organic substances and precipitation of authigenic minerals. Soluble ions or molecules will move through the system in migrating ground water. Organic and mineral detritus can also enter the system suspended in surface water.

Schnitzer and Khan (1972) suggested that interaction between metals and humic substances could be by ion exchange, chelation, coagulation of soluble organic molecules or peptization of humic colloids. Bonding of metals to humic functional groups can be largely due to the electrostatic attraction of charged ions or by formation of stronger, covalent linkages. Complexing and chelation are terms often used to describe covalent bonding between metals and humic or fulvic fractions. Complexing involves donation of electrons by single active

ligand to a metals ion and may be shown in the following example.



Where an organic molecule has several potential electron donating groups a chelate may be formed.



Several experimental methods have been used to demonstrate that trace metals will form complexes with humic and fulvic fractions. Broadbent and Ott (1957) concluded that the large increase in optical density, observed when humic acid and copper sulphate solutions were mixed together, was due to formation of copper-humate complexes. Rashid and Leonard (1973) studied variation in infrared spectra occurring when cupric ions were added to solutions of humic substance extracted from a marine sediment. They concluded from these variations that carboxyl groups, attached to humic substances, formed bonds with copper and were important in metal retention. Goodman and Cheshire (1973;1976), however, concluded from results of electron paramagnetic resonance measurements that the copper in peat samples was linked to nitrogen associated with heterocyclic porphyrin molecules. Nitrogen content of peat humic acids has been found to be generally less than 5 percent. A relatively small proportion of total copper in organic matter may be bound to nitrogen compared to that associated with humic fractions (Ennis 1962, Davis et al. (1969).

Carboxylic and phenolic hydroxyl functional groups have been shown to play a significant role in humic-metal complexing. Ennis (1962) observed that the cation exchange capacity of peat could be decreased by the addition of organic reagents which reacted with specific functional groups to 'block' their metal complexing ability. Experimental results indicated that carboxyl groups were responsible for 30% and hydroxyl groups 60% of the total exchange capacity. Lewis and Broadbent workers (1961;1961) studied continuous copper and zinc exchange, by hydrogen ions, from metal saturated peat, humic acid and synthetic phenol-carboxylic acid. The authors concluded from their data that groups of phenolic, carboxylic and unidentified strongly acid ligands were largely responsible for trace metal complexing in humic substances. Solution pH which reflected acidity and type of the functional groups was also shown to control the extent to which metals were complexed. Monovalent  $\text{CuOH}^+$  ions were thought to bond with carboxyl groups with cupric ions demonstrating preference for phenolic sites.

Potentiometric titrations have often been used to investigate humic and fulvic metal complexing reactions (Beckwith 1959; Khanna and Stevenson 1962; Cross 1975). This technique measures pH variation after known volumes of bases are added to humic solutions. Sigmoidal titration curves in the absence of metal ions suggest that the humic and fulvic acid fractions could be both monobasic or polybasic in nature. Gamble and Schnitzer (1973) concluded from studies of proton release (pH decrease) occurring when copper ions were added to a fulvic acid fraction solution that two reactions were possible. These in-

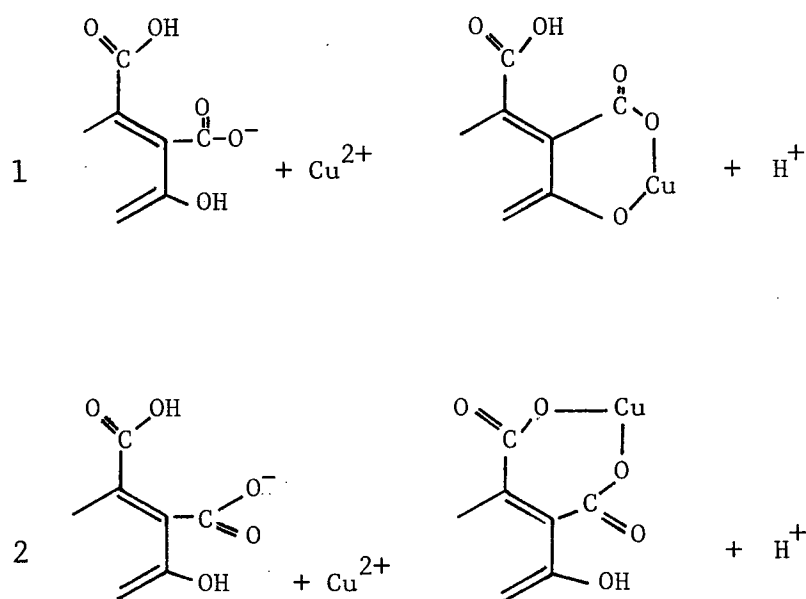


Figure 1-3: Reactions between copper and fulvic acid fraction (Gamble and Schnitzer 1973).

volve bonding of copper to phenolic hydroxyl and carboxyl groups. The carboxyl groups are ortho relative to the phenolic hydroxyl groups attached to the fulvic acid molecule. Two possible reactions with copper are shown in Fig. 1-3 and number 1 is considered the most probable.

Several workers (Beckwith 1959; Khanna and Stevenson 1962; Khan 1969) found that the sequences of potentiometric curves obtained from reaction of different metals with humic solutions resembled the theoretical order of organo-transition metal complexes established by Irving and Williams (1948). Relative strength of complex stabilities decreases in the order of lead > copper > nickel > zinc > cadmium > iron > manganese. Schnitzer and Skinner (1966;1967), however, found that relative strengths of metal-humate complex stabilities, measured at pH 3.5, did not follow the Irving-Williams sequence. They found the order to be copper > iron > nickel > lead > cobalt > zinc > manganese. The observed variations between measured humate-metal or fulvate-metal complex stabilities and the Irving-Williams series could be due to different experimental methods used in determinations or different source material for humic substances. Cross (1975), for example, demonstrated in titration curves obtained for reactions of copper with humic acid solutions that the shape of the curves reflected soils of varying maturity. Davis et al. (1969) found that, using copper, the exchange capacity of a humic fraction extracted from peat was greater than the maximum exchange capacity of the original peat. They concluded from these results that during the alkaline extraction of the humic

fraction additional exchange sites were made available for bonding with copper.

The formation of humate and fulvate complexes can increase mobility of metals through several possible interactions. Rashid and Leonard (1973) observed that humic acid solutions will markedly increase the solubility of transition metal sulphides, hydroxides and carbonates. Baker (1973) found that the solubility of metal-humates of such metals as lead, zinc and copper increased with the addition of further humic acid solution. Coagulation of humic and fulvic acid solutions commonly occurs when metal ions are added to these substances. Khan and Schitzer (1972) suggested that coagulation is due to formation of negatively charged hydrophilic colloids. The critical concentration of different metals necessary to peptize these colloids is related to ionic valence, ionic strength and pH. Ong and Bisque (1968) proposed that the Foss effect can explain relative mobility of metal humate and fulvate colloids. Carboxylic and phenolic hydroxyl functional groups, attached to the humic macro molecules, are almost completely dissociated in the presence of low cation activities. Increasing metal ion concentrations will, however, decrease the mutual repulsion between the functional groups due to the bonding of these groups with metal ions. The Foss effect is a structural change from a stretched colloid shape to a coiled form due to the attraction between the different groups. This structural change will also result in the colloid changing from a hydrophilic to a hydrophobic state and, in the process, coagulating.

## I-5 DIAGENESIS IN BOGS

Reactions between minerals, microorganisms and the enclosing fluids which occur after the sediment has been deposited, but before metamorphism are termed diagenesis (Bluck 1969). Photosynthesis, fermentation and anaerobic decomposition are basic diagenetic reactions which occur in organic rich bog sediments (Berner 1971). Aerobic bacteria and aquatic plants, living in surface pore water layers, use oxygen for their metabolic processes. These reactions decompose organic substances producing low molecular weight organic acids such as acetic acid which, with carbon dioxide decreases pore water pH. Berner (1969) observed that in the absence of neutralizing bases such as amines or calcium, bog sediment waters can show decrease in pH falling to below 5.0. The progressive consumption of oxygen diffusing downward through the pore water by aerobic bacteria also decreases Eh in the deeper sediments.

Reducing conditions, produced through the removal of oxygen, favour the activity of anaerobic bacteria. These bacteria are important in fermentation reactions and other organic decompositions. Bacterial processes catalyse the reduction of various anions such as sulphate under conditions which are thermodynamically unfavourable for corresponding inorganic reactions. Energy for these biological processes is obtained by oxidation of simple organic substrates such as glucose. Different biogenic reactions will only occur within certain Eh and pH ranges. Stumm and Morgan (1970) demonstrate that in the pH range 7 to 8 and with abundant organic substrate, nitrogen is initially re-

duced to elemental nitrogen, followed by reduction of sulphate to hydrogen sulphide and finally reduction of carbon dioxide to methane. This sequence reflects increasing electron density as a result of each reaction and also parallel ecological ranges in which different bacteria are active at a certain Eh. Products of reduction reactions increase pore water pH and diffuse upward through the sediment. Oxidation of reduced species will occur when these products diffuse into pore waters having a higher dissolved oxygen concentration. The point at which oxidation occurs in a vertical sedimentary column may be termed the oxidation-reduction boundary (Berner 1969). This boundary can form relatively close to the surface of bogs where strongly reducing organic soils are in contact with the atmosphere.

Several quantitative models have been proposed for the formation of metal sulphides during marine sediment diagenesis (Sweeney and Kaplan 1973; Rickard 1970; Love 1963; Ramm and Bella 1974; Lambert and Bubela 1970; Bass Becking and Moore 1961). Presence of certain metal sulphide textures, commonly formed during diagenesis, are often used as evidence for syngenetic origin of many sedimentary ore deposits. These textural forms, known as framboids, consist of small ( $50\mu\text{m}$ ) spheroidal accumulations of microcrystalline pyrite, galena or sphalerite. Love (1963) originally proposed that framboids represented fossil bacteria colonies. More recent studies, however, have demonstrated that they may be formed by precipitation, under laboratory conditions, without presence of bacteria (Sweeney and Kaplan 1973; Rickard 1970; Berner 1969; Kallioskoski 1969;

Kribeek 1975). Framboidal pyrite textures, although generally associated with marine environments, have also been identified in lake sediments (Vallentyne 1962), esturine sediments (Miedema 1973) and bogs (Papunen 1966).

Papunen (1966) suggested that framboid formation in fresh water sediments initially involved the association of ferric ions with spherical humic colloids. Where these entered a zone rich in hydrogen sulphide the iron would be reduced to sulphide minerals which would be retained in the characteristic spheroidal shape. Papunen concluded that humic acids only participated in the mechanism by forming stable colloidal iron-hydroxide systems which protected the developing framboid form. Berner (1969) also demonstrated that elemental sulphur, in addition to the hydrogen sulphide is essential for formation of initially the iron monosulphide, mackinawite, and finally pyrite.

Although no direct biological interaction may be involved in framboid formation bacteria are essential, indirectly, to provide a source of sulphide anions. Variables which control precipitation of metal sulphides include cation sulphate and organic substrate concentrations, their relative diffusion rates to sites of precipitation and the rate of bacterial sulphate reduction. In organic rich marine sediments the extent of sulphide formation will be a function of the available metal ion concentration and ionic diffusion rates (Berner 1971). Sulphate contents of freshwater sediments, however, are generally much lower than in marine environments. Ramm and Bella (1974) studied the sources for hydrogen sulphide commonly found in re-

duced, intertidal sediments. They determined, experimentally, that below dissolved sulphate concentrations of 300 ppm, the rate of sulphate reduction, by bacteria, depends on relative concentrations of sulphate and of organic substrates such as carbohydrate and amine.

Casagrande et al. (1977) found that 25% of the total sulphur (which ranged from 0.17 to 0.21%) in peat samples from Minnie's lake, Okefenokee swamp, Georgia was in the form of ester sulphate (sulphur in a C-O-S linkage, often termed HI reducible) and 1% was pyritic sulphur. Lowe (private communication, 1977) reported that undecomposed sedge peat can have total sulphur ranging from 1 to 1.6% which is significantly higher than contents reported by Casagrande et al.

#### 1-6 STUDIES OF TRACE METAL DISTRIBUTION IN BOGS

Many factors may contribute to the final concentration of metals in bogs. Discrimination between anomalous trace metal distributions which could reflect significant mineral sources and high background levels in organic materials is often difficult. Usilk (1968) reviewed geochemical prospecting methods in peatlands and concluded that determination of background data would require knowledge of geological, geomorphological, hydrological, chemical and ecological characteristics of bogs.

Trace metals in peat have been found to range from 1 ppm to several percent where bogs are located in mineralized areas. Walsh and Barry (1958) determined that the copper content of organic materials from several Irish blanket bogs did not exceed 20 ppm and values for all elements progressively decreased with

depth. This trend suggested that the metals were introduced to the system through surface precipitation rather than by ground water. Similar, very low, transition and rare earth contents were found by Kochenov et al. (1967); Tarakanova(1971) as a result of numerous metal distribution studies in Russian bogs.

Tarakanova observed, however, that providing surficial clays between bedrock and peat were comparatively thin, distribution of the metals in organic material would reflect underlying geology. Other investigations have demonstrated similar relationships. Gleeson and Coope (1966) found that copper and zinc increased from levels below 50 ppm in peat to above 200 ppm in the glaciolacustrine clays beneath an Ontario bog. Soil pH also increased with depth and Salmi (1967) noted that values in several Finnish bogs reflected underlying granites or limestones. Manaskaya et al. (1960) concluded that low copper contents in sedge and sphagnum peats were related, primarily, to low bedrock levels. Copper distribution was also thought to depend on distance from underlying basement and degree of ground water migration.

Trace metals may enter bogs by diffusion through underlying sediments, lateral movement of mineralized ground water or surface water transport of clay sized detrital grains (Tarakanova, 1971; Borovitskii 1970). Areas where water discharges into a bog system can correspond to large trace metal accumulation in organic sediment and especially at the edge of bogs. Zinc values up to 8.8% were found, by Cannon (1955) in peat samples from bog margins. The source of metal, transported to the bog

by ground water, was a small base-metal sulphide concentration hosted in dolomite. Fraser (1961) and Boyle (1977) found that high copper values approaching 1% in a New Brunswick bog were related to entry of ground water through springs and seepages. Mehrtens et al. (1973) traced similar copper levels (2%) in a small Welsh bog to movement of ground water through a buried stream channel.

Different trace metal patterns can often be used to indicate direction of ground water movement and location of a mineralized source. Maximum contrast of copper and nickel anomalies in peat from a Finnish bog sampled by Nieminen and Yliruokanen (1976) follows a horizontal layer at an intermediate depth in the bog. This distribution reflects lateral migration of ground water solutions from partially exposed bedrock on the till covered bog floor. Eriksson and Eriksson (1976) observed that copper, lead and zinc anomalies in the Hinson bog, Sweden, reflected drainage from weathering metal sulphides outcropping on the hill side above the bog. Higher lead and copper values occurred close to the edge of the bog, but zinc was concentrated in peat at a greater distance from the point of ground water entry. Relative distribution of these metals indicate that ground water flow and mobility of metal-humate complexes control migration. The even, vertical distribution of copper in the Whipsaw creek bogs studied by Gunton and Nichol (1975) suggested significant mineral sources below the copper-rich materials. Vertical migration of copper was not apparently strongly influenced

by variation in the organic matter content.

Vegetation, environment pH and Eh may have a strong effect on trace metal dispersion through bogs. Salmi (1960) considered that the difference in distribution of manganese, iron, molybdenum and lead in surface peat of Finnish bogs from concentration of nickel, titanium and vanadium at depth reflected different solubilities when metal ions migrated through zones of decreasing pH. He also observed accumulation of copper and zinc reaching 3000 ppm in the Ledum shrub twig ash compared to levels below 300 ppm for these metals in the host peat. The relationship of copper and molybdenum ion mobilities to pH of the secondary environment has been discussed, in detail, by Hansuld (1966). Horsnail and Elliott (1971) studied several central B.C. bogs, located close to mineral occurrences, and found accumulation of molybdenum, but depletion of copper in the acid, fibrous surface peat. A reverse relationship between these metals was observed, however, in deeper, more decomposed organic sediments. From the results of a regional geochemical prospecting program conducted through central B.C. Boyle et al. (1975) concluded that molybdenum accumulated in alkaline bogs, whereas, copper values were greater in acid swamps.

Effect of environment, vegetation cover and organic matter on copper accumulation has been studied in detail by Fraser (1961) who investigated the Tantramer swamp, New Brunswick. Organic material from an exposed peat bank resting on sandy loam within a small, open clearing contained up to 10% copper. Copper

values reaching 1% occurred in samples of the sandy loam collected close to ground water seepages. Copper contents below 1%, however, were found in surface material from an area of swampy forest which partly surrounded the clearing. Values sharply increased, with depth, reaching 5% copper in peat layers three feet below the swampy forest floor. Fraser concluded that the original clearing formed when copper rich spring water destroyed the primary forest growth. Following accumulation of the peat bank evaporation from its exposed surface induced upward migration of solutions and concentration of copper in the organic material. Low copper values in surface layers of the swampy forest reflect decreased evaporation beneath the tree cover. Larger copper abundances in deeper layers, however, are due to lateral movement of copper-rich ground water solutions into the peat. Absence of visible syngenetic copper minerals in organic sediment was thought to be due to the oxidizing, alkaline nature of the environment. Formation of nitrogen bonded metal complexes was considered to be the major factor responsible for copper accumulation in the peat. Later studies, however, have shown that the association of metals with organic nitrogen forms may be a relatively minor effect.

Copper and other iron minerals may form in bogs by precipitation from dilute ground water solutions under favourable Eh and pH conditions. Native copper grains ranging from 1 to 10mm size associated with fine grained pyrite were identified by Eckel (1949) in a Colorado bog. An occurrence of native copper also in an organic accumulation has been reported by

Lovering (1928). Cannon (1955), using X-ray diffraction identified lead and zinc sulphides in peat samples containing more than 8% zinc from the Bergen bog, New York state. Papunen (1966) described framboidal pyrite in an iron sulphide layer exposed in a Finnish peat bog. Postma (1977) also reported the presence of iron sulphide (mackinawite), iron carbonate and iron phosphate (vivianite) in a Danish river bog. He found that the pH of the organic rich sediments containing the iron sulphide ranged from 5.5 to 7.4 and the Eh ranged from +100 to +250 mv.

#### 1-7 SUMMARY

Factors which could influence mobility of metals in bogs include the nature of the peat forming environment, chemical changes produced through organic diagenesis, formation of humic substances and interaction of metals with these humic substances. Numerous investigators have demonstrated that metals such as copper, lead, cobalt, nickel and zinc form strong complexes with humic and fulvic acid fractions in soil. Stability of these complexes will reflect relative strength of bonding between the metals and the humic or fulvic acid fractions, pH and ionic strength of solutions containing the metals. The physical state of the humic and fulvic colloids may also affect mobility of the metal-organic complexes. A small proportion of the metals could also be strongly bound to soil nitrogen groups. Authigenic metal sulphides can occur in reducing organic accumulations although organic sulphur forms are most abundant in peat.

Metal distribution patterns in bogs have been frequently

studied during the past thirty years and investigators have found that the metals were generally concentrated by the organic matter from dilute ground water solutions. Interpretation of geochemical anomalies associated with bogs is, however, often complicated by the complex chemical and physical interactions which lead to the accumulation of metals.

## CHAPTER 2

## DESCRIPTION OF THE STUDY AREA

## 2-1 LOCATION AND ACCESS

The study area covering roughly one square kilometre forms part of a mineral claim group located 29 km northwest of Princeton, British Columbia (Fig. 2-1). Access to the property from the Hope-Princeton highway is by 19 km of gravelled summer roads which follow the east side of Whipsaw creek.

## 2-2 PHYSIOGRAPHY, DRAINAGE AND CLIMATE

Mean elevation of the study area is 158 m and the surrounding regional topography reflects transition between higher relief of the Cascade mountains in the west and the Thompson plateau to the east. Locally there is a marked topographic change corresponding, roughly, to the 1350 m contour. Above this elevation are rolling, wooded hills with gentle slopes and broad valleys. Land surfaces below 1350 m, however, are often dissected by deep valleys through which flow major streams e.g. Whipsaw creek. Relief on the property is 200 m and land surface gradients range from 5 to 40 degrees.

The gentle undulating plateau north of the study area is drained by streams which flow south into Whipsaw creek through steep walled valleys. These probably reflect surface expression of geological faults or zones of higher rock fracture density. External property drainage is through a subdendritic network of small streams. First order streams often rise in small hillside bogs which are relatively common throughout the region and range from 10 to several thousand square metres in area. The location of the central bog, the outline of the



Plate 2-1: A west looking view of the west end of the central bog. Station G 1.0 is approximately located in the center of the open area shown in the foreground of the photograph.

study area and other bogs on the property are shown in Fig.2-2.

The central bog occupies an elongate irregularly shaped depression sloping to the southeast at a 5 to 10 degree gradient. Surface features are illustrated in Plate 2-1. Several smaller marshy areas surrounding the main depression at slightly higher elevations correspond to points of ground water discharge from the break in slope separating the steep hill side from the concave bog basin. Larger springs northwest of the bog probably reflect water rising to the surface through fault zones. Water also discharges continuously from one diamond drill hole collared on the hill side north of the bog.

First order streams flow from springs and marshy seepage areas to form a meandering, dendritic pattern of channels on the bog floor. Shallow, semi-stagnant ponds are also common on the bog surface and reflect the very poor internal drainage of the organic soil. The streams combine into a single channel which drains the lower part of the basin through a shallow valley; the stream gradient in this valley increases from 10 to 15 degrees over 1000 m distance from the bog margin to confluence with a larger stream draining the northern bog.

Climate of the study area reflects a transition from high rainfall, typical of the coastal mountains, to a semi-arid, interior environment. Annual precipitation of roughly 70 cm at the property elevation is represented by several metres of compacted snow which can persist on the ground until late June. Large fluctuations of water table, observed in a deep sample pit on the interfluvium south of the bog, reflect aquifer recharge from this accumulation early in the summer. Stream water flow

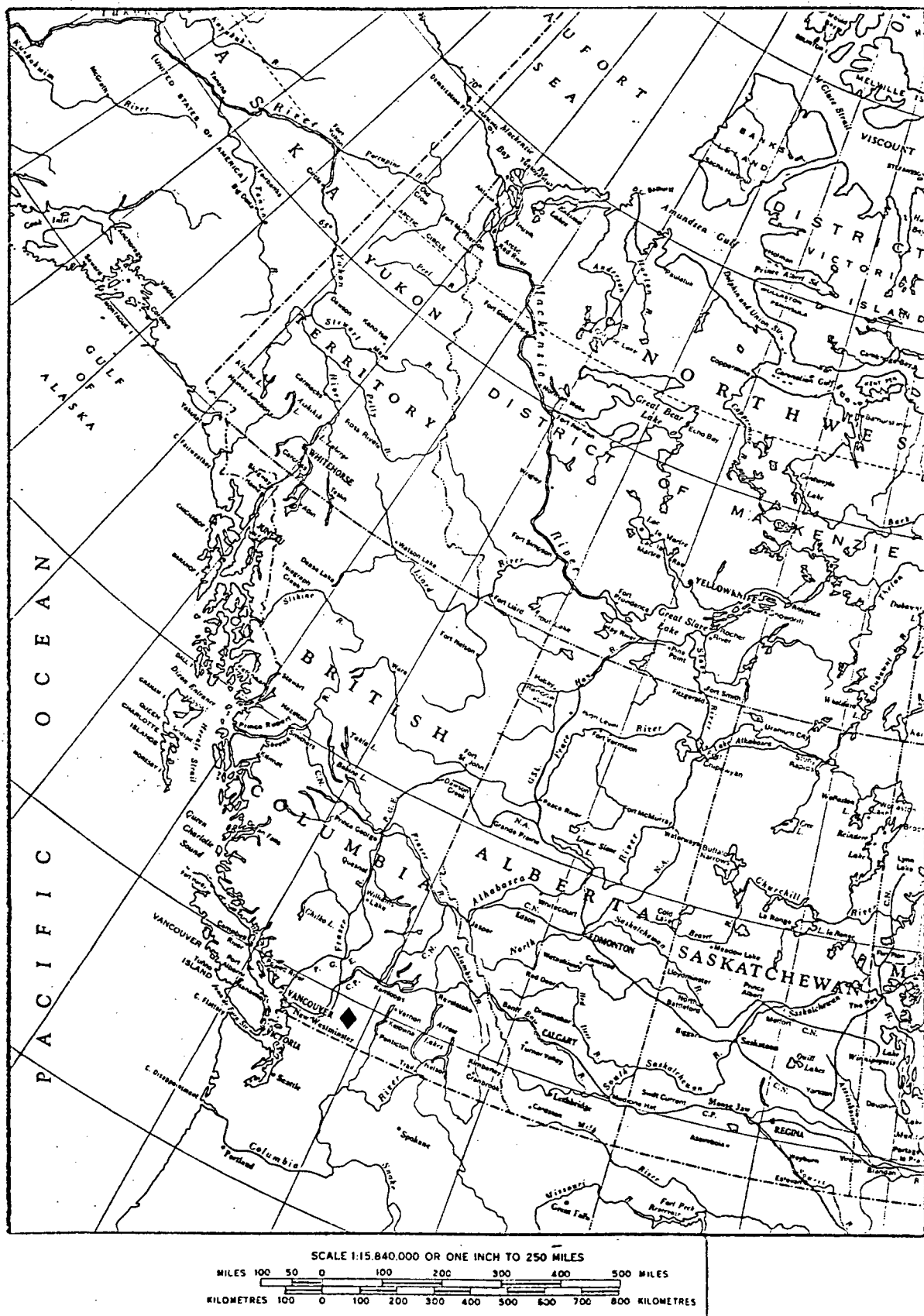


Figure 2-1. Location (◆) of the study area.

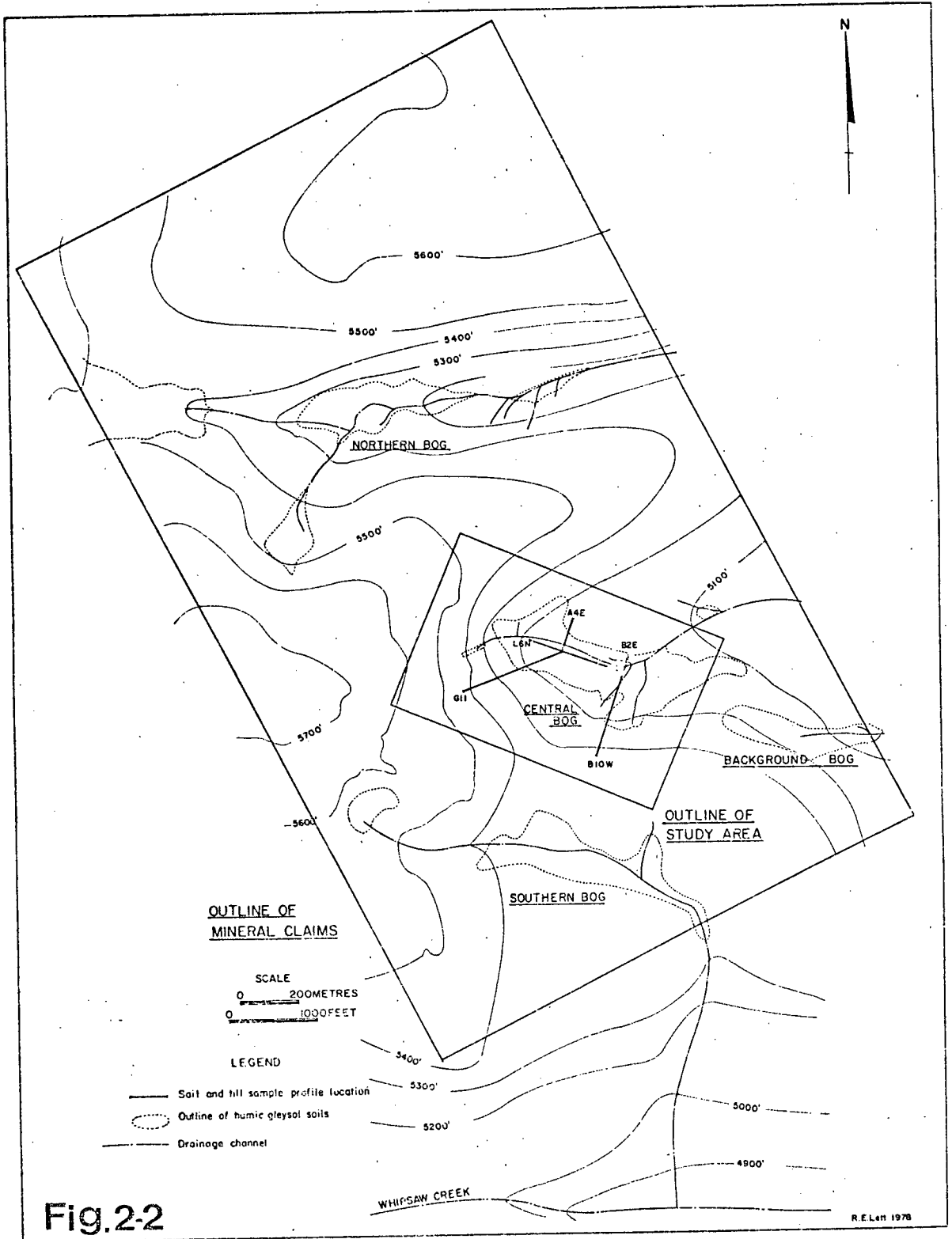


Figure 2-2: Outline of mineral property and location of bogs.

decreases from a June maximum and may cease completely in first order channels during late summer.

## 2-3 EFFECTS OF GLACIATION AND PLEISTOCENE DEPOSITS

Orientation of glacial striae and outcrop shape indicate two possible Pleistocene ice advances from the northeast (Hills 1960). Thick continental ice sheets covering the region may have reached elevations of 2500 m above sea level (Mathews 1944) and deposited extensive basal till on a mature weathered land surface. Average basal till thickness in the study area is 2 to 3 m and ranges from 1 m on ridge crests to 12 m below the bogs. Moderately oxidized olive brown (Munsell colour 2.5Y 5/4) basal till consisting of sandy clay or sandy loam may contain up to 50% subangular rock clasts. Reduced, dark olive grey (Munsell colour 5Y 3/2) sandy clay till forms a layer 1 to 2 m thick immediately below the till-bog interface. Rock clasts in the till are dominantly schistose, granitic and volcanic rock types cropping out over a wide area to the north and east. They range from pebbles to boulders and may have long axes aligned parallel to the till-bedrock contact. This orientation of clasts in deeper till layers reflects compression and flow of the till below the moving ice sheet.

The bedrock surface beneath the till is deeply weathered and although vestigial rock fabric is frequently preserved, most of the silicate minerals, other than quartz, have completely weathered to clays. The effect is visible in trenches where the Eagle granodiorite is weathered to a depth of 3 m below the original bedrock surface. Elongate, highly weathered, comminuted granodiorite lenses occur within the basal till. The

lenses have sharp contacts with the till which have a similar dip angle to the hill slope gradient. An example of the relationship between lenses and till from a trench north of the central bog is shown in Fig. 2-5a. The lenses were probably surface bedrock layers which were removed by moving ice and forced into the basal till along shear planes (Ashley, Personal Communication 1976).

During final retreat of the ice, glaciers blocked normal drainage in several of the major valleys. A proglacial lake formed behind ice dams in the upper Whipsaw creek valley and drained, initially, south into Copper Creek. Hills (1960) has suggested that this occurred through a melt water channel which occupied a small pass at the 1430 m elevation located due south of the property. Terraced fill and the irregularly distributed, well sorted, subsurface gravels above the 1600 m may have been deposited during this period. A succession of lakes probably developed in the Whipsaw valley with progressive wasting of glaciers and an extensive white silty clay, exposed on the valley side close to the Hope-Princeton highway, may represent glacio-lucustrine deposits.

Post Pleistocene uplift of the land surface north of the study area rejuvenated drainages. Bogs started to develop in gently sloping depressions where ground water discharged to the surface. Streams rising in these depressions are actively eroding the area. Regionally, the east-west channel systems which dominated Pre-Pleistocene topography have been replaced by north-south draining creeks.

## 2-4 GEOLOGY OF THE STUDY AREA

The study area is on the western margin of a 2000km linear belt of Triassic and Lower Jurassic volcanics and sediments known as the Quesnel Trough. These rocks, referred to as the Nicola-Takla-Stuhini volcanic assemblage, are bounded by the Omineca Crystalline Belt, to the east, and by the Coast Crystalline Belt, to the west. Volcanic lithofacies of the Nicola Group rocks are dominated by calc-alkaline basalt and andesitic flows which were formed during subaqueous eruptions from regional faults. Sedimentary lithofacies are represented by argillite, limestone, chert, quartzite and thin interbedded volcanic members. Pyroclastic and epiclastic rocks, complex intrusives, breccias and dyke swarms are associated with the development of large volcanic centers during a late stage of the volcanic cycle. Economic copper-molybdenum-precious metal deposits, stockwork and disseminated sulphide deposits are closely related to alkalic intrusives e.g. Copper Mountain. Sulphides were emplaced during late stage fumarolic activity close to volcanic centers. (Barr et al. 1976)

Other types of deposits in the Quesnel Trough include skarn, vein and small copper occurrences associated with porphyry stocks or dykes. Copper sulphides, hosted by Nicola volcanics, close to a small porphyry stock on the Whipsaw Creek property may be typical of mineralization which was related to the emplacement of intrusions along faults during later periods of deformation. Geology of the study area and surrounding mineral claims, shown in Fig. 2-3, has been compiled from mapping, geophysical data and diamond drilling results which were obtain-

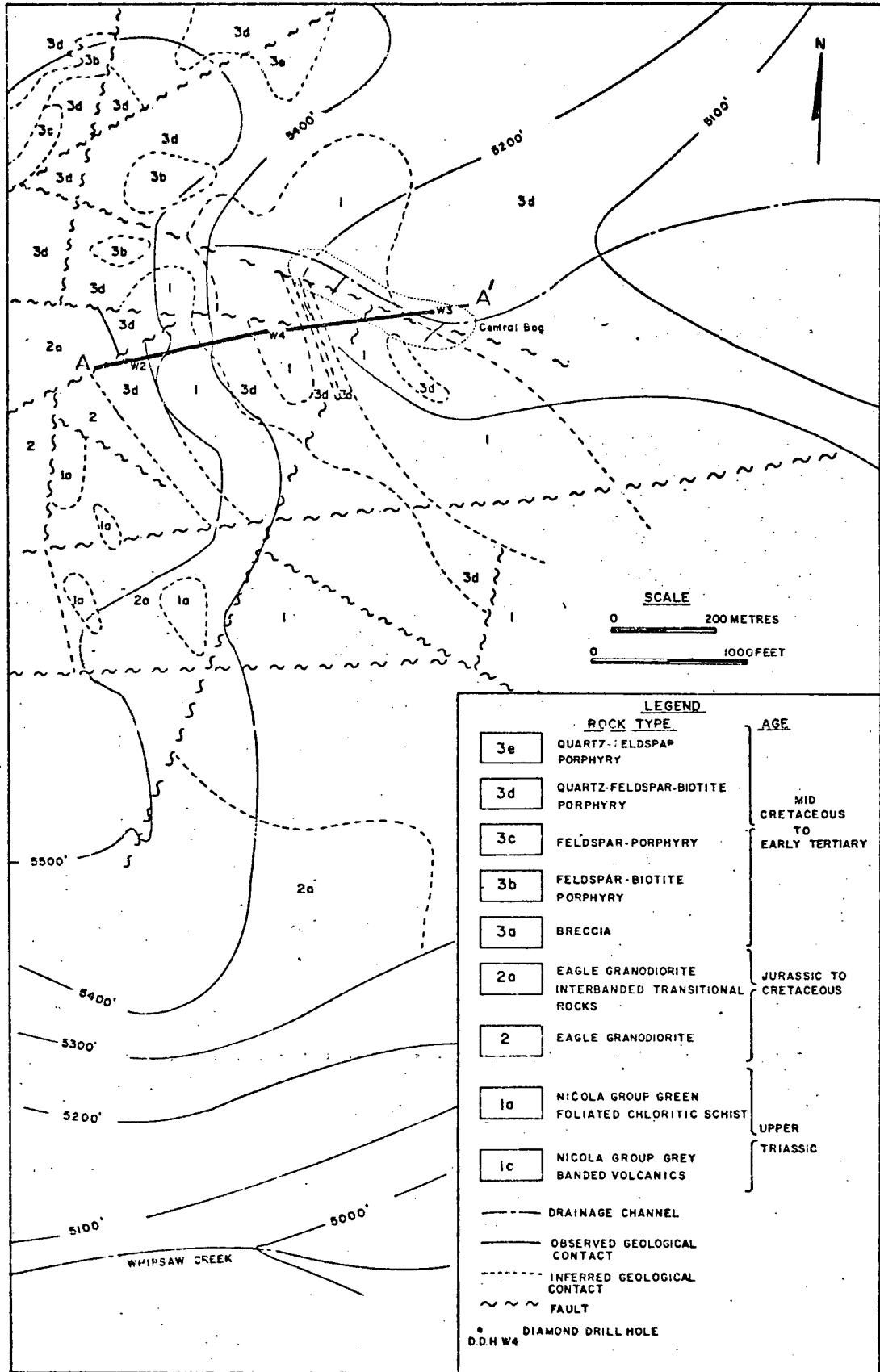


Figure 2-3: Geology of the mineral property (after Mustard 1968).

ed during a property evaluation conducted by AMAX EXPLORATION (Mustard 1968).

Oldest rocks which crop out are metamorphosed Nicola Group volcanic rocks represented by chlorite and amphibole schists. These are strongly foliated and, in the western part of the property, are also in contact with the intrusive Eagle pluton. This intrusive is Jurassic-Cretaceous in age and consists of pale grey, coarse grained biotite granodiorite with marginal aplite and pegmatitic phases. Both the granodiorite and aplite are foliated along a 150-160 degree strike which is parallel to that of the adjacent schists. Coarse feldspar-quartz-biotite pegmatites, skarn lenses containing epidote, grossularite and base metal sulphides also occur in the intrusive in addition to the aplite.

A transition zone several hundred metres wide is characteristic of the contact between the Eagle granodiorite and the Nicola schists. Rock types in sequence through a typical west to east section are granodiorite, rafts of volcanic rocks in granodiorite, alternating volcanic and granodioritic layers, injection gneisses, chloritic schists with occasional aplite stringers and, finally chlorite schists. A small porphyry stock with a related dyke swarm has also intruded the Nicola Group-Eagle granodiorite contact. The age of this intrusion is thought to be late Cretaceous to mid Tertiary (Anderson 1974). Rock types within the stock include feldspar-biotite porphyry, biotite porphyry, quartz-feldspar-biotite porphyry and quartz porphyry. A breccia, consisting of schist, granodiorite and altered porphyry fragments in a matrix of comminuted porphyry occurs at intervals along the intrusive contact. Leucocratic

quartz-feldspar-biotite porphyry is most common and crops out on a ridge north and west of the central bog. It also occurs in dykes and interpretation of geophysical data has suggested that these have intruded chloritic schists which extend beneath the bog.

Porphyry rocks have been altered hydrothermally and during this process several mineral assemblages developed. Propylitic alteration resulted in the formation of abundant epidote and chlorite which are visible in all porphyry types. Argillic alteration with the development of kaolinite and minor chlorite from minerals in the porphyritic rocks occurs close to their contact with the Nicola Group schists. Quartz sericite alteration is generally confined to the quartz-feldspar-porphyry dykes. Local, commonly intense, silicification of aplites and breccia is associated with concentration of sulphide minerals.

Copper, lead, zinc, iron and molybdenum sulphides have been identified on the property. Sphalerite, galena, chalcopyrite and molybdenite are found associated with skarn lenses in the granodiorite. Pyrite is the most abundant sulphide and occurs as fracture fillings in schist, aplite or marginal porphyry or as coarse disseminations comprising up to 20% volume of porphyritic and schistose rocks. Chalcopyrite, closely associated with pyrite, occurs disseminated or as fracture fillings in breccia, porphyry, schist and aplite. Assay values of 1% copper over one . six m interval of exposed breccia and chloritic schist have been found adjacent to the porphyry-Nicola Group contact.

Bornite, less abundant than chalcopyrite, only occurs as

fine disseminations in porphyry or, at one location, in breccia. Thin blebs or rounded coatings of covellite and chalcocite on chalcopyrite are found in the porphyry dykes cropping out west of the central bog. Molybdenite is, in general, closely associated with the porphyry stock margins and forms fine coatings on fractures and in quartz veins. Magnetite is concentrated in the chlorite schist close to the porphyry contact, as fracture fillings in breccia, as disseminations in the porphyry and as massive lenses in scarn. Hematite generally occurs as disseminations in feldspar porphyry and feldspar-biotite porphyry rocks

Three diamond drill holes, completed in 1969, are located within the study area. A geological cross section for part of the area beneath the central bog has been constructed from drill logs for these holes and from geophysical data. Hole # W-2, collared west of the bog, intersected a sequence of green chloritic schist, altered feldspar porphyry dykes, biotite-feldspar porphyry dykes and terminated in grey banded volcanics at a vertical depth of 40 m (Fig. 2-4). Average copper grade of the rocks was 0.2% and a 3 m interval of quartz veined chloritic schist assayed 0.5% copper and 0.16% molybdenite. A similar sequence of rocks with comparable copper grade was also found in diamond drill hole #69-4, collared on the western edge of the central bog. Fractured zones up to one m wide cutting the drill core at intervals indicate the presence of large faults. These have also been identified from air photographs and appear to be normal, steeply dipping with a northwest strike. Several of the faults intersect in

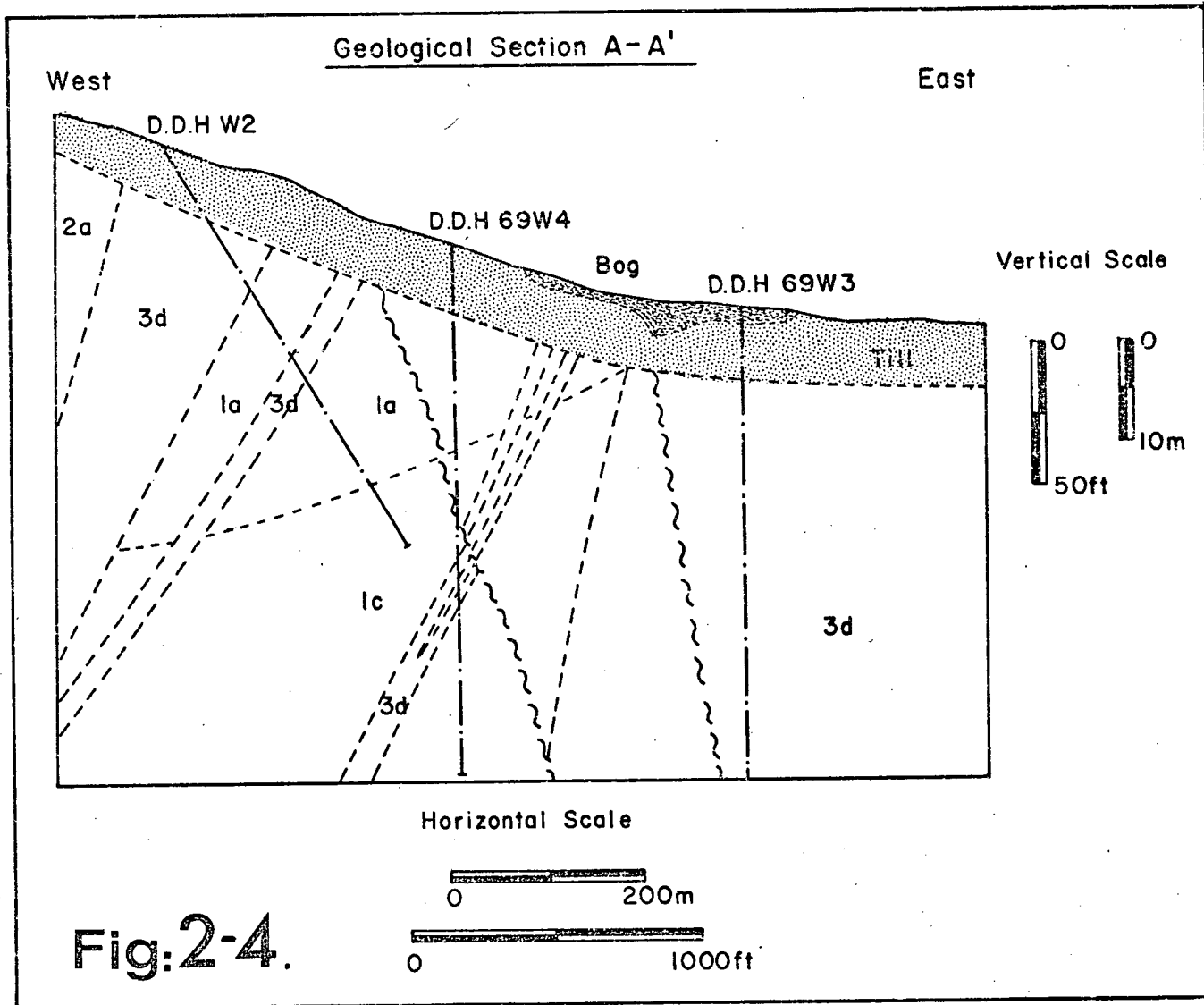


**Fig:2-4.**

the region of the central bog.

## 2-5 MINERAL EXPLORATION HISTORY AND PREVIOUS GEOCHEMICAL INVESTIGATIONS

Copper-molybdenum mineral occurrences were first discovered by Texas Gulf Sulphur in 1968 following a regional stream sediment sampling program. Detailed examination of the mineral claims was conducted from 1960 to 1964 by Texas Gulf and Dome Exploration. Geochemical sampling established that bogs close to the porphyry stock margins contained abundant copper. Amax Exploration conducted additional exploration of the property during 1968. From geological mapping, detailed soil sampling, geophysics, diamond drilling and trenching they concluded that the concentration of base-metal sulphides was closely related to intrusion of the porphyry stock. Further exploration targets proposed, but not investigated, were suggested to be in the area on Nicola Group-porphyry contacts buried beneath the central and northern bogs. Horsnail (1968) carried out applied geochemical orientation studies over the bogs and concluded that migrating ground water transported metal ions from weathering sulphides into organic material where copper was accumulated by humic substances.

The diamond drilling, described in Section 2-4, was carried out by Texas Gulf in 1969. Anderson (1971) who completed a detailed geological and petrological study outlined concentric molybdenite, pyrite, chalcopyrite, sphalerite and galena zones radiating outwards from a quartz stockwork 1500 m north-west of the study area. Results of diamond drilling, an induced polarization survey and geochemical sampling, carried out

by Newmont Mines in 1972 over the northern margin of the porphyry stock outlined a broad zone of copper sulphide mineralization with copper assay values to 0.28%. Gunton (1974) analysed till samples collected by over-burden drilling from beneath the central and northern bogs. He also analysed organic soils from the central bog for copper, iron, manganese, and organic matter by loss on ignition. Organic matter abundance was found to decrease down profiles through the bog where as copper values often remained high in the till beneath the bog. A possible copper source to explain the high values was suggested directly below the central bog.

#### 2-6 PEDOLOGY AND FLORA OF THE STUDY AREA

Nature of the parent materials, surface relief, vegetation, external climate and time are all factors influencing soil genesis. Characteristics of those soils which have formed from the same parent material will often strongly reflect physiography. This may be illustrated by relating different soil types on a relief catena. A catena through the study area is defined by brunisolic, gleysolic and organic soils (Fig. 2-5). The spatial relationship between these soils, the characteristic flora which they support and surface drainage patterns are shown in Fig. 2-6.

Brunisolic soils with medium internal drainage form on the gently undulating ridge crests and convex parts of hill slopes. Solum thickness varies from 20 to 40 cm and the soil supports mature growth of lodgepole pine (*Pinus contorta*), Englemann Spruce (*Picea engelmannii*), White Spruce (*Picea glauca*) and Alpine Fir (*Abies lasiocarpa*). The characteristic soil is an

orthic dystric brunisol which may be distinguished from the other great soil groups by thin Ah horizons ( 5 cm) and a low base status (pH 5.5). A typical soil profile (A) from the study area is shown in Fig. 2-5a.

Alpine dystric brunisols with thicker, turfy Ah horizons form beneath small, open, grassy hillside clearings west of the bog. Degraded dystric brunisols, identified by having a thin, eluviated, Aej horizon have also developed on the undulating ridge crests. Gleyed dystric and sombric brunisols result from poor internal drainage at the base of hill slopes and form a transition between orthic brunisols and humic gleysols.

Humic gleysols have developed on the lower, concave parts of the hill slopes and form a margin around the central bog. Water table in this area is generally within 10 to 20 cm of the surface. The characteristic soil is an orthic humic gleysol which has a thick Ah horizon ( 8cm) containing between 3 and 30% organic matter. Prominent orange-red and occasionally black mottles are also visible in the B and C soil horizons. A typical profile (B) is illustrated in Fig. 2-5b. Humic gleysols support abundant growth of Mountain Labrador Tea (Ledum glandulosum), White Rhododendrum (Rhododendrum albiflorum), Skunk Cabbage (Lysichiton kamschatcense), White Spruce and Englemann Spruce. Orthic humic gleysols with up to 40 cm accumulation of moderately decomposed organic material are known as peaty phases. These have formed in seepage areas, generally less than 10 square metres in size, where appreciable ground water is discharging at the surface. Vegetation, typical of mineralotrophic bog environments includes sedge

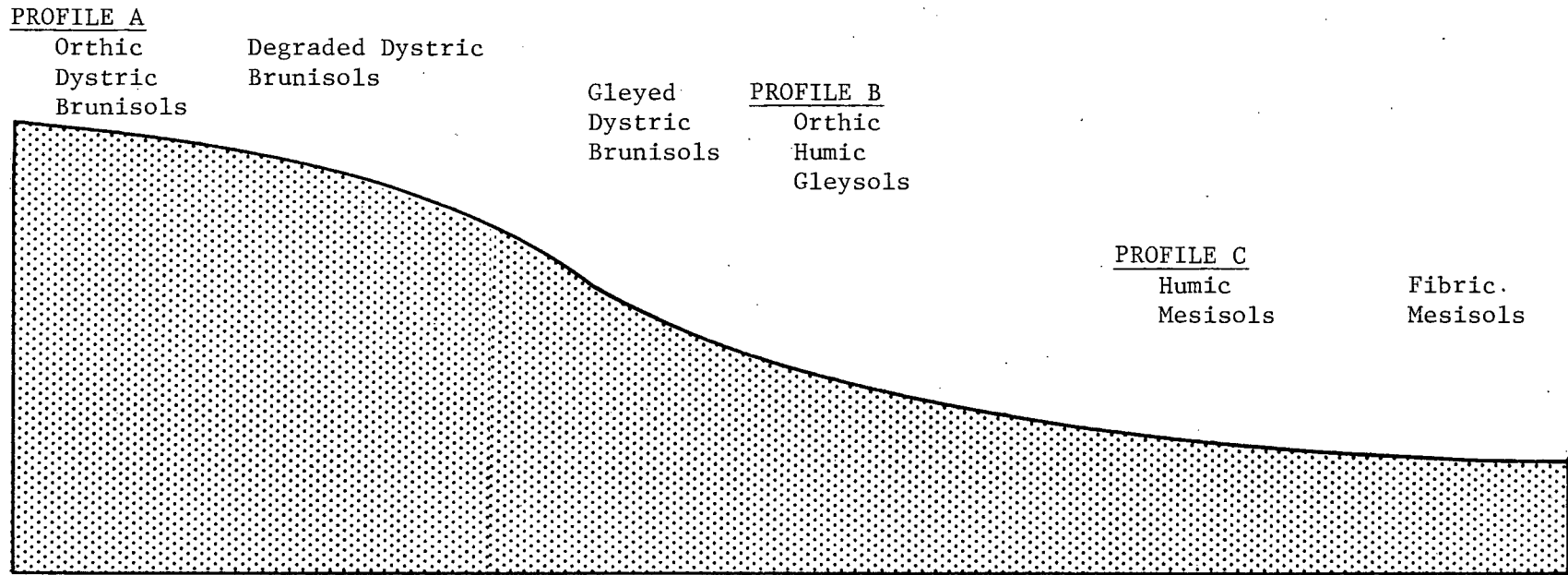


Figure 2-5: Soil catena through the study area.

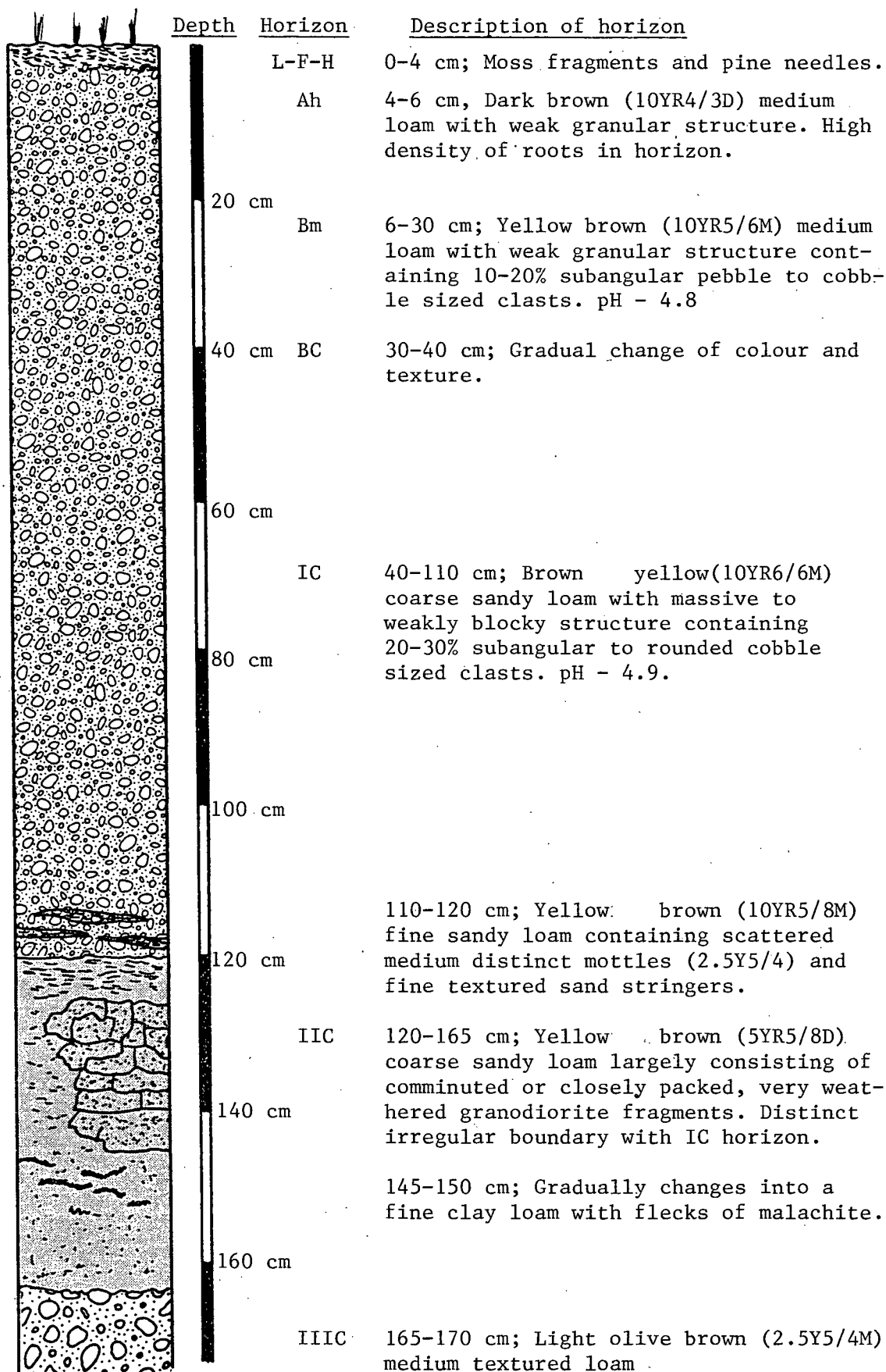


Figure 2-5.a PROFILE A.

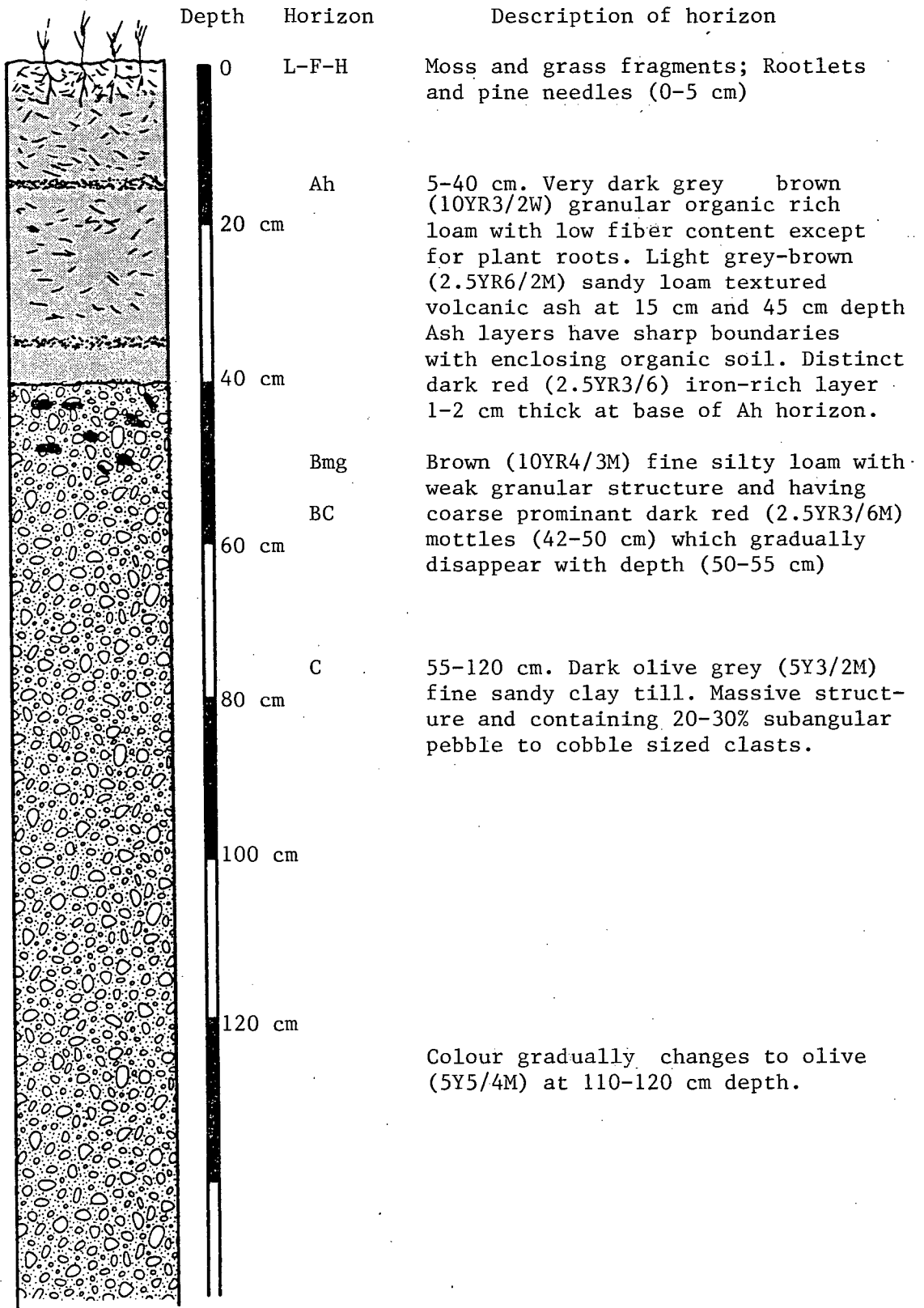


Figure 2-5b:PROFILE B.

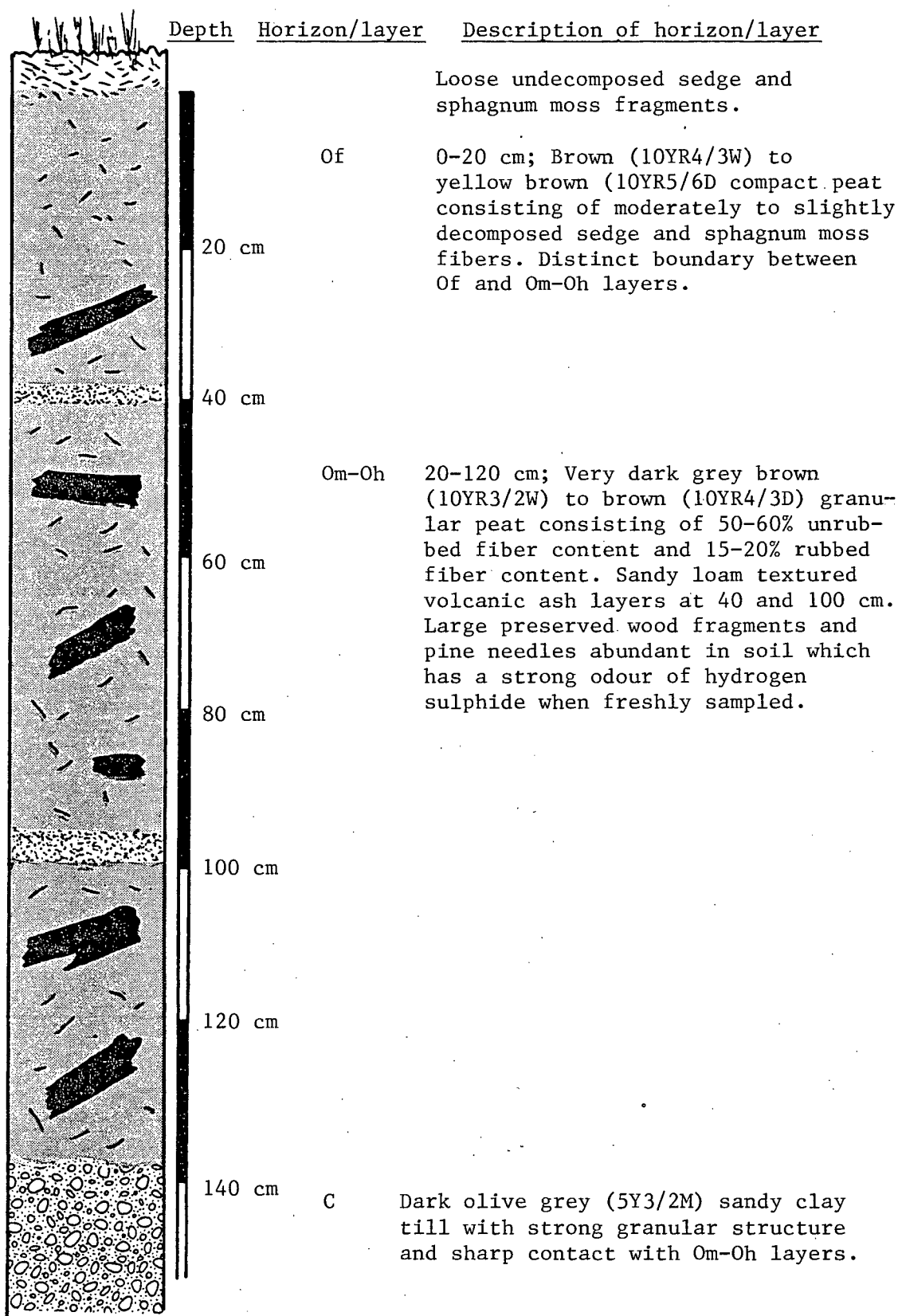


Figure 2-5c:PROFILE C.

(Carex sp.), Horsetail (Equisetum arevanse), Skunk Cabbage, Labrador Tea (Ledum groenlandicum) and mosses including Sphagnum Sp.

Organic soils are defined in the System of Soil Classification for Canada (Canadian Department of Agriculture 1974) as those soils where organic accumulations are greater than 40 cm thick and contain more than 30% organic matter. Further classification of these soils into suborders is based on those features observed in a typical profile known as the control section. A control section profile through the central bog is 130 cm thick and consists of a soil surface tier from 0 to 30 cm depth, a soil middle tier from 30 to 90 cm depth and a lower tier from 90 to 130 cm depth. Organic soil suborders are defined from unrubbed fiber contents, rubbed fiber contents and colour of sodium pyrophosphate solution extracts from soil samples of the middle tier. This method provides a rough index of the degree of natural decomposition of the organic soil.

Typical material from the middle tier in a central bog profile contains between 50 and 60% unrubbed fiber content, 15 to 20% rubbed fiber content and has a sodium pyrophosphate extract colour of 10YR 5/6 on the Munsell scale. Based on these criteria the characteristic soil is a humic mesisol. A profile, illustrated in Fig. 2-5c, consists of the least decomposed, fibric layer (Of) above more mature mesic (Om) and humic (Ch) layers. Beneath a small area in the northwest part of the bog where there is abundant Sphagnum moss growth the fibric (Of) layer may reach 50 cm thickness. The soil is then classified as a fibric mesisol. Total thickness

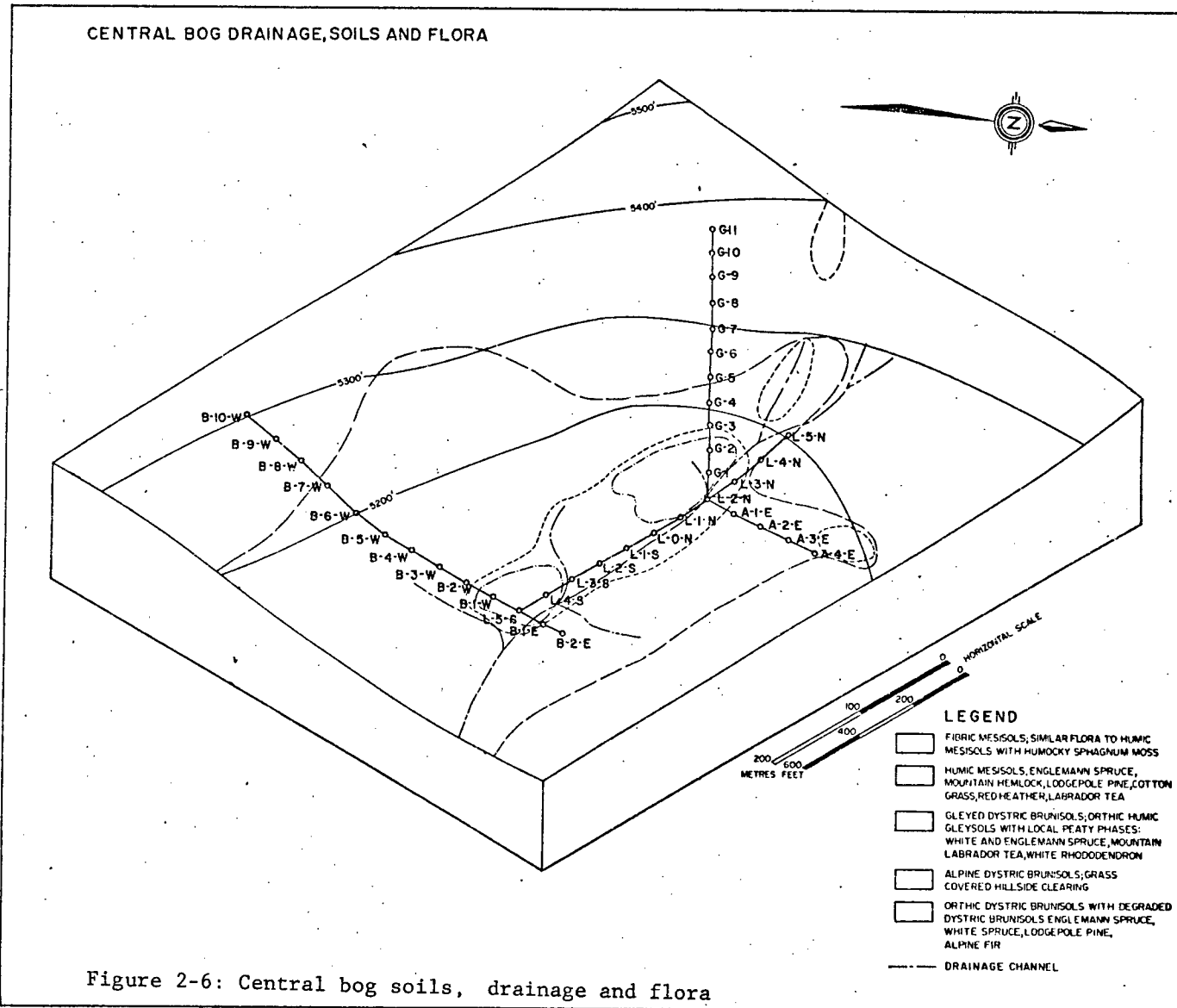


Figure 2-6: Central bog soils, drainage and flora

of fibric, mesic and humic layers in the humic mesisols ranges from 1.5 to 2 m. Accumulation of organic soil may, however, reach 4 m in the area of fibric mesisols and corresponds to prominent depressions in the organic soil- till interface.

The central bog is a mineralotrophic, hillslope type and vegetation is, in general, similar to that formed on peaty phases in humic gleysol soil. Restricted Sphagnum moss growth is mixed with Sedges (*Saxifraga* Sp.), Cotton grass, Labrador Tea, Skunk Cabbage, Red Heather (*Phyllodoce empetrifolia*) and Blueberry (*Vaccinium membranaceum*). Scattered stands of Englemann Spruce, Mountain Hemlock (*Tsuga mertensiana*) and Lodgepole Pine also occur. Abundant Sphagnum moss growth in the upper, northwest part of the bog is characteristic of ombrotrophic or raised bog environments. The water table may be up to 50 cm below the humicky moss covered surface in this area.

Light grey-brown (Munsell colour 2.5Y 5/6) layers of fine sandy-loam textured material found at intervals in organic soil profiles are volcanic ash. Samples from these layers consist of submicroscopic, silky, translucent glass fragments mixed with small quantities of magnetite, hornblende and a green mineral which may be hypersthene. The layers have sharp contacts with the soil and are 1 to 4 cm thick. They commonly occur in organic soil profiles at two intervals between 20 to 40 cm depth and also between 70 to 180 cm depth. Two distinct layers also occur in the Ah horizon of humic gleysolic soil at 20 cm and at 40 cm depth. Presence of two distinct layers in the soil suggests that volcanic ash may have covered the bog sur-

face at two, separate time intervals. Continuity of the layers in the bog cannot be demonstrated, however, due to the small number of samples available for mineralogical analysis. In addition the ash which fell on the bog surface may have been reworked by stream water action soon after deposition.

Two separate ash falls have been deposited over southern British Columbia in Recent times. Mullineau (1974) described an early, widespread ash deposit, dated by carbon 14 isotope method, at 6,600 years B.P. This originated from the pre-historic Mount Mazama which was located in the present Crater Lake, Oregon, area. The ash contained a small proportion of hypersthene, but no hornblende. Repeated, later eruptions from Mount St. Helens in Washington also deposited ash, but over a small area. The ash from this eruption contained hornblende and cummingtonite with minor pyroxenes. St. Helens ash has been identified at 85 cm depth in a peat bog located in the Otter Creek valley roughly 60 km west of the study area Fulton and Armstrong (1965).

Source of the ash in the bog is uncertain although mineralogy of one sample from the deeper layer exposed in a humic gleysol profile suggests that it may represent the St. Helens eruption. Upper layers in soil may also be related to periodic ash falls which were related to the event.

## CHAPTER 3

## SAMPLING AND ANALYTICAL TECHNIQUES

## 3-1 SAMPLING METHODS AND FIELD OBSERVATIONS

Soil and till samples were collected by several methods from vertical profiles at stations located between 10 and 60 metres apart along traverses crossing the central bog. Sampling control was provided by a geophysical grid which had been previously established over the property. Profile and sample locations are shown in Fig. 3-1 and Fig. 3-2. Mineral soils and shallow till samples were obtained by excavating pits at stations on the hillslopes above the bog. Each sample represented a 10 cm long vertical channel cut in the wall of the pit. Samples were taken at 30 to 40 cm intervals down profiles exposed in the pits and detailed observations of environment, soil type, topography, sample colour, sample consistency clast rock type, clast shape and clast orientation were made at each location. Till samples deeper than one metre were obtained using a Boro overburden sampler mounted on a Cobra percussion drill. At each location an attempt was made to collect material with the Boro sampler from the till bedrock interface. This was often unsuccessful owing to the very hard, compact till. Ten cm long till cores were obtained at 50 to 100 cm intervals down profiles through the till.

Organic soil material was collected using a Hiller peat auger. Continuous 40 to 50 cm long cores were obtained with this equipment at 50 cm intervals down profiles in the bog. A complete core was found to be necessary to provide sufficient dried material for analysis. Subsamples were however taken

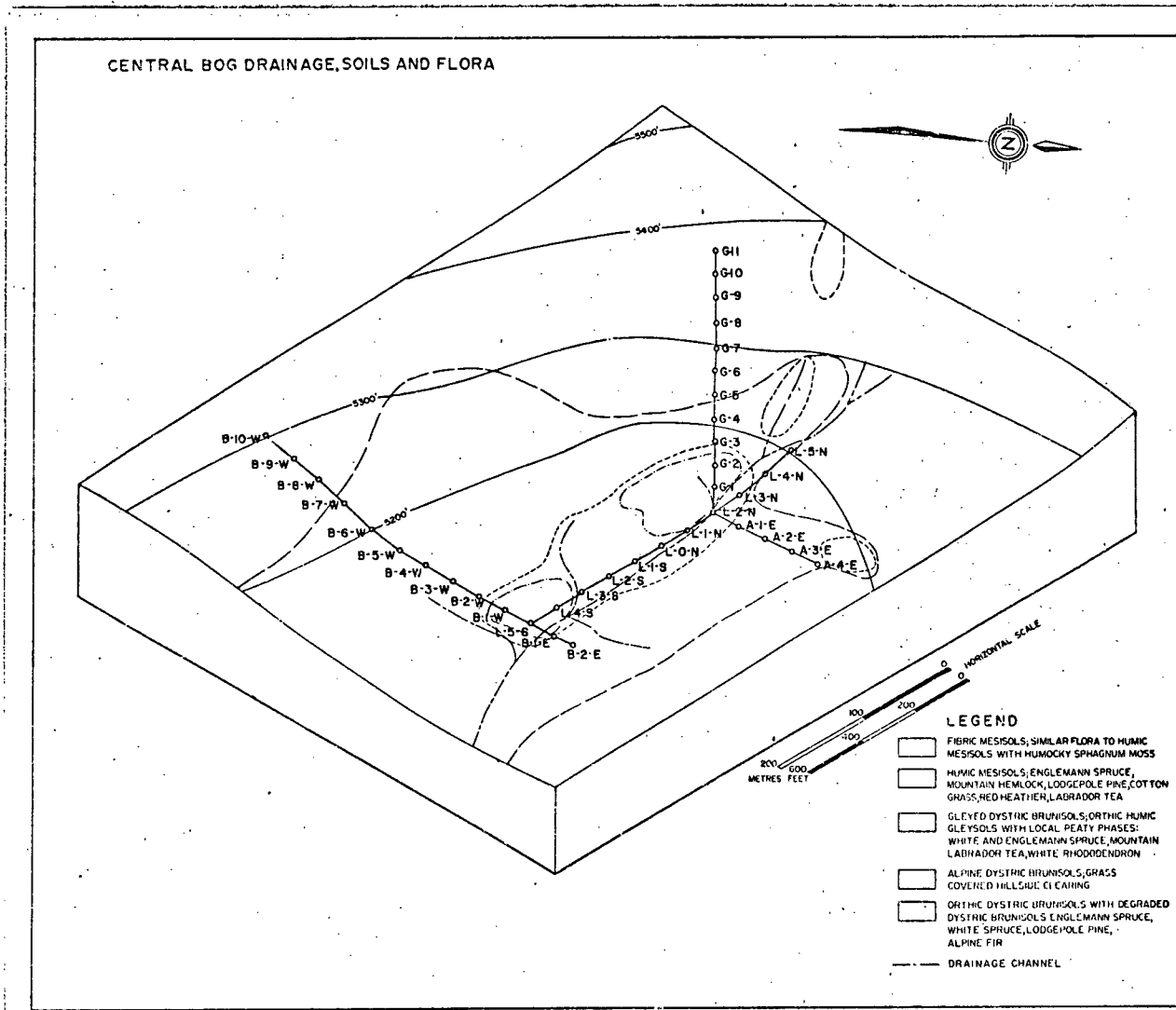


Figure 3-1: Location of soil and till profiles

from the core when conspicuous texture or colour variations could be seen within an interval. Freshly collected organic soil, mineral soil and till material was transferred from the sampler to Kraft paper bags and allowed to air dry. Several bulk organic soil samples, each consisting of several combined cores were placed in acid washed plastic cartons, quickly transported in an insulated container to Princeton and stored in a cold storage at  $-5^{\circ}\text{C}$ .

Volcanic ash samples were obtained from layers exposed in the organic soil cores. The ash, however, was commonly mixed with organic material and ultimately only two relatively uncontaminated samples were analysed for trace metals. Leaf and stem samples representing new seasonal growth, were taken from Ledum glandulosum shrub and sphagnum moss growing in the central bog. These samples were washed with distilled water and stored in paper bags. Specimens of typical bog flora were also preserved for later identification.

Water samples were collected from a number of sources in the study area (Fig. 3-3). These included seepages from till-bedrock interfaces exposed in trenches, springs from probable fault zones and water discharging from a diamond drill hole north of the central bog. Springs and seepages from the area dominated by humic gleysolic soils were also sampled. A number of samples were collected from water accumulating in semi-stagnant bog pools and from water flowing in streams crossing the bog floor. Subsurface bog waters were sampled through cased bore holes at ten locations within the bog. Holes were cased with 3cm diameter PVC pipe to depths ranging from 1 to 2 m.



At some of the locations this depth represented the organic soil-till interface. Water was allowed to accumulate to the top of the casing and they completely removed several times with a small hand pump. A sample was finally collected through a smaller PVC tube attached to the pump and lowered to the bottom of the casing.

All water samples were filtered in the field under pressure through a 0.45  $\mu$ m millipore membrane filter, acidified with HCl, and stored in 125 ml or 500 ml acid washed PVC bottles. Water pH was generally measured at each sample site with British Drug Houses Universal Indicator. The pH of the water in the cased bore holes was measured using a combination glass-reference electrode attached to an Orion model 404 meter. Problems occurred with this method of pH determination owing to instrumental drift possibly resulting from the long lead connecting the electrode to the instrument. The Eh of several surface water samples, one ground water sample and the interstitial water from a freshly sampled core was measured with a platinum-glass electrode attached to the Orion 404 instrument. Sulphate content of several water samples was determined in the field by a barium chloride turbidimetric method described in Appendix B.

### 3-2 ANALYSIS OF SAMPLES FOR TRACE METALS

Mineral soil, organic soil, till and vegetation samples were oven dried at 110°C. Mineral soils and till samples were gently disaggregated and sieved through an 80 mesh nylon screen. It was often found necessary to grind the organic soil samples in a mortar before sufficient material could be obtained for sieving. Vegetation samples were ground in a Wiley mill. A



<u>Element</u>	<u>Flame</u>	<u>Wavelength (Å)</u>	<u>Current(mA)</u>	<u>Slit (u)</u>	<u>Background Correction</u>
Ca	Air-acetylene	4226.7	4	100	No <sup>a</sup>
Co	"	2410	20	300	Yes <sup>b</sup>
Cu	"	3247.5	3	50	No <sup>a</sup>
Fe	"	3719.9	5	25	No <sup>a</sup>
Mn	"	2794.8	10	50	No <sup>a</sup>
Mo	Nitrous oxide- acetylene	3132.0	5	100	No <sup>a</sup>
Ni	Air-acetylene	2324	20	300	Yes <sup>b</sup>
Zn	"	2138.6	6	100	No <sup>a</sup>

a - Varian Techtron IV

b - Perkin-Elmer 303

Table 3-1: Instrumental operating conditions for  
atomic absorption spectrophotometers

weighed portion of the sieved soil, till or ground vegetation was digested for twelve hours in a 3:1 mixture of nitric and perchloric acids. At the end of this digestion, carried out on an air bath at 200°C, a dry residue is obtained. This residue was leached with 2 ml of 6M HCl for several minutes and the solutions then diluted to 10 ml with distilled water. The solutions were then analysed for copper, cobalt, iron, manganese, nickel and zinc by atomic absorption spectrophotometry.

The solutions were also analysed for molybdenum by atomic absorption spectrophotometry, but with a nitrous oxide-acetylene flame rather than an air-acetylene flame. Before analysing the solutions 200 mg of aluminium chloride (hexahydrate) were added to each 10 ml as a releasing agent. The same proportion of aluminium chloride was also added to the standards. Operating conditions for the atomic absorption spectrophotometers are given in Table 3-1, analytical results for elements are given in Appendix A and analytical precision for elements in Table 3-2.

Filtered water samples were aspirated directly into the atomic absorption spectrophotometer and analysed for copper, iron, manganese and zinc. A 10 ml portion of each water sample was also mixed with 2 ml of 5% lanthanum solution in a 50 ml volumetric flask, the solution made up to 50 ml with distilled water and analysed for calcium by atomic absorption spectrophotometry. Dissolved organic carbon content of water samples was measured using a Beckmann model 915 total carbon analyser by injecting 50 µl of the filtered, acidified water with a microsyringe into the sample port of this instrument. The sample is carried by a stream of oxygen gas through a furnace

heated to 950°C where the carbon is oxidized to carbon dioxide. The concentration of carbon dioxide evolved from each sample was measured using a Beckmann model 865 Infrared analyser attached to the total carbon analyser. Before samples were analysed the instrument was calibrated with a series of sucrose solution standards. Analytical results are given in Appendix A.

### 3-3 ANALYSIS OF WATER SAMPLES FOR 2-2 BIQUINOLINE EXTRACTABLE COPPER

Approximate proportions of ionic copper and copper bound as natural organic complex were determined by a method based on that described by Stanton (1966). This technique is based on the reaction between  $\text{Cu}^+$  ions and 2-2 biquinoline forming a pink coloured complex and the intensity of this coloured complex will depend on the concentration of the copper in solution. The determinations are made by adding 1 ml of a buffer solution, consisting of 200 g of sodium acetate (trihydrate), 100 g of potassium sodium tartrate (tetrahydrate) and 20 g of ascorbic acid in 1:1 of distilled water to 20 ml of the filtered water sample in a test tube. The buffer solution reduces  $\text{Cu}^{2+}$  to  $\text{Cu}^+$ , prevents precipitation of iron and aluminium and adjusts pH to 6.0. One ml of a 0.02% 2-2 biquinoline solution in iso-amyl alcohol is then added and the tube stoppered and shaken for 30 seconds. The colour of the immiscible alcohol layer is visually compared to a standard series generally ranging from 5 ppb to 100 ppb. Larger copper concentrations were measured by diluting the water sample with distilled water.

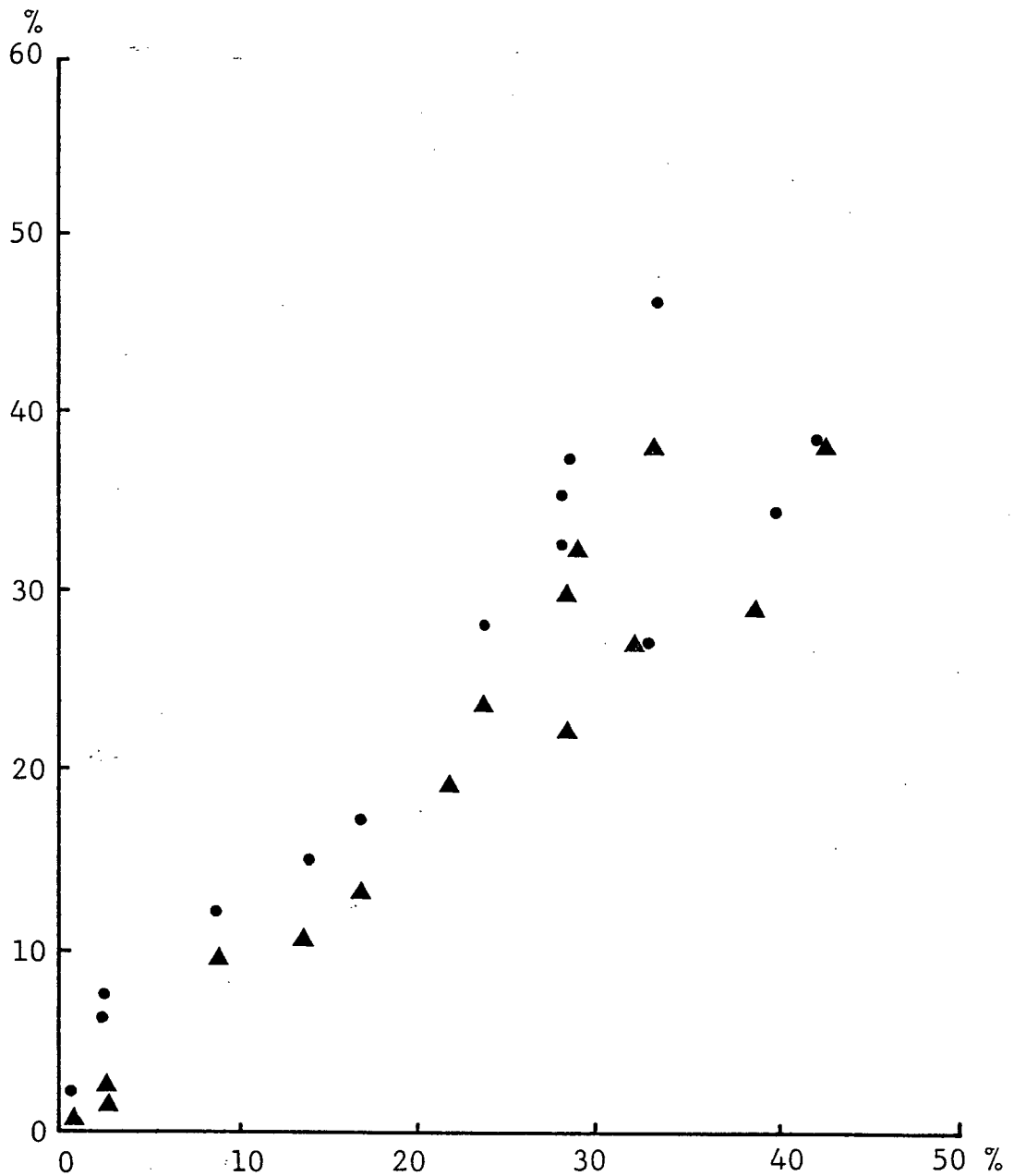
### 3-4 ORGANIC CARBON ANALYSIS

Soil and till samples were analysed for organic carbon by

a modified Schollenberger wet oxidation method (Royal School of Mines, Geochemical Prospecting Research Center, 1962). A potassium dichromate-sulphuric acid solution is used to oxidize the carbon in the sample at roughly  $100^{\circ}\text{C}$ . The potassium dichromate which is not used during the reaction is measured by titrating the solution with ferrous ammonium sulphate using diphenylalanine as an indicator. Additional details of the method are outlined in Appendix B.

Several previous studies have established that between 60 and 80% of the total carbon present will be oxidized to  $\text{CO}_2$  by the dichromate. Results obtained by wet oxidation methods are therefore generally adjusted by a correction factor to compensate for the partial carbon recovery. The correction factor used to calculate organic carbon values given in the present study was determined by analysing a group of samples by the Leco combustion technique. A correction factor of 1.3 was obtained by comparing results of organic carbon analyses by wet oxidation and Leco combustion methods. This factor can be compared to that of 1.12 for the Walkley-Black method and to 1.33 for the Schollenberger method. Analytical precision for the two methods at the 95% confidence levels is 18.2% for the wet oxidation technique and 8.8% for the Leco combustion method.

Loss of weight after sample ignition at  $550^{\circ}\text{C}$  was also determined in the same samples analysed by wet oxidation and Leco techniques. A scatter diagram (Fig. 3-4) indicates a strong linear variation between wet oxidation and Leco combustion analyses and between wet oxidation and loss on ignition analyses of identical samples. Loss on ignition in samples with



- ▲ %Organic carbon by wet oxidation against % carbon by Leco
- %Organic carbon by wet oxidation against %  $\frac{\text{Loss on ignit.}}{1.724}$

Figure 3-4: Comparison of organic carbon analyses of 15 samples by wet oxidation, Leco method and loss on ignition at 550°C.

less than 10% carbon, however, shows a departure from the linear trend suggesting that clay minerals could also contribute to the weight loss, during ignition, by releasing water. A comparison of wet oxidation and loss on ignition results indicates that they differ by a mean ratio of 1.8 which is similar to the Van Bemmelen factor of 1.724 used to convert organic carbon values to organic matter contents.

### 3-5 SULPHUR ANALYSIS

A number of organic soil and till samples were analysed for sulphur content by a hydriodic acid reduction technique (Tabatabai and Bremner 1970) followed by bismuth colorimetry (Kowalenko and Lowe 1972), described in Appendix B. This method measures organic sulphate and mineral sulphate fractions in soils. These forms are reduced to hydrogen sulphide at 110°C with a mixture of hydriodic and hypophosphorous acids. The hydrogen sulphide which is generated is carried in a nitrogen stream into a solution of bismuth nitrate where bismuth sulphide is precipitated and the concentration of suspended bismuth sulphide is measured in a spectrophotometer at a wavelength of 400 nm. Analytical precision for this method at the 95% confidence limit was 58.56%.

Total sulphur analyses were also attempted using X-ray fluorescence, but were largely unsuccessful owing to problems of sample preparation. Pressed discs of the organic soil material mixed with bakelite resin tended to fracture when these were removed from the hydraulic press used to prepare the discs. Analyses were attempted with the organic material held between two mylar films in the samples holder of the instrument. This

approach may introduce unknown variations when results are compared with those obtained from standards prepared from crushed rocks. Semiquantitative sulphur abundances in organic rich samples range from 0.5 to 2.1%.

### 3-6 PREPARATION OF POLISHED SECTIONS FROM HEAVY MINERAL SEPARATES AND ORGANIC SOIL FRAGMENTS

A heavy mineral fraction was separated from 100 minus 80-mesh sized soil and till samples using bromoform (S.G. 2-9). Mineral grains were easily separated from organic soils by this method. Till samples, however, commonly contained appreciable rock flour which separated with the minerals. Heavy mineral separates were initially examined under a binocular microscope. Small portions from fifty of the mineral separates samples were mounted on microscope slides in epoxy-resin at about 110°C. Organic fragments from several of the frozen bulk organic soil samples were thawed, air dried and also mounted in epoxy-resin. Freeze drying of the material was also attempted to minimize damage to remnant plant structures when fragments were mounted. This approach was unsuccessful because the very friable freeze dried material tended to disperse on contact with the epoxy-resin. Mineral grain and organic soil fragment mounts were polished and then examined under a reflecting microscope.

### 3-7 SCANNING ELECTRON MICROPROBE ANALYSES AND ELECTRON MICROSCOPE STUDIES

Several of the polished mounts containing mineral grains and organic soil fragments were analysed for copper, iron and sulphur with an Applied Research Ltd., Scanning Electron Microprobe Quantometer. This instrument is capable of spectro-

chemical analyses for elements in areas as small as 0.05  $\mu\text{m}$  by directing a finely focused electron beam onto the surface of polished, carbon coated mounts containing the mineral grains and organic fragments. Due to the interaction of the high-energy electrons with atoms of the elements present characteristic X-ray spectra of these elements originate. Relative intensities of X-rays at  $\text{CuK}\alpha$ ,  $\text{FeK}\alpha$  and  $\text{SK}\alpha$  wave lengths produced from the mineral grains and organic fragments were measured by X-ray spectrometers calibrated with pure iron, pure copper and sphalerite standards.

Relative intensities of X-ray radiation at  $\text{CuK}\alpha$ ,  $\text{FeK}\alpha$  and  $\text{SK}\alpha$  wave lengths was observed by directing the radiation onto a fluorescent cathode screen where the intensities appeared as contrasting light and dark areas. These were recorded by exposing polaroid film (A.S.A. 3000) to the X-rays for periods ranging from 30 to 100 seconds corresponding to the time required for the electron beam to scan a small area of the polished mount. A scanning time of 100 seconds and a camera f stop of 5.6 were used to analyse the organic fragments. Sulphide mineral grains, however, were generally scanned at 30 seconds. Several of the mineral grains were also photographed at different magnifications with an ETEC autoscan scanning electron microscope.

### 3-8 ANALYTICAL PRECISION

Each batch of 24 soil, till or vegetation samples, analysed by atomic absorption spectrophotometry, included a U.B.C. standard rock sample, one duplicate sample and a blank. Precision at the 95% confidence level was calculated from results of the

<u>Element</u>	<u>Analytical Method</u>	<u>Number of paired samples</u>	<u>Precision <math>\bar{\pm}</math>% (95% confidence)</u>
Ca <sup>a</sup>	Direct A.A.	3	27.5
C <sup>b</sup>	Wet oxidation	12	18.2
C <sup>a</sup>	IR-Total carbon	5	31.6
Cu <sup>b</sup>	HNO <sub>3</sub> -HClO <sub>4</sub> - A.A.	12	14.1
Cu <sup>a</sup>	Direct A.A.	5	11.3
Co <sup>b</sup>	HNO <sub>3</sub> -HClO <sub>4</sub> - A.A.	12	3.6
Fe <sup>b</sup>	"	12	5.8
Fe <sup>a</sup>	Direct A.A.	5	*
Mn <sup>b</sup>	HNO <sub>3</sub> -HClO <sub>4</sub> - A.A.	12	5.8
Mn <sup>a</sup>	Direct A.A.	5	*
Mo <sup>b</sup>	HNO <sub>3</sub> -HClO <sub>4</sub> - A.A.	15	26.0
Ni <sup>b</sup>	"	12	6.6
Zn <sup>b</sup>	"	12	4.3
Zn <sup>a</sup>	Direct A.A.	5	*
S <sup>b</sup>	HI Red.-Bi Col.	5	58.6

a - Water samples.

b - Soil, till and vegetation samples.

\* - Not determined due to insufficient data.

Table 3-2: Analytical precision

paired duplicate samples in each batch by a procedure outlined by Garrett(1969;1973) on the UBC IBM 370/168 computer. The same approach was used to estimate precision of analytical techniques for elements in water, organic carbon and HI reducible sulphur in soils although in several cases only a small number of duplicate samples were analysed. Analytical precision for each element and method is given in Table 3-2.

## CHAPTER 4

## GEOCHEMICAL RESULTS

## 4-1 TRACE AND MINOR ELEMENT ABUNDANCES AND pH IN SOILS AND TILL

Information collected from vertical and horizontal profiles has been used to construct fence diagrams illustrating three dimensional relationships between different soils, the till and element abundances in the bog. The metal, organic carbon and pH value ranges plotted in symbol form on these diagrams have been selected arbitrarily from the shape of frequency histograms.

Contrasting vertical variations of organic carbon content are found in different parts of the bog. Abundances increase from less than 31% in the fibric (Of) layer to more than 40% in the mesic-humic (Om-Oh) layers down several profiles between stations LON to L2N (Fig. 4-1). Variations on a typical organic soil profile are shown in Fig. 4-2 and Fig. 4-3. Organic carbon sharply decreases down profiles between stations L2N to G4 from more than 40% in the fibric layer to less than 15% in material at 2 to 3 m depth. Between stations L5S to L4S organic carbon varies slightly down profiles and values range from 16 to 32%. Values generally decrease sharply at the base of the bog and the underlying till has less than 5% organic carbon. Abundances ranging from 5 to 8% in the till at station L3N may be due to sample contamination during augering.

Copper is most abundant in the mesic-humic organic soil layers between stations B2W to L4S and LON to G2 (Fig. 4-4). Soil in these areas has more than 30% organic carbon (roughly equivalent to 60% organic matter) and contains up to 2.5% copper. The lateral variations of copper in the study area

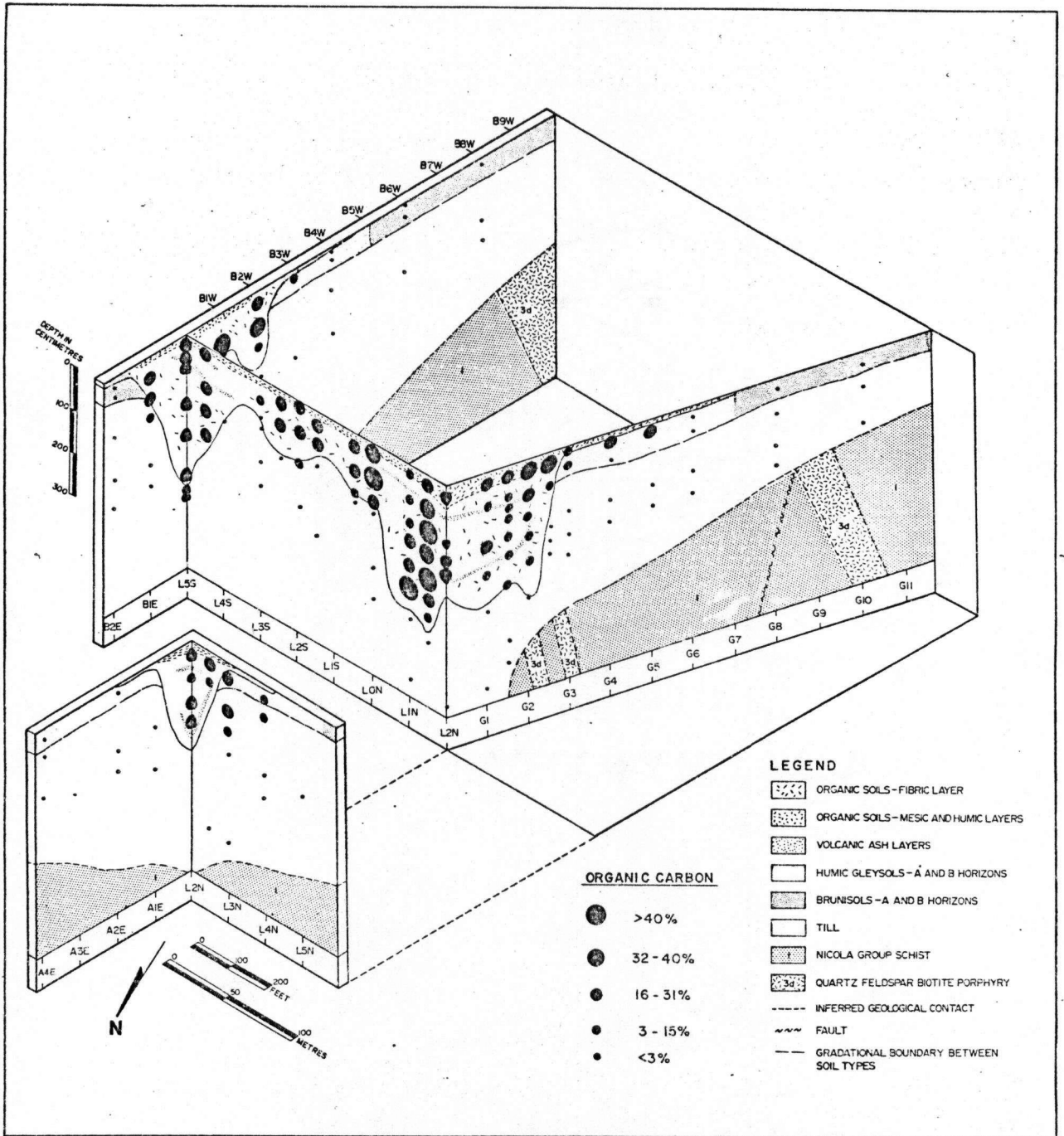


Figure 4-1: Organic carbon in soils and till.

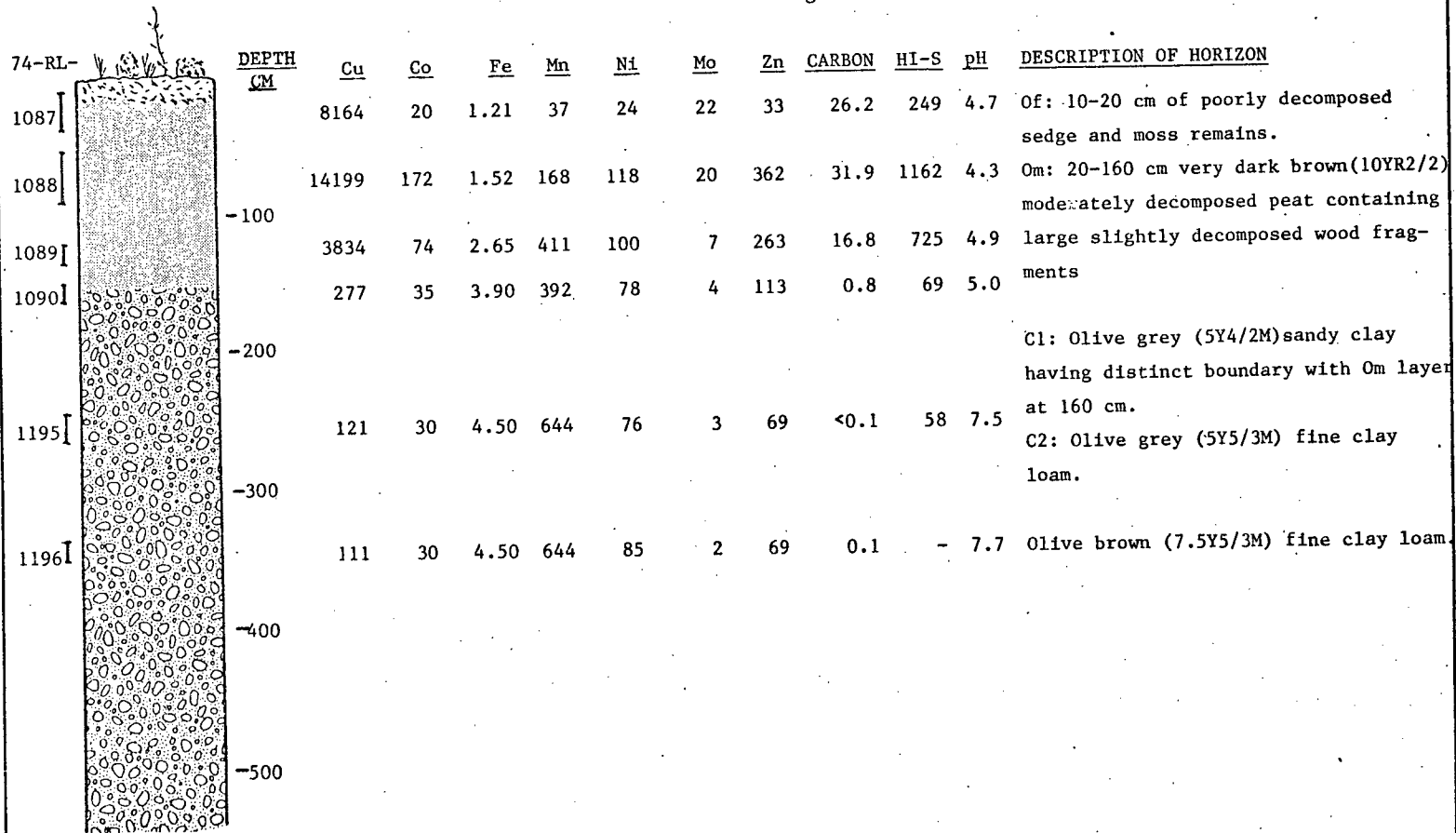
PROFILE 2. LOCATION: Station L1N. ENVIRONMENT AND SOIL TYPE: Fibric mesisol supporting humicky sphagnum moss, sedges, scattered lodgepole pine and hemlock.

74-RL-	DEPTH CM	Cu	Co	Fe	Mn	Ni	Mo	Zn	CARBON	HI-S	pH	DESCRIPTION OF HORIZON
1091		2174	10	4.06	56	19	<2	28	13.7	118	5.3	Of: 0-50 cm of slightly decomposed sedge and moss fibers. Volcanic ash layer at 40 cm.
1092	-100	8508	271	0.13	149	73	16	283	16.0	449	4.3	Om1: 50-140 cm very dark brown (10YR3/2W) moderately decomposed silty granular peat.
1093		17038	153	0.72	243	98	<2	321	26.1	1360	4.3	140-145 cm. Light brown volcanic ash.
1094	-200	23073	164	0.44	271	125	7	577	32.0	906	4.1	Om2-Oh: 145-320 cm. Very dark grey brown moderately to highly decomposed peat containing large wood fragments and pine needles. Material has a strong odour of hydrogen sulphide when freshly sampled.
1095		17748	122	0.43	532	139	20	535	39.4	1418	4.5	
1096	-300	13755	287	0.95	635	162	74	651	42.6	906	4.5	
1097	-400	692	49	3.64	381	75	2	100	1.3	104	4.4	C1: 320-400 cm. Olive grey (5Y3/2M) sandy clay containing 10-20% pebble sized clasts.
1194	-500	161	28	4.30	604	71	3	70	0.18	-	7.5	C2: 400- 500 cm. Olive grey(5Y5/2M) fine silty clay.

Cu, Co, Mn, Ni, Zn, Mo and HI reducible sulphur (HI-S) are in ppm, Organic carbon and Fe are in percent.

Figure 4-2: Variation of metals, organic carbon and sulphur on a fibric mesisol profile.

PROFILE 3. LOCATION - Station LON. ENVIRONMENT AND SOIL TYPE - Humic mesisol supporting mixed sedge and sphagnum moss growth. Water table within 10 cm of surface



Cu, Co, Mn, Ni, Mo, Zn and HI reducible sulphur (HI-S) are in ppm, Organic carbon and Fe are in percent.

Figure 4-3: Variation of metals, organic carbon and sulphur on a humic mesisol profile.

reflect transitions between different soil types. Copper increases from less than 210 ppm in brunisols to more than 1300 ppm in the Ah horizon of humic gleysols across the boundary between these two soils at station G7. Copper generally increases down organic soil profiles, as shown in detail in Fig. 4-2, and then decreases sharply across the organic soil-till interface from 1.38% in the humic-mesic soil layers to less than 700 ppm in the till. This decrease is also shown on Profile #3 (Fig. 4-3) located at station LON where organic material at 1.3 m depth contains 3834 ppm copper compared to 277 ppm in the underlying till at 1.5 m depth.

The till from profiles between stations G1.5 to G3 (Fig. 4-4) contains from 730 ppm to 0.5% copper compared to values ranging from 0.5% to 1.6% in the overlying organic soil. Copper values greater than 1300 ppm are also found in the till at station A4E, where overburden thickness may be less than 3 m, and at station B3W. The variation of copper through a brunisolic soil and the till is shown on Profile 1 (Fig. 4-5). Copper exceeds 310 ppm in the Bm soil horizon and the upper till (IC) layer. Values fall from 466 ppm in this layer to less than 294 ppm in the underlying IIC till layer and this decrease occurs at the sharp contact between the two layers. Copper content of the deeper IIC and IIIC till layers is less than 305 ppm.

Cobalt in the humic-mesic organic soil layers ranges from 125 ppm to more than 580 ppm and values generally increase down profiles, but fall sharply to less than 50 ppm in the underlying till. (Figs. 4-2, 4-3 and 4-6). The fibrous organic soil layer

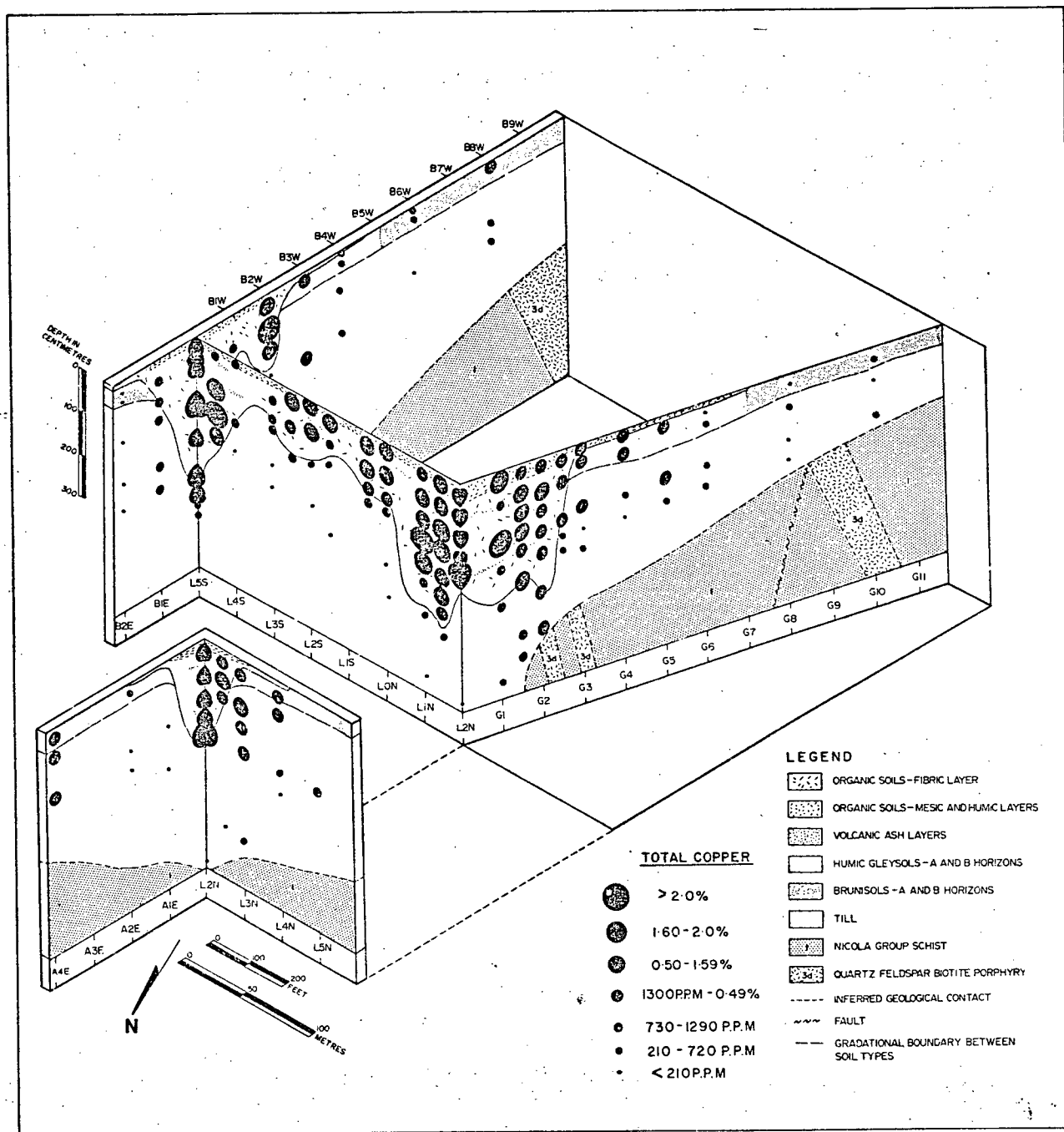


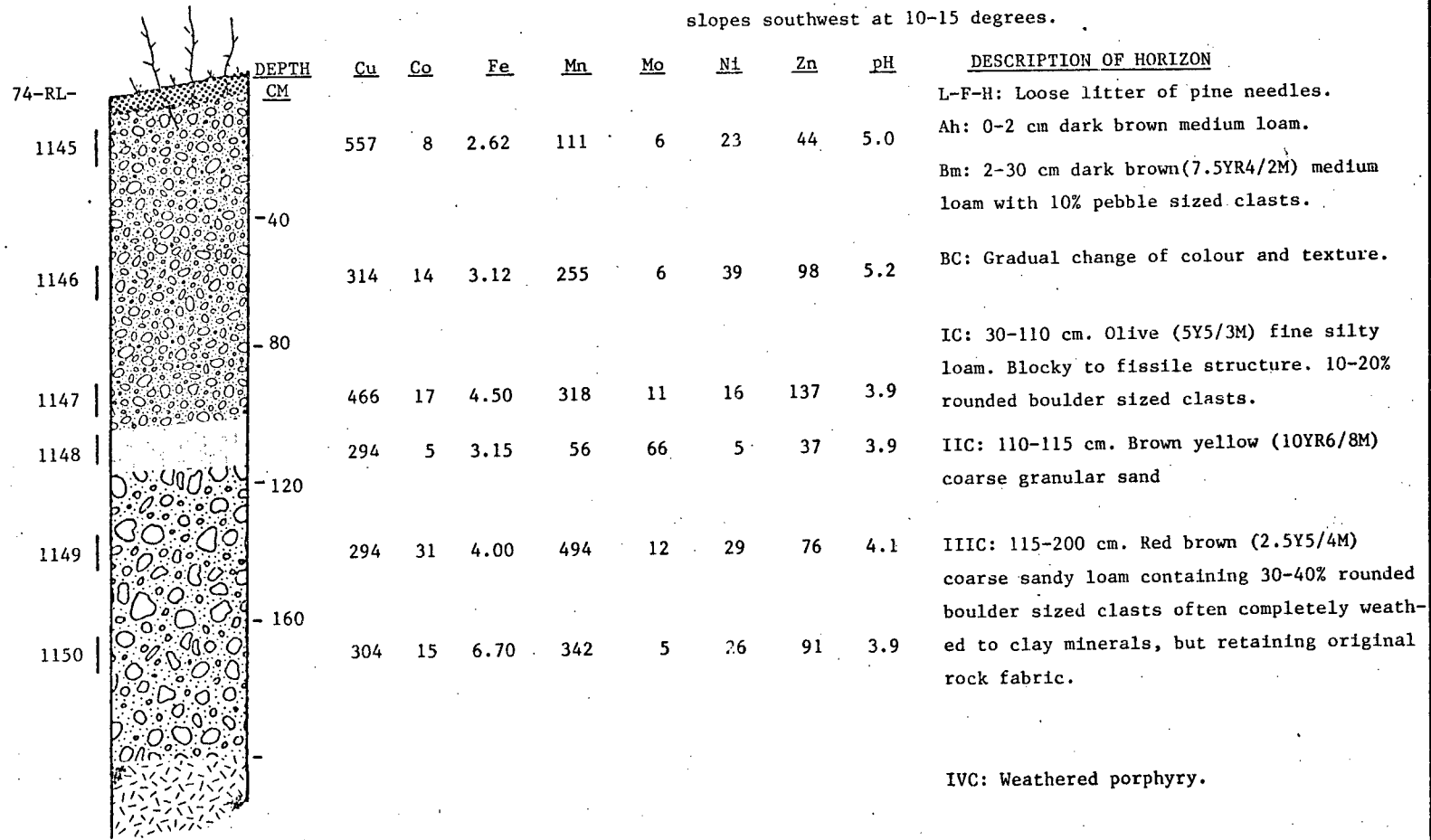
Figure 4-4: Copper in soils and till.

and the Ah horizon of the humic gleysol normally has less than 25 ppm cobalt although values exceeding 580 ppm are found, locally, in fibrous material between stations L2S and L5S (Fig. 4-6). The fibrous layer in this part of the bog also contains more than 1280 ppm manganese and more than 5% iron. Organic material from the fibrous layer and humic gleysols in the western part of the bog, however, has less than 100 ppm manganese. Iron and manganese levels increase at the boundary between the humic gleysolic and brunisolic soils.

The humic-mesic organic soil layers commonly have less than 440 ppm manganese and less than 3% iron (Figs. 4-5, 4-7 and 4-8). Concentrations increase in the underlying till where manganese exceeds 650 ppm and iron is greater than 3%. Manganese and iron increase down profiles through the till and material from 3 m depth at station B2E typically contains more than 1050 ppm manganese. The deeper, oxidized till close to the weathered bedrock, shown in Profile 1, (Fig. 4-5) has more than 6.0% iron and till from 2.5 m depth at station G2.5 contains more than 4.2% iron.

Nickel in the mesic-humic soil layers ranges from 61 to more than 250 ppm and the highest values are found at 1-3 m depth between stations L5S to L4S (Fig. 4-9). Nickel increases down profiles through organic soil, but falls to less than 150 ppm in the underlying till. Humic-mesic soil layers between stations L1N to L2N have nickel ranging from 91 to 250 ppm. Nickel also increases slightly down profiles through brunisolic soil and till from less than 60 ppm in the mineral soil to more than 90 ppm in the till. The fibric organic

PROFILE 1. LOCATION: 300 m south of station L2N. ENVIRONMENT AND SOIL TYPE: Orthic dystric brunisol formed on till supporting growth of Hemlock and Engelmann spruce. Surface slopes southwest at 10-15 degrees.



Cu, Co, Mn, Mo, Ni and Zn are in ppm, Fe is in percent.

Figure 4-5: Variation of metals and pH on an orthic dystric brunisol profile.

soil layer throughout the bog has less than 40 ppm nickel and similar levels are found in the humic-mesic layers between stations G1.5 to G2.0. A sharp decrease of nickel occurs at the boundary between the brunisols and the humic gleysols.

The zinc content of the fibrous organic layer is less than 30 ppm and values increase down profiles to more than 1420 ppm in the humic-mesic layers at the eastern end of the bog (Fig. 4-10). Profiles through these layers between stations G1.5 to G2.0, however, have less than 30 ppm zinc. The till underlying the organic soil normally has less than 210 ppm although values greater than 500 occur on a profile at station A4E. Till layers IC, IIC, and IIIC, shown in Profile 1 (Fig. 4-5) have contrasting zinc contents. A sharp decrease from 137 to 37 ppm occurs across the boundary between the silty textured IC material and the sandy textured IIC layer. Zinc increase in the underlying IIIC layer and there are similar variations in manganese, iron, nickel and molybdenum abundances on this profile from 80 to 120 cm depth.

Molybdenum contents ranging from 26 to 100 ppm occur in several parts of the bog. The fibrous organic layer between stations L2N, L3N and G2 has more than 25 ppm molybdenum although levels in the fibrous material from the eastern part of the bog are generally less than 6 ppm. Molybdenum values greater than 25 ppm are also found in the humic-mesic layers between stations L4S to L2N where the metal is most abundant on profiles close to the till-bog interface. The underlying till generally has less than 6 ppm molybdenum although values

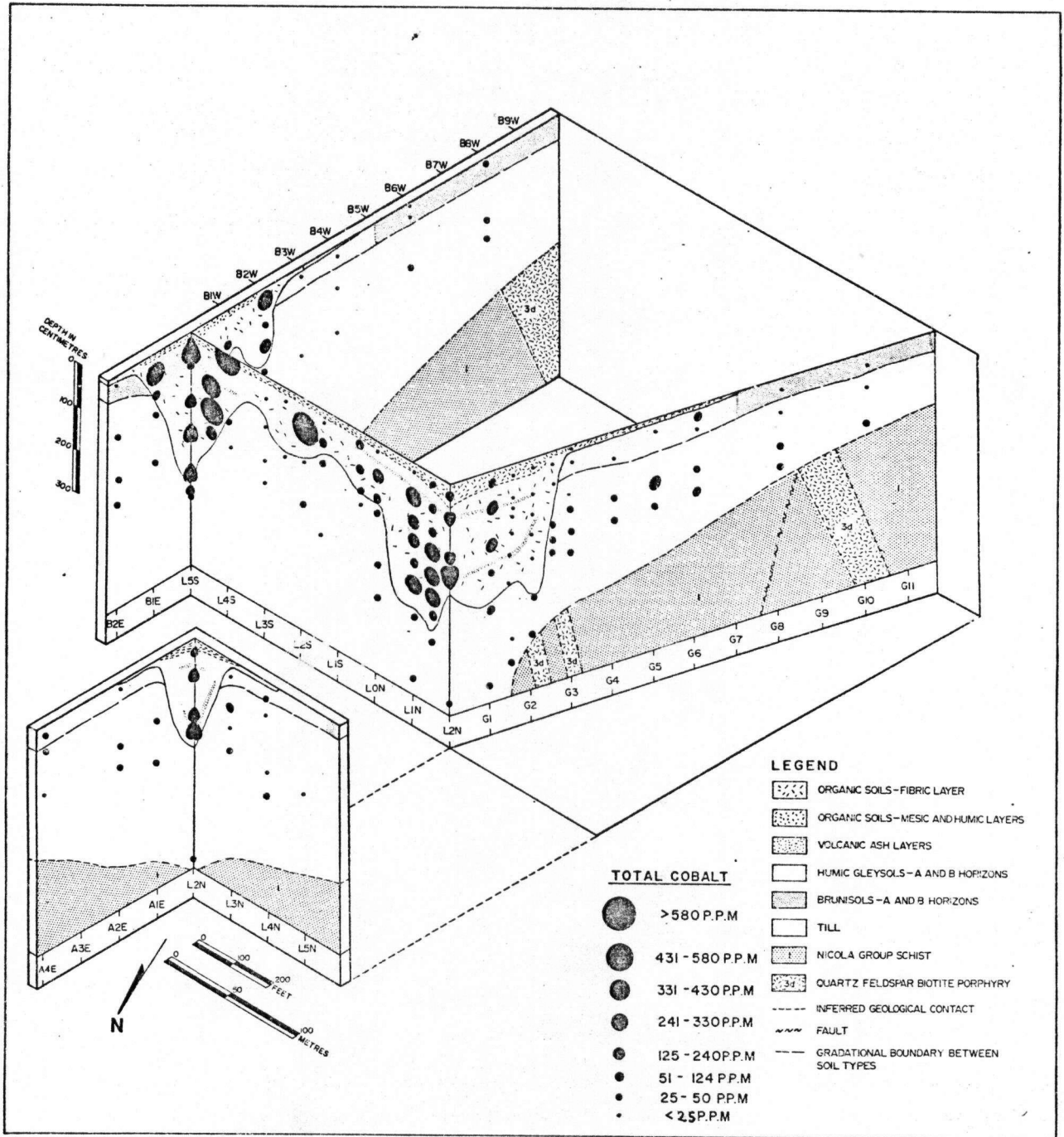


Figure 4-6: Cobalt in soils and till.

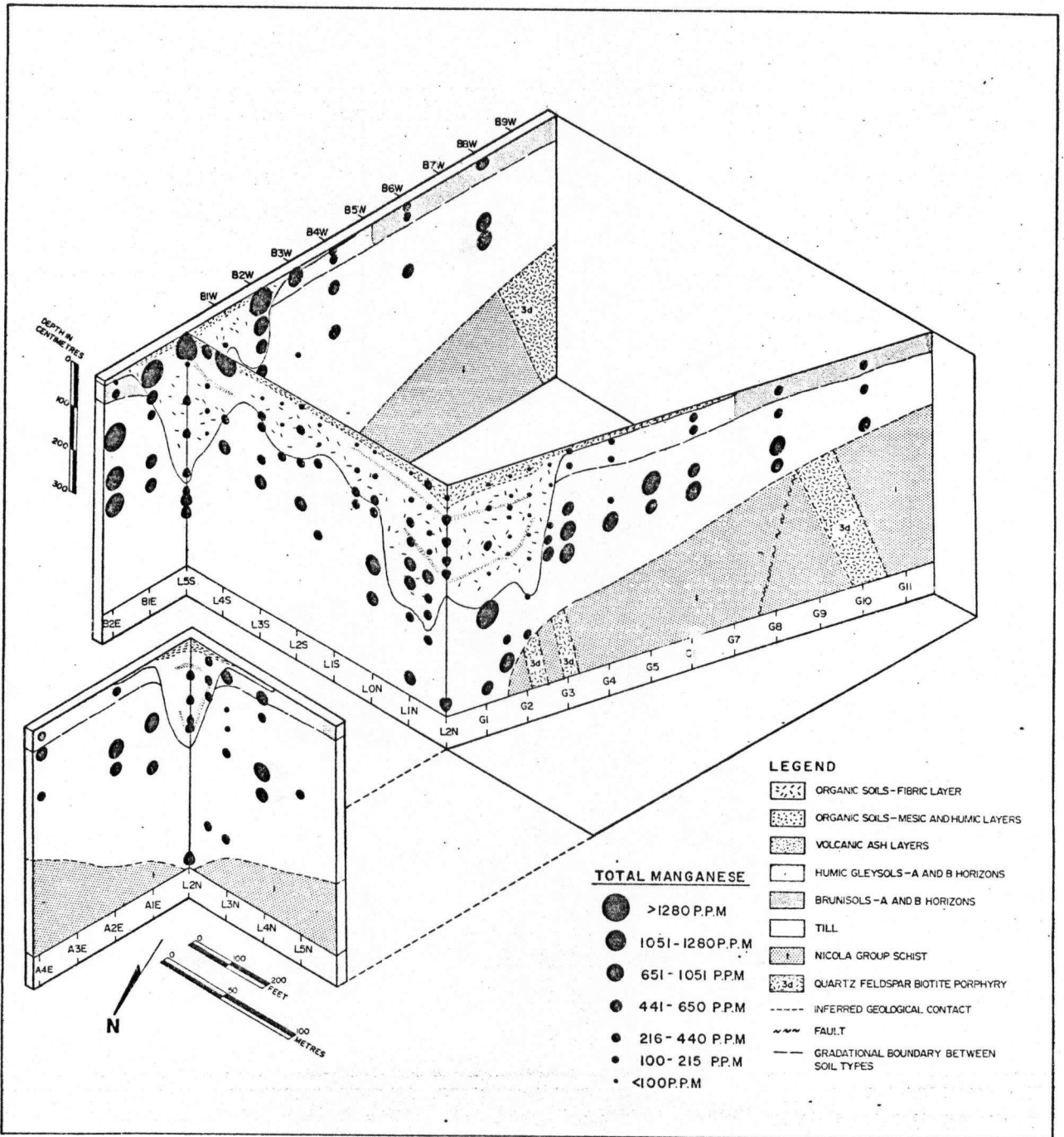


Figure 4-7: Manganese in soils and till.

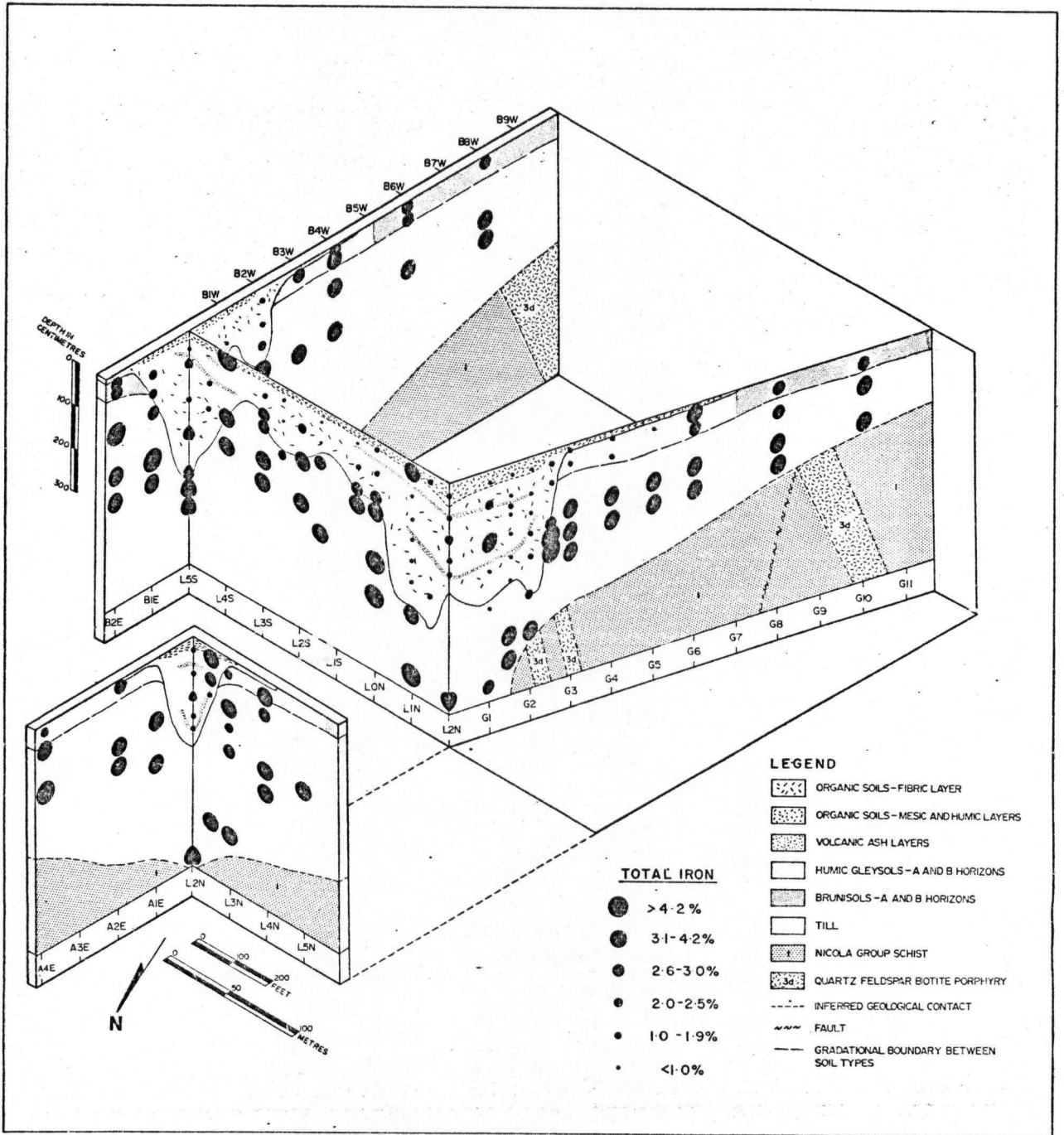


Figure 4-8: Iron in soils and till.

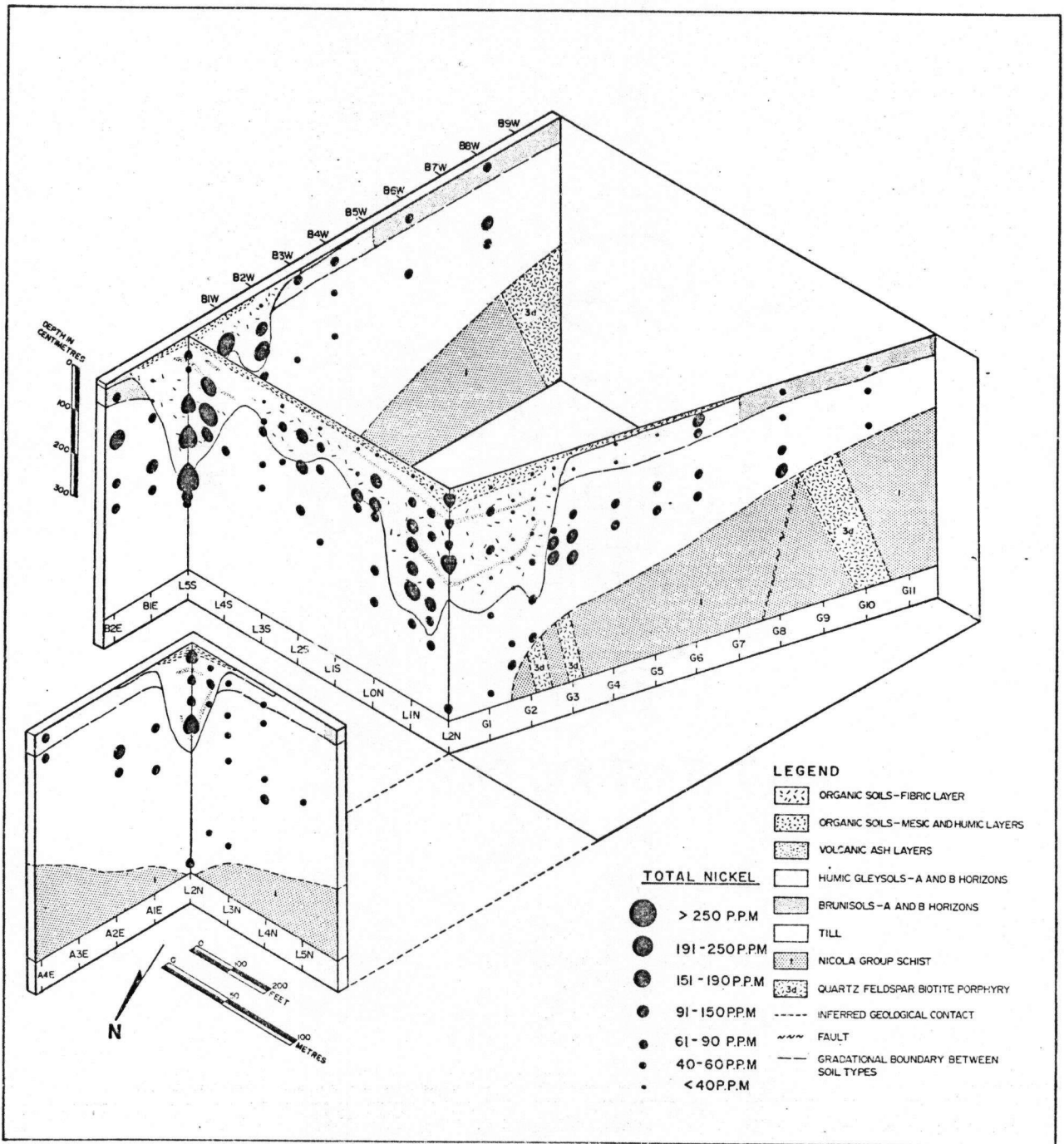


Figure 4-9: Nickel in soils and till.

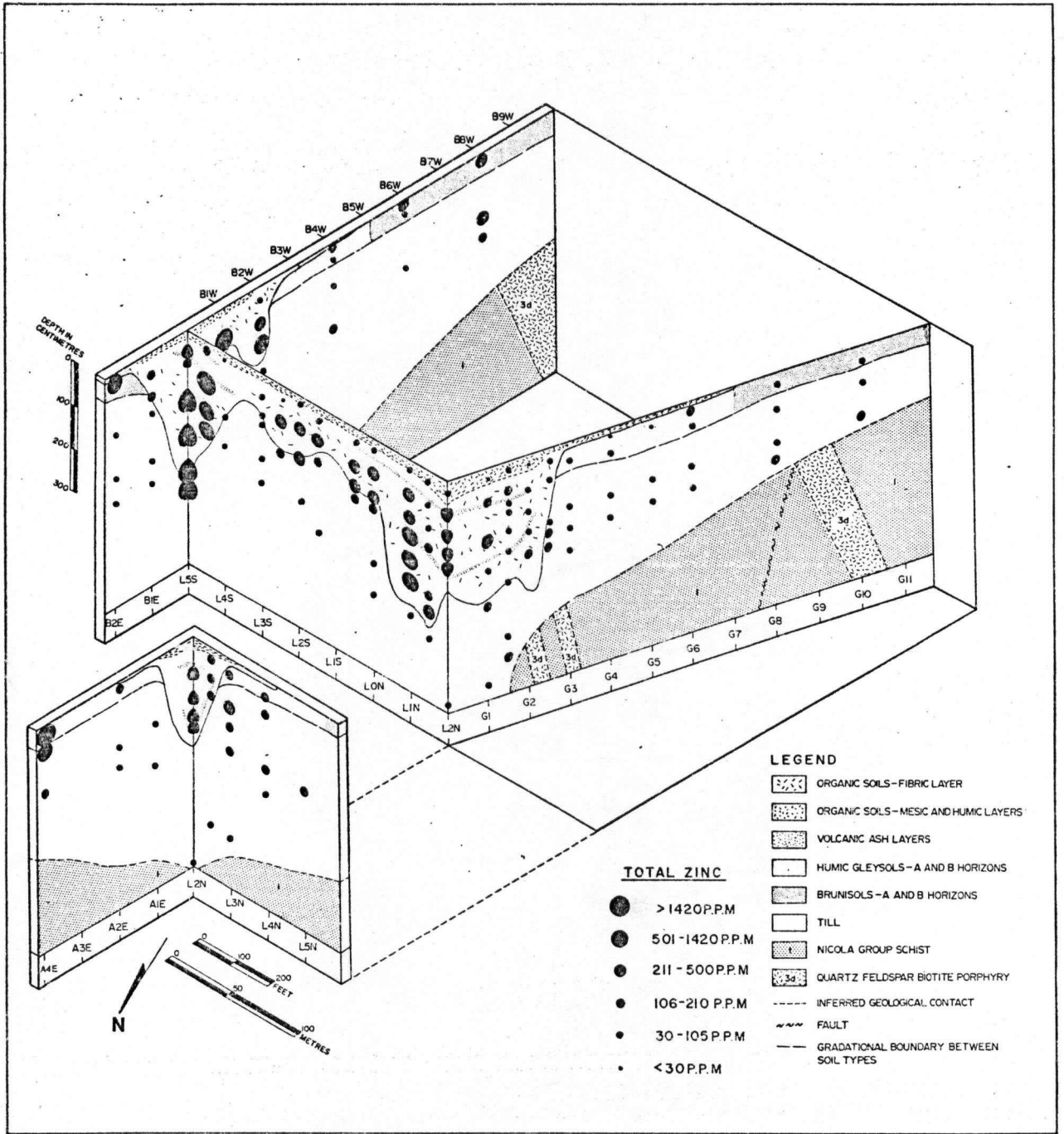


Figure 4-10: Zinc in soils and till.

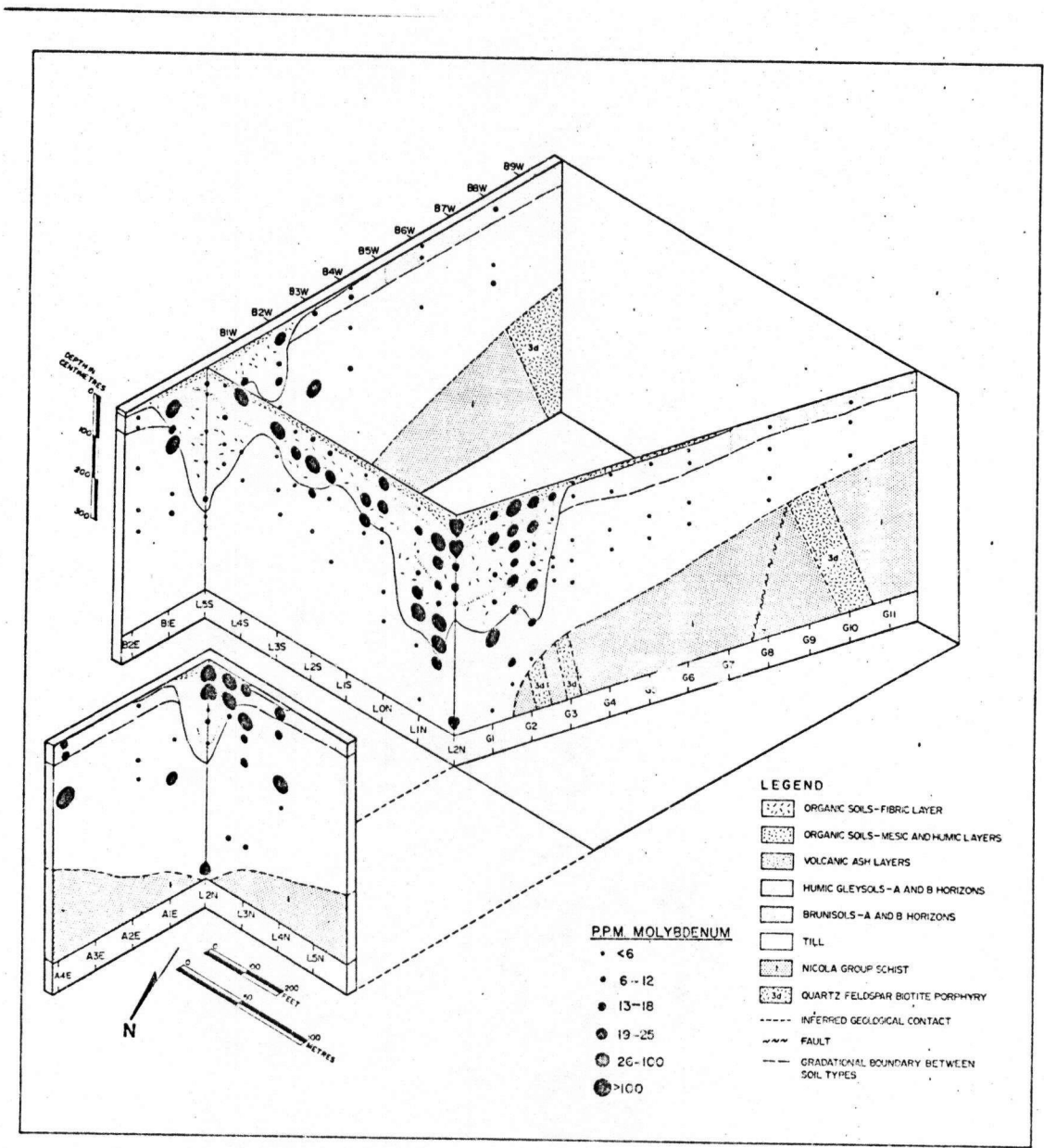


Figure 4-11: Molybdenum in soils and till.

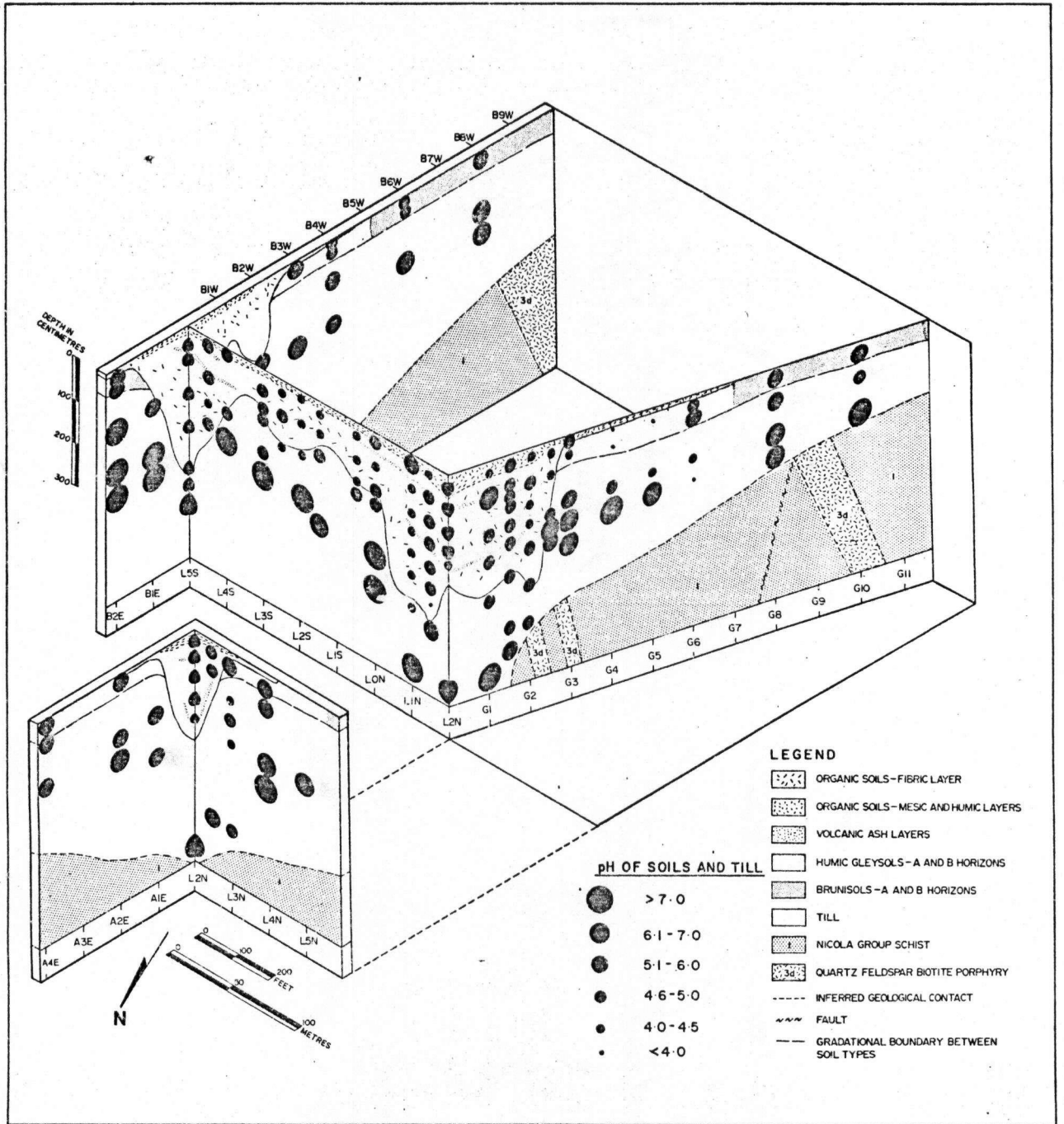


Figure 4-12: pH of soils and till.

ranging from 18 to 25 ppm occur on profiles at B3W, L4N, G1, L2N and A1E. Very high molybdenum with values exceeding 100 ppm occurs on a profile at station A4E at 2-3 m depth (Fig. 4-11).

Iron, manganese and pH show a concomitant increase down profiles through the till underlying organic soils. The pH of the grey-green till below the humic-mesic organic layers ranges from 5.0 to 6.0, while pH of deeper, moderately oxidized till is greater than 7.0 (Fig. 4-12). A small area of copper-rich till from 3 to 4 m depth on profiles at G1.5 and G2 has pH ranging from 5.0 to 6.0. The pH of organic soil ranges from 4.0 to 5.0 and is relatively constant down soil profiles. The pH of brunisolic soils is greater than 5.0 and the pH of humic gleysols between stations G3.5 to G5.0 is less than 4.0.

#### 4-2 STATISTICAL TREATMENT OF THE DATA

Ranges and means of elemental distributions in different soil types, soil horizons and parent materials can be determined by separating the distributions based on the physical characteristics of the samples. However, boundaries between the soil types and horizons in the bog are often indistinct or transitional and a clear separation of the sample groups, necessary for calculating statistics, is impossible. Histograms and probability graphs have also been used to establish statistical parameters of elemental distributions.

Histograms representing density distributions are commonly used to organize geochemical data so that their

characteristics can be summarized. Symmetrical, bell-shaped density distributions reflect populations consisting of normally distributed values about a population mean. Trace and minor geochemical abundances, however, are commonly logarithmically distributed and log-transformed values follow a symmetrical, bell-shaped distribution curve. Histograms are often positively or negatively skewed and several separate peaks can occur along the 'tail' of a positively skewed distribution. The peaks represent statistical populations which have been combined into the total distribution. Each population may reflect a different range of values associated with contrasting soil types, overburdens, rocks or horizons.

Interpretation of geochemical data using cumulative frequency histograms, also known as probability graphs, has been described by Lepeltier (1969), Parslow (1974) and Sinclair (1976). The graphs are generally prepared by plotting element abundances on the ordinates of logarithmic or arithmetic probability paper against cumulative frequency of the abundance on the abscissa. A straight line graph on logarithmic probability paper will represent a single, lognormal distribution. The graphs commonly have a sinuous shape indicating that distributions are polymodal, that is several populations are present.

Individual populations can be partitioned from the graph by estimating the proportion of each in the total distribution from inflection points along the smoothed cumulative frequency curve. Based on these proportions cumulative frequencies

<u>Element</u>	<u>Population</u>	<u>Proportion(%)</u>	<u>X+2S</u>	<u>X+1S</u>	<u>X</u>	<u>X-1S</u>	<u>X-2S</u>	<u>Log S</u>
Organic carbon(%)	A	100.0	48.0	34.8	21.3	12.3	7.2	0.237
Co(ppm)	A	55.0	640	334	161	78	41	0.315
Co(ppm)	B	45.0	107	43	21	9	4	0.368
Cu(%)	A	32.0	3.30	2.35	1.75	1.30	0.93	0.128
Cu(%)	B	54.0	1.10	0.80	0.58	0.44	0.35	0.119
Cu(%)	C	14.0	0.70	0.35	0.18	0.092	0.056	0.289
Fe(%)	A	25.0	4.935	3.837	2.831	2.094	1.625	0.132
Fe(%)	B	75.0	2.979	1.625	0.850	0.437	0.216	0.263
Mn(ppm)	A	5.6	3700	3113	2683	1994	1718	0.129
Mn(ppm)	B	94.4	1186	486	172	66	20	0.452
Mo(ppm)	A	75.0	51	31	19	12	17	0.221
Mo(ppm)	B	25.0	12	7	4	2	1	0.247
Ni(ppm)	A	75.0	299	154	78	37	19	0.295
Ni(ppm)	B	25.0	37	28	21	16	12	0.124
pH	A	100.0	-	5.01	4.67	4.34	-	0.531
Zn(ppm)	A	12.0	3131	2321	1600	1098	701	0.162
Zn(ppm)	B	88.0	945	385	135	47	18	0.455

Table 4-1: Geometric mean (X), mean + 2 standard deviation, mean + 1 standard deviation and Log standard deviation (S) of populations representing 90 soil samples.

<u>Element</u>	<u>Population</u>	<u>Proportion(%)</u>	<u>X+2S</u>	<u>X+1S</u>	<u>X</u>	<u>X-1S</u>	<u>X-2S</u>	<u>Log S</u>
Organic	A	20.0	1.14	0.32	0.09	0.03	-	0.550
Carbon(%)	B	80.0	1.29	0.92	0.77	0.55	0.39	0.146
Co(ppm)	A	4.2	87	71	61	52	43	0.066
Co(ppm)	B	95.8	47	36	27	21	16	0.116
Cu(ppm)	A	6.0	4000	3250	2650	2180	1750	0.089
Cu(ppm)	B	10.0	1500	1400	1350	1250	1200	0.033
Cu(ppm)	C	84.0	720	350	180	92	45	0.289
Fe(%)	A	100.0	4.91	4.37	3.77	3.23	2.76	0.064
Mn(ppm)	A	2.2	1580	1450	1380	1320	1250	0.021
Mn(ppm)	B	92.8	1270	710	550	430	305	0.111
Mn(ppm)	C	5.0	600	370	280	220	165	0.121
Mo(ppm)	A	5.0	66	49	38	29	22	0.120
Mo(ppm)	B	6.2	22	19	17	15	13	0.054
Mo(ppm)	C	88.8	9	5	3	1	-	0.222
Ni(ppm)	A	100.0	123	93	71	51	39	0.125
pH	A	40.0	7.8	7.5	7.3	7.0	6.7	0.018
pH	B	60.0	6.7	6.1	5.6	4.8	4.1	0.067
Zn(ppm)	A	15.0	330	260	195	150	110	0.125
Zn(ppm)	B	85.0	118	95	71	51	39	0.097

Table 4-2: Geometric mean (X), mean +2standard deviation, mean + 1standard deviation and Log standard deviation (S) for 96 till samples.

are recalculated and replotted on the graph as linear graphs from which geometric mean and standard deviations for each population are extrapolated from the 50 and 84 percent probabilities.

Graphs were plotted for cobalt, copper, iron, manganese, nickel, molybdenum, zinc, organic carbon and pH in 96 till and 90 soil samples by a program written by Fox and Sinclair (1973) for the U.B.C. IBM 370/168 computer. These graphs are shown in Appendix C. Geometric means, log standard deviations and values for mean  $\pm$  1S and mean  $\pm$  2S for populations partitioned from the graphs are given in Tables 4-1 and 4-2. The convention followed to define populations in the description of the graphs will be: Geometric mean, Mean plus two standard deviation, Mean minus two standard deviation.

Cumulative frequency graphs for cobalt in the till (Appendix Fig. C-1) and cobalt in soils (Appendix Fig. C-2) have the form of bimodal, non-intersecting distributions. Overlap between till population A (61,87,43) and till population B (27,47,16) is less than 10% and values greater than 43 ppm probably represent cobalt in the till between stations G1 and G6 (Fig. 4-6). Although there is appreciable overlap of the two cobalt populations in soils values greater than 161 ppm, representing the upper 50% of population A, can be explained by cobalt in the mesic-humic organic soil layers. Population B is largely an expression of cobalt in the fibrous soil layer.

Three copper populations are present in the till (Appen-

dix Fig. C-3). The till population C (180,720,45), containing 84% of the values, reflects 'background' copper levels in the till. Populations A and B have little overlap with each other or with C. Ranges of values representing these populations reflect distribution patterns in the till below the western part of the bog. Soil population A (1.75%, 3.3%, 0.93%) has negligible overlap with distributions B and C. These populations could be explained by distribution patterns in the organic soil associated with different forms of copper.

Distribution of iron in the till could be explained by either normal or lognormal curves (Appendix Fig. C-5). Two non-intersecting iron distributions are present in soils (Appendix Fig. C-6). Soil population B, containing 75% of the values, is an expression of low iron abundances generally found in the organic soil layers. Population B (2.83,4.93, 1.63), however, is probably due to scattered high iron values in the organic soil and Ah horizon (Fig. 4-8). Three manganese distributions are present in the till (Appendix Fig. C-7) although the shape of the curve suggests that a fourth population could be present. Population A (1320,1580,1250) is an expression of manganese in the till between stations G1 and A2E. Populations reflect manganese in the reduced till layer and in the oxidized till layer. Soil population A (2683,3700,1718), represented by 4 values is an expression of the high manganese levels in the fibrous layer at the eastern end of the bog. Population B reflects manganese in the humic-mesic organic soil layers (Appendix Fig. C-8).

The probability graph for molybdenum in till follows a non-intersecting, trimodal distribution with inflection points at 5% and 11% cumulative frequency (Appendix Fig. C-9). Values exceeding 18 ppm representing populations A and B reflect mineralized material in the till. Two molybdenum populations are present in the soil (Appendix Fig. C-10) and population A (19,51,7) is an expression of high values in the organic soil layers at the western end of the bog. (Fig. 4-11). A single, lognormal nickel distribution is present in the till (Appendix Fig. C-11). Two non-intersecting lognormal populations are present in soils (Appendix Fig. C-12) and population A (78,299,19) is an expression of nickel distribution patterns in the humic-mesic layers. Values less than 37 ppm are largely due to population B which reflects nickel in the fibric organic layer and the Ah horizon of the humic gleysol soil.

Two zinc distributions are present in soils and in the till (Appendix Fig. C-13). Till population A (195,330,110), containing 15% of the values, is an expression of zinc in the deeper till on the south side of the bog shown in Fig. 4-10. The soil population A (1600,3131,701) reflects the high zinc levels in the humic-mesic soil layers at the eastern end of the bog. Population B (135,945,18) is probably due to zinc in organic soils and the Ah horizon of the humic gleysol throughout the central and western parts of the bog.

The till organic carbon population A (0.77,0.96,0.55) (Appendix Fig. C-15) can be explained by slightly higher

carbon levels in the till close to the organic soil-till interface. There is, however, considerable overlap between till populations A and B. Population B is largely due to very small organic carbon concentrations generally less than 0.1% in the deeper till. Organic carbon values in soils follow a single distribution (Appendix Fig. C-16) although the curve tends to exhibit a degree of flattening above 80% cumulative frequency. This could be due to truncation or the presence of a second population represented by organic carbon values less than 10%.

The pH values in the till follow a non-intersecting, bimodal distribution (Appendix Fig. C-17) and population A (7.3, 7.8, 6.7) is clearly due to the pH of the deeper, oxidized till layer. Values less than 6.7 represent population B which is an expression of the pH of the reduced till layer beneath the organic soil. The pH of soils follows a single distribution (Appendix Fig. C-18) although the curved shape of the probability graph could indicate that both normal and lognormal distributions are present.

#### 4-3 STATISTICAL CORRELATIONS BETWEEN METALS, ORGANIC CARBON AND pH IN SOILS

The spatial distribution patterns, described in section 4-1, show that several of the metals and organic carbon apparently have a common association. The mesic-humic organic soil layers with organic carbon contents ranging from 16 to 42% are typically enriched with copper, cobalt, zinc, nickel and molybdenum, but generally have low iron and manga-

<u>C</u>	<u>C</u>	<u>pH</u>	<u>Co</u>	<u>Cu</u>	<u>Fe</u>	<u>Mn</u>	<u>Ni</u>	<u>Zn</u>
<u>C</u>	1.00							
<u>pH</u>	-0.26	1.00						
<u>Co</u>	0.43	-0.13	1.00					
<u>Cu</u>	0.46	-0.09	0.51	1.00				
<u>Fe</u>	-0.08	0.23	0.21	-0.15	1.00			
<u>Mn</u>	0.27	0.01	0.60	0.09	0.37	1.00		
<u>Ni</u>	0.43	-0.11	0.49	0.38	0.18	0.15	1.00	
<u>Zn</u>	0.32	-0.05	0.54	0.51	0.13	0.17	0.86	1.00

Table 4-3: Correlation matrix for soil samples with organic carbon content greater than 5%; (n = 63; r =  $\bar{r}$  0.25 significant at 95% confidence level).

<u>C</u>	<u>C</u>	<u>pH</u>	<u>Co</u>	<u>Cu</u>	<u>Fe</u>	<u>Mn</u>	<u>Ni</u>	<u>Zn</u>
<u>C</u>	1.00							
<u>pH</u>	-0.08	1.00						
<u>Co</u>	0.05	-0.19	1.00					
<u>Cu</u>	0.30	-0.04	0.56	1.00				
<u>Fe</u>	-0.25	0.22	0.08	-0.03	1.00			
<u>Mn</u>	0.04	0.05	0.19	-0.10	0.26	1.00		
<u>Ni</u>	0.17	0.08	0.09	0.23	0.15	-0.28	1.00	
<u>Zn</u>	0.02	0.15	0.31	0.43	0.20	-0.15	0.77	1.00

Table 4-4: Correlation matrix for soil samples with organic carbon content greater than 16%; (n = 33; r =  $\bar{r}$  0.35 significant at 95% confidence level).

nese levels. Associations between high nickel and zinc values in the humic-mesic layers and between iron and manganese in the fibrous layer are especially evident at the eastern end of the bog. The statistical significance of these associations was determined by calculating correlation coefficients and plotting scatter diagrams using the program TRP written by Chin Le and Tenisci (1977) for the UBC IBM 370/168 computer.

Correlation coefficients measure the degree of linear relationship between two variables and represent a ratio of the covariance of the variables to the product of their standard deviation (Dixon and Massey 1969). The coefficients which do not depend on units used to measure the variables range from +1.0 (indicating a perfect sympathetic relationship) through zero (a total absence of any relationship) to -1.0 (indicating a perfect inverse relationship). Large positive or negative coefficients can also result from the presence of a few spuriously high or low values in the data and scatter diagrams are therefore commonly plotted to visually examine the correlation between the variables (Chapman 1976).

Geochemical data for 63 soil samples with organic carbon ranging from 5% to 42% was used in a preliminary analysis. This data includes values from several combined populations as described in section 4-2. Metal values were log transformed before correlation coefficients were calculated since Chi squared testing of the data indicated that most distribu-

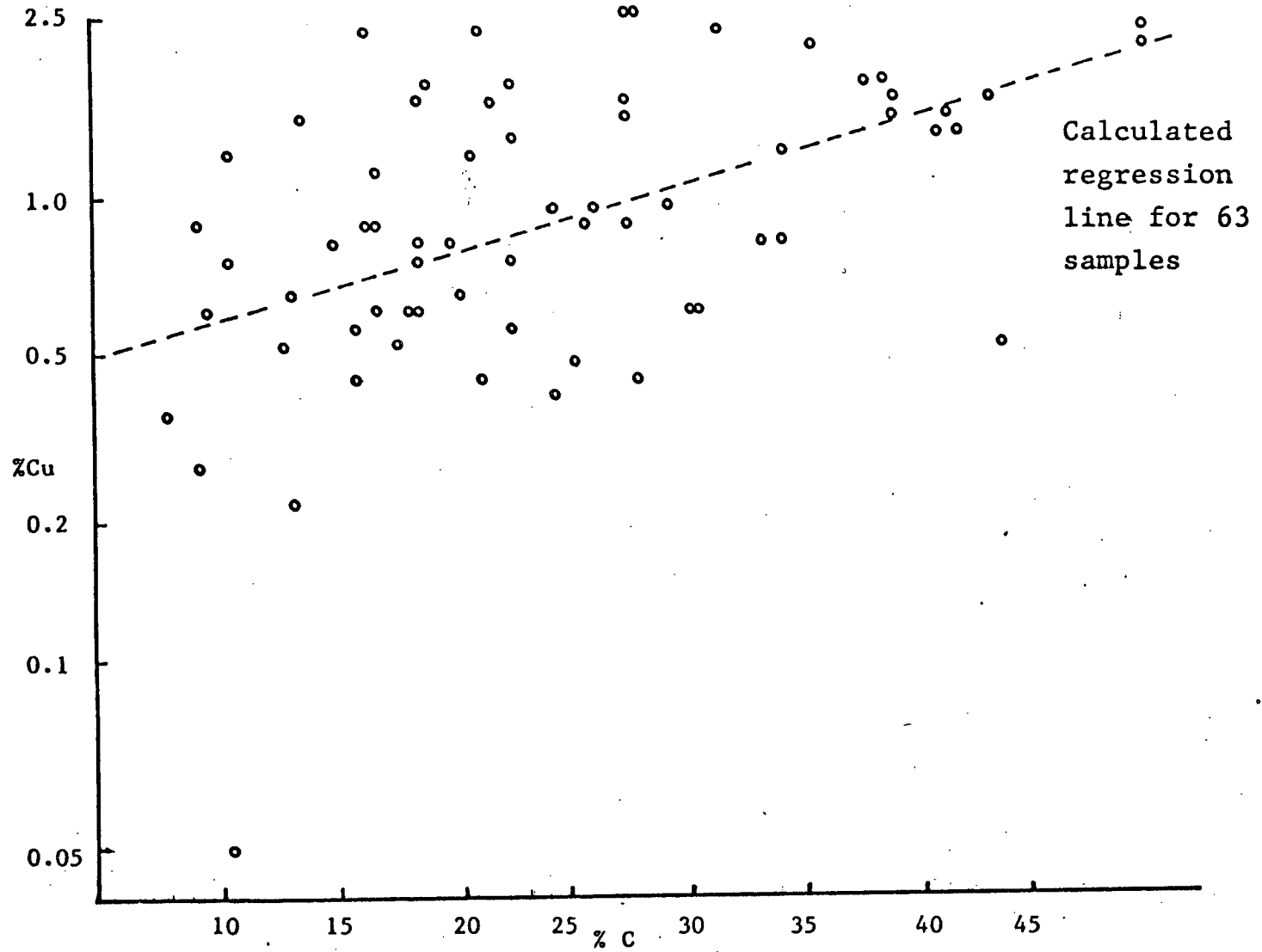


Figure 4-13. Scatter diagram for  $\text{Log}_{10}$  Cu against Organic Carbon.

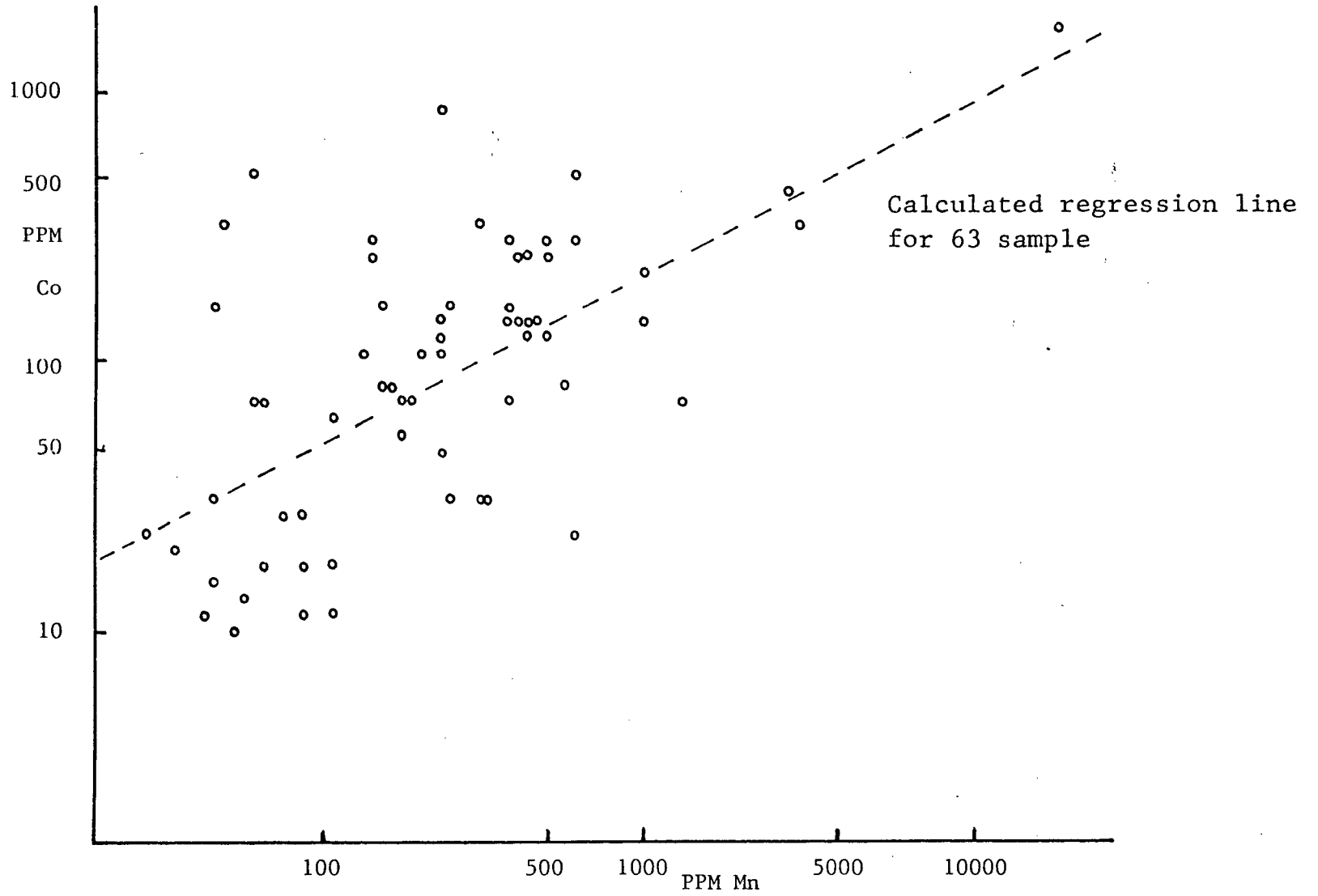


Figure 4-14. Scatter diagram for  $\text{Log}_{10}\text{Co}$  against  $\text{Log}_{10}\text{Mn}$ .

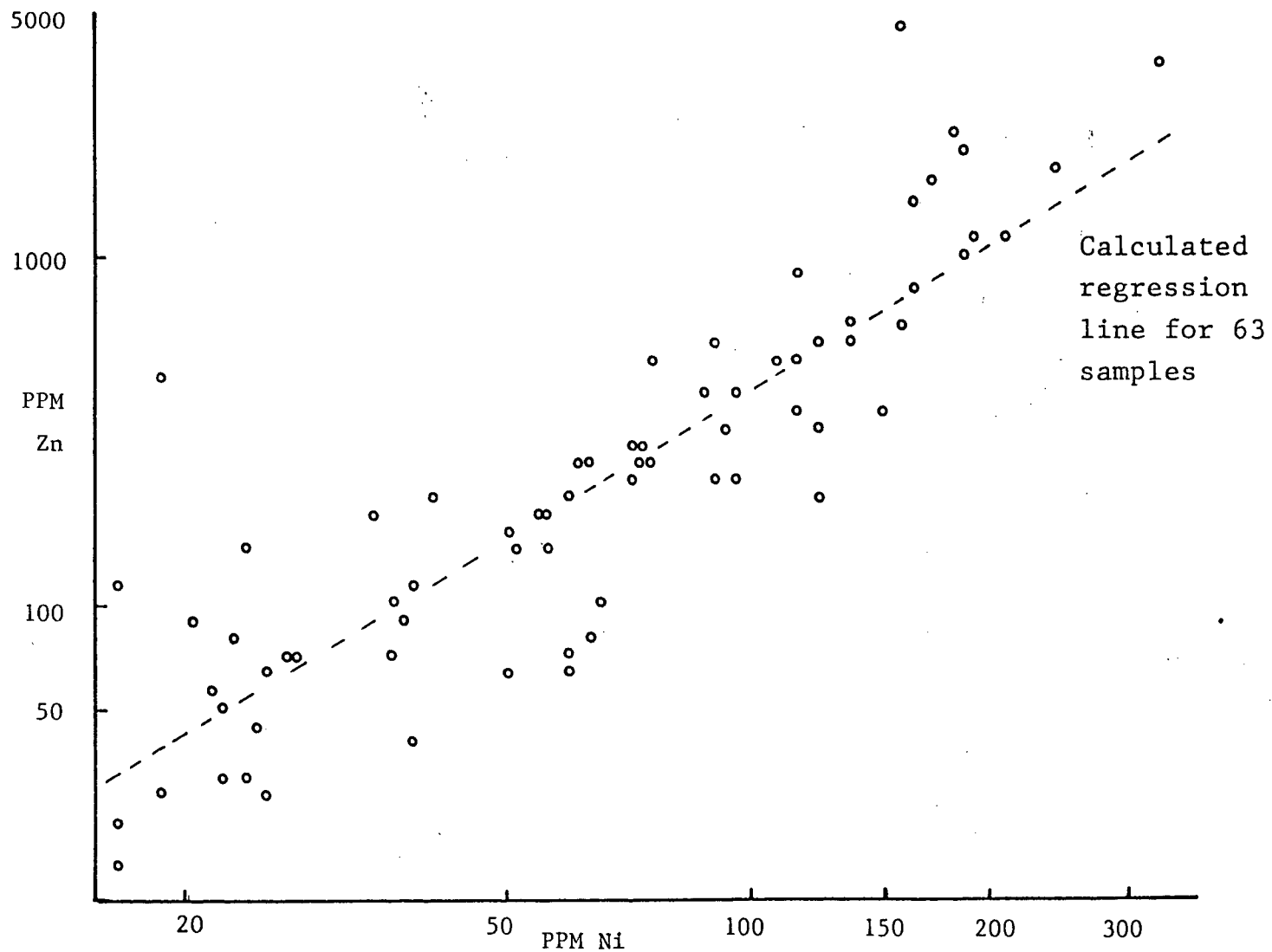
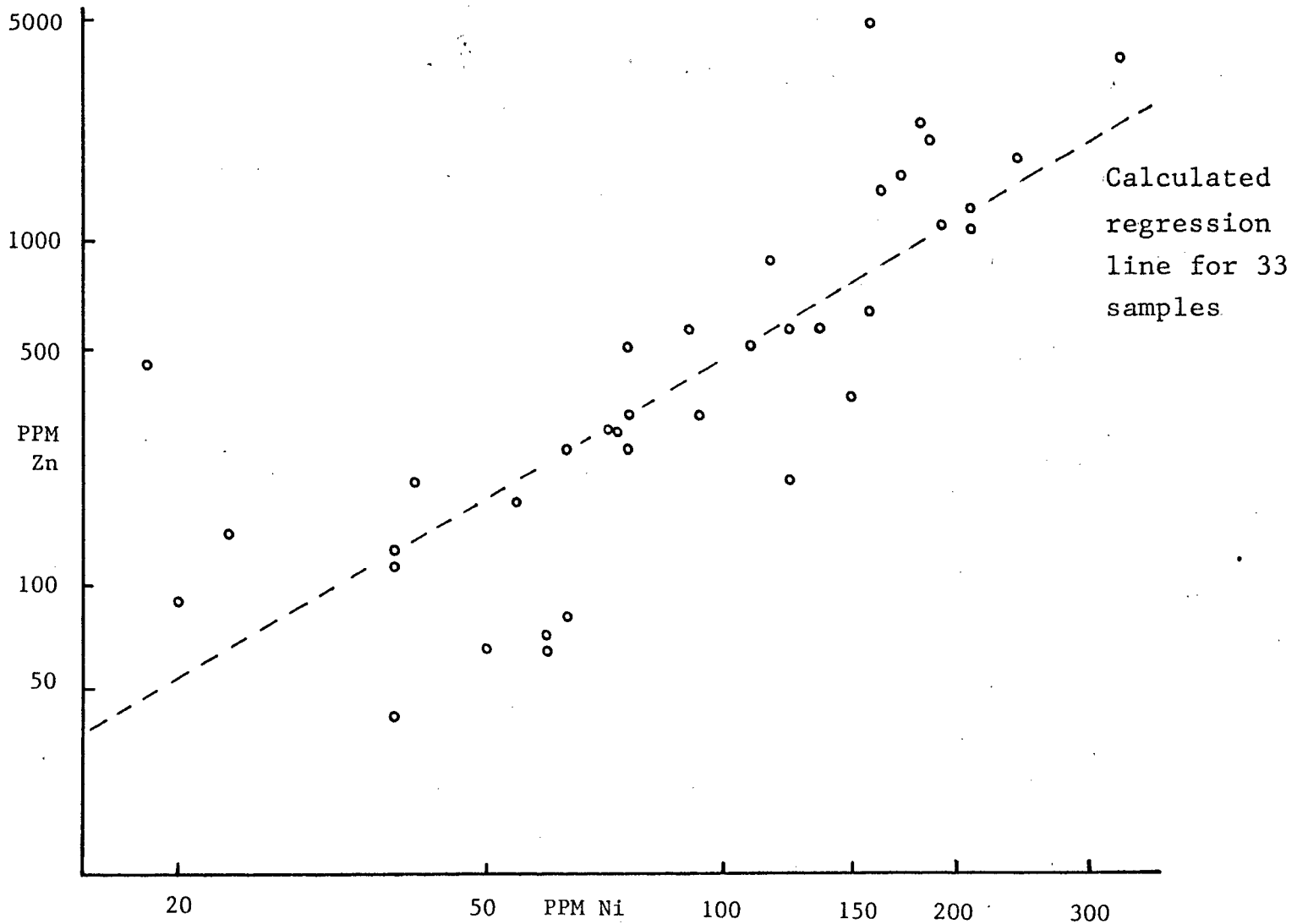


Figure 4-15. Scatter diagram for  $\text{Log}_{10}$  Zn against  $\text{Log}_{10}$  Ni

tions were approximately log normal. No transformation of organic carbon or pH values were made, however, and since a proportion of molybdenum values were below detection limit this metal was also excluded from the analysis. A correlation matrix calculated from data representing the 63 samples is shown in Table 4-3.

The minimum correlation coefficient ( $r$ ) which will be significant at the 5% significance level in a sample size of 63 (60 degrees of freedom) is  $\pm 0.25$  (Phillips and Thompson, 1967, Table F-8). Correlation coefficients greater than  $\pm 0.25$  in Table 4-3 will indicate that there is a linear relationship between two variables. This relationship, however, will be relatively weak below a coefficient of  $\pm 0.5$  since at this level only 25% of the variation can be attributed to the linear association between variables. Coefficients greater than  $+0.5$  in Table 4-3 are Co-Cu ( $+0.51$ ), Co-Mn ( $+0.60$ ), Co-Zn ( $+0.54$ ), Cu-Zn ( $+0.51$ ) and Zn-Ni ( $+0.86$ ). The coefficient between zinc and nickel indicates that more than 60% of the variation can be explained by a linear relationship and the scatter diagram for  $\text{Log}_{10}$  zinc against  $\text{Log}_{10}$  nickel (Fig. 4-15) demonstrates that points cluster relatively closely along a linear trend. A diagram of  $\text{Log}_{10}$  copper plotted against % organic carbon (Fig. 4-13) shows that points are widely scattered although a weak trend of increasing copper and organic carbon can be seen. Similar scattering occurs in the diagram of  $\text{Log}_{10}$  Cobalt plotted against  $\text{Log}_{10}$  manganese (Fig. 4-14). The higher correlation coefficient

Figure 4-16. Scatter diagram for  $\text{Log}_{10}\text{Zn}$  against  $\text{Log}_{10}\text{Ni}$ .



(+0.60) for Co-Mn than Cu-Carbon (+0.46) could be due to a single, high cobalt-manganese value.

The correlation matrix was recalculated for the same variables, but using samples with more than 16% organic carbon (Table 4-4). The minimum coefficient for a sample size of 33 at the 5% significance level is  $\pm 0.35$ . Those variables with coefficients greater than + 0.50 are Cu-Co (+ 0.56) and Ni-Zn (+ 0.71). A scatter diagram for  $\text{Log}_{10}$  zinc plotted against  $\text{Log}_{10}$  nickel (Fig. 4-16) shows that there is a relatively strong linear relationship between the two metals above values of 250 ppm zinc and 50 ppm nickel. The coefficients for Co-Cu and Ni-Zn, while indicating a clear linear relationship between these metals, do not necessarily prove that variations of cobalt depend on those of copper or that nickel variations will depend on those of zinc. The common association of these metals in the highly organic soils could be completely fortuitous and the spatial distribution patterns could reflect common sources for the metals or similar concentrating mechanisms.

#### 4-4 TRACE METALS IN VOLCANIC ASH

Results of analyses of two volcanic ash samples are shown in Table 4-5. Ash sample 77-RL-1 is from a layer between 30 to 40 cm deep in the Ah horizon of a humic gleysol profile 125 m south from station L6S. Sample 77-RL-2 is of similar textured material, but at 100 cm depth on a profile through fibric mesisolic soil. Both of these samples may be of ash that was deposited during the St Helens ash fall. Very low metal

<u>Number</u>	<u>Location</u>	<u>Co</u>	<u>Cu</u>	<u>Fe</u>	<u>Mn</u>	<u>Ni</u>	<u>Zn</u>
77-RL-1	125 m south of station L6S	ND	79	0.12	9	9	33
77-RL-2	1 m deep at station 1.5G	4	359	0.20	12	14	116

Table 4-5: Metal contents of volcanic ash samples.  
Cu, Co, Mn, Ni and Zn are in ppm; Fe is  
in %.

---

<u>Number</u>	<u>Location</u>	<u>Cu</u>	<u>Fe</u>	<u>Mn</u>	<u>Zn</u>
73-RL-533 <sup>a</sup>	L5S	44	197	154	48
73-RL-535 <sup>a</sup>	B1E	96	215	90	31
73-RL-570 <sup>a</sup>	L2N	37	167	132	29
73-RL-573 <sup>a</sup>	A1W	228	206	240	21
73-RL-530 <sup>b</sup>	B1W	13	73	707	63
73-RL-534 <sup>b</sup>	B1E	19	82	805	49
74-RL-1357 <sup>b</sup>	A2W	17	56	391	34
74-RL-1363 <sup>b</sup>	G2	10	60	548	27
74-RL-1364 <sup>b</sup>	G4	16	66	430	44
74-RL-1365 <sup>b</sup>	L1N	14	68	290	41
74-RL-1366 <sup>b</sup>	L0N	17	57	548	32
74-RL-1381 <sup>b</sup>	L1S	20	77	612	42
74-RL-1382 <sup>b</sup>	L3S	19	71	1503	35

Table 4-6: Metal contents in ppm of vegetation  
samples; a - Sphagnum moss;  
b - Labrador Tea.

contents appear to be typical of the volcanic ash except for the high copper content in sample 77RL-2. Presence of small organic fragments in this sample and the dark yellow to brown colour of the material suggests that the copper may have been introduced with organic matter after deposition of the ash.

#### 4-5 TRACE METALS IN BOG VEGETATION

A small number of sphagnum moss and labrador tea samples were analysed for copper, iron, manganese and zinc and results are given in Table 4-6. These results are for nitric-perchloric acid digested material and no ash weights were determined. Results indicate, however, that copper and iron are relatively more abundant in the sphagnum moss growing on the water saturated fibrous material than in the labrador tea shrub. The labrador tea, in contrast to the moss, has higher levels of manganese.

#### 4-6 TRACE ELEMENTS IN GROUND AND SURFACE BOG WATERS

Water flowing from till-bedrock seepages, a diamond drill hole (#68-W-5), humic gleysol seepages, semi-stagnant bog surface pools, surface streams and water accumulating at the bottom of cased auger holes was analysed for total copper, iron, manganese, zinc, organic carbon, calcium and pH. A number of the surface and subsurface water samples were also analysed for sulphate and biquinoline extractable copper. Arithmetic means, standard deviations and concentration ranges for the different sample types are given in Table 4-7. Means and standard deviations for those sample groups where a proportion of the analytical values are below instrumental

<u>Sample type</u>		<u>Carbon</u>	<u>Ca</u>	<u>Cu</u>	<u>Fe</u>	<u>Mn</u>	<u>pH</u>	<u>Zn</u>
Till-bed-	X	1.6	24	70	30	33	6.0	10
rock seeps	R	<0.5-5.0	<5-125	<10-290	<20-153	<20-41	5.5-7.0	<6-54
n = 14	S	1.4	32	98	76	8	0.5	22
	P(%)	79	100	71	21	31	100	50
Humic-gley-	X	1.6	19	178	87	35	6.2	25
sol seeps	R	<0.5-8.0	<5-120	<10-590	<20-143	<20-60	4.0-7.3	<6-70
n = 17	S	2.2	30	162	102	17	1.0	22
	P(%)	15	12	100	24	24	100	82
Surface	X	1.4	19	441	30	40	5.0	27
pools	R	<0.5-7.0	<5-30	<10-750	<20-276	<20-62	4.0-7.0	<6-50
n = 13	S	3.6	7	230	117	13	0.9	12
	P(%)	69	100	100	39	77	100	85
Subsurface	X	7.4	21	185	263	106	7.4	12
waters	R	2.0-16.0	<16-28	<10-1060	<20-2328	<20-204	6.0-7.5	<6-40
n = 10	S	4.2	5	324	744	60	0.6	14
	P(%)	100	100	70	80	100	100	60
Stream	X	2.2	22	104	38	<u>No</u>	6.6	8
waters	R	<0.5-3.0	<17-25	<10-425	<<20-123	<u>Data</u>	4.5-7.8	<6-22
	S	1.0	6	111	38		0.9	6
	P(%)	90	100	95	50		100	70

Table 4-7: Arithmetic means (X), standard deviations(S) and ranges (R) for elements in water. Cu, Fe, Mn, and Zn in ppb; C and Ca in ppm. P = % values detection limit

detection limit have been calculated by the method described by Miesch (1967). These statistics are only approximations in those sample groups with more than 50 percent of values below the detection limit.

Horizontal variations of copper in bog waters and surrounding seepages are shown in Fig. 4-17. Weakly acid (pH 5.5-7.0) till-bedrock seepages generally have less than 50 ppb copper, less than 2 ppm organic carbon and no detectable iron or manganese. Spring water draining from a probable fault zone 50 m north of station G 11 contains 290 ppb copper although no copper was detected in water flowing from diamond drill hole 68-W-5. This water contained 125 ppm calcium, 120 ppm sulphate and 54 ppb zinc. Seepages from humic gleysols have pH values ranging from 4.0 to 7.0 and a higher mean copper content (178 ppb) than the till-bedrock seepages. Water from seepages on the west side of the bog has up to 590 ppb copper (Fig. 4-17). Most of the seepages do not have detectable levels of iron or manganese. Dissolved organic carbon up to 8 ppm occurs in water accumulating in pits on the north and south sides of the bog. Seepages and springs flowing from the north side of the bog have up to 120 ppm calcium. Zinc contents up to 70 ppb are found in seepages draining the hill side on the southeast margin of the bog.

The pH of semi-stagnant surface pools can be as low as 4.0 and water standing on the bog surface between stations LON to G2 contains up to 750 ppb copper. The high copper concentrations are found in semi-stagnant pools less than 10 cm



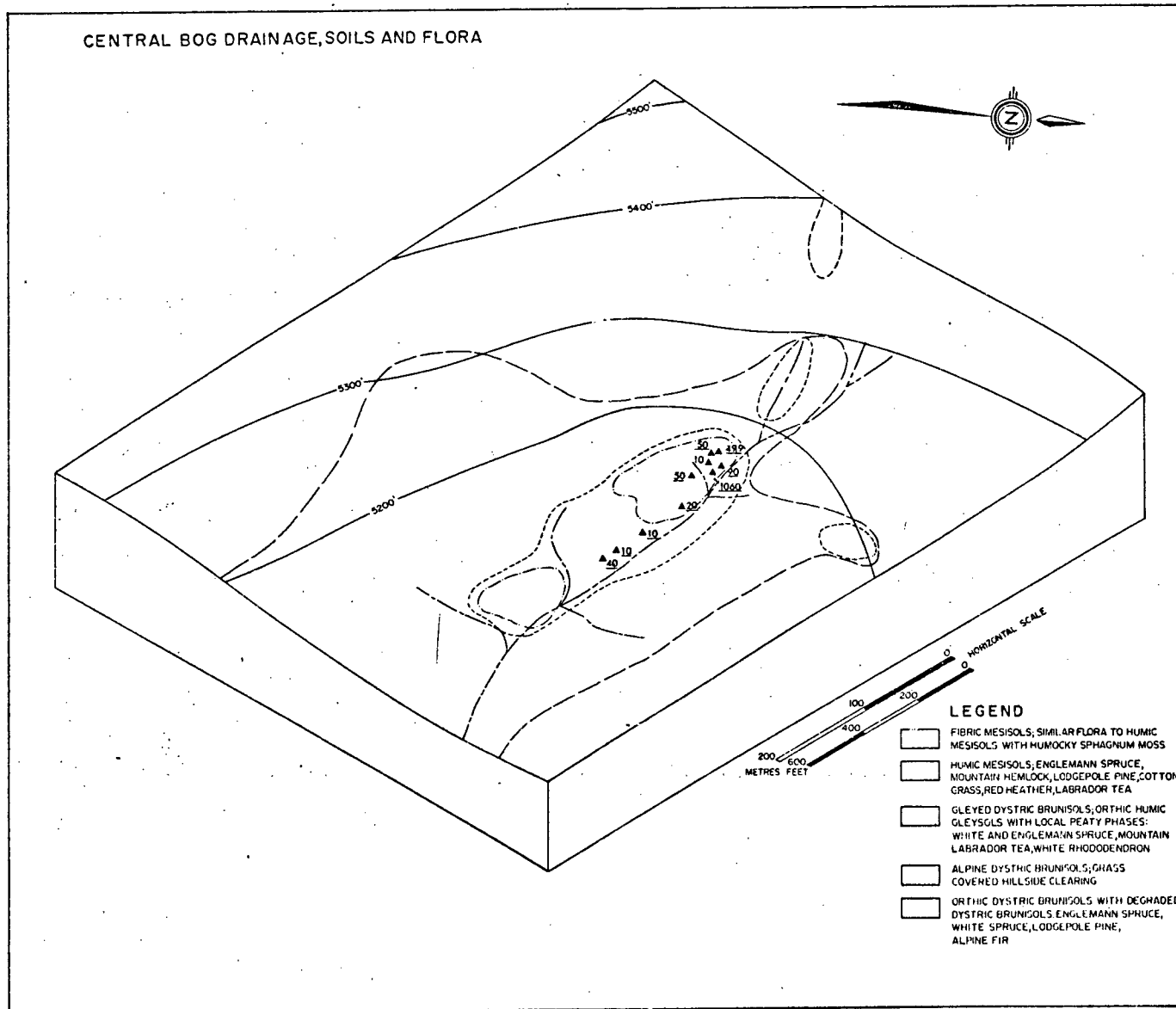


Figure 4-18: Copper ( ppb) in subsurface water samples

deep formed over fibric mesisols. Bottom sediment in these pools consisting of partially decomposed vegetation fragments, is occasionally coated with a white precipitate identified as sulphur. Iron hydroxide precipitates are more common on the bottom of pools and surrounding seepages at the western end of the bog. The mean dissolved organic carbon content (1.4 ppm) and range of values are lower than those determined for the humic gleysol seepages. Surface water pools also have less than 30 ppb iron, below 30 ppb manganese and less than 50 ppb zinc.

The largest chemical variations are found between surface waters and waters accumulating at the bottom of cased auger holes. Mean pH of the subsurface waters (7.4) is higher than surface waters and values range from 6.0 to 7.5. The mean copper content (185 ppb) of the subsurface waters is markedly lower than that of surface waters, but is similar to the mean of the humic gleysol seepage samples (178 ppb). Most subsurface water samples have less than 50 ppb copper (Table 4-9) except in a small area at the western end of the bog where copper exceeds 1000 ppb in the water (Fig. 4-18). The area where these high copper values occurs is underlain by copper-rich till. Subsurface bog water samples also have higher mean dissolved iron, manganese and organic carbon abundances than do surface waters (Table 4-7). One sample, for example, collected at 1.5 m depth at station G2 contains more than 2000 ppb dissolved iron, but less than 50 ppb dissolved copper. The mean dissolved calcium content of the

<u>Sample number</u>	<u>Ppb Cu by A.A. spectrophotometry</u>	<u>Ppb Cu by biquinoline</u>	<u>% Cu not extracted by biquinoline</u>	<u>Organic carbon (ppm)</u>	<u>pH</u>
74-RL-					
1290	125	180	-	2.0	5.8
1291	117	90	23	2.5	5.0
1292	175	120	31	2.0	5.5
1293	241	150	38	2.5	5.5
1294	158	110	30	2.0	5.8
1314	658	650	2	<0.5	5.0
1315	699	700	<1	<0.5	4.5
1316	749	800	<1	<0.5	4.0
1318	62	80	<1	2.0	6.0
1320	395	350	11	<0.5	4.0
1323	146	110	25	<0.5	5.5
1324	146	50	66	3.0	4.0
1326	220	150	32	2.0	7.0
1508	645	520	19	5.0	n.a
1427*	21	10	50	9.5	6.0
1428*	10	8	20	9.0	7.5
1429*	50	8	84	16.0	7.0
1439*	499	450	10	2.0	6.0
1442*	50	20	60	4.0	6.2
1443*	90	50	44	3.5	6.0

Table 4-8: Surface and subsurface(\*) water samples analysed by atomic absorption spectrophotometry and by 2-2 biquinoline colorimetry. n.a = not determined.

subsurface water samples is similar to that of surface waters and sulphate values, ranging from 27 to 80 ppm, are slightly higher in surface pools. One Eh measurement made on subsurface water recorded -260 mv. This Eh and the odour of  $H_2S$  from freshly sampled water suggests that subsurface bog water is moderately reducing. Measured dissolved sulphate values will therefore be a product of sulphate derived from mineral sources and sulphate from the oxidation of  $H_2S$ .

Organic carbon values ranging from 2 to 16 ppm in subsurface water and from 0.5 to 7 ppm in surface water may represent concentrations of dissolved, metal-complexing organic substances (fulvic acid fraction). The proportion of copper which may be bound to organic matter or other substances in the water has been measured using 2-2 biquinoline and results are given in Table 4-8. Several of the samples analysed have a biquinoline extractable copper value that is greater than the concentration determined by atomic absorption spectrophotometry. The reason for this inconsistency may be analytical error of the biquinoline extractable copper method or poor precision at high copper concentrations. Biquinoline generally extracts more than 60% of the copper from samples having low dissolved carbon contents and low pH which are from the surface pools (Table 4-8). A smaller proportion of the total copper is removed from subsurface water samples having a greater organic carbon content indicating that a higher percentage of the copper could be bound to the organic matter.

<u>Sample number</u>	<u>Depth-Location</u>	<u>Organic carbon</u>	<u>Ca</u>	<u>Cu</u>	<u>Fe</u>	<u>Mn</u>	<u>pH</u>	<u>SO<sub>4</sub></u>	<u>Zn</u>
1326	S; A0.5W	2.0	19	200	61	<20	7.0	n.r	31
1427	G; L1N	9.5	n.r	21	30	204	6.0	45	15
1323	S; G0.8	5.0	8	146	<20	23	5.5	n.r	22
1428	G; G0.8	9.0	25	<10	110	136	7.5	40	10
1324	S; A1W	3.0	7	146	<20	<20	4.0	n.r	20
1429	G; A1W	16.0	11	50	172	74	7.0	27	22
1315	S; G2.2	<0.5	23	699	<20	43	4.5	75	28
1439	G; G2.2	2.0	18	499	398	43	6.0	60	22
1317	S; G2.0	<0.5	29	708	<20	51	5.2	80	37
1442	G; G2.0	4.0	23	50	2328	51	6.2	62	<6
1314	S; G1.5	<0.5	23	658	<20	43	5.0	65	30
1443	G; G1.5	3.5	25	90	441	100	6.0	62	<6
1320	S; G1.0	<0.5	16	395	<20	34	4.0	50	39
1444	G; G1.0	4.0	25	1060	61	43	n.r	65	39
1493	S; LON	7.0	n.r	633	<20	57	4.0	n.r	15
1492	G; LON	9.0	16	<10	30	165	n.r	27	<6
1508	S; L1S	5.0	13	645	61	62	4.8	40	25
1507	G; L1S	12.0	28	<10	92	71	n.r	30	<6

Table 4-9: Element contents in surface(S) and subsurface (G) bog water samples. Cu, Fe, Mn, Zn are in ppb; Carbon, Ca, and SO<sub>4</sub> are in ppm. n.r = not recorded.

Biquinoline extractable copper data are, however, based on a comparison between 6 subsurface and 12 surface water samples.

Stream waters are weakly acid and have dissolved iron, zinc, and organic carbon levels similar to those found in till-bedrock seepages. Streams draining semi-stagnant pools covering the western end of the bog have water pH values below 5.0 and samples contain more than 400 ppb copper. Thick precipitates of iron hydroxide often occur in channels through this part of the bog. Below these incrustations, however, the organic rich stream sediment has a dark blue-grey colour and has a strong  $H_2S$  odour. Water flowing in the main stream draining the lower end of the bog has higher pH than water in the channel at the western end. The dissolved copper content also decreases from above 400 ppb at the western end to less than 70 ppb in samples from the channel draining the lower, eastern end of the bog.

#### 4-7 HI REDUCIBLE SULPHUR CONTENTS OF SOIL AND TILL

The soil and till samples analysed for hydriodic acid reducible sulphur (HI reducible sulphur) are from four vertical organic soil-till profiles including Profile 2 (Fig. 4-2) and Profile 3 (Fig. 4-3). Results given in Table 4-10 show that HI reducible sulphur is 10 to 20 times greater in organic soil layers than in underlying till and sulphur generally increases down profiles from the fibric layer into the humic-mesic layers, but falls sharply at the organic soil-till interface. The correlation coefficient for HI reducible

<u>Sample Number</u>	<u>Location-Depth in cm</u>		<u>HI-Sulphur(ppm)</u>	<u>Organic C</u> (%)	
73-RL-117	Station	B1E	0-50	788	26.4
" 118	"	"	50-100	350	19.0
" 119	"	"	100-110	105	4.0
" 139	"	"	250-260	19	0.5
" 140	"	"	300-310	26	0.1
73-RL-120	"	L5S	0- 50	1114	39.5
" 121	"	"	50-100	1360	32.0
" 122	"	"	100-150	1445	22.9
" 123	"	"	150-200	1181	50.6
" 141	"	"	350-360	24	0.1
" 142	"	"	380-390	30	0.4
74-RL-1087	"	LON	0-40	249	34.1
" 1088	"	"	50-100	1162	41.4
" 1089	"	"	100-130	725	21.9
" 1090	"	"	130-140	69	1.0
74-RL-1091	"	L1N	0-40	118	13.7
" 1092	"	"	50-100	449	16.7
" 1093	"	"	100-150	1360	26.1
" 1094	"	"	150-200	906	32.0
" 1095	"	"	200-250	1418	39.4
" 1096	"	"	250-300	906	42.6
" 1097	"	"	325-350	104	1.3

Table 4-10: Hydriodic acid reducible sulphur and organic carbon contents of samples from four profiles.

sulphur and organic carbon is + 0.82 indicating that more than 65% of the variation can be explained by a linear relationship between sulphur and carbon. This relationship and the marked increase of sulphur in organic soil compared to levels in the till suggests that a large proportion of the HI reducible sulphur present occurs as organic sulphate and possibly as sulphide.

## CHAPTER 5

## SULPHIDE MINERALS IN ORGANIC SOILS AND TILL

## 5-1 INTRODUCTION

Bromoform separated heavy mineral fractions from roughly one hundred soil and till samples were initially examined under a binocular microscope. Visible, non-sulphide minerals included angular to subangular grains of quartz, feldspar, a green pyroxene and magnetite. Small, subangular shaped pyrite grains, often partially altered to limonite could be identified in separates from till samples. Clusters of small bronze coloured concretion less than 0.5 mm in size were visible in separates from organic soil samples. A single concretion was analysed by X-ray diffraction using a Debye-Scherrer powder camera and the mineral was identified as pyrite. Dark brown to yellow dendritic grains, smaller than the concretion clusters were also present in the organic soil separates. To identify these mineral grains and to carry out additional examination of the concretion textures roughly fifty heavy mineral separate samples were mounted in epoxy-resin, polished and the sections examined under a reflecting microscope. Several of the individual grains in the sections were also examined and analysed for relative copper, iron and sulphur abundances with a scanning electron microscope.

## 5-2 COMPOSITION AND TEXTURES OF SULPHIDE MINERAL GRAINS

Several forms of pyrite were identified in the sections made from the heavy mineral separates. Small angular pyrite grains mainly occur in the till although these were occasionally present in organic soils. The most common form of pyrite

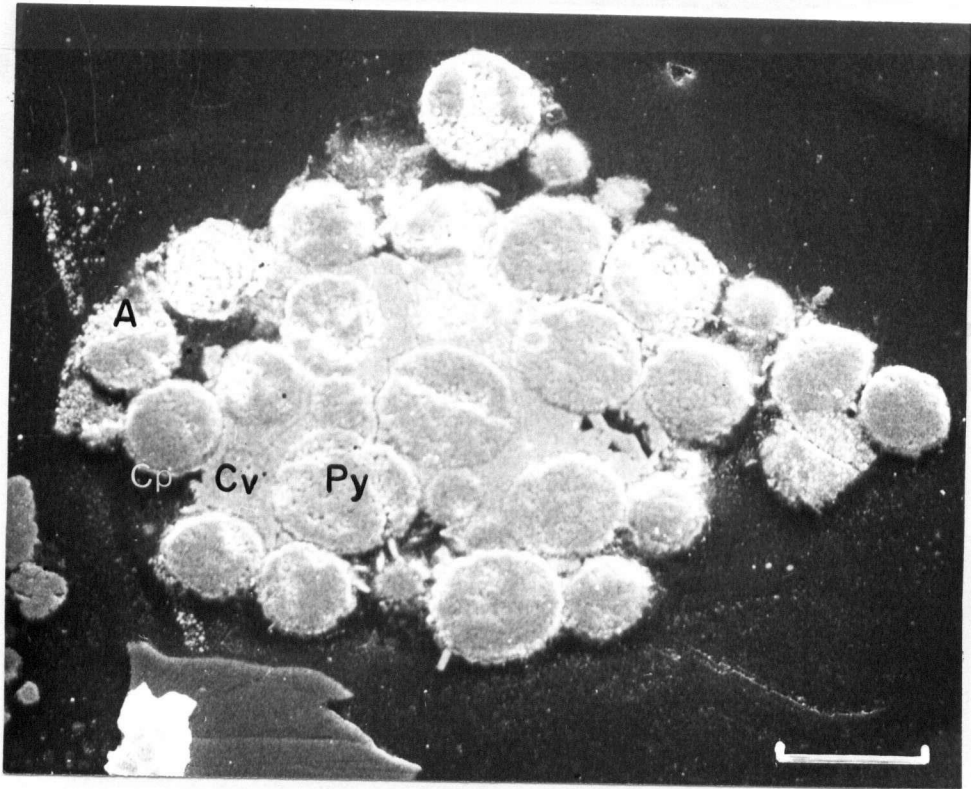


Plate 5-1: Electron micrograph of a framboidal pyrite cluster in a polished mount made from a heavy mineral separate of soil sample 74-RL-1119. Spherical pyrite concretions (Py) are rimmed with softer sulphides consisting of chalcopyrite (Cp) and covellite (Cv). Sample 74-RL-1119 is from station G1.0 at 2.5 m depth. Bar scale measures 50  $\mu\text{m}$ .

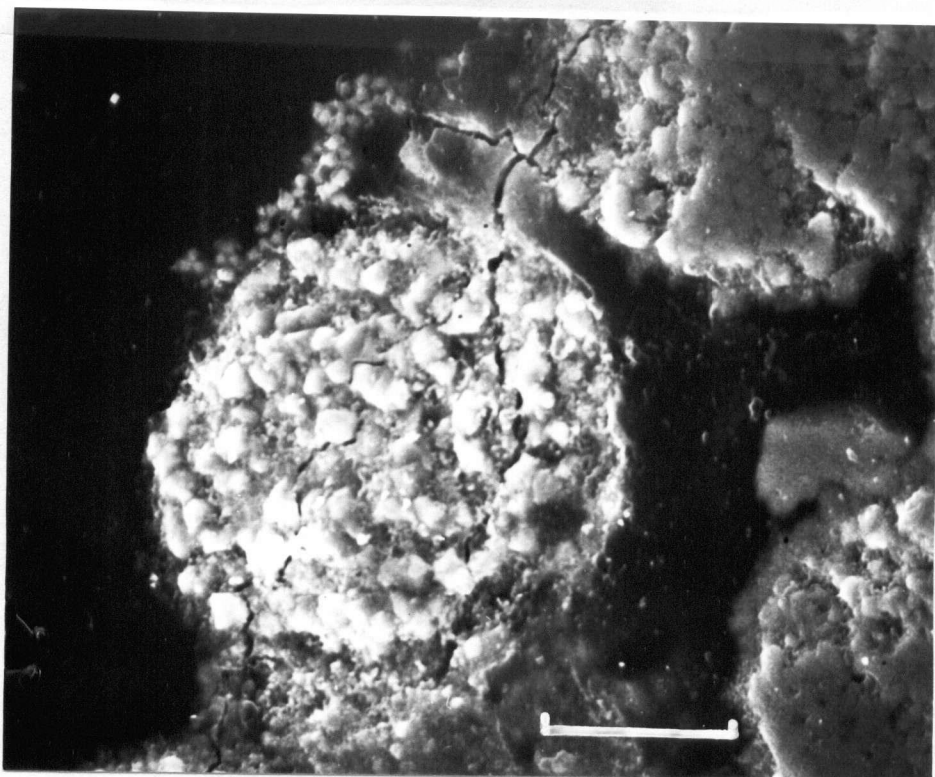


Plate 5-2: Electron micrograph of an individual pyrite framboid ('A') from the cluster shown in Plate 5-1. The pyrite microcrystals are less than 10  $\mu\text{m}$  across and are randomly oriented. Cubic forms are visible in several of the microcrystals. Bar scale measures 20  $\mu\text{m}$ .

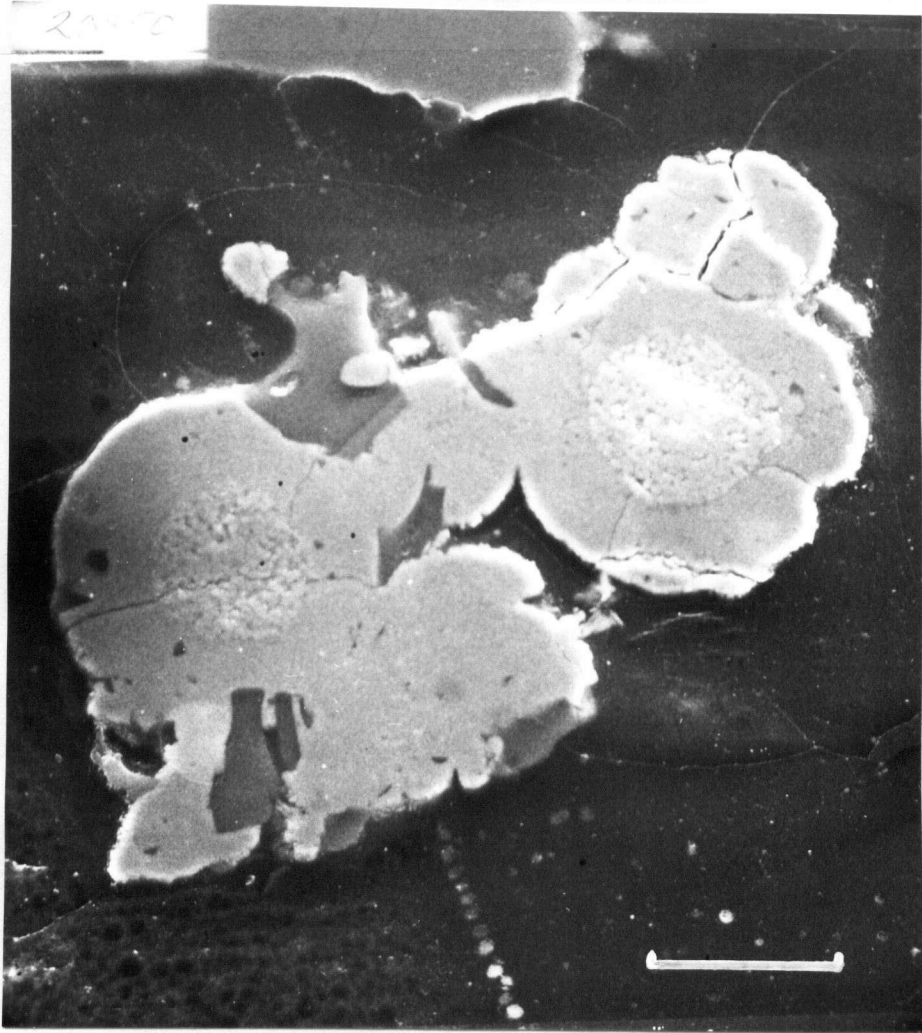


Plate 5-3: Electron micrograph of pyrite framboids from sample 74-RL-1119. The microcrystalline framboid core is coated with a concentric layer of massive, slightly softer sulphide that has a composition similar to  $\text{FeS}_2$ . Bar scale measures 20  $\mu\text{m}$ .

in organic soil is as spherical concretions or clusters of concretions resembling bunches of grapes. The individual concretions are between 20 and 30  $\mu\text{m}$  diameter and generally consist of loosely packed pyrite microcrystals. Microcrystals in a typical concretion, shown in Plates 5-1 and 5-2, are roughly cubic and the length of each crystal is less than 5  $\mu\text{m}$ . Comparable features have been described in framboidal pyrite reported in recent sediments from widely ranging environments. Framboids described in these sediments commonly have the individual microcrystals orientated along well defined planes, but the microcrystals which make up the framboid in Plate 5-2 appear to be randomly orientated. Several of the framboids found in the organic soils have a microcrystalline core that is enclosed by a roughly spherical envelope consisting of massive iron sulphide that is slightly softer and darker coloured than that in the core (Plate 5-3). The envelope is 8-10  $\mu\text{m}$  thick and is often cut by both radiating and concentric fractures. Relative iron and sulphur abundances, determined by scanning electron microprobe analysis, are almost uniform throughout these framboids although, however, the core has a slightly iron content than the envelope.

Individual framboids are apparently non-magnetic and the cubic shape of the microcrystals in the core indicates that they are pyrite. The softer sulphide which comprises the surrounding envelope could, however, have a composition closer to that of greigite-melnikovite ( $\text{Fe}_3\text{S}_4$ ) which has a hardness ranging from 4.0-5.0 compared to 5.0 for pyrite. Papeunen (1966) has reported framboids from a pyritic layer in a Finish peat

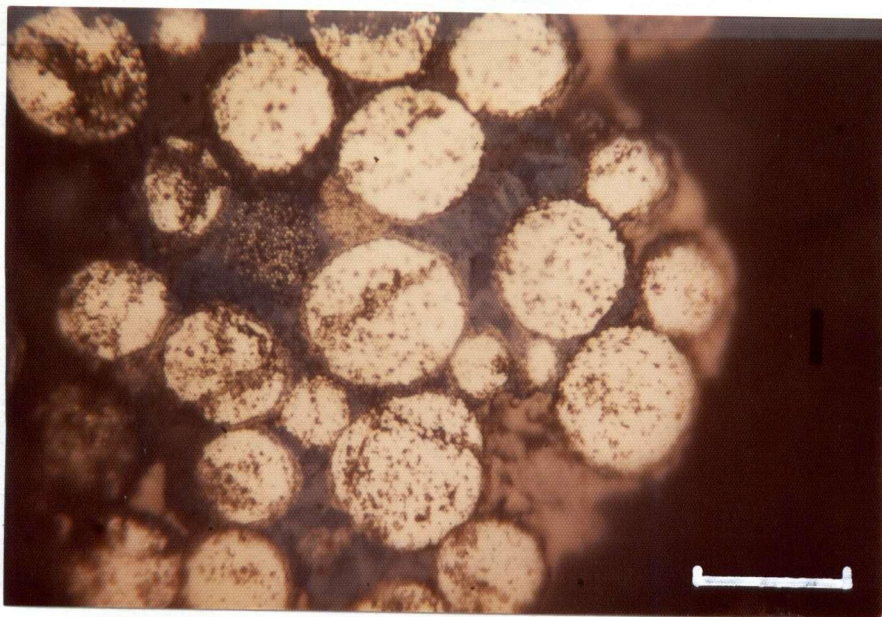


Plate 5-4: Photomicrograph of the framboidal cluster shown in Plate 5-1. The softer, darker yellow chalcopyrite coating the pyrite framboids is clearly visible. Blue covellite lamellae fill the interstices between the framboids. Bar scale is 50  $\mu\text{m}$ .

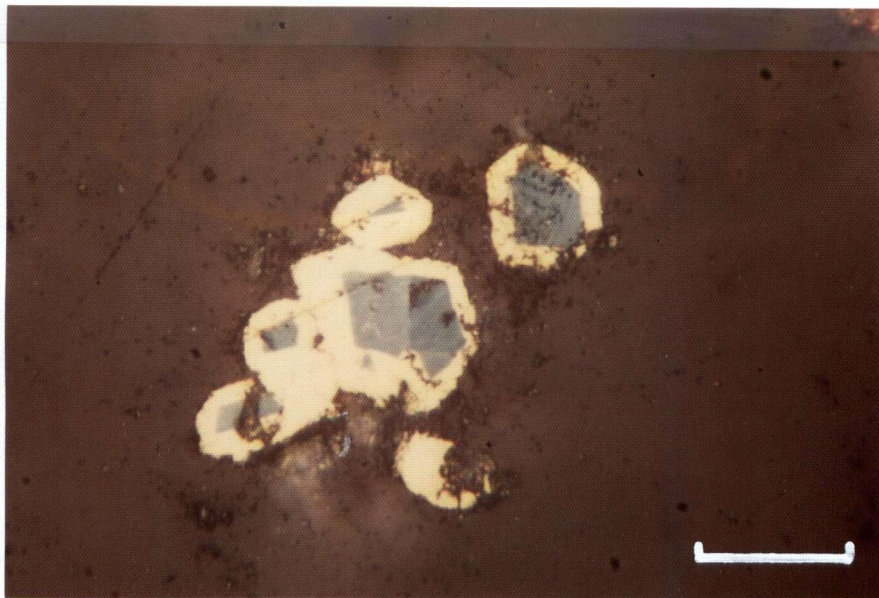


Plate 5-5: Photomicrograph of a polished mount from sample 74-RL-1127 collected at station G 1.5 at 2.5 m depth. Idiomorphic covellite 'crystals' less than 20  $\mu\text{m}$  across are rimmed by chalcopyrite. The outer shape of the chalcopyrite envelope is sub-parallel to the shape of the covellite core and one of the grains has a roughly hexagonal form. Bar scale is 10  $\mu\text{m}$ .

bog which exhibited similar textures to those described above. He determined, by X-ray diffraction that the core and concentric envelope surrounding the core both consist of pyrite.

Framboids commonly occur in clusters containing approximately 20 to 30 concretions and one example, shown in Plate 5-4, measures roughly 200  $\mu\text{m}$  across. Microcrystalline pyrite is clearly visible in several of the framboids in this cluster and blue covellite lamellae partially fill the interstices between the pyrite concretions. Chalcopyrite is also present as a thin concentric layer surrounding several of the pyrite framboids and also as larger, irregularly shaped areas on the outer edge of the cluster partially enclosing the covellite. The irregular shape of the framboidal pyrite cluster suggests that it may have been larger, but was broken up during sample disaggregation.

Grains of chalcopyrite mixed with covellite, covellite and native copper were also identified in polished mounts made from heavy mineral separates of organic soils. Idiomorphic covellite grains are less than 20  $\mu\text{m}$  and consist of deep blue, twinned lamellae or roughly hexagonal forms. The covellite is strongly anisotropic and red to brown polarization colours are visible under crossed nicols. Examples of these grains are shown in Plate 5-5 where the covellite is rimmed by a thin envelope of green-yellow chalcopyrite. The outer edge of the grains is subparallel to the internal boundary between the covellite core and the chalcopyrite rim. Larger copper-iron sulphide grains ranging from 20  $\mu\text{m}$  to more than 60  $\mu\text{m}$  have more complex textural relationships between the constituent minerals than do the

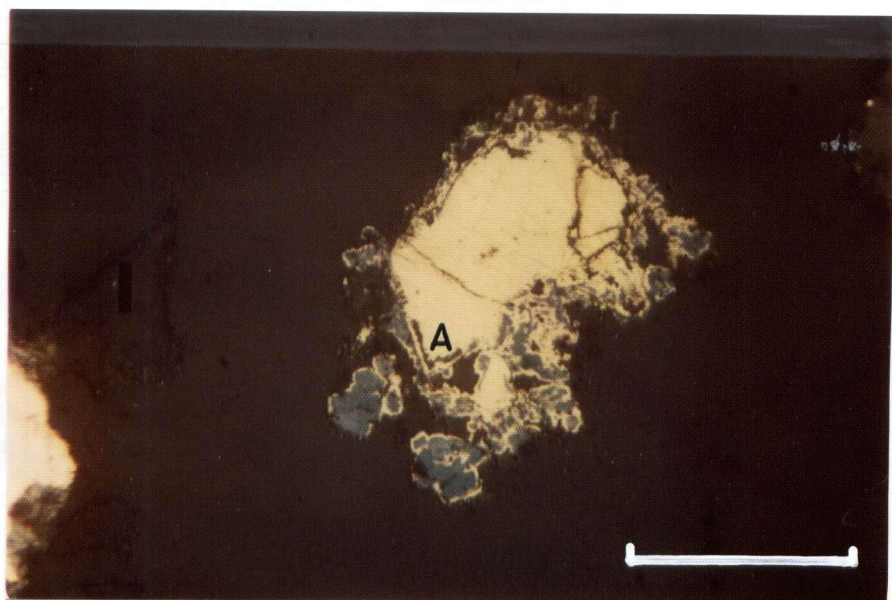


Plate 5-6: Photomicrograph of a polished mount from sample 74-RL-1117 collected at station G 1.0 at 1.5 m depth. Covellite occurs as a discontinuous margin along the highly irregular, deeply corroded outer edge of the chalcopyrite grain. Two surfaces in this grain (area 'A') appear to intersect at roughly  $90^\circ$ . Smaller (less than  $20\ \mu\text{m}$ ) covellite grains are rimmed by chalcopyrite. Bar scale measures  $40\ \mu\text{m}$ .

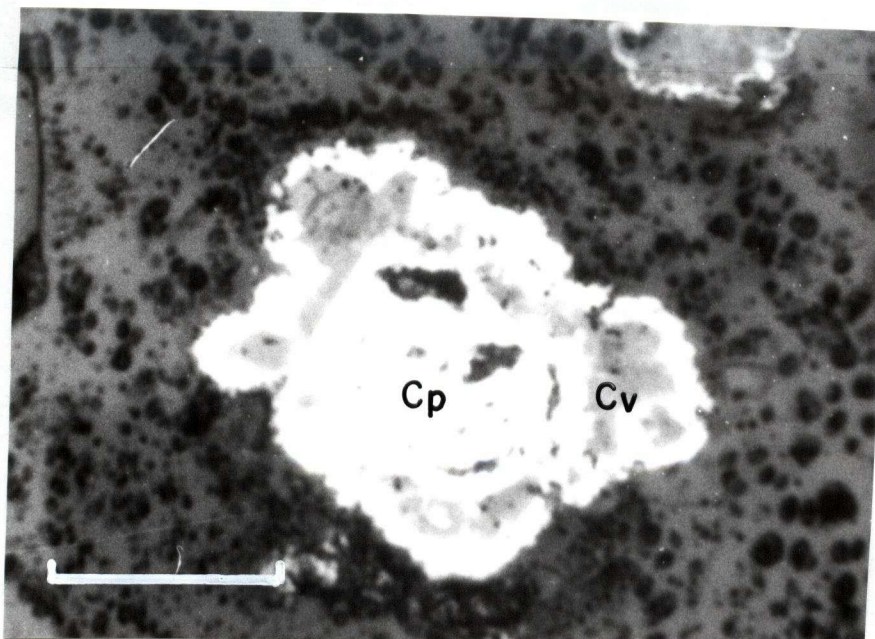


Plate 5-7: Photomicrograph of a chalcopyrite-covellite grain from sample 74-RL-1119. The chalcopyrite (Cp) core is sub-hedral and has a sharp contact with enclosing layers of chalcopyrite and covellite (Cv). Dark, non-sulphide inclusions are present in the core forming a discontinuous, concentric layer. Bar scale on Plates 5-7 and 5-8 measures 50  $\mu\text{m}$ .

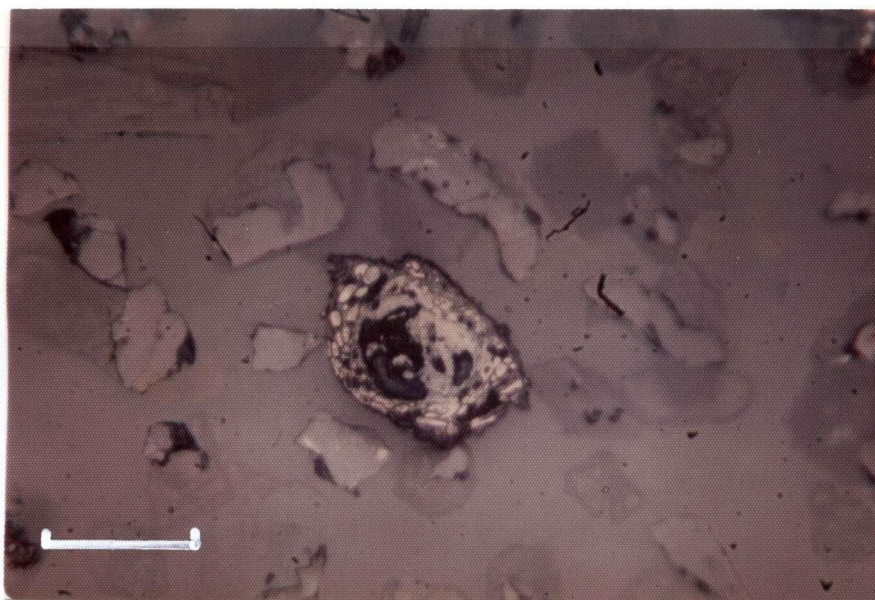


Plate 5-8: Photomicrograph of a grain from sample 74-RL-1113. Concentric layers of almost spherical chalcopyrite granules surround an irregularly shaped silicate mineral grain.

smaller covellite grains.

Chalcopyrite may be present forming the grain 'core' with covellite occurring as small irregularly shaped zones close to the outer edge of the grain. Within the chalcopyrite core of the grain shown in Plate 5-6 are indications that two regular surfaces, intersecting at roughly  $90^{\circ}$ , (Area "A" in Plate 5-6), form a contact between the chalcopyrite core and the enclosing chalcopyrite-covellite margin. These surfaces enclose two small subparallel areas that may be fractures or inclusions of non-sulphide mineral matter. The regularity of these surfaces contrasts markedly to the deeply embayed, corroded outer edge of the grain where covellite, the dominant sulphide, and is usually rimmed by chalcopyrite. Similar features are also visible in a second example of a grain shown in Plate 5-7 where the chalcopyrite core has a subhedral shape and appears to enclose roughly concentric zones of a non-sulphide material which are sub-parallel to the core envelope boundary. The outer boundary of this grain consists of an envelope of both chalcopyrite and covellite. The edge of this grain is also very irregular and appears to be deeply corroded. These textures may represent two stages of sulphide mineral formation where a preexisting chalcopyrite grain formed the nucleus for later covellite-chalcopyrite accretion and replacement.

An unusual association of sulphide with a silicate mineral is shown in Plate 5-8. This grain consists of a subhedral quartz core surrounded by roughly concentric layers of almost spherical chalcopyrite granules smaller than 20  $\mu\text{m}$  and having a slightly blue core suggesting that they may be partially covell-

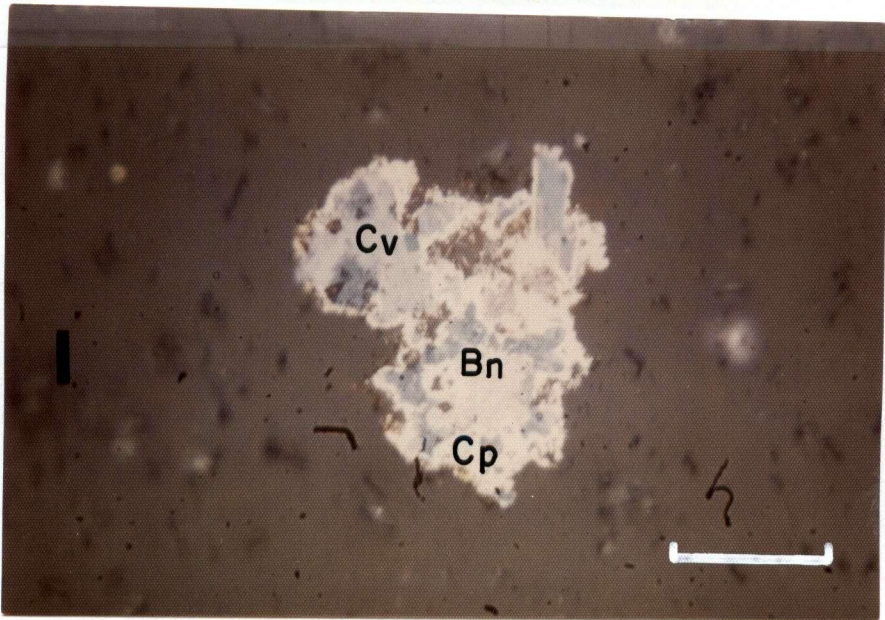


Plate 5-9: Photomicrograph from sample 74-RL-1119 showing chalcopyrite intergrown with covellite. Blue covellite (Cv) occurs as lamellae or roughly concentric zones in the chalcopyrite (Cp). A pale brown mineral enclosed by the chalcopyrite in the grain center could be bornite (Bn). Bar scale measures 50  $\mu\text{m}$ .

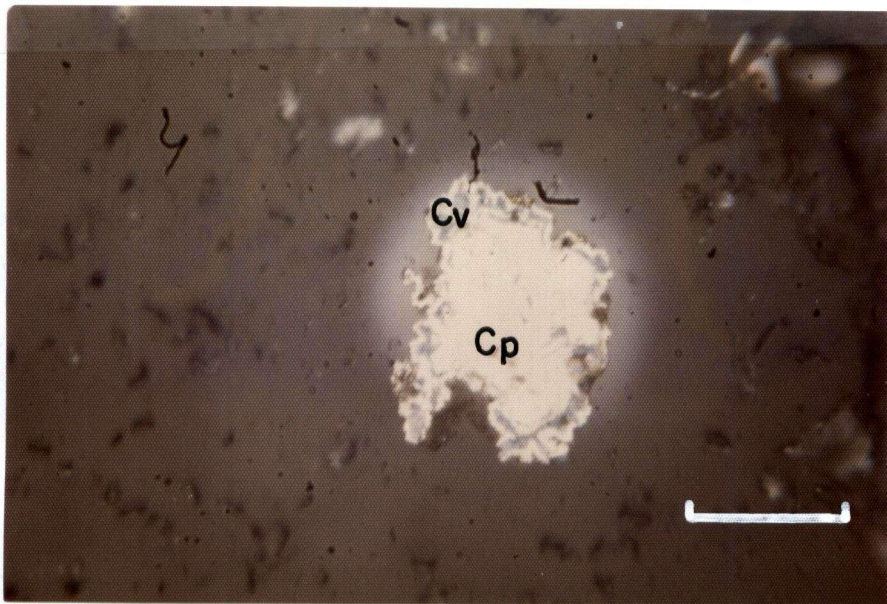


Plate 5-10: Photomicrograph from sample 74-RL-1119 showing covellite (Cv) forming discontinuous, roughly concentric layers in chalcopyrite (Cp). Both the grains illustrated in Plates 5-9 and 5-10 have deeply embayed, corroded outer boundaries and this feature is typical of copper-iron sulphide grains larger than 40  $\mu\text{m}$  across. Bar scale measures 50  $\mu\text{m}$ .

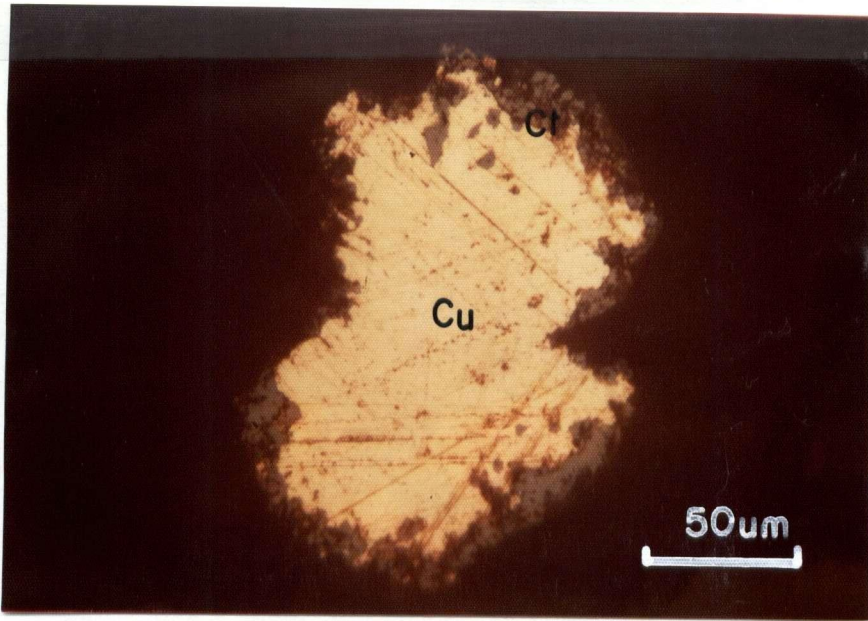


Plate 5-11: Photomicrograph of a grain from sample 74-RL-1127. Native copper (Cu) is partially rimmed by cuprite (Ct).

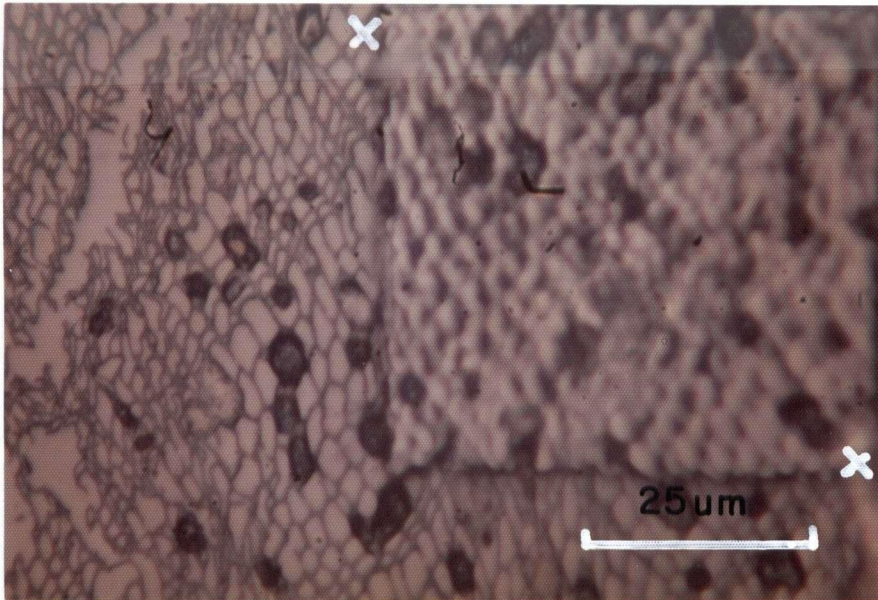


Plate 5-12: Photomicrograph of a polished mount made from a fragment of sample 73-RL-340. The reticulate cell-wall structures visible in this mount may have originally been sphagnum moss tissue. Several of the cells are filled by opaque material that could be iron oxide. The eroded area represents partial destruction of the surface by the electron beam during microprobe analysis. Reference marks X are included to orientate photomicrographs with microprobe patterns.

ite. Formation of this association is uncertain although it could represent accretion of copper sulphide onto a mineral grain during organic sediment diagenesis.

Larger copper-iron sulphide grains (40-60  $\mu\text{m}$  across) also common in the organic soil show evidence of a chalcopyrite core and surrounding covellite envelope. An intimate mixture of sulphides is often visible in the grains. Twinned covellite laths are rimmed with chalcopyrite and the covellite, in turn, encloses an area of darker yellow to brown coloured sulphide in a grain shown in Plate 5-9. This latter sulphide may be bornite although the mineralogy has not been confirmed. No chalcocite has been observed in any of the grains although indistinct dark brown areas in corroded chalcopyrite grains may represent this sulphide. Covellite also forms discontinuous roughly concentric zones within chalcopyrite (Plate 5-10) that are sub-parallel to the outer edge of the grain. Both the grains, described in Plates 5-9 and 5-10 have highly irregularly shaped, embayed and deeply corroded outer edges and are typical of those seen in mounts of the organic soil separates.

Native copper grains were visible in one sample which also contained covellite and chalcopyrite (Plate 5-5). Grains range from 40 -60  $\mu\text{m}$  across and have a moderately corroded outer edge. The bronze coloured native copper has parallel cleavages on the exposed face (Plate 5-11) and is partially rimmed with dark grey cuprite. Mineralogy of the native copper was confirmed by microprobe analysis.

### 5-3 DISTRIBUTION OF COPPER AND IRON MINERAL GRAINS

The horizontal and vertical distribution of copper sulphide,

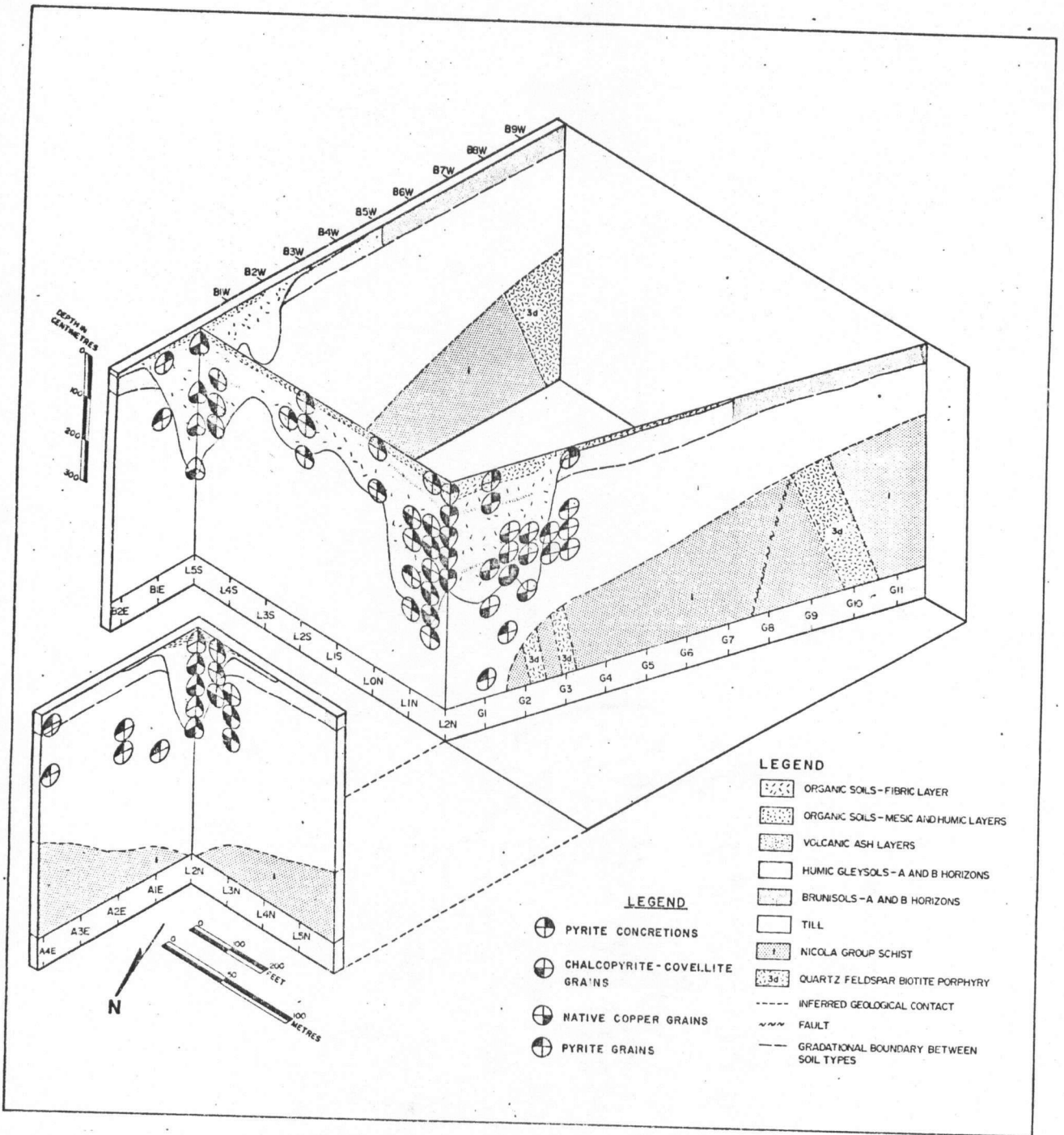


Figure 5-1: Distribution of mineral grains in organic soils and till.

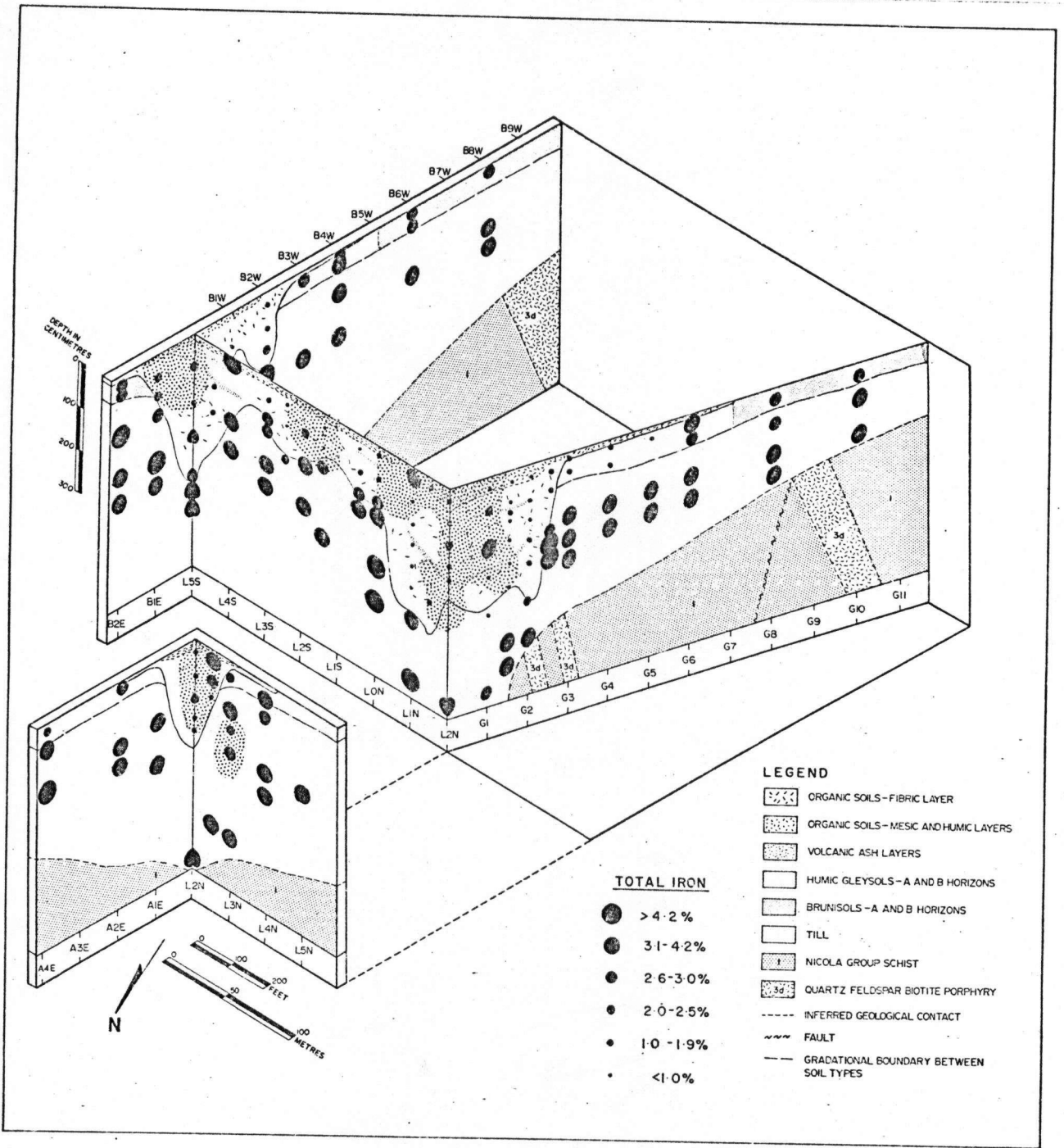


Figure 5-2: Distribution (●) of framboidal pyrite.

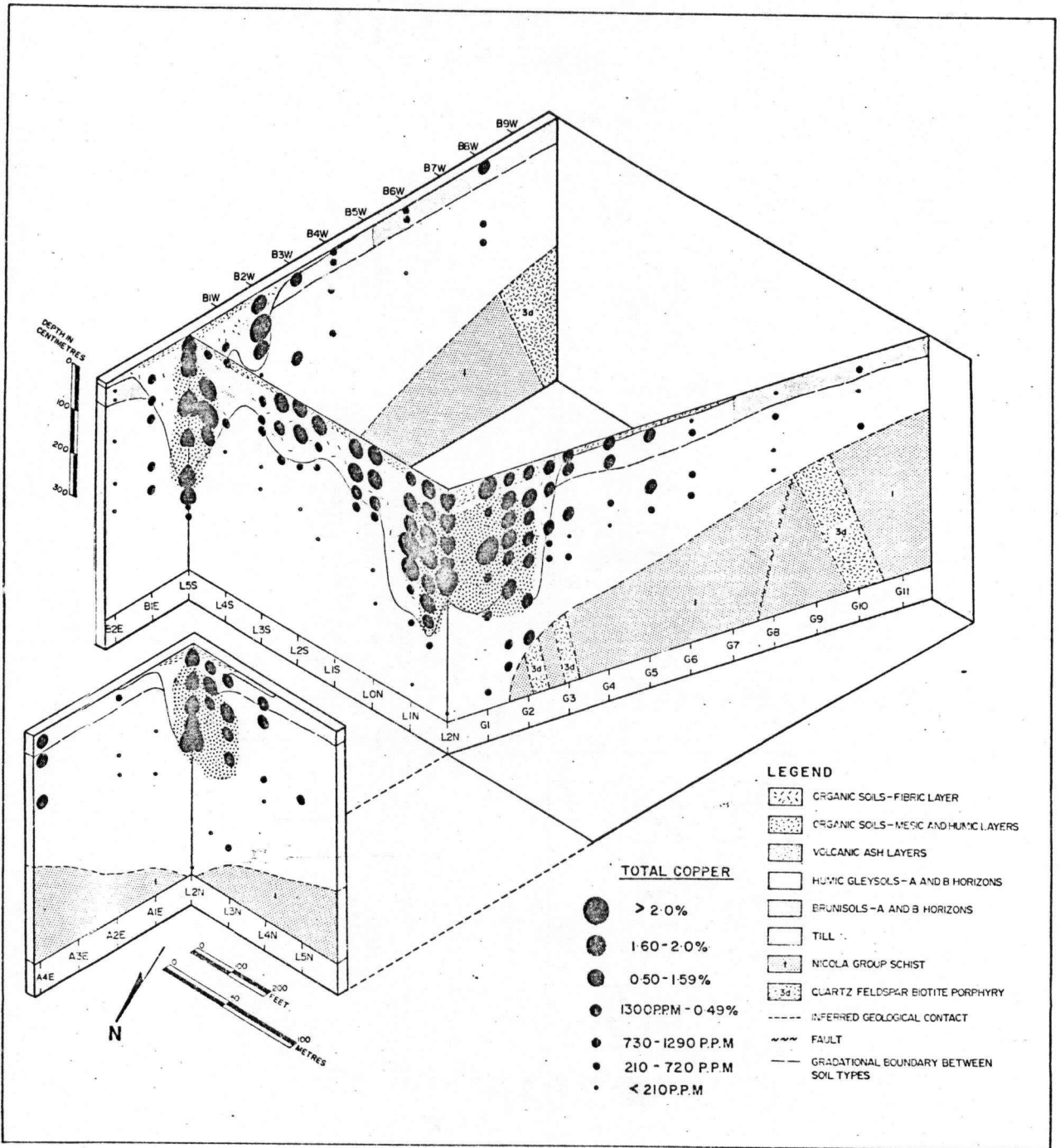


Figure 5-3: Distribution (●) of covellite, covellite-chalcopyrite and native copper-cuprite grains.

copper-iron sulphides, iron sulphides and native copper grains is shown in Fig. 5-1. Angular to subangular shaped pyrite grains are more common in the till than in organic soils. Iron content of till samples having visible pyrite grains is greater than 3.1% (Fig. 5-2). No copper-iron or copper sulphide grains were found in deeper till samples although the copper content of the till at station G1.5 is greater than 1300 ppm. Framboidal pyrite occurs at all depths in organic soils from the fibric soil layer to the base of the bog. The framboids appear to be most common in the mesic-humic soil layers and in the upper 10 cm of reduced till. Iron content of organic soils containing pyrite framboids is often higher than soils having no visible concretions. Pyrite abundance in organic soils, however, probably does not exceed 0.1% of the total sample weight.

Occurrence of covellite, covellite-chalcopyrite and native copper grains is more restricted than that of framboidal pyrite (Figs. 5-2;5-3) and these grains are most common above the two depressions in the till-bog interface. Copper mineral grains do not occur in the fibric organic soil layer, but are present in the humic-mesic layers and in the upper 1-2 cm of reduced till underlying the bog. Copper content of soils containing copper mineral grains ranges from 1300 to 2.5% (Fig. 5-3), but there is no apparent relationship between copper in soils and semi-quantitative estimates for abundance of mineral grains. The larger covellite and covellite-chalcopyrite grains (greater than 50  $\mu\text{m}$  across) occur between 1 to 3 m in the organic soil above the two depressions. Grains of native copper rimmed

by cuprite and idiomorphic covellite enclosed by chalcopyrite smaller than  $40\ \mu\text{m}$  occur close to the base of the bog at station G 1.5 at a depth of 2.5 m. Framboidal pyrite partially rimmed by chalcopyrite and covellite (Plate 5-1) also occurs in the same area from station G2 at 2.5 m depth.

#### 5-4 RESULTS OF MICROPROBE ANALYSES OF ORGANIC SOIL FRAGMENTS

Several chemical methods are commonly used to distinguish different modes of trace metal occurrence in soils and other weathered materials. These include the application of oxidizing agents, chelating agents or alkaline solutions which liberate and extract metals bound to the organic fraction in soil. Changes in the character of the humic substances can occur during chemical extraction processes and concentrations of those metals released may not be a true indication of the original form of the metal present in the soil. In situ analysis of soil for metals can be made using the scanning electron microprobe. This method has been used to determine relative abundances of copper, iron and sulphur in dried organic soil fragments from several parts of the bog. Location of the samples from which fragments were obtained and results of analyses for total trace metals and organic carbon are given in Table 5-1.

Results of microprobe analyses indicate that copper may be present in two different associations in the organic soil. A polished section of fragments from sample RL-340 containing 1.11% copper is shown in Plate 5-12. Preserved plant cell structure is clearly visible in this fragment and the reticulate pattern of the cell walls is reflected in the patterns for the  $\text{CuK}\alpha$  and  $\text{SK}\alpha$  X-radiation intensities that are shown in

<u>Sample Number</u>	<u>Location and description</u>	<u>Co</u>	<u>Cu</u>	<u>Fe</u>	<u>Mn</u>	<u>Ni</u>	<u>Zn</u>	<u>Organic Carbon</u>
73-RL-323	300 m south of L5S; 1.5 m depth; Dark brown silty peat.	3	141	0.49	120	29	514	16.4*
73-RL-338	L5S; 1 m depth; Dark brown silty peat.	277	11313	1.81	1821	80	541	22.2*
73-RL-340	L3S; 1 m depth; Dark brown silty peat.	82	11104	1.05	102	61	210	21.2*

Co, Cu, Mn, Ni, Zn are in ppm; Fe and organic carbon are in %

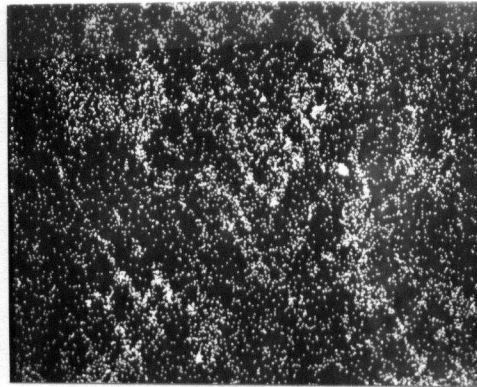
\* Organic carbon determined by Leco method.

Table 5-1: Metals and organic carbon in soil samples used for microprobe analyses.

Plates 5-13 and 5-14. The pattern for the  $\text{FeK}\alpha$  radiation does not, however, correspond to those of copper or sulphur. High  $\text{FeK}\alpha$  radiation intensity (Plate 5-15) from this fragment may be due to iron oxide infilling plant cells. This appears in the polished section (Plate 5-12) as opaque material filling several of the cells. The relative intensities of the copper and sulphur  $\text{K}\alpha$  X-radiation, illustrated by these Plates, suggests that these elements are in some way associated with plant cell walls. No indication of copper and sulphur concentrations associated with the plant structures could be obtained from the analysis. Fragments of soil from a sample containing 141 ppm copper, collected 300 m south east from station L5S were also analysed for copper, iron and sulphur by electron microprobe. Cellular plant structures are also visible in fragments (Plate 5-16) although it is doubtful if the original vegetation is of the same species to that in Plate 5-12. Relative intensities of  $\text{CuK}\alpha$  and  $\text{SK}\alpha$  X-radiation do not correspond to the plant cell structures (Plates 5-17 and 5-19) although the high  $\text{FeK}\alpha$  intensity indicates that iron is abundant in the material.

Small mineral sulphide grains are also visible in amorphous organic matter and this association being best shown by a polished section (Plate 5-20) of a fragment from sample RL-340 containing 1.11% copper. The sulphide grains are less than  $20\mu\text{m}$  diameter and are subangular to rounded shape. Areas of relatively high  $\text{CuK}\alpha$ ,  $\text{FeK}\alpha$  and  $\text{SK}\alpha$  X-radiation correspond to these grains indicate that they are probably chalcopyrite (Plates 5-21, 5-22, 5-23). Sulphide mineral grains were also identified in a fragment from sample RL-338 containing 1.13% copper and are

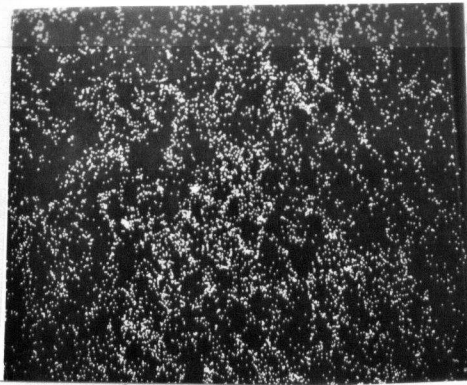
X



X

Plate 5-13: Intensity pattern of CuK $\alpha$  X-radiation in sample 73-RL-340

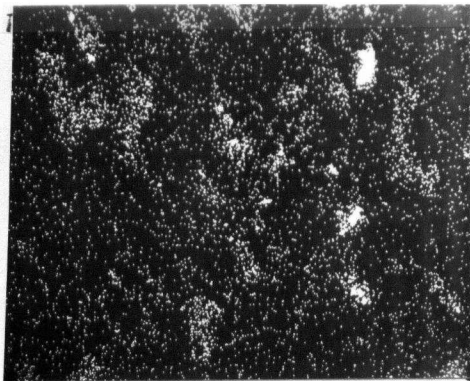
X



X

Plate 5-14: Intensity pattern of SK $\alpha$  X-radiation in sample 73-RL-340

X



X

Plate 5-15: Intensity pattern of FeK $\alpha$  X-radiation in sample 73-RL-340

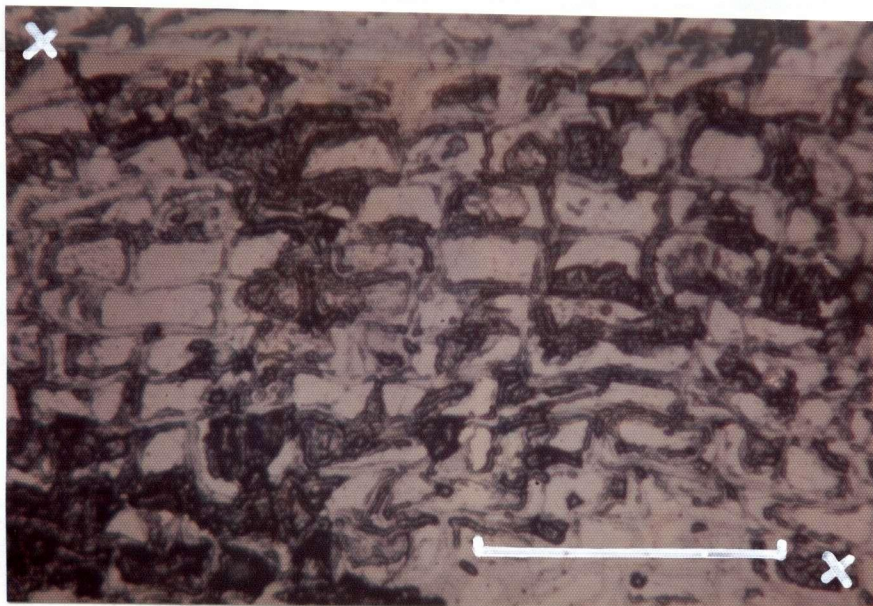
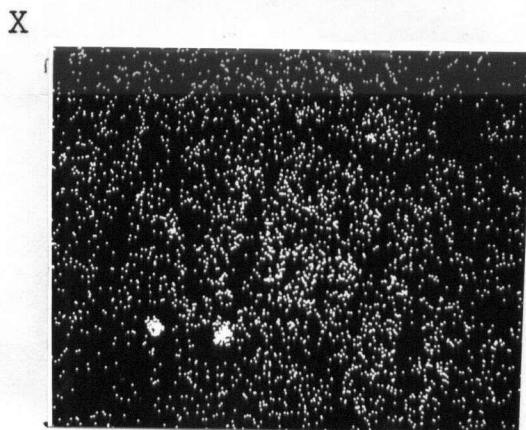
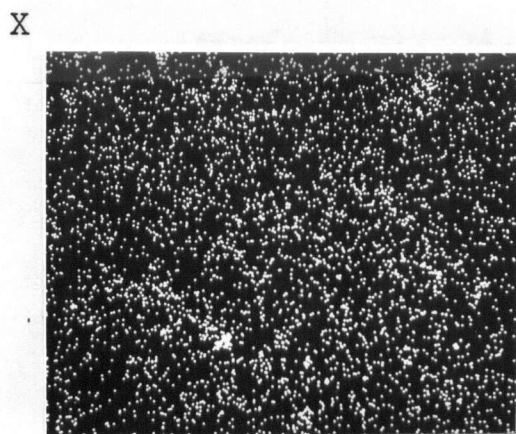


Plate 5-16: Photomicrograph of a polished mount from sample 73-RL-323. The cell structures in this mount may represent root tissue. The bar scale measures 20  $\mu\text{m}$ .



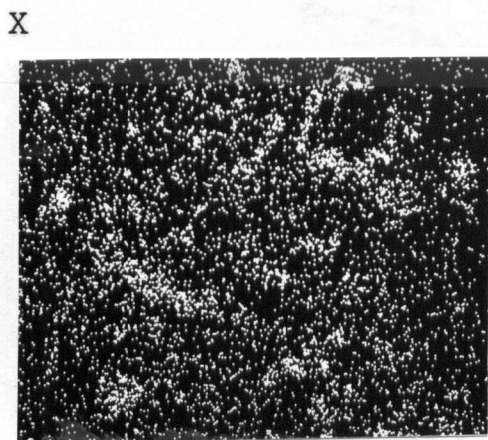
X

Plate 5-17: Intensity pattern of  $\text{CuK}\alpha$  X-radiation in sample 73-RL-323



X

Plate 5-18: Intensity pattern of  $\text{SK}\alpha$  X-radiation in sample 73-RL-323



X

Plate 5-19: Intensity pattern of  $\text{FeK}\alpha$  X-radiation in sample 73-RL-323

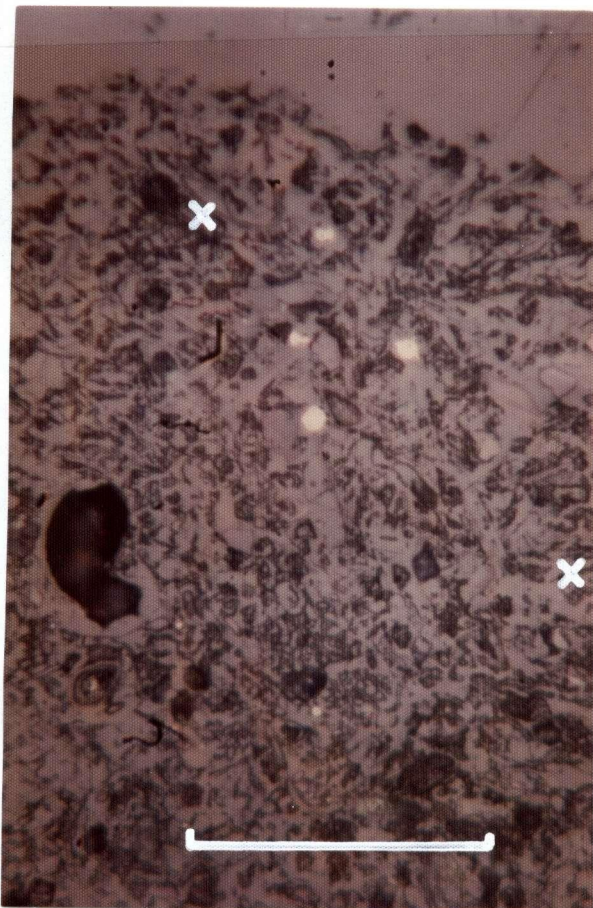


Plate 5-20: Photomicrograph of a polished mount from sample 73-RL-340. Small sulphide granules less than 10  $\mu\text{m}$  across are visible in the fine textured organic matter. The bar scale measures 50  $\mu\text{m}$ .

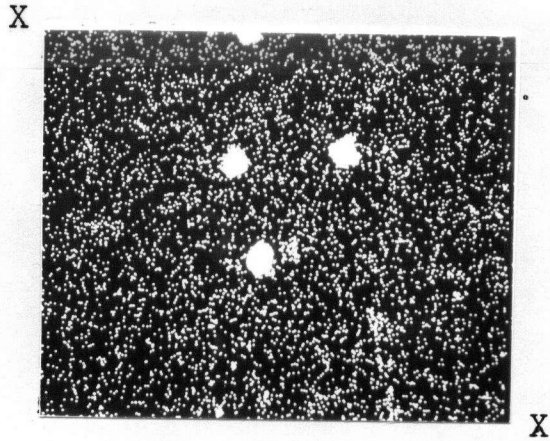


Plate 5-21: Intensity pattern of  $\text{CuK}\alpha$  X-radiation in sample 73-RL-340

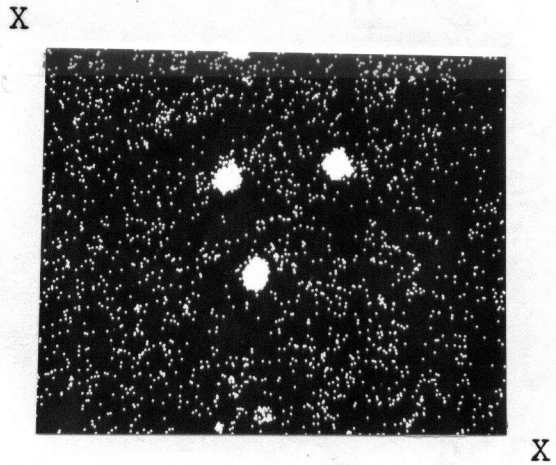


Plate 5-22: Intensity pattern of  $\text{SK}\alpha$  X-radiation in sample 73-RL-340



Plate 5-23: Intensity pattern of  $\text{FeK}\alpha$  X-radiation in sample 73-RL-340

shown in Plates 5-24 to 5-27. Higher  $\text{CuK}\alpha$  and  $\text{SK}\alpha$  radiation intensities also outline a tissue fragment in the section that was probably originally a plant stem. Chalcopyrite grains present in this fragment are in the amorphous organic matter and are not associated with remnant plant structures.

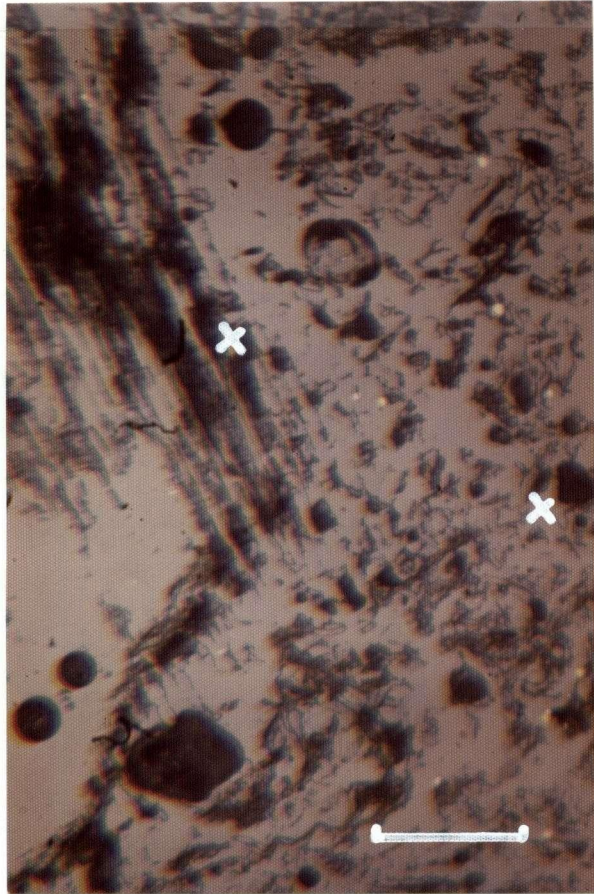
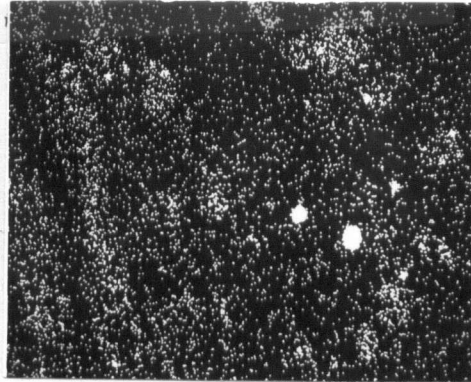


Plate 5-24: Photomicrograph of a polished mount made from sample 73-RL-338. A longitudinal section through a plant stem or a wood fragment is visible on the left hand side of the field. Small sulphide mineral granules are present in fine textured organic matter on the right hand side of the photomicrograph. The bar scale measures 50  $\mu\text{m}$ .

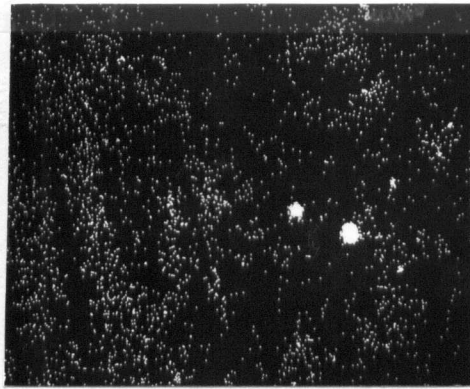
X



X

Plate 5-25: Intensity pattern of  $\text{CuK}\alpha$  X-radiation in sample 73-RL-338

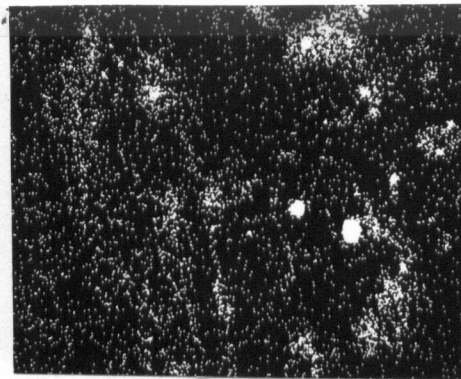
X



X

Plate 5-26: Intensity pattern of  $\text{SK}\alpha$  X-radiation in sample 73-RL-338

X



X

Plate 5-27: Intensity pattern of  $\text{FeK}\alpha$  X-radiation in sample 73-RL-338

## CHAPTER 6

## DISCUSSION

## 6-1 SUMMARY OF RESULTS

Results of geochemical and mineralogical investigations are summarized below.

(1) Organic soils and the Ah horizon of humic gleysolic soil have between 5 and 51% organic carbon. Organic carbon can increase or decrease down profiles and there is a positive correlation of values with HI reducible sulphur.

Organic soil pH ranges from 4.0 to 5.5 and values increase down profiles to more than 7.0 in the deeper, oxidized till.

(2) Copper in A and B mineral soil horizons sharply increases across the boundary between brunisols and humic gleysols whereas cobalt, zinc, nickel, manganese and pH markedly decrease in the Ah horizon of humic gleysolic soil. Low abundances of cobalt, nickel, zinc and manganese are typical in the fibrous organic layer although extremely high manganese, iron and cobalt occurs, locally, in fibrous material at the eastern end of the bog and high molybdenum values are present at the western end of the bog. Humic-mesic layers contain from 0.1 to 2.5% copper and are enriched in cobalt, zinc, nickel and molybdenum. These metals are most abundant where more than 3 m of organic material have accumulated and values generally increase down profiles, but fall sharply in the till. Iron and manganese, however, are higher in the till than in organic soils. Copper content of the till is less than 210 ppm although a small area beneath

the western end of the bog contains up to 0.5% copper.

(3) Cumulative frequency graphs show that cobalt, nickel, zinc, iron, manganese and molybdenum values in soils and till generally follow bimodal, lognormal non-intersecting distributions or unimodal distributions. Organic carbon and pH values are normally distributed. Three lognormal, non-intersecting copper distributions are present in soils and the till. Correlation coefficients for the variation of metals with organic carbon show that a very small proportion of this variation is due to linear relationships. Stronger linear relationships are present, however, between copper and cobalt and between nickel and zinc in soils containing more than 16% organic carbon.

(4) Volcanic ash layers have very low copper and other metals abundances compared to those in surrounding organic soils.

(5) Sphagnum moss contains up to 228 ppm copper compared to less than 20 ppm in Labrador tea leaves.

(6) Subsurface, reducing bog waters generally have lower copper, but higher organic carbon, iron and manganese than surface waters. Surface water from semi-stagnant pools in the western part of the bog commonly has pH less than 5.0 and extremely high dissolved copper content. Underlying subsurface water generally has much less copper except in the western part of the bog where samples from 1.5 m depth have more than 500 ppb copper and up to 16 ppm organic carbon. Biquinoline extracts more than 40% of the copper from surface

water and less than 50% from subsurface water. Seepages from the till and possible faults zones draining into the western end of the bog have up to 290 ppb copper. Seepages draining humic gleysolic soil in this area have up to 590 ppb copper. Water flowing from a diamond drill hole on the northwest side of the bog has no detectable copper, but has high sulphate and calcium levels. Stream waters have more than 400 ppb copper with maximum concentration in the channel at the western end of the bog decreasing to less than 70 ppb at the eastern end of the depression.

(7) Scanning electron microprobe analyses for copper, iron and sulphur distribution in organic soil fragments demonstrates that copper and sulphur are commonly associated with remnant plant cell wall structure. Samples from which the fragments were obtained contained more than 1% copper. Small chalcopyrite grains less than 10 $\mu$ m diameter were also identified by microprobe analysis in the amorphous fraction of organic soil.

(8) Framboidal pyrite, small subangular pyrite grains, native copper grains, chalcopyrite and covellite grains ranging from 10 to 60 $\mu$ m occur in heavy mineral separates of organic soils. Pyrite framboids are occasionally coated with covellite and chalcopyrite. Idiomorphic covellite grains less than 30 $\mu$ m across are rimmed with chalcopyrite. Covellite also occurs as roughly concentric layers in larger chalcopyrite grains which typically have highly irregular outer boundaries. Framboidal pyrite is found in organic

soils throughout the bog. Copper sulphide and native copper grains only occur in the mesic-humic soil layers, above depressions in the till-organic soil interface at the eastern and western ends of the bog.

#### 6-2 DEVELOPMENT OF THE BOG AND ORGANIC DIAGENESIS

The relief catena, described in Chapter 1, consists of brunisolic soils, gleysolic soils and organic soils. Transition from well-drained dystric brunisols to humic gleysols is marked by a line of springs surrounding the bog and the secondary environment changes from the moderately oxidizing, weakly acidic conditions, typical of brunisolic soils, to strongly reducing, moderately acidic conditions in the humic gleysols.

Gleysolic and organic soils form in areas where the soil is periodically or continuously water saturated. The thin organic horizons, typical of mineral soils, are due to microbial oxidation of organic matter proceeding at the same rate as accumulation. Inundation of the soil by water, however, lowers the dissolved oxygen concentration in soil pore water and therefore decreases microbial activity. Due to this decreased activity the net accumulation of organic matter is greater than the rate of oxidation. Accumulation of organic matter in the bog could also be increased by the continuous discharge of mineral rich water favouring abundant growth of a flora dominated by sedges and sphagnum moss. Mature timber growth may be inhibited in areas where thick organic soils are forming due to the absence of nutrients

and toxic copper concentrations in the water (Fraser 1961).

An average rate of organic soil accumulation of 0.3 mm / year can be calculated from the 3 m maximum thickness of material in the bog assumed to have accumulated following final deglaciation of the area at roughly 9300 years B.P. Grosse-Brackmann et al. (1964) determined that the average rate of peat formation in a European bog was 0.4 mm/year. Volcanic ash layers at two depth intervals in humic gleysolic and organic soils suggests that both soils formed contemporaneously, but the shallow Ah horizon of humic gleysols indicates that this organic matter is forming at only 0.01 mm/year compared to the faster rate of organic soil accumulation. The age of each ash layer is uncertain and it is therefore difficult to establish if the rate of organic soil formation has varied through time.

Vertical Eh and pH variations in the bog are due to the thick accumulation of decomposing organic matter. Aerobic bacteria break down organic substrates dissolved in the near surface soil pore water forming carbon dioxide. This process, however, quickly lowers the dissolved oxygen concentration in the deeper, more decomposed soil and will also decrease pore water pH through formation of carbonic acid. An ecological succession of different anaerobic bacteria become active down vertical organic soil profiles due to the progressive decrease in oxygen concentration and the corresponding redox potential change from positive to negative values. These bacteria mediate reduction of

nitrogen to ammonium ion, sulphate to  $H_2S$  and carbon dioxide to methane and hydrogen. Nitrogen reduction can occur within an Eh range from +150 to +200 mv (Bell, 1969). Sulphate reduction, however, will proceed when redox potential are more negative than -100 mv and methane forms when the redox potential is more negative than -300 mv (Cappenburge 1974; Bell 1969).

The presence of detectable  $H_2S$  in freshly sampled organic soil and water from vertical profiles through the Central bog indicates that the redox potential of the moderately decomposed organic material is more negative than -200 mv. Measured Eh of water saturated organic soil and of one subsurface water sample ranged from -200 to -250 mv. Reduction of carbon dioxide to methane and buffering action by dissolved calcium, magnesium and basic amines (Berner 1968) could explain the higher pH of the subsurface bog water compared to that of surface water. Values ranging from 6.0 to 7.2 in the subsurface waters are similar to the pH of reduced organic material in a river bog studied by Postma (1977). Oxidation reactions could occur simultaneously with microbial reductions especially close to the boundary separating oxidizing from reducing conditions. Small accumulations of a white precipitate on the bottom of shallow surface pools, identified as sulphur, represent the oxidation of  $H_2S$  diffusing from deeper reduced soil.

### 6-3 ACCUMULATION OF METALS IN ORGANIC SOILS

Horizontal and vertical variations of metals in soils, water, till and vegetation have been described in Chapter 4 with the object of establishing mechanisms for metal migration and concentration in the bog and probable sources for the metals. Chemical and physical adsorption can remove transition metals from dilute solutions migrating through the organic soils. Minerals such as carbonates, hydroxides and sulphides may be precipitated or dissolved due to changes in pore water chemistry or abundance of dissolved organic matter in the water (Rashid and Leonard 1973). High metal contents could therefore be due to both organic or inorganic interactions and the relative importance of these processes must be established to explain the metal distribution patterns found in the bog.

Several mechanisms, reviewed in Chapter 1, have been proposed to account for high metal values commonly found in natural organic accumulations. Goodman and Cheshire (1973) established experimentally that metals could be strongly bound to nitrogen associated with heterocyclic groups present in soil organic matter. Organic soils, however, typically have low nitrogen contents suggesting that a large proportion of the metal is associated with other components and numerous studies have shown that humic substances can play a major role in concentrating transition elements. These substances are complex natural polymers thought to exist in two basic forms known as humic and fulvic acid fractions. Although

humic and fulvic acid fractions probably have different polymer structure and shape they have similar chemical reactions with metals. Both fractions are abundant in organic soil and Given and Dickenson (1975), for example, reported that peat formed from decomposing forest vegetation contained from 30 to 70% humic substances. Undecomposed sphagnum moss forming the fibric organic layer, however, was found to have less than 10% humic substances.

Reactions between metals and soil organic matter will depend on the physical nature of humic fractions, the relative stability of the fractions and their abundance. Fulvic acid fractions are more water soluble than are humic acid fractions and may represent a large proportion of the dissolved organic carbon content of bog waters (Reuter and Perdue 1977). Both humic and humic acid fractions have been shown to exist in dispersed or peptized colloidal states. The colloids are dispersed through mutual repulsion due to a net negative charge originating from ionized function groups. This charge can be neutralized by metal ions resulting in coagulation of the humic and fulvic acid fractions (Van Dijk 1971; Ong and Bisque 1968). Changes in pore water chemistry could therefore have a marked effect on the translocation of humic and fulvic acid fractions in organic soils.

Reactions can also involve ion exchange, surface adsorption and chelation (Kahn 1969). Many workers have investigated the relative stabilities of complexes thought

to form when metals are bound to humic or fulvic acid fraction exchange sites. Schnitzer and Hanson (1970), Schnitzer and Skinner (1967), Gamble and Schnitzer (1973) demonstrated that the relative stability of the metal-fulvate complexes decreased in the order of  $Fe > Ni > Co = Pb > Cu > Zn > Mn > Ca$ . Kahn (1969) found that metal-humate complexes follow a similar sequence of stabilities where  $Fe > Al > Cu > Zn > Ni > Co > Mn$ . Complex stabilities are generally determined by reacting metals with humic or fulvic acids which have been extracted from soil using alkaline solutions. This process may change the structure of the humic substance and the number of available cation exchange sites. As a result retention of metals by the extracted humic substances can be different from that of the untreated raw material (Davis et al. 1969). Reaction between metals and extracted humic substances may also vary with different types of soil used to provide the extracts (Cross 1975). Reported stabilities for metal-humate and metal-fulvates can therefore only be used to indicate the relative affinities of the metals for soil organic matter due to the variations introduced by the extraction methods.

The maximum amount of copper that could be adsorbed by organic materials in the bog can be estimated from the results of experiments made by Ong and Swanson (1966). They measured the copper content of peat samples after these had been immersed in solutions with concentrations ranging from 1 to 1500 ppm copper. Copper content of peat placed in solutions with more than 1500 ppm copper was found to be

1%. Using solutions with less than 50 ppm, however, they found that copper enrichment in the peat at a pH of 4.5 was by a factor of 200. Peat immersed in a solution containing 1 ppm copper, for example, will adsorb a total of 200 ppm copper. The authors also found that the adsorption capacity of peat increased after removal of humic acid and concluded that reactions of copper with peat involved both surface adsorption and ion exchange.

Subsurface bog waters have been found, locally, to contain more than 1 ppm dissolved copper. Organic matter would adsorb up to 200 ppm copper from this dilute solution based on the enrichment factor given by Ling Ong and Swanson (1966). Dried soil samples from the bog typically have more than 2% copper and freshly sampled organic material has more than 90% water content. A copper content of 2% in a dry sample is therefore equivalent to 2000 ppm in the original, water saturated material. This value is ten times greater than the estimated maximum of 200 ppm which could theoretically be concentrated through adsorption. This difference could be explained by soil pore water copper concentrations higher than those found in subsurface bog water, formation of complexes by mechanisms other than adsorption or the presence of authigenic copper minerals in the soil.

Other metals will be adsorbed from dilute bog water solutions and this accumulation will depend on the concentration of metals in the water and the relative affinity

of metals for the organic matter. Concentration of metals could reflect the relative strength of complexes formed with humic and fulvic acid fractions. Correlation coefficients calculated for metals, organic carbon and pH in soils containing more than 16% organic carbon indicate a moderate linear relationship of nickel with zinc. The copper-cobalt relationship can be compared to the similarity between copper-fulvate and cobalt-fulvate complex stabilities although the difference between nickel-fulvate and zinc fulvate stabilities does not explain the strong relationship between these metals. The stabilities of nickel-humate and zinc-humate complexes are, however, similar. Relatively weak manganese-humate complexes could explain low manganese levels in the mesic-humic organic soil layers. Although metal associations suggest that complexes have formed with humic and fulvic acid fractions, the size and shape of distribution patterns will also depend on the stability of the humic substances and the chemistry of water flowing through the bog.

Correlation coefficients indicate that there are no linear relationships between metals and organic carbon in the bog. This could be due to the large surface area available for metal adsorption, low metal concentrations in aqueous solutions migrating through the organic material, dilution of decomposing organic soil by material from the area surrounding the bog (Garrett and Hornbrook 1976) or very large differences between ranges of metal and organic carbon

values used to calculate the correlation coefficient matrix.

Probability graphs for cobalt, nickel, zinc and molybdenum in organic soils have the form of bimodal, non-intersecting distributions reflecting metal abundances associated with the different soil layers. High cobalt, nickel, zinc and molybdenum concentration ranges (population 'A') can be explained by accumulation of metals through adsorption and other processes in the mesic-humic layers. The very low cobalt, nickel and zinc values (population 'B') reflect metal associated with the fibrous organic layer. These low concentrations, in contrast to the enhanced values in the underlying humic-mesic layers, suggest that cobalt, zinc and nickel are not adsorbed by the organic material and may be desorbed due to the high concentration of hydrogen ions in the surface water pools. Three populations can be partitioned from the distribution graph for copper in organic soil although there is considerable overlap of values representing each population. The separate copper distributions could reflect presence of different metal associations in the soil. Values greater than 1.3% copper (population 'A') are found chiefly in the mesic-humic layers above the depressions in the till-organic soil interface.

Extremely high, local concentrations of iron, manganese and molybdenum in the fibrous organic layer contrast sharply to the low metal abundances typical of this material. Clearly processes other than interaction with organic substances are responsible for concentration of these metals.

The high molybdenum in the fibrous layer at the western end of the bog can be explained by formation of readily immobilized acid molybdenate ions ( $\text{HMoO}_4^-$ ) in acid bog surface water. Accumulation of molybdenum in deeper, humic-mesic layers is probably due to precipitation of molybdenum sulphide in the reducing organic material. Extremely high manganese and iron in fibrous material at the eastern end of the bog could be the result of secondary hydrous oxide formation. Colloidal iron hydroxide commonly occurs on the bog surface and especially in an area surrounding small seepages at the eastern end of the bog. No manganese oxides were found although these have been described as coatings on clastic material in streams draining marshy areas elsewhere (Horsnail *et al.* 1969).

Although no systematic studies were made to establish the form of manganese in the fibrous layer, a small number of stream sediments from the bog were treated with 1M strength hydroxylamine hydrochloride solution. The stream sediments are from the eastern end of the bog close to station L5S and contain up to 12360 ppm Mn, 14980 ppm Cu, 980 ppm Co. Hydroxylamine hydrochloride extracted more than 65% of the manganese, but less than 9% of the copper and only 4% of the cobalt. These proportions suggest that a relatively high proportion of manganese is present in the form of a secondary oxide, but that the copper and cobalt are mainly associated with organic matter or other components in the organic soil (Chao, 1972; Carpenter *et al.*, 1975; 1977).

Garrels and Christ (1964) demonstrated that manganite and hematite are stable minerals in aqueous solutions where  $\text{Fe}^{2+}$  and  $\text{Mn}^{2+}$  concentrations exceed  $10^{-4}\text{M}$ , pH is greater than 6.0 and the Eh is more positive than +200 mv. Moreover, although oxidation of  $\text{Mn}^{2+}$  to  $\text{MnO}_2$  is inhibited below pH 8.5 and oxidation of  $\text{Fe}^{2+}$  to  $\text{Fe}_2\text{O}_3$  is very slow below pH of 6.0, high concentrations of  $\text{Co}^{2+}$  and  $\text{Cu}^{2+}$  in the water will greatly increase these oxidation rates (Stumm and Morgan 1970). Ferric hydroxide commonly forms in oxidized environments through activity of iron bacteria such as Gallionella. Other bacteria such as Metallogenium are known to mediate oxidation of  $\text{Mn}^{2+}$  to  $\text{Mn}^{4+}$ .

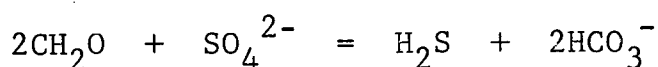
Dissolved manganese concentrations greater than 200 ppb and dissolved iron concentrations exceeding 2 ppm are found in several of the subsurface bog water samples. These high values are in contrast to very low levels of Fe and Mn typical of surface waters. The large local concentrations of iron and manganese in the fibrous layer at the eastern end of the bog may be explained by discharge of metal rich water onto the bog surface. Oxidation of  $\text{Fe}^{2+}$  and  $\text{Mn}^{2+}$ , catalysed by the high dissolved copper content of the surface water and by activity of bacteria, may be involved in formation of immobile hydrous oxides. The high cobalt values found in the fibrous material at the eastern end of the bog may, however, be due to local adsorption on organic matter rather than adsorption onto the surface of secondary oxides.

#### 6-4 BOG WATER CHEMISTRY

Surface water samples have a markedly different trace metal chemistry compared to that of subsurface water samples. Moderately to strongly acid surface waters have abundant copper, but low concentrations of iron, manganese, and zinc. Subsurface waters, however, are weakly acid to neutral and generally have low copper, but higher iron, manganese and dissolved organic carbon values than do surface waters. Zinc, calcium and sulphate contents show little vertical variation compared to large concentration gradients typical of other elements. Although copper values are much lower in subsurface waters than in surface water contents greater than 1 ppm occur at 1.5 m depth above an area of copper-rich till at the western end of the bog. Vertical chemical gradients found in the bog could reflect metal rich ground water discharging from the till-organic soil interface, variations in the soil-water flow rate (Sperling 1965), variations in ionic diffusion rates (Berner, 1971) and chemical changes in the system due to processes of organic diagenesis.

Dissolved sulphide concentrations, Eh and pH will be important factors influencing the solubility of minerals in water saturated organic soil. Sulphide ion activity in reducing, subsurface bog water was not measured during the investigation and dissolved sulphate contents represent original sulphate content plus sulphate derived from post sampling oxidation of ionic species such as  $\text{H}_2\text{S}$ ;  $\text{HS}^-$ ;  $\text{S}^{2-}$ ;

$S_2O_3^{2-}$ . The maximum possible concentration of hydrogen sulphide formed through biological reduction of sulphate can be calculated from dissolved sulphate and organic matter contents where the rate of sulphate reduction will be limited by the available sulphate and the available organic substrate. The most common organic substrates in natural waters are carbohydrates and amino acids which are oxidized in the following reaction proposed by Ramm and Bella (1968).



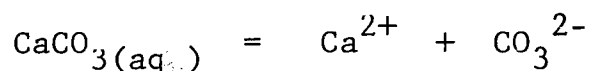
Three mg of sulphate would be reduced to 1 mg of  $H_2S$  and 0.75 mg of carbohydrate would be oxidized in this reaction.

Less than 10% of the total dissolved organic matter in natural waters has been estimated to be in the form of carbohydrates and amino acids (Midwood and Felbeck 1968). The most abundant form of organic matter in filtered natural water samples has been found to be the fulvic acid fraction (Reuter and Perdue 1977). Central bog water samples having more than 10 ppm dissolved organic carbon could contain between 1 and 2 ppm carbohydrate which could be oxidized, by bacteria, to produce 1 ppm ( $10^{-4}M$ ) hydrogen sulphide through the reduction of 3 ppm of sulphate. Concentrations of  $S^{2-}$  and  $HS^-$  will depend on Eh and pH and will generally be very small compared to the concentration of dissolved hydrogen sulphide. Measured dissolved sulphide ion concentrations in reducing, water saturated lake sediments range from  $10^{-8}M$  (Timperly and Allan 1974) to  $10^{-12}M$  at pH 7.5 (Emerson 1976).

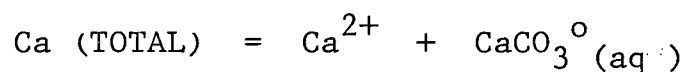
## 6-5 THEORETICAL MODELS FOR WATER CHEMISTRY AND PREDICTION OF MINERAL SOLUBILITIES.

The distribution of ionic and complexed species from natural water compositions can be calculated using thermodynamic data for all possible chemical equilibria in the water. Various models have been proposed to predict elemental distribution in sea water (Garrels and Thompson 1962), the distribution of organic species in sea water (Thorstenson 1976) and the distribution of simple organic complexes in sea water (Gardner 1974). The basic principles underlying the calculations have been described by Garrels and Christ (1965) and involve the following stages.

- (1) Define all possible interactions between cations and anions; eg.,



- (2) Write mass balance equations for each component present; eg.,



- (3) Calculate concentration of the *i*th component from mass action equations written in terms of the appropriate equilibrium constants ( $K_i$ ), molalities ( $m_i$ ) and activity coefficients ( $\gamma_i$ ); eg.,

$$\frac{(m\text{Ca}^{2+} \gamma\text{Ca}^{2+}) (m\text{CO}_3^{2-} \gamma\text{CO}_3^{2-})}{(m\text{CaCO}_3 \gamma\text{CaCO}_3)} = K$$

Mass action equations can generally be simplified in fresh water chemical models by assuming that the activity coefficient  $\gamma$  is unity.

(4) Substitute mass action equations in the mass balance equations and simultaneously solve these in terms of total element concentrations; eg.,

Ca (TOTAL), C (TOTAL), Cu(TOTAL), S(TOTAL)

Species distributions for six subsurface central bog water samples (74-RL-1428, 1429, 1439, 1442, 1443 and 1444) were calculated from total dissolved copper, zinc, iron, manganese, bicarbonate, sulphate and sulphide concentrations, pH and oxygen fugacity by the program DISTRIB written by Brown and Perkins (1977) on the UBC IBM 370/168 computer.

Several assumptions have been made in calculating the species distributions for the bog waters.

(1) The first assumption is that the chemical equilibria models include all major ions and complexes and account for all reactions between these species. Most models, however, will be simplified because elements such as magnesium, sodium, nickel and cobalt, inorganic complexes such as  $\text{CuOH}^+$  and  $\text{Cu}(\text{OH})_3^-$  and metal-organic complexes such as copper-humic acid fraction associations could exist in a natural system but, due to the paucity of analytical and thermodynamic data, they have been excluded from the models.

(2) The system is assumed to represent an equilibrium state and no interactions occur between solid and aqueous phases. This assumption may be made if the models are applied to a small volume of bog water. In the natural state it is unlikely that the macro system will approach equilibrium due to the different rates of biological reactions. Moreover metals will be removed from solution by precipitation as sulphides, oxides

and carbonates or by adsorption to organic matter or adsorption to particulate iron hydroxide.

(3) The system is assumed to be closed and no material transfers occur into or out of the aqueous phase other than those dissolved elements specified as solution constraints.

Solution constraints used in calculating species distributions are the copper, zinc, iron, manganese, calcium and sulphate values obtained by analysis of filtered, subsurface water samples and given in Table 4-9. Although no subsurface water samples were analysed for bicarbonate this anion was measured in a small number of seepage water samples from the transition between the humic gleysolic soil and organic soils. These samples contained less than 10 ppm bicarbonate ( $2 \times 10^{-4} \text{M}$ ) and this concentration was entered as an additional solution constraint in the models.

A number of preliminary calculations were carried out using DISTRIB to establish the probable range of oxygen activity by assuming that solid chalcopyrite and pyrite were in equilibrium with an aqueous solution equivalent to the composition of water sample 74-RL-1429. The two solid phases were substituted for total dissolved copper and iron as solution constraints in the distribution of species calculations which were repeated at Log oxygen activities of -66.5, -66.0 and -65.5. Equilibrium constants (Log K) and reaction quotients (Log Q) for several, common copper, iron, and zinc sulphides, oxides and carbonates are calculated by the program DISTRIB. Equilibrium constants are based on free energy changes associated with mineral formation whereas reaction quotients are determined from equilibrium

DISTRIBUTION OF SPECIES FOR WATER SAMPLE 73-RL-1429 IN  
# 1429 IN THE PRESENCE OF 1 GR CP AND PY

DISTRIBUTION OF SPECIES CALLED AT STEP 0

AQUEOUS SPECIES

SPECIES	MOLALITY	LOG MOL	ACTIVITY	LOG ACT	ACT COEF	LG ACT C	GRAMS/KGM H2O	PPM	LOG PPM
CA++	0.30259E-03	-3.519	0.26022E-03	-3.595	0.85498E+00	-0.066	0.12128E-01	12.127	1.084
FE++	0.27910E-07	-7.554	0.24002E-07	-7.620	0.85998E+00	-0.066	0.15587E-05	0.002	-2.807
FE+++	0.52231E-22	-22.282	0.37583E-22	-22.425	0.71956E+00	-0.143	0.29169E-20	0.000	-17.535
CU+	0.41730E-15	-15.379	0.40150E-15	-15.396	0.96168E+00	-0.017	0.26528E-13	0.000	-10.576
CU++	0.14293E-19	-19.845	0.12292E-19	-19.910	0.85998E+00	-0.066	0.90818E-18	0.000	-15.042
S--	0.34847E-17	-17.458	0.29919E-17	-17.524	0.85859E+00	-0.066	0.11173E-15	0.000	-12.952
SO4--	0.27033E-03	-3.567	0.23215E-03	-3.634	0.85718E+00	-0.067	0.26016E-01	26.015	1.415
CO3--	0.34107E-08	-8.467	0.29260E-08	-8.534	0.85789E+00	-0.067	0.20467E-06	0.000	-3.689
DH-	0.10690E-07	-7.971	0.10285E-07	-7.938	0.96208E+00	-0.017	0.18182E-06	0.000	-3.740
H+	0.10371E-05	-5.984	0.10000E-05	-6.000	0.96419E+00	-0.016	0.10454E-05	0.001	-2.981
H2O	0.55508E+02	1.744	0.99999E+00	-0.000	0.18015E-01	-1.744	0.10000E+04	999948.132	6.000
O2(AQ)	0.33881E-69	-69.470	0.33881E-69	-69.470	0.10000E+01	0.0	0.10842E-67	0.000	-64.965
CACO3	0.95365E-09	-9.021	0.95395E-09	-9.020	0.10003E+01	0.000	0.95450E-07	0.000	-4.020
CASO4	0.10149E-04	-4.994	0.10153E-04	-4.993	0.10003E+01	0.000	0.13817E-02	1.382	0.140
H2SO4-	0.22955E-07	-7.639	0.22089E-07	-7.656	0.96229E+00	-0.017	0.22282E-05	0.002	-2.652
HS-	0.23537E-09	-9.628	0.22644E-09	-9.645	0.96208E+00	-0.017	0.77841E-08	0.000	-5.109
H2S	0.23441E-08	-8.630	0.23449E-08	-8.630	0.10003E+01	0.000	0.79888E-07	0.000	-4.098
HCO3-	0.64590E-04	-4.190	0.62167E-04	-4.206	0.96248E+00	-0.017	0.39411E-02	3.941	0.596
H2CO3	0.13541E-03	-3.868	0.13545E-03	-3.868	0.10003E+01	0.000	0.83986E-02	8.398	0.924
FE(OH)+	0.13870E-08	-8.858	0.13347E-08	-8.875	0.96229E+00	-0.017	0.10105E-06	0.000	-3.995

IONIC STRENGTH = 0.117973E-02

ELECTRICAL BALANCE = 0.484106E-13

GASES

-----

NAME	LOG K	ACTIVITY	LOG ACTIVITY
OXYGEN GAS	0.0	0.31623E-66	-66.50000
CARBON DIOXIDE	-7.83540	0.42556E-02	-2.37163
STEAM	1.50517	0.31248E-01	-1.50518
SULFUR GAS	192.34951	0.76212E-24	-24.11798
HYDROGEN SULFIDE	125.01049	0.22660E-07	-7.64473
HYDROGEN GAS	41.66022	0.33884E-08	-8.41023
METHANE	135.90718	0.76978E-13	-13.11363

Table 6-1: Distribution of aqueous species in water sample 74-RL-1429 at Log oxygen activity of -66.5.

DISTRIBUTION OF SPECIES FOR WATER SAMPLE 73-RL-1429 IN  
# 1429 IN THE PRESENCE OF 1 GR CP AND PY

DISTRIBUTION OF SPECIES CALLED AT STEP 0

AQUEOUS SPECIES

SPECIES	MOLALITY	LOG MOL	ACTIVITY	LOG ACT	ACT COEF	LG ACT C	GRAMS/KGM H2O	PPM	LOG PPM
CA++	0.30107E-03	-3.521	0.25891E-03	-3.537	0.85997E+00	-0.066	0.12067E-01	12.066	1.082
FE++	0.15689E-05	-5.804	0.13492E-05	-5.870	0.85997E+00	-0.066	0.87620E-04	0.088	-1.057
FE+++	0.39154E-20	-20.407	0.28173E-20	-20.550	0.71954E+00	-0.143	0.21866E-18	0.000	-15.660
CU+	0.52674E-15	-15.254	0.53540E-15	-15.271	0.96167E+00	-0.017	0.35375E-13	0.000	-10.451
CU++	0.25417E-19	-19.595	0.21858E-19	-19.660	0.85997E+00	-0.066	0.16150E-17	0.000	-14.792
S--	0.34853E-18	-18.458	0.29925E-18	-18.524	0.85858E+00	-0.066	0.11175E-16	0.000	-13.952
SO4--	0.27088E-03	-3.567	0.23219E-03	-3.634	0.85717E+00	-0.067	0.26021E-01	26.020	1.415
CO3--	0.34107E-08	-8.467	0.29260E-08	-8.534	0.85788E+00	-0.067	0.20467E-06	0.000	-3.689
OH-	0.10690E-07	-7.971	0.10285E-07	-7.988	0.96208E+00	-0.017	0.18182E-06	0.000	-3.740
H+	0.10371E-05	-5.984	0.10000E-05	-6.000	0.96418E+00	-0.016	0.10454E-05	0.001	-2.931
H2O	0.55508E+02	1.744	0.99999E+00	-0.000	0.18015E-01	-1.744	0.10000E+04	999948.103	6.000
O2(AQ)	0.10714E-68	-68.970	0.10714E-68	-68.970	0.10000E+01	0.0	0.34284E-67	0.000	-64.465
CACO3	0.94882E-09	-9.023	0.94913E-09	-9.023	0.10003E+01	0.000	0.94967E-07	0.000	-4.022
CASO4	0.10100E-04	-4.996	0.10103E-04	-4.996	0.10003E+01	0.000	0.13750E-02	1.375	0.133
HSO4-	0.22959E-07	-7.639	0.22093E-07	-7.656	0.96228E+00	-0.017	0.22286E-05	0.002	-2.652
HS-	0.23251E-10	-10.628	0.22648E-10	-10.645	0.96208E+00	-0.017	0.77855E-09	0.000	-6.109
H2S	0.23446E-09	-9.630	0.23453E-09	-9.630	0.10003E+01	0.000	0.79903E-08	0.000	-5.097
HCO3-	0.64590E-04	-4.190	0.62167E-04	-4.206	0.96248E+00	-0.017	0.39411E-02	3.941	0.596
H2CO3	0.13541E-03	-3.868	0.13545E-03	-3.868	0.10003E+01	0.000	0.83986E-02	8.398	0.924
FE(OH)+	0.77971E-07	-7.108	0.75030E-07	-7.125	0.96228E+00	-0.017	0.56805E-05	0.006	-2.246

IONIC STRENGTH = 0.117990E-02

ELECTRICAL BALANCE = 0.145868E-13

GASES

-----

NAME	LOG K	ACTIVITY	LOG ACTIVITY
OXYGEN GAS	0.0	0.10000E-65	-66.00000
CARBON DIOXIDE	-7.83540	0.42556E-02	-2.37103
STEAM	1.50517	0.31248E-01	-1.50518
SULFUR GAS	192.34951	0.24109E-25	-25.61782
HYDROGEN SULFIDE	125.01049	0.22664E-08	-8.64466
HYDROGEN GAS	41.66022	0.21866E-08	-8.66023
METHANE	135.90718	0.76978E-14	-14.11363

Table 6-2: Distribution of aqueous species in water sample 74-RL-1429 at Log oxygen activity of -66.0.

DISTRIBUTION OF SPECIES FOR WATER SAMPLE 73-RL-1429 IN  
# 1429 IN THE PRESENCE OF 1 GR CP AND PY

DISTRIBUTION OF SPECIES CALLED AT STEP 0

AQUEOUS SPECIES

SPECIES	MOLALITY	LOG MOL	ACTIVITY	LOG ACT	ACT COEF	LG ACT C	GRAMS/KGM H2O	PPM	LOG PPM
CA++	0.21569E-03	-3.664	0.13625E-03	-3.730	0.85951E+00	-0.066	0.86851E-02	8.685	0.939
FE++	0.86596E-04	-4.063	0.74430E-04	-4.128	0.85951E+00	-0.066	0.48361E-02	4.836	0.684
FE+++	0.28836E-18	-18.540	0.20725E-18	-18.683	0.71873E+00	-0.143	0.16104E-16	0.000	-13.793
CJ+	0.74253E-15	-15.129	0.71397E-15	-15.146	0.96153E+00	-0.017	0.47181E-13	0.000	-10.326
CU++	0.45223E-19	-19.345	0.33869E-19	-19.410	0.85951E+00	-0.066	0.28735E-17	0.000	-14.542
S--	0.35209E-19	-19.453	0.30213E-19	-19.520	0.85811E+00	-0.066	0.11289E-17	0.000	-14.947
SO4--	0.27364E-03	-3.563	0.23443E-03	-3.630	0.85669E+00	-0.067	0.26286E-01	26.285	1.420
CO3--	0.34125E-08	-8.467	0.29259E-08	-8.534	0.85740E+00	-0.067	0.20478E-06	0.000	-3.689
OH-	0.10692E-07	-7.971	0.10285E-07	-7.988	0.96195E+00	-0.017	0.18184E-06	0.000	-3.740
H+	0.10373E-05	-5.984	0.10009E-05	-6.000	0.96406E+00	-0.016	0.10455E-05	0.001	-2.991
H2O	0.55508E+02	1.744	0.99999E+00	-0.000	0.18015E-01	-1.744	0.10000E+04	999946.540	6.000
O2(AQ)	0.33881E-68	-68.470	0.33881E-68	-68.470	0.10000E+01	0.0	0.10842E-66	0.000	-63.965
CACU3	0.68253E-09	-9.166	0.68274E-09	-9.166	0.10003E+01	0.000	0.68314E-07	0.000	-4.166
CASO4	0.73355E-05	-5.135	0.73379E-05	-5.134	0.10003E+01	0.000	0.99867E-03	0.999	-0.001
HSO4-	0.23183E-07	-7.635	0.22306E-07	-7.652	0.96215E+00	-0.017	0.22504E-05	0.002	-2.648
HS-	0.23771E-11	-11.624	0.22857E-11	-11.641	0.96195E+00	-0.017	0.78617E-10	0.000	-7.105
H2S	0.23672E-10	-10.626	0.23679E-10	-10.626	0.10003E+01	0.000	0.80673E-09	0.000	-6.093
HCO3-	0.64596E-04	-4.190	0.62164E-04	-4.206	0.96235E+00	-0.017	0.39415E-02	3.941	0.596
H2CO3	0.13540E-03	-3.868	0.13544E-03	-3.868	0.10003E+01	0.000	0.83982E-02	8.398	0.924
FE(OH)+	0.43019E-05	-5.366	0.41391E-05	-5.383	0.96215E+00	-0.017	0.31341E-03	0.313	-0.504

IONIC STRENGTH = 0.11885E-02

ELECTRICAL BALANCE = -0.387176E-11

GASES

-----

NAME	LOG K	ACTIVITY	LOG ACTIVITY
OXYGEN GAS	0.0	0.31623E-65	-65.50000
CARBON DIOXIDE	-7.83540	0.42555E-02	-2.37105
STEAM	1.50517	0.31248E-01	-1.50518
SULFUR GAS	192.34951	0.77717E-27	-27.10949
HYDROGEN SULFIDE	125.01049	0.22883E-09	-9.64049
HYDROGEN GAS	41.66022	0.12296E-08	-8.91023
METHANE	135.90718	0.76975E-15	-15.11365

Table 6-3: Distribution of aqueous species in water sample 74-RL-1429 at Log oxygen activity of -65.5.

<u>Log oxygen activity</u>		<u>-66.5</u>		<u>-66.0</u>		<u>-65.5</u>	
<u>MINERAL</u>	<u>Log K</u>	<u>Log Q</u>	<u>Log K</u>	<u>Log Q</u>	<u>Log K</u>	<u>Log Q</u>	
Bornite	167.18	168.23*	167.18	166.73	167.18	165.24	
Chalcocite	83.79	84.11*	83.79	83.37	83.79	82.62	
Chalcopyrite	0.0	0.0	0.0	0.0	0.0	0.0	
Covellite	84.82	84.12	84.82	83.87	84.82	82.62	
Cuprite	-16.36	-33.25	-16.36	-33.0	-16.36	-32.75	
Hematite	-431.68	-436.21	-431.68	-432.46	-431.68	-428.73*	
Magnetite	-629.39	-637.69	-629.39	-632.20	-629.39	-626.72*	
Native Copper	4.84	0.0	4.84	0.0	4.84	0.0	
Pyrite	0.0	0.0	0.0	0.0	0.0	0.0	
Siderite	-208.26	-211.69	-208.26	-209.94	-208.26	-208.20*	

Table 6-4: Equilibrium constants (Log K) and reaction quotients (Log Q) for water sample 74-RL-1429 at Log oxygen activities of -66.5, -66.0 and -65.5 and at 25°C in the presence of solid chalcopyrite and pyrite. Oversaturation of minerals compared to equilibrium conditions is indicated by \* . Solution constraints are  $\text{SO}_4^{2-}$ ,  $\text{HCO}_3^-$ ,  $\text{Ca}^{2+}$ ,  $\text{H}^+$  and Log oxygen activity. Distribution of species are balanced on  $\text{Ca}^{2+}$  ion.

concentration of the reactants and products and the difference between Log K and Log Q values is an indication of the degree of mineral saturation in the solution.

Distribution of species in water sample 74-RL-1429; Log K and Log Q values at Log oxygen activities of -66.5, -66.0 and -65.5 are given in Tables 6-1, 6-2, 6-3 and 6-4. Results of these calculations indicate that, when chalcopyrite and pyrite are assumed to be in equilibrium with the solution at Log oxygen activity of -66.5, bornite and chalcocite are oversaturated and covellite slightly undersaturated (Table 6-4). Concentration of iron ( $\text{Fe}^{2+} + \text{Fe}^{3+}$ ) in solution is less than  $10^{-8}\text{M}$ , sulphide ion is below  $10^{-18}\text{M}$  and copper concentration ( $\text{Cu}^+ + \text{Cu}^{2+}$ ) is less than  $10^{-16}\text{M}$  (Table 6-1). Bornite and chalcocite are undersaturated when Log oxygen activity is increased from -66.5 to -66.0 (Table 6-4) and the iron concentration ( $\text{Fe}^{2+} + \text{Fe}^{3+}$ ) is increased to  $10^{-6}\text{M}$  (88 ppb). The concentration of sulphide ion, however, is decreased to  $10^{-19}\text{M}$ . (Table 6-2). Magnetite, hematite and siderite are oversaturated in solution when Log oxygen activity is increased from -66.0 to -65.5 and the predicted equilibrium iron concentration ( $\text{Fe}^{2+} + \text{Fe}^{3+}$ ) of  $8.65 \times 10^{-3}$  (4836 ppb) greatly exceeds measured total dissolved iron (172 ppb) in the water sample 74-RL-1429. (Table 6-3). Equilibrium copper concentration ( $\text{Cu}^+ + \text{Cu}^{2+}$ ) is relatively constant at  $10^{-16}\text{M}$  despite variations of oxygen activity and is considerably lower than the measured copper concentration ( $10^{-7}$ ) in the water.

The calculations indicate that the degree of mineral saturation is extremely sensitive to variations

of oxygen activity. Species distributions also demonstrate that chalcopyrite, pyrite, covellite, bornite, chalcocite and iron oxides approach partial chemical equilibrium with an aqueous solution containing sulphate between Log oxygen activities of -66.0 and -66.5. Aqueous species distributions were recalculated for the six subsurface central bog water samples using total measured dissolved copper, zinc, iron, manganese, calcium, sulphate, bicarbonate, pH and Log oxygen activity of -66.5 as system constraints. An example of the program output for sample 74-RL-1429 is shown in Appendix D. Log K and Log Q values for eleven copper and iron minerals are given in Table 6-5 and these indicate that the degree of cuprite, hematite, magnetite, native copper, pyrite, sphalerite and siderite saturation in the waters is generally less than five orders of magnitude from predicted equilibrium compositions. Bornite, chalcocite, covellite and chalcopyrite, however, are greatly oversaturated in all water samples and Log Q values are often larger than Log K values by more than ten orders of magnitude.

Oversaturation of copper and copper-iron sulphides and the large excess of copper ( $\text{Cu}^+ + \text{Cu}^{2+}$ ) above that for a solution where pyrite, chalcopyrite, covellite, bornite and chalcocite are in equilibrium (Tables 6-1, 6-2 and 6-3) could be explained by the formation of copper complexes. The aqueous species distribution calculations are based on the assumption that the dissolved metal concentrations largely consist of simple ions. Copper, however, can form hydroxo complexes such as  $\text{CuOH}^+$ ,  $\text{Cu}_2(\text{OH})_2^{2+}$  in dilute aqueous systems (Stumm and Morgan 1970) and can also form very stable complexes with dissolved humic

Table 6-5: Equilibrium constants (Log K), reaction quotients (Log Q) and relative degree of mineral saturation in central bog subsurface water samples at Log oxygen activity of -66.5.

MINERAL	74-RL-1428		74-RL-1429		74-RL-1439		74-RL-1442		74-RL-1443		74-RL-1444	
	LOG K	LOG Q	LOG K	LOG Q	LOG K	LOG Q	LOG K	LOG Q	LOG K	LOG Q	LOG K	LOG Q
BORNITE	499.74	544.16**	499.74	549.18**	499.74	555.71**	499.74	551.53**	499.74	551.86	499.74	556.42**
CHALCOCITE	134.47	152.08**	134.47	153.34**	134.47	155.63**	134.47	153.64**	134.47	154.16**	134.47	156.31**
CHALCOPYRITE	231.20	240.00**	231.20	242.50**	231.20	244.44**	231.20	244.23**	231.20	243.55**	231.20	243.80**
COVELLITE	110.16	116.67**	110.16	118.73**	110.16	120.03**	110.16	119.04**	110.16	119.10**	110.16	120.18**
CUPRITE	34.32	37.57*	34.32	35.98*	34.32	37.96*	34.32	35.96*	34.32	36.87*	34.32	39.01*
HEMATITE	-19.96	-15.62*	-19.96	-20.44 <sup>U</sup>	-19.96	-19.77*	-19.96	-18.23*	-19.96	-18.91*	-19.96	-20.63 <sup>U</sup>
MAGNETITE	-11.81	-6.82*	-11.81	-14.04 <sup>U</sup>	-11.81	-13.03 <sup>U</sup>	-11.81	-10.23*	-11.81	-11.74*	-11.81	-14.32 <sup>U</sup>
NATIVE COPPER	30.81	35.41*	30.81	34.61*	30.81	35.61*	30.81	34.60*	30.81	35.06*	30.81	36.13*
PYRITE	205.86	204.59 <sup>U</sup>	205.86	207.88*	205.86	208.83*	205.86	209.62*	205.86	208.49*	205.86	207.66*
SIDERITE	-2.40	-2.44 <sup>U</sup>	-2.40	-3.81 <sup>U</sup>	-2.40	-3.47 <sup>U</sup>	-2.40	-2.70 <sup>U</sup>	-2.40	-3.11 <sup>U</sup>	-2.40	-3.97 <sup>U</sup>
SPHALERITE	120.46	122.32*	120.46	122.59*	120.46	122.74*	120.46	122.40*	120.46	122.40*	120.46	123.00*

\*\* - Highly oversaturated compared to equilibrium solution composition

\* - Slightly oversaturated compared to equilibrium solution composition

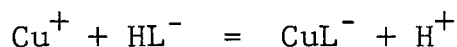
<sup>U</sup> - Undersaturated compared to equilibrium solution composition

and fulvic acid fractions in natural waters. Nissenbaum and Swaine (1976), for example, found that more than 80% of copper, but less than 5% of calcium and manganese concentrations in a shallow marine sediment pore water was associated with humic substances. The actual simple copper ion concentration in organic rich natural waters could be very small compared to measured abundances. Soil pore water chemistry could be different from that of water accumulating at the bottom of cased auger holes. Nissenbaum et al. (1971) found that shallow marine sediment pore water contained up to 148 ppm dissolved organic carbon compared to less than 5 ppm in overlying sea water.

Studies by Rashid and Leonard, (1973), Baker, (1973) have shown that the solubility of base-metal sulphides, hydroxides and carbonates increases in the presence of solutions containing humic acid fractions. A major proportion of copper and other metals could be bound to humic and fulvic acid fractions forming soluble complexes despite small concentrations of organic matter in natural waters. The percentage of organically bound copper can be approximately calculated from known data for metal-fulvate complex stabilities. Estimates are, however, very approximate since interactions with other inorganic and organic ligands has been ignored and metal-fulvate stability constants were determined at pH 3.0.

The concentration of fulvic acid fraction available for metal complexing is based on an average molecular weight for fulvic acid of 1000. From this molecular weight Gamble and Schnitzer (1973) calculated that a solution containing 1 ppm of

organic carbon was equivalent to  $3 \times 10^{-6}$  M metal complexing sites. Concentrations of metal-fulvate complexes were calculated by the same method as that used for the species distribution. The mass action equation for the reaction of copper with the fulvate ligand is shown below.



$$\bar{K}_4 = \frac{m(\text{CuL}^-) m(\text{H}^+)}{m(\text{HL}^-) m(\text{Cu}^+)}$$

$m(\text{CuL}^-)$  is the molality of the site bound bidentate copper ligand.

$m(\text{H}^+)$  " " " " hydrogen ion.

$m(\text{Cu}^+)$  " " " " cuprous ions.

$m(\text{HL}^-)$  " " " " ionized fulvate fraction complexing sites.

$\bar{K}_4$  is the mass action quotient for the reaction. Mass action quotients have been calculated for copper, calcium, zinc and manganese by Gamble and Schnitzer (1973) and are listed below. An estimate for the mass action quotient for iron has been made from data given by Schnitzer and Skinner (1966).

<u>Metal</u>	<u>Mass action quotient <math>\bar{K}_4</math> (at pH 3.0)</u>
Cu	23
Fe	20
Ca	15
Zn	1.8
Mn	0.37

<u>Sample Number</u>	<u>Ca</u>	<u>Cu</u>	<u>Biquino- ine Cu*</u>	<u>Fe</u>	<u>Mn</u>	<u>Zn</u>	<u>Organic carbon**</u>
74-RL-1428	4.16	35.67	20.0	33.00	0.81	1.96	9.0
" 1429	16.46	71.59	84.0	68.64	2.96	7.44	16.0
" 1439	0.89	11.24	10.0	9.97	5.51	0.30	2.0
" 1442	1.22	13.50	60.0	12.00	0.22	0.66	4.0
" 1443	1.44	15.60	44.0	14.14	0.27	0.65	3.5
" 1444	1.44	16.27	n.r	13.17	0.26	0.67	4.0

Table 6-6: Proportion of metals (%) theoretically bound to the fulvic acid fraction in subsurface bog water samples.

\* Represents %Cu not extracted by 2-2 biquinoline.

\*\*Dissolved organic carbon content in ppm.

Percentages of copper, zinc, iron, manganese and calcium bound to fulvic substances in six subsurface water samples are given in Table 6-6. Relative proportions of metals bound in complex form reflect the decreasing stabilities of the copper, iron, calcium, zinc and manganese complexes. More than 70% of the copper is present in the form of a fulvate complex in water sample 1429 containing 16 ppm dissolved organic carbon. The 2-2 biquinoline extracted only 16% of the copper from this sample emphasizing that a large proportion of the metal is bound in a relatively stable complex form. Water samples 1442, 1443, 1444 and 1439 containing less than 5 ppm dissolved organic carbon have smaller proportions of metals in the form of metal-fulvate complexes. Although calculations indicate that less than 16% of the total copper in samples 1442 and 1443 is bound to organic matter, extraction of copper using 2-2 biquinoline suggests that more than 40% of the metal is present in complexed forms. The difference between calculated and extracted complexed copper values could reflect interaction of metals with other organic and inorganic ligands to form stable complexes in addition to association with fulvic and humic acid fractions.

#### 6-6 STABILITY OF COPPER AND IRON MINERALS IN THE ORGANIC SOILS

Thermodynamic models have demonstrated that chalcopyrite, chalcocite, covellite and bornite are oversaturated compared to equilibrium concentrations calculated from subsurface, central bog water sample compositions. However, precipitation will only occur if anion and cation concentrations satisfy mineral

solubility product relationships. Predicted equilibrium sulphide ion concentrations ( $10^{-15}\text{M}$ ) are smaller than measured sulphide ion abundances in lake sediment pore waters ( $10^{-12}\text{M}$ ) reported by Emerson (1976). The calculated hydrogen sulphide concentration ( $10^{-6}\text{M}$ ) is also smaller than that which could theoretically be produced as a result of biogenic sulphate reduction ( $10^{-4}\text{M}$ ). Although sulphide ion concentrations are apparently large enough for precipitation of mineral sulphides the concentration of metal ions may be insufficient for formation of large authigenic mineral accumulations due to development of complexes.

Stability relationships among copper and iron minerals which could be formed in the organic soils reflect variations of pH, Eh, total metal concentration and total sulphur concentration. Eh of the system can be calculated from Log oxygen activity by the relationship for the stability of water.

$$\text{Eh} = 1.23 + \frac{0.059}{4} \text{Log } \text{O}_2 - 0.059\text{pH}$$

Calculated Eh from this relationship at Log oxygen activity of -66.0 and pH 6.0 would be -98mv. Copper and iron mineral relationships as a function of Eh and pH at a total sulphur activity of  $10^{-4}$  are shown in Fig. 6-1 where approximate limits to the central bog system, based on Eh and pH measurements, are shown as a shaded area.

An aqueous solution having a pH of 6.0 and Eh -98 mv would plot in the covellite-pyrite stability field on Fig. 6-1. This mineral association occurs in a grain shown in Plate 5-4 where covellite lamellae fill the interstices between pyrite



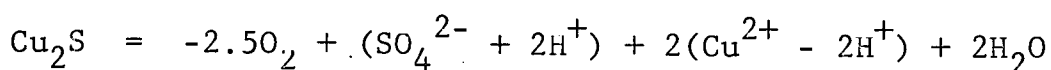
framboids. The mineral relationships most commonly observed in the heavy mineral grains, however, are small, idiomorphic covellite granules coated with chalcopyrite (Plate 5-5) or covellite as roughly concentric zones within chalcopyrite grains (Plate 5-7). The covellite and chalcopyrite stability fields in Fig. 6-1 are separated by chalcocite and bornite fields and these minerals would be expected to be present in an assemblage containing chalcopyrite and covellite. No chalcocite and bornite have been positively identified in any of the mineral grains.

Idiomorphic covellite-chalcopyrite grains, smaller than 40  $\mu\text{m}$  across and the presence of framboidal pyrite in the bog strongly suggests that the sulphide minerals are authigenic. Framboidal pyrite probably formed by adsorption of particulate ferric hydroxide onto the surface of spherical humic acid colloidal droplets followed by reaction of iron with sulphide ions and elemental sulphur to form pyrite (Papunen 1966, Berner 1969, Rickard 1970). Pyrite framboids are occasionally enclosed by a layer of massive, softer sulphide which is almost identical to pyrite composition (Plate 5-3). This concentric, massive pyritic layer could represent later precipitation of an iron sulphide gel onto the original framboid due to local chemical variations in the organic soil pore water. Although mineralogy of the concentric layer is most likely  $\text{FeS}_2$ , other metastable iron sulphides such as mackinawite and griegite ( $\text{Fe}_3\text{S}_4$ ) which have been experimentally produced by Sweeney and Kaplan (1973) may be also present.

Chalcopyrite granules smaller than 10  $\mu\text{m}$  diameter occur in

the central bog organic soils (Plates 5-20 and 5-24). and these could represent the initial stage of sulphide precipitation from soil pore water solutions. The elliptical chalcopyrite granules coating a silicate mineral grain shown in Plate 5-8 may also have formed by precipitation of sulphide onto an existing surface. Textures exhibited by chalcopyrite-covellite grains smaller than 40  $\mu\text{m}$  across could be explained by a sequence of sulphide mineral depositions. The idiomorphic covellite lamellae (Plate 5-4) represent the first stage of precipitation and the subparallel chalcopyrite layer surrounding the covellite was deposited onto existing mineral surface due to changing Eh, pH or solution composition. Covellite often forms roughly concentric layers in chalcopyrite grains larger than 50  $\mu\text{m}$  across (Plates 5-7 and 5-10) resembling Leisegang rings which are commonly found in colloform structures. These rings are thought to form as a result of rhythmic mineral precipitation in a gel and could also form where authigenic sulphide grains have developed through sequential deposition.

The effect of sulphur activity variations on mineral stabilities in the Cu-S-O-H and Fe-S-O-H systems at 25°C is shown in Figs. 6-2a and 6-2b. Mineral stabilities were determined as a function of varying Log oxygen activity and Log sulphate activity + 2pH<sup>2</sup>. The phase boundaries were established by writing balanced equations for the oxidation of each mineral in terms of oxygen, (SO<sub>4</sub><sup>2-</sup> + 2H<sup>+</sup>), Cu<sup>2+</sup>, Fe<sup>2+</sup> and H<sub>2</sub>O. A typical reaction for chalcocite oxidation would be:-



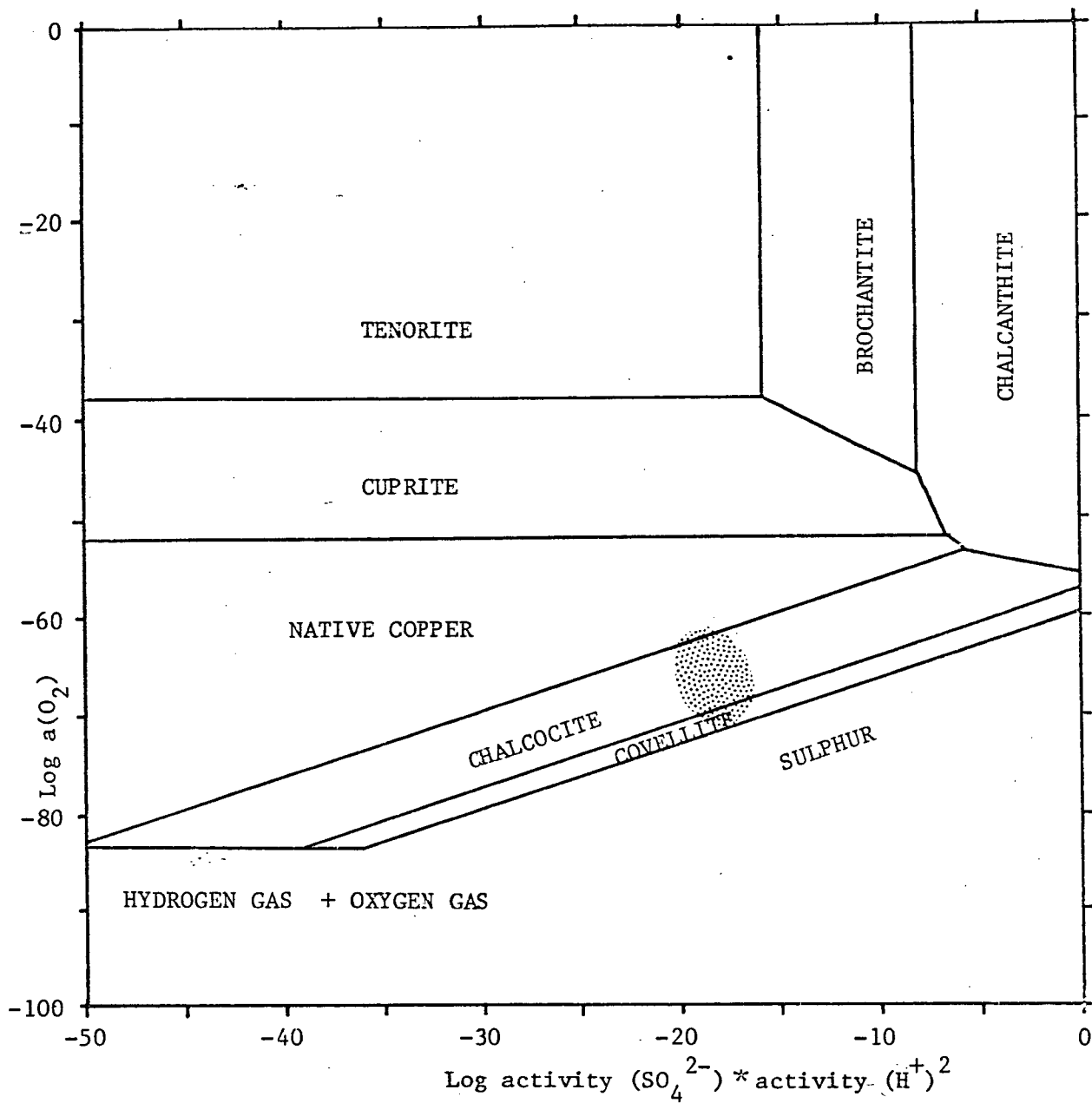


Figure 6-2a: Stability relationships between copper minerals in water at 25°C and 1 atmosphere pressure as a function of Log activity oxygen gas and Log activity sulphate \* activity hydrogen ion <sup>2</sup>. The shaded area  indicates the approximate limits of subsurface bog water sample compositions at pH 6.0 and Eh -100 mv.

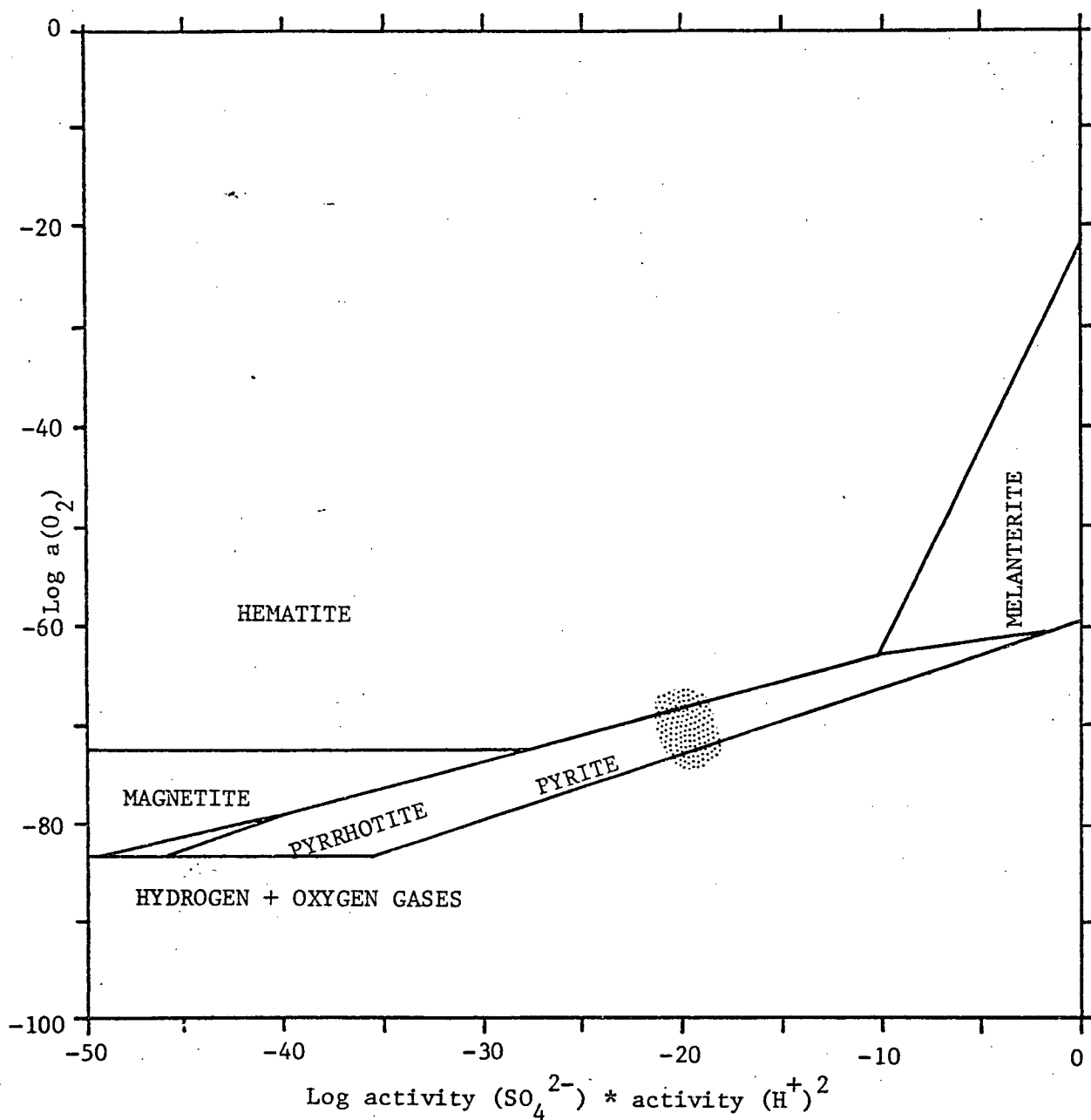


Figure 6-2b: Stability relationships between iron minerals in water at 25°C and 1 atmosphere pressure as a function of Log activity oxygen gas and Log activity sulphate \* activity hydrogen ion<sup>2</sup>. The shaded area  indicates approximate limits of subsurface bog water sample compositions at pH 6.0 and Eh -190mv.

Equilibrium constants,  $K$ , for each reaction and components indicated by the reaction were used as controls for the plotting program DIAG (Brown 1970) on the UBC IBM 370/168 computer to prepare the phase diagrams. Probable oxygen activity and sulphate concentration limits to the bog system, based on water sample analyses are shown as shaded areas on the diagrams. The chalcopyrite stability field has not been indicated on the diagram although this mineral would be formed by reaction of copper sulphides with pyrite. Water sulphate-pH values at Log oxygen activity of -66.0 plot in the chalcocite field on Fig. 6-2a close to the chalcocite-native copper boundary and in the pyrite field on Fig. 6-2b close to the pyrite-hematite boundary. Increasing oxygen activity and decreasing sulphate concentration would favour the formation of native copper and hematite whereas decreasing oxygen activity and increasing sulphate concentration would favour the formation of pyrite, covellite and chalcopyrite.

The phase diagrams 6-1, 6-2a and 6-2b indicate that chalcopyrite and pyrite, chalcocite, covellite, native copper, cuprite, and hematite would become progressively stable in sequence when oxygen activity is increased or sulphate concentration is decreased. Native copper grains, rimmed by cuprite, and idomorphic covellite-chalcopyrite grains (Plates 5-11 and 5-5) occur together in sample 74-RL-1119 suggesting large, but local variations of Eh, pH and/or sulphur activity. Chalcocite is not visible in any of the mineral grains although bornite may be present in one grain shown in Plate 5-9. The absence of chalcocite in the system where conditions are favourable for

formation and stability could be explained by predominantly low oxygen activity and high sulphur activity. Since the native copper is present in only one sample from close to the organic soil-till interface the mineral grains may be detrital rather than authigenic.

The absence of chalcocite could also be due to high solubility of the mineral in aqueous solutions containing abundant dissolved humic substances. Baker (1973) demonstrated that chalcocite is extremely soluble in humic acid fraction solutions whereas, by contrast, chalcopyrite and pyrite are only weakly soluble. Chalcocite may therefore be quickly dissolved soon after precipitation by dissolved humic fractions present in the bog waters. The corroded outer edges, typical of the larger chalcopyrite-covellite grains, could also reflect partial solution of sulphides by the dissolved organic matter.

Thermodynamic models and mineral textures provide strong evidence that the sulphide minerals formed by precipitation from aqueous solutions during organic diagenesis. Covellite and chalcopyrite probably formed initially in the organic soil as colloidal aggregates which formed a nucleus for later growth. The sulphides could also have replaced existing organic fragments or could have accreted onto the surface of silicate mineral grains. Textures interpreted as due to replacement of wood by chalcocite and chalcopyrite are described by Papenfus (1928) Hagni and Gann (1976) also describe replacement of fossil spores by chalcocite in a red-bed copper deposit. The small, dark, opaque mineral inclusions in the core of a chalcopyrite-covellite grain, shown in Plate 5-7, could

represent almost complete replacement of an organic fragment by copper sulphide.

Copper, transported into the bog by circulating ground water, is immobilized as sulphide minerals and copper-humate or copper-fulvate associations. Microprobe analyses have also demonstrated that copper and sulphur are associated with cell-wall structures preserved in organic soil fragments. This association was probably formed as a result of copper absorption, by living plants such as sphagnum moss or sedges, from copper-rich water flowing over the bog surface. The copper may be bound to sulphur containing amino acids which form the plant cell membrane proteins. Release of copper from the plant material will only occur when the material is completely decomposed. High organic carbon values in deeper samples from several vertical profiles, however, suggest that a significant proportion of the organic matter has not undergone decomposition. A large proportion of the total copper in this material could therefore be bound in a relatively stable form and could reflect copper concentration on the surface water flowing over the bog at the time when the surface was exposed. Quantitative analyses of copper, sulphur and carbon in organic soil components at different depths are necessary to establish the validity of this hypothesis.

## 6-7 A CONCEPTUAL MODEL FOR METAL DISPERSION

Secondary dispersion of metals in the bog and surrounding area can be summarized by the model shown in Fig. 6-3. Iron, cobalt, nickel, zinc, molybdenum and manganese are largely derived through reduction of the till beneath the organic soil. Copper and iron are also introduced by ground water flowing from fault zones buried under the till or by surface streams draining hill slopes on the western side of the bog. The small area of concealed copper-rich till at the western end of the bog could reflect upward migration of solutions from a fault zone. The copper and iron dissolved in this water are derived from oxidation of sulphides disseminated through the Nicola volcanic rocks. Subsurface bog waters have less than 70 ppm sulphate suggesting that the circulating ground water has a low oxygen fugacity or that a relatively small part of the rock is exposed to the oxidizing water. High calcium and sulphate values in water flowing from a diamond drill hole, intersecting porphyritic and volcanic rocks, indicates local weathering of these rocks and local oxidation of iron sulphides.

The metals are transported through the organic soil by migrating water as complex ions or as soluble complexes including those formed with humic acid fractions, fulvic acid fractions, amines and polysaccharides. Copper, zinc, cobalt and nickel are adsorbed from these dilute solutions by the abundant colloidal humic aggregates forming a major

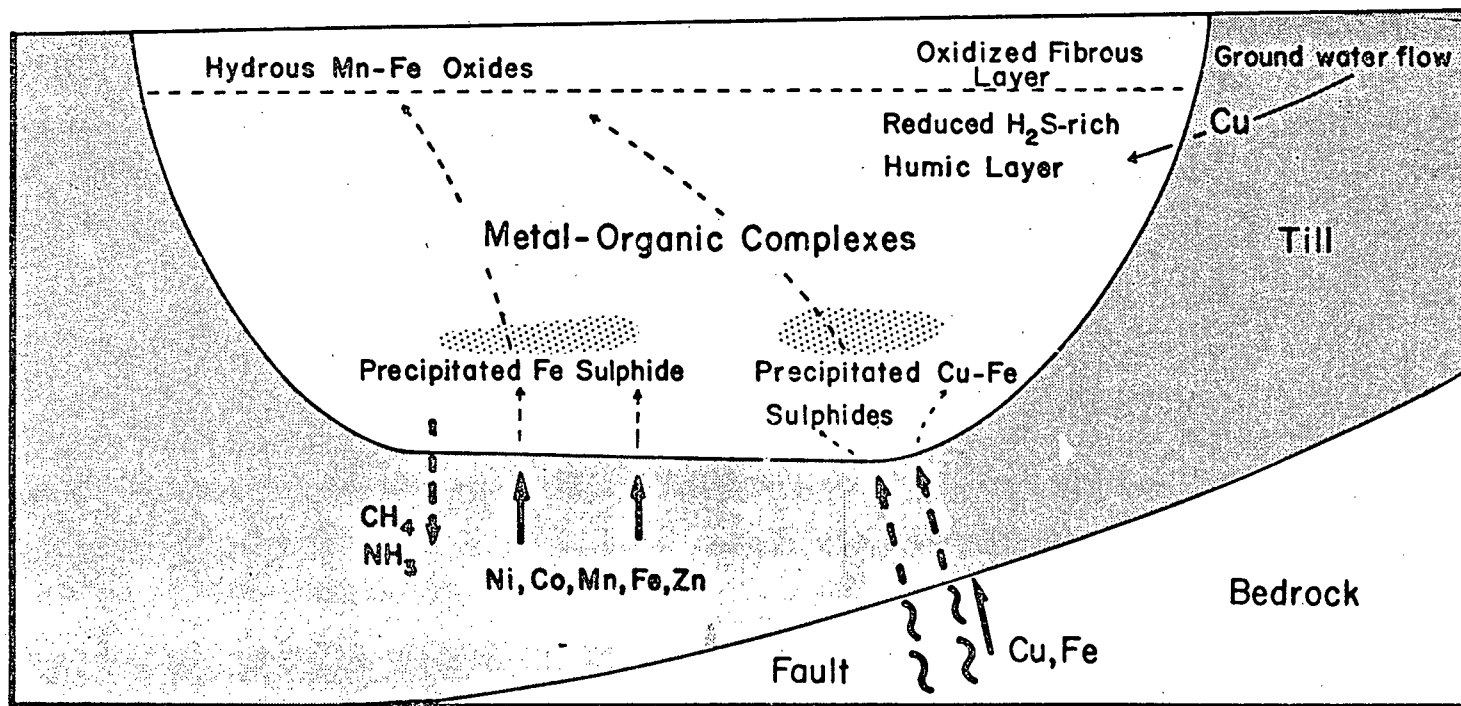


FIGURE 6-3: CONCEPTUAL MODEL FOR DISPERSION OF METALS IN THE BOG

component of the organic soil. The degree to which these metals are enriched in the soil will depend on the dissolved metal contents in the soil pore water, relative strengths of complexes formed between metals and humic substances, pH, Eh, and the abundances of these substances in the soil. Iron and manganese are only weakly adsorbed by the humic and fulvic acid fractions and therefore remain in solution.

Framboidal pyrite, chalcopyrite, covellite and native copper will precipitate from reducing, weakly acid subsurface bog water solutions. Framboidal pyrite forms largely as a result of reaction between iron migrating from the till and sulphide ions produced from biogenic reduction of sulphate. Copper sulphide and native copper grains, however, are formed in those parts of the bog where copper and iron rich waters discharge from faults. Sphalerite and molybdenite could also be precipitated in the organic soil although these minerals have not been identified. The absence of pyrite or copper-iron sulphide layers in the soil could reflect the comparative slow diffusion rates of metals and sulphide to reaction sites or may reflect the small vertical concentration gradients developed in the bog.

Oxidation of dissolved metal-humate or metal-fulvate complexes in water flowing through the reducing-oxidizing boundary will increase cation activities in surface waters. Secondary iron and manganese hydrous oxides form close to the bog surface or on the surface and especially in areas where large volumes of water discharge. Molybdenum will

be immobilized as acid molybdenate ions in the acid surface water. Copper migrating to the surface and transported laterally into the bog by streams can be absorbed into the tissues of surface vegetation. This copper will be relatively stable and may only be released from the plant tissues in highly decomposed soils.

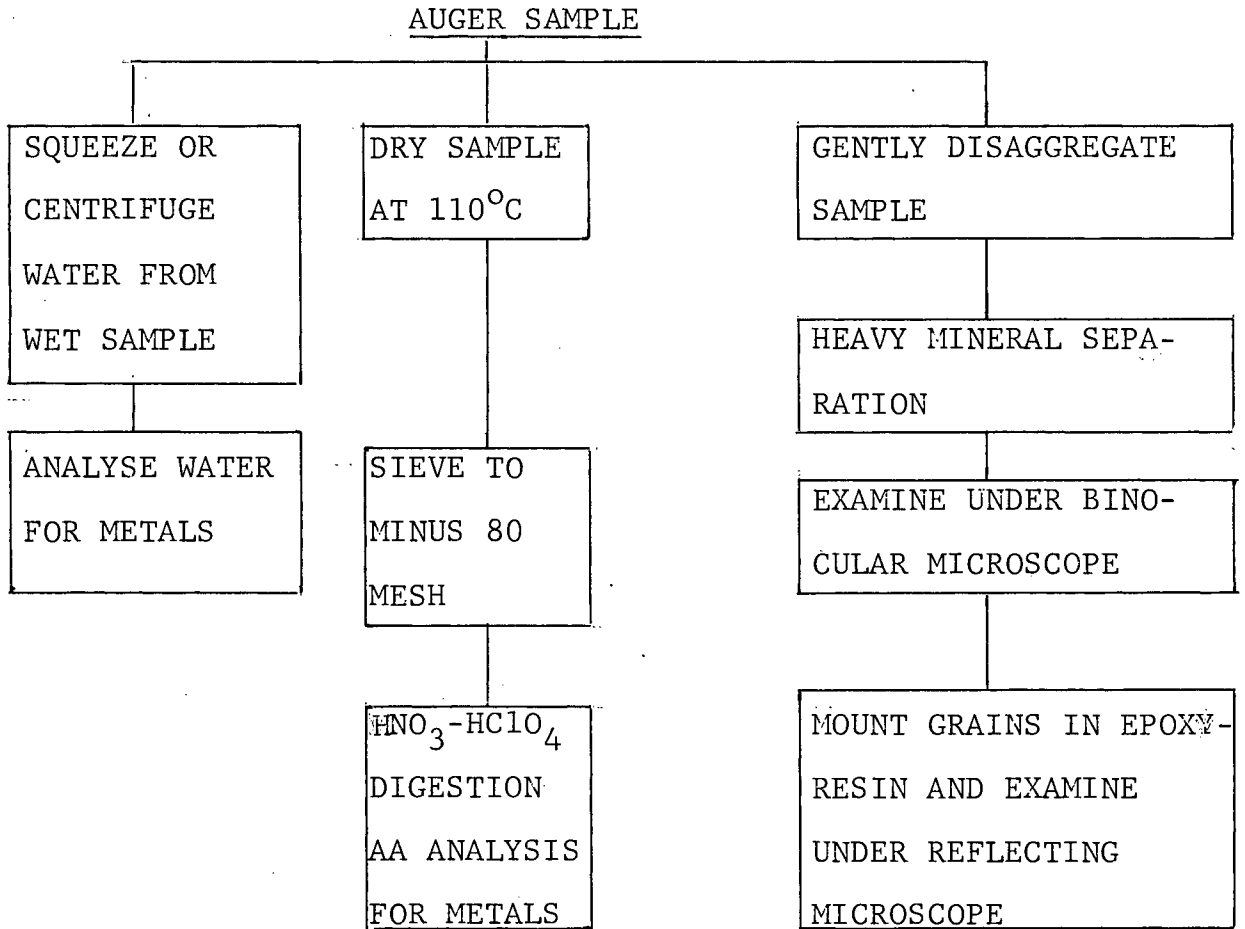
#### 6-8 APPLICATIONS TO MINERAL EXPLORATION

Several previous studies have demonstrated that organic soil geochemistry can be successfully used to locate concealed mineral occurrences. Nieminen and Yliruokunen (1976), for example, traced copper, nickel and zinc anomalies in a Finnish peat bog to a small bedrock exposure through the till-bog interface and concluded that metal distribution patterns reflected metalliferous water flowing from this bedrock.

Results of the present investigation indicate that copper, nickel, cobalt and zinc are most abundant in the deeper, decomposed material in parts of the central bog where organic soil thickness exceeds 3 m. Copper generally decreases from more than 0.5% in humic-mesic soil layers to less than 210 ppm in the underlying till except at the western end of the bog where a small area of buried till contains up to 0.5% copper. Horizontal and vertical variations of copper in the organic soil layers do not show a clear relationship with the copper-rich till and distribution patterns have largely formed through concentration of copper and other metals from migrating ground water solutions.

Authigenic chalcopyrite, chalcopyrite-covellite and native copper-cuprite grains form, locally, in two areas through reaction of sulphide ions with metals transported into the organic soil from the till-bog interface. The grains are abundant in soil between 1 to 3 m depth above the copper-rich till. Subsurface bog water in this area of the bog where the grains are most abundant have high copper and iron contents. Distribution of small, authigenic grains in organic soils and subsurface bog water chemistry could be used to locate concealed metal sources. Seepages draining the hill slope on the west side of the bog also have high copper concentration suggesting that metals have been introduced into the bog by laterally flowing water as well as by discharging ground water.

Overburden sampling is often used to outline areas of mineralized till or bedrock concealed by bogs, but this method is relatively expensive (current costs are roughly \$20/m) and slow (1 to 2 samples/hour) compared to stream sediment and soil sampling. An exploration target size could be effectively decreased before application of overburden sampling by sampling organic material from close to the base of a bog with a Hiller peat auger. Identification of mineral grains, examination of grain textures and measurement of metal concentrations in bog waters could be important in establishing the source for the metal. A flow diagram describing physical and chemical analyses of augered soil samples and water samples is shown below.



Analysis of water from squeezed or centrifuged organic soils for trace metal contents would be faster than sampling cased auger holes in the bog, but additional studies must be conducted, however, to determine if there are any significant variations between organic soil pore water and water collected from the cased auger holes.

Microprobe analyses of organic soil samples for metals are generally too expensive for routine mineral exploration application. Quantitative scanning electron microprobe analysis could, however, be used to establish the distribution of metals between different organic soil components.

Results could then be compared with those obtained from relatively simple sequential extraction or ion exchange methods. These techniques may then be confidently used to determine the mode of metal occurrence in soils.

## CHAPTER 7

## CONCLUSIONS

(1) The principle forms of copper in organic soils in order of relative abundance are:-

- (a) Copper bound by physical and chemical adsorption to soil organic matter. The soil components largely responsible for these processes are humic and fulvic acid fractions.
- (b) Copper bound to protein molecules forming the cell wall membranes of plant fragments preserved in the decomposed material comprising the humic-mesic organic soil layers.
- (c) Copper in the form of authigenic chalcopyrite, chalcopyrite-covellite, covellite and native copper-cuprite mineral grains.

(2) Copper, cobalt, nickel and zinc are adsorbed by the organic matter from dilute aqueous solutions migrating through the bog. The cobalt, nickel and zinc are largely derived from the reduced till beneath the organic soils and from humic gleysols surrounding the bog. Copper concentrations are also introduced by surface water flowing from seepages on the west side of the bog and by subsurface ground water discharging from a fault zone beneath organic soils and the till. The source of this copper is probably disseminated copper-iron sulphides in contact with oxidizing, deeply circulating ground water. The degree of copper, cobalt, nickel and zinc enrichment through adsorption will depend

on the activity of metal ions in the soil pore water, relative stabilities of complexes formed with humic and fulvic acid fractions, soil pore water pH and Eh.

(3) Scattered pyrite framboids occur throughout the bog and form by reaction of iron rich bog waters with sulphide ions produced through biogenic reduction of sulphate.

Framboids found in organic soil above copper-rich till at the western end of the bog are occasionally coated with chalcopyrite and covellite indicating that the copper-sulphides were precipitated on the framboid surface. Textures of chalcopyrite-covellite grains, found in the same area, reflect alternating deposition of sulphides where copper and iron rich solutions, flowing from the fault, mix with sulphide ions.

(4) Significant concentrations of iron and manganese also enter the bog from the reduced till. These metals are not adsorbed by the reducing, organic soils although iron will be immobilized as framboidal pyrite. Iron and manganese hydroxides form in the surface fibrous organic layer where metal rich solutions flow from the reducing into the oxidizing environment. Molybdenum is also concentrated in this fibrous material due to the low pH of the bog surface water.

BIBLIOGRAPHY

- Anderson, P., 1971. Geology, petrology, origin and metamorphic history of the Eagle granodiorite and Nicola Group, Princeton area, southern British Columbia. Unpublished B.Sc Thesis, University of British Columbia, 201 p.
- Barr, D.A., Fox, P.E., Northcote, K. and Petro, V.A., 1976. The alkaline suite porphyry deposits: A summary. In: Porphyry deposits of the Canadian Cordillera. (Sutherland-Brown, A., Ed.), pp. 359-367.
- Baker, W.E., 1973. The role of humic acids from Tasmanian podzolic soils in mineral degradation and metal mobilization. Geochim. Cosmochim. Acta. Vol. 37, pp. 269-281.
- Baas Becking, L.G.M. and Moore, D., 1961. Biogenic sulphides Econ. Geol. Vol. 56, pp. 259-272.
- Beckwith, R.S., 1959, Titration curves of soil organic matter. Nature. Vol. 184, pp. 745-746.
- Bell, R.G., 1969. Studies of the decomposition of organic matter in flooded soil. Soil Biol. Biochem. Vol 15, pp. 105-115.
- Berner, R.A., 1969. Migration of iron and sulphur in anaerobic sediment during diagenesis. Am. J. Sci. Vol. 267, pp. 19-42.
- Berner, R.A., 1971. Principles of chemical sedimentology. McGraw-Hill International Series in the Earth Sciences, New York. 240 p.
- Bluck, B.J., 1969. Introduction to sedimentology. In: Organic Geochemistry, (Eglinton, G., and Murphy, M.M.J., Eds.), Springer-Verlag, New York. pp. 245-257.
- Brown, T.H., 1970. Theoretical predictions of equilibria and mass transfer in the system  $\text{CaO-MgO-SiO}_2\text{-H}_2\text{O-NaCl-HCl}$ . Unpublished Ph.D thesis, Northwestern University. 136 p.
- Borovitskii, V.P., 1970. The application of bog sampling in prospecting for ore deposits in perennial regions. Jour. Geoch. Expl., Vol. 5, No. 1, pp. 65-70.
- Boyle, R.W., 1977. Cupriferous bogs in the Sackville area, New Brunswick, Canada. Jour. Geoch. Expl., Vol. 8, No. 3, pp. 495-528.

- Boyle, D.R. and Troup, A.G., 1975. Copper-molybdenum porphyry mineralization in central British Columbia, Canada: An assessment of geochemical sampling media useful in areas of glaciated terrain. In: Prospecting in areas of glaciated terrain. (Jones, M.L., Ed.), Institution of Mining and Metallurgy, London. pp. 6-15.
- Broadbent, F.E. and Ott, J.E., 1957. Soil organic matter complexes: 1. Factors affecting retention of various cations. Soil Sci. Vol. 83, pp. 419-423.
- Canadian Department of Agriculture, 1974. The system of soil classification for Canada. Published by the Canadian Department of Agriculture, Ottawa. 255 p.
- Cannon, H.L., 1955. Geochemical relationships of zinc bearing peat to the Lockport dolomite, Orleans Co., New York. U.S. Geol. Surv. Bull. No. 1000-D
- Carpenter, R.H., Pope, T.A. and Smith, R.L., 1975. Iron-manganese oxide coatings in stream sediment geochemical surveys. Jour. Geoch. Exp., Vol. 4, No. 3, pp 349-363
- Cappenberg, Th. E., 1974. Interrelations between sulphate-reducing bacteria and methane producing bacteria in bottom deposits of a fresh water lake: 1. Field observations. Antonie van Leeuwenhoek. Vol. 40, pp. 285-295.
- Casagrande, D.J., Siefert, K., Berschinski, C. and Sutton, N., 1977. Sulphur in peat-forming systems of the Okefenokee swamp and Florida Everglades: Origins of sulphur in coal. Geochim. Cosmochim. Acta., Vol. 41, pp. 161-167.
- Chao, T.T., 1972. Selective dissolution of manganese oxides from soils and sediments with hydroxylamine hydrochloride. Soil Sci. Soc. Am. Proc., Vol. 36, pp. 764-768.
- Chapman, R.P., 1976. Limitations of correlation and regression analysis in geochemical exploration. Trans. Inst. Min. Metall. London, Vol. 85, pp. B279-283.
- Chin Le. and Tenisci, T., 1977. TRP: a triangular regression program package, University of British Columbia Computing Center. 183 p.
- Cross, C.H., 1975. The relationship of metals and soil organic components with particular reference to copper. Unpublished Ph.D thesis, University of British Columbia, Canada. 170 p.
- Davis, R.I., Cheshire, M.V. and Graham-Bryce, I.J., 1969. Retention of low levels of copper by humic acid. Jour. Soil. Sci. Vol. 20, No. 78, pp. 65-71.

- Dixon, W.J. and Massey, F.J., 1969. Introduction to statistical analysis. McGraw-Hill, 638 p.
- Eckel, E.B., 1949. Geology and ore deposits of the La Plata District, Colorado. U.S. Geol. Surv. Prof. Paper., No. 219, pp. 55-64.
- Emerson, S., 1976. Early diagenesis of anaerobic lake sediments: chemical equilibria in interstitial water. Geochim. Cosmochim. Acta. Vol. 40, pp. 925-934.
- Ennis, M.T., 1962. The chemical nature of copper complexes in peat. Irish Jour. Agric. Res., Vol. 2, pp. 147-155.
- Erriksson, K. and Erriksson, G., 1976. Hinsén: Heavy metals in peat and till. Jour. Geoch. Explor., Vol. 5, No. 7, pp. 232-235.
- Erriksson, K. and Erriksson, G., 1976. Stromo: Heavy metals in peat close to a boulder train. Jour. Geoch. Explor., Vol. 5, No. 7, pp. 342-343.
- Felbeck, G.T., 1971. Chemical and Biological characterization of humic matter. In: Soil Biochemistry, Vol. 2, (McLaren, A.D. and Skujins, J., Eds.), pp. 36-59.
- Flaig, W., 1972. An introductory view on humic substances: aspects of research on their genesis, their physical and chemical properties and their effects on organisms. Proceedings of the International Meeting on Humic Substances, (Povoleds, D. and Bolterman, H.L., Eds.). pp. 19-41.
- Fox, M. and Sinclair, A.J., 1973. Unpublished program for plotting probability graphs. Department of Geological Sciences, University of British Columbia.
- Fraser, D.C., 1961. A syngenetic copper deposit of recent age. Econ. Geol., Vol. 56, pp. 951-962.
- Fraser, D.C., 1961. Organic sequestration of copper. Econ. Geol., Vol. 56, pp. 1063-1078.
- Fulton, R.J. and Armstrong, J.E., 1965. Field conference J. 7th. Meeting of the International Association for Quaternary Research, 1965. pp. 746-747.

- Gamble, D.S. and Schnitzer, M., 1973. The chemistry of fulvic acid and its reaction with metal ions. In: Trace metals and metal-organic interactions in natural waters, (Singer, P.C., Ed.), Science Publishers Inc., Ann Arbor, Michigan, pp. 265-301.
- Gardener, L.R., 1974. Organic versus inorganic trace metal complexes in sulphidic marine waters: some speculative calculations based on available stability constants. *Geochim. Cosmochim. Acta*, Vol. 38, pp. 1297-1302.
- Garrels, R.M. and Thompson, M.E., 1962. A chemical model for seawater at 25 degrees centigrade and one atmosphere total pressure. *Am. Jour. Sci.* Vol. 260. pp. 57-66.
- Garrels, R.M. and Christ, C.H., 1965. *Solutions, Minerals and Equilibria*. Published by Harper Interscience, 450 p.
- Garrett, R.G. and Hornbrook, E.H.W., 1976. The relationship between zinc and organic content in centre-lake bottom sediments. *Jour. Geoch. Explor.*, Vol. 5, No. 1, pp. 31-38.
- Garret R.G., 1973. The determination of sampling and analytical errors in exploration geochemistry (discussion). *Econ. Geol.*, Vol. 68, pp. 282-283.
- Garret R.G., 1969. The determination of analytical errors in exploration geochemistry. *Econ. Geol.*, Vol. 64, pp. 568-574.
- Given, P.C. and Dickinson, C.H., 1975. Biochemistry and microbiology of peats. In: *Soil biochemistry*, (Pauli, E.M., and McLaren, A.D., Eds.), pp. 123-213.
- Gleeson, C.F. and Coope, J.A., 1966. Some observations on the distribution of metals in swamps in eastern Canada. *Geological Survey of Canada Paper No. 66-54*, pp. 145-166.
- Goodman, B.A. and Cheshire, M.V., 1973. Electron paramagnetic resonance evidence that copper is complexed in humic acid by nitrogen of porphyrin groups. *Nature, New Biology*, London, Vol. 244, pp. 158-159.
- Goodman, B.A. and Cheshire, M.V., 1976. The occurrence of copper-porphyrin complexes in soil humic acids. *Soil. Sci.* Vol. 27, pp. 337-347.
- Grosse-Brauckmann, C. and Puffe, D., 1964. *Über zersetzungsprozesse und stoffbilanz im wachsenden moor*. In: *Proceedings of the 8th International Congress of Soil Science*, Bucharest.
- Gunton, J.E. and Nichol, I., 1974. *Deliniation and interpre-*

- tation of metal dispersion patterns relating to mineralization in the Whipsaw Creek area. Trans. Can. Inst. Min. Metall., Vol. 77, pp. 32-41.
- Hagi, R.D. and Gann, D.E., 1976. Microscopy of copper ore at the Creta mine, southwestern Oklahoma. In: Stratiform copper deposits of the midcontinental region, Oklahoma Geol. Surv. Circ. , No. 77, pp. 40-50.
- Hansuld, J.A., 1966. The behaviour of molybdenum in secondary dispersion media. Min. Eng. December, 1966. pp. 73-77.
- Hills, L.V., 1962. Glaciation, stratigraphy, structure and micropaleobotany of the Princeton coalfield, British Columbia. Unpublished M. Sc. thesis, University of British Columbia, 141 p.
- Horsnail, R.F., Nichol, I. and Webb, J.S., 1969 Influence of variations in the surface environment on metal distribution in drainage sediments. Q. J. Colorado School of Mines, Vol. 64, No. 1, pp. 307-322.
- Horsnail R.F. and Elliott, I.L., 1971. Some environmental influences on the secondary dispersion of molybdenum and copper in western Canada. In: Can. Inst. Min. Metall., Special Vol. 2, (Boyle, R.W. and McGerrigle, J.I., Eds) pp. 166-175.
- Irving, H. and Williams, R.J.P., 1948. Order of stability of metal complexes. Nature, Vol. 162. pp. 746-747.
- Kallioskoski, J. and Cathles, L., 1969. Morphology, mode of formation and diagenetic changes in framboids. Bull. Geol. Soc. Finland., Vol. 41, pp. 125-134.
- Khanna, S.S. and Stenevson, F.J., 1962. Metal-organic complexes in soil:1. Potentiometric titration of some soil organic matter isolates in the presence of transition metals. Soil. Sci., Vol. 93, pp. 298-305.
- Khan, S.U. and Schnitzer, M., 1972. The retention of hydrophobic organic compounds by humic acids. Geochim. Cosmochim. Acta, Vol. 36, pp. 745-754.
- Khan, S.U., 1969. Interaction between the humic acid fraction of soil and certain metallic cations. Soil Sci. Soc. Am. Proc., Vol. 33. pp. 851-854.
- Kochkenov, A.V. and Kreshtapova, V.N., 1967. Rare and dispersed elements in the peat of the northern part of Russian Platforms. Geochem. Intern., No. 4. pp. 286-292.
- Kononova, M.M., 1961. Soil organic matter. Pub. by Pergamon, Oxford, 450 p.

- Kowalenko, C.G. and Lowe, L.E., 1972. Observations on the bismuth method for sulphate analysis in soil. Comm. Soil. Sci. Pl. Anal., Vol. 3, pp. 79-86.
- Kribek, B., 1975. The origin of framboidal pyrite as a surface effect on sulphur grains. Minera. Deposita, Vol. 10, pp. 389-396.
- Kuznetsov, S.I., Ivanov, M.V. and Lyakikova, N.N., 1963. Introduction to geological microbiology. International Series in the Earth Sciences. (Broneer, P.T., Trans., Oppenheimer, C.H., Ed.), 252 p.
- Lambert, I.B. and Bubela, B., 1970. Banded sulphide ores: The experimental production of monomineralic sulphide ores in sediments. Minera. Deposita., Vol. 5, pp.97-102.
- Lepeltier, G., 1969. A simplified statistical treatment of geochemical data by graphical representation. Econ. Geol., Vol. 64, pp. 538-550.
- Lewis, T.E. and Broadbent, F.E., 1961. Soil organic matter-metal complexes: 3. Exchange reactions of model compounds. Soil. Sci., Vol. 91, pp. 341-347.
- Lewis, T.E. and Broadbent, F.E., 1961. Soil organic matter-metal complexes: 4. Nature and properties of exchange sites. Soil. Sci., Vol. 91, pp. 393-399.
- Lindsay, W., 1972. Inorganic phase equilibria of micro-nutrients in soils. In: Micronutrients in Agriculture, (Mortvedt, J.J., Giordano, P.M. and Lindsay, W.L., Eds.), Symposium cosponsored by the Tennessee Valley Authority and Soil Science Society of America, pp. 41-57.
- Love, L.G., 1963. Early diagenetic pyrite in fine-grained sediments and the genesis of sulphide ores. In: Sedimentology and ore genesis, (Amstutz, G.C. Ed. ), Developments in Sedimentology, Vol. 2, pp. 11-17.
- Lovering, T.S., 1928. Organic precipitation of metallic copper. U.S.Geol. Surv. Bull., No. 795-C, pp. 45-52.
- Manaskaya, S.M. and Drozdova, T.V., 1960. Distribution of copper in peat of Byellorussia. International Series of Monographs on the Earth Sciences, Vol. 28, pp. 243-250.
- Manaskaya, S.M. and Drozdova, T.V., 1968. Geochemistry of organic substances. (Shapiro, L., Trans., Breger, I.A., Ed. ), Pergamon, 435 p.
- Mathews, W.H., 1944. Glacial lakes and ice retreat in south central British Columbia, Trans. R. Soc. Can. Sect. 4., Vol. 38, pp. 39-57.

- Midwood, R.B. and Felbeck, G.T., 1969. Analysis of yellow organic matter from fresh water. Jour. Am. Waste Water Assoc., Vol. 60, pp. 357-366.
- Miesch, A.T., 1967. Methods of computation for estimating geochemical abundance. U.S. Geol. Surv. Paper 574B, pp. 1-15.
- Mehrtens, M.B., Tooms, J.S. and Troup, A.G., 1973. Some aspects of geochemical dispersion from base metal mineralization within glaciated terrain in Norway, North Wales and British Columbia, Canada. In: Proceedings of the 4th International Geochemical Exploration Symposium, 1972. (Jones, M.J. Ed.), Published by the Institution of Mining and Metallurgy, London, pp. 105-116.
- Miedema, R., Jongmans, A.G. and Slager, S., 1973. Micromorphological observations on pyrite and its oxidation products in four Holocene alluvial soils in the Netherlands. Proceedings of the fourth International Working Meetings on Soil Microbiology, (Rutherford, G.K. Ed.), pp. 772-794.
- Moore, P.D. and Bellamy, D.J., 1974. Peatlands. Published by Springer-Verlag, New York, 221 p.
- Mullineaux, D.R., 1974. Pumice and other pyroclastic deposits in Mount Rainier National Park, Washington. U.S. Geol. Surv. Bull., No. 1362, 81 p.
- Mustard, D.K., 1968. Property examination of the Whipsaw Creek property. Unpublished Assessment Report by Amax Exploration, Vancouver, 48 p.
- Nason, A. and McElroy, W.D., 1963. Modes of action of essential mineral elements. In: Plant Physiology, (Stward, F.C., Ed.), Vol. 3, pp. 449-536.
- Nieminen, K. and Yliruokanen, I., 1976. Kitee: The copper-nickel anomalies of the Lietsosud peat bog. Jour. Geoch. Expl., Vol. 5, No. 3, pp. 348-353.
- Nissenbaum, A. and Swaine, D.J., 1976. Organic matter-metal interactions in Recent sediments: the role of humic substances. Geochim. Cosmochim. Acta., Vol. 33, pp. 809-816.
- Nissenbaum, A., Baedecker, M.J. and Kaplan, J.R., 1971. Studies of dissolved organic matter from the interstitial water of a reducing fjord. In: Advances in organic geochemistry, (Ingerson, E., Ed.), Vol. 33, pp. 427-440.
- Ong, H.L. and Bisque, R.E., 1968. Coagulation of humic colloids by metal ions. Soil Sci., Vol. 106, pp. 220-224.

- Ong, H.L. and Swanson, V.E., 1966. Adsorption of copper by peat, lignite and bituminous coal. *Econ. Geol.*, Vol. 61, pp. 1214-1231.
- Papenfus, E.B., 1931. "Red-bed" copper deposits in Nova Scotia and New Brunswick. *Econ. Geol.*, Vol. 26, pp. 314-330.
- Papunen, H., 1966. Framboidal texture of the pyritic layer found in a peat bog in southeast Finland. *Comptes Rendus de la Societe Geologique de Finlande*, No. 38, pp. 117-125.
- Parslow, G.R., 1974. Determination of background and threshold in Exploration Geochemistry. *Journ. Geoch. Expl.*, Vol. 3, No. 4, pp. 319-336
- Pauli, F.W., 1968. Some recent developments in biogeochemical research. *Geol. Can. Proc*, Vol. 19, pp. 45-49.
- Phillips, J.S. and Thompson, R.F., 1967. *Statistics for nurses*. Macmillan and Co, 550 p.
- Postma, D., 1977. The occurrence and chemical composition of iron-rich carbonates in a river bog. *Jour. Sed. Pet.* Vol. 47, No. 3, pp. 1089-1098.
- Ramm, A.E. and Bella, D.A., 1974. Sulphide production in an-aerobic microcosms. *Limnol. Oceanogr.*, Vol. 19, pp. 110-118.
- Randhawa, N.S. and Broadbent, F.C., 1965. Soil organic matter-metal complexes:5. Reactions of zinc with model compounds and humic acid. *Soil Sci.*, Vol. 99, No. 5, pp. 295-300.
- Rashid, M.A. and Leonard, J.D., 1973. Modification in the solubility of various metals as a result of their interaction with sedimentary humic acid. *Chemical Geology*, Vol. 11, pp. 89-97.
- Reuter, J.H. and Perdue, E.M., 1977. Importance of heavy metal-organic matter interactions in natural waters. *Geochim. Cosmochim. Acta.*, Vol. 41, pp. 325-344.
- Rickard, D.T., 1970. The origin of framboids. *Lithos*, Vol. 3, pp. 269-293.
- Ramanov, V.V., 1961. *Hydrophysics of bogs*. Published by the Israel Program for Scientific Translations, 299 p.
- Royal School of Mines Geochemical Prospecting Research Centre., 1962. Determination of sulphate in natural water. *Technical Communication No. 27*, 2 p.
- Royal School of Mines Geochemical Prospecting Research Centre., 1962. Determination of organic carbon in soil and sediment samples. *Technical Communication No. 32*, 2 p.

- Salmi, M., 1967. Peat in prospecting: Applications in Finland. In: Geochemical prospecting in Fennoscandia, (Kvalheim, A., Ed.), pp. 113-125.
- Schnitzer, M. and Khan, S.U., 1972. Humic substances in the environment. Marcel Dekker Inc., New York, 320 p.
- Schnitzer, M. and Hansen, E.H., 1970. Organo-metallic interactions in soils 8: An evaluation of methods for the determination of stability constants of metal-fulvate acid complexes. Soil Sci., Vol. 109, pp. 333-349.
- Schnitzer, M. and Skinner, S.I.M., 1966. Organo-metal interactions in soils 5: Stability constants of  $\text{Cu}^{++}$ ,  $\text{Fe}^{++}$ , and  $\text{Zn}^{++}$  fulvic acid complexes. Soil Sci., Vol. 102, pp. 361-365.
- Schnitzer, M. and Skinner, S.I.M., 1967. Organo-metal interactions in soils 7: Stability constants of  $\text{Pb}^{++}$ ,  $\text{Ni}^{++}$ ,  $\text{Mn}^{++}$ ,  $\text{Co}^{++}$ ,  $\text{Ca}^{++}$ , and  $\text{Mg}^{++}$  fulvic acid complexes. Soil Sci., Vol. 103, pp. 247-252.
- Sinclair, A.J., 1976. Application of probability graphs in mineral exploration. Association of Exploration Geochemists, Special Vol. 4, 95 p.
- Sperling, J.H., 1965. Studies on the relationship between water movement and water chemistry in mires. Can. Jour. Botany, Vol. 44, pp 747-758.
- Stanton, R.E., 1966. Rapid methods of trace metal analysis. Edward Arnold Ltd., London, 96 p.
- Stevenson, F.J. and Butler, J.H.A., 1969. Chemistry of humic acids and related pigments. In: Organic Geochemistry, (Eglinton, G. and Murphy, M.T.J., Eds.), pp. 534-556.
- Stumm, W. and Morgan, J.J., 1970. Aquatic chemistry. Wiley Interscience, New York, 583 p.
- Sweeney, R.E. and Kaplan, I.R., 1973. Pyrite framboids formation: Laboratory synthesis and marine sediments. Econ. Geol., Vol. 68, pp. 618-634.
- Tabatabai, M.A. and Bremner, J.M. 1970. An alkaline oxidation method for determination of total sulphur in soils. Soil Sci. Soc. Am. Proc., Vol. 34, pp. 62-65.
- Tarakanova, E.I., 1971. Distribution of accessory elements in modern peat bogs. U.S.S.R. Academy of Sciences, Transactions of the Institute of Geology and Geochemistry, No. 90, pp. 55-63.
- Tarnocai, C., 1970. Classification of peat landforms in Mani-

toba. Canadian Dept. of Agriculture Research Station, Pedology Unit, Winnipeg, Man., 45 p.

- Thorstenson, D.C., 1970. Equilibrium distribution of small organic molecules in natural waters. *Geochim. Cosmochim. Acta.*, Vol. 34, pp. 745-770.
- Timperly, M.H. and Allan, R.J., 1974. The formation and detection of metal dispersion haloes in organic lake sediments. *Jour. Geoch. Expl.*, Vol. 3, No. 2, pp. 167-190.
- Turner, R.G., 1969. Heavy metal tolerance in plants. In: Ecological aspects of the mineral nutrition of plants. *Brit. Ecol. Soc. Symp. No. 9.* Blackwell Scientific Publications, Oxford, pp. 399-410.
- Usilk, L., 1968. Comparison of geochemical and geobotanical prospecting methods in peatlands. *Geol. Surv. Can. Paper 68-66.*
- Vallentyne, J.R., 1962. A chemical study of pyrite spherules isolated from sediments of Little Round Lake, Ontario. In: Biochemistry of sulphur isotopes, (Jensen, M.L., Ed.), *National Science Symposium*, pp. 144-152.
- Van Dijk, H., 1971. Colloidal chemical properties of humic matter. In: Soil Biochemistry (McLaren, A.D. and Skujins, J., Eds.), Vol. 2, pp. 16-35.
- Walsh, T. and Barry, T.A., 1958. The chemical composition of some Irish peats. *Proceedings of the Royal Irish Academy*, Vol. 59, Sect. B, No. 15, pp. 308-325.
- Waksman, S.A. and Stevens, K.R., 1929. Contribution to the chemical composition of peat:V. The role of microorganisms in peat formation and decomposition. *Soil Sci.*, Vol. 4, pp. 315-325.

APPENDIX A: Results of soil and till sample analyses.

ANALYTICAL RESULTS FOR SOIL AND TILL SAMPLES									
NUMBER	PPM CD	PPM CU	PPM FE	PPM MH	PPM NI	PPM ZN	% CARBON	PH	PPM MO
73-RL-18	122.5	11114.2	1.268	203.5	131.8	50.1	24.40	5.10	55.5
19	125.1	8803.3	1.540	226.9	76.1	336.0	0.0	4.80	28.9
20	30.1	2533.4	2.526	326.8	77.4	249.8	9.53	4.80	11.4
21	137.6	15533.8	1.243	420.7	152.1	254.9	19.23	4.80	13.7
22	353.5	24423.9	0.754	326.2	18.9	454.3	27.85	4.20	11.4
28	79.7	941.8	2.980	393.5	58.2	264.1	0.75	7.00	26.6
29	35.0	388.0	2.970	416.2	126.3	57.1	0.29	5.10	0.0
30	33.2	134.5	3.652	639.2	110.5	64.4	0.18	6.50	0.0
31	41.1	131.3	4.196	904.1	111.7	65.6	0.15	6.00	0.0
32	39.0	202.9	4.143	800.5	77.5	89.0	0.21	6.40	0.0
33	38.0	240.7	3.847	755.0	8.2	165.5	0.26	7.30	6.1
34	7.9	397.4	4.464	175.9	8.0	77.9	0.13	5.70	13.7
35	12.3	345.9	3.856	172.6	77.3	66.8	0.16	5.80	9.1
36	38.4	261.3	3.834	889.6	78.0	233.5	0.16	6.10	0.0
37	26.6	46.3	2.690	454.1	63.7	167.4	1.53	5.20	0.0
38	30.4	84.5	3.523	309.3	50.3	80.9	0.02	5.20	0.0
40	32.4	46.3	3.386	303.0	51.4	556.7	1.00	5.10	0.0
41	27.4	41.6	2.728	195.5	22.4	88.8	1.53	5.00	1.5
42	26.7	145.9	3.322	277.7	30.7	187.8	1.51	5.00	0.0
43	34.8	194.8	3.730	276.2	33.3	205.8	0.74	5.30	1.5
44	26.8	51.5	2.307	198.5	28.5	238.8	1.30	5.70	0.0
45	29.5	92.7	2.907	270.5	43.8	246.2	0.26	5.70	1.5
46	25.1	80.0	2.404	195.5	44.2	259.0	1.51	5.30	0.0
47	30.9	112.5	3.334	356.3	54.0	80.2	0.38	5.40	1.5
48	30.8	116.6	2.618	175.3	59.0	319.2	1.24	5.00	5.5
49	36.2	1521.7	2.135	366.3	86.9	1797.9	1.17	5.90	17.7
50	31.4	2173.6	4.103	621.1	98.4	323.8	0.48	6.00	16.7
51	17.3	235.4	2.689	219.7	40.6	242.0	1.14	6.20	4.6
52	52.4	1231.9	3.388	527.1	67.5	75.3	2.43	5.70	1.5
53	51.7	1352.8	3.924	583.8	77.9	78.7	2.34	5.30	2.4
54	27.2	66.8	2.622	195.8	38.0	49.3	2.46	5.20	0.0
55	25.8	96.5	2.822	220.9	44.5	57.0	1.72	5.30	0.0
56	27.0	56.4	2.588	196.4	32.2	51.3	2.41	4.80	0.0
57	34.3	99.3	3.310	346.3	53.9	61.0	0.48	5.20	0.0
58	23.6	105.7	2.801	200.9	44.7	76.0	1.65	5.20	1.5
59	27.3	138.6	3.353	298.6	58.9	76.8	0.86	5.20	0.0
60	26.5	188.6	3.342	285.7	52.8	257.8	1.65	5.10	0.0
61	29.4	138.1	3.128	350.3	55.9	68.3	0.68	5.30	0.0
68	18.2	44.3	2.596	572.5	37.6	392.4	2.08	5.60	1.0
69	26.4	126.1	3.802	366.7	52.5	241.7	0.61	6.90	1.0
90	23.6	39.7	2.901	535.9	42.7	207.1	1.17	6.00	1.0
91	25.5	75.3	3.721	366.4	52.4	83.9	0.38	5.60	0.0
92	17.5	65.9	2.195	135.3	28.8	65.2	1.14	5.20	1.0
93	29.2	129.6	3.801	472.2	60.4	62.3	0.73	5.50	1.0
94	37.5	511.3	5.566	320.7	84.4	396.6	2.65	5.70	2.0
95	31.4	239.9	4.334	431.1	59.5	75.9	0.90	5.70	1.0
96	22.7	61.9	2.368	449.5	47.9	62.6	1.14	5.60	1.0
97	30.4	69.9	3.747	521.2	81.1	60.9	1.29	5.70	1.0
98	21.5	228.0	3.159	609.9	57.6	171.0	3.35	5.60	9.2
99	26.0	152.2	2.990	325.0	55.8	76.0	1.00	5.50	6.1

ANALYTICAL RESULTS FOR SOIL AND TILL SAMPLES

NUMBERS	PPM CU	% FE	PPM MN	PPM VJ	PPM ZN	% CARBON	PH	PPM MO
73-RL-100	26.9	3.520	440.8	70.1	59.3	0.29	5.40	0.0
101	25.1	2.808	211.0	57.6	88.2	0.52	5.20	6.1
102	16.6	2.149	314.8	33.9	40.4	0.23	5.10	0.0
103	21.8	2.806	198.5	58.8	77.0	1.03	5.00	0.0
104	26.7	3.079	365.8	72.2	56.9	0.04	5.30	0.0
105	19.0	2.605	163.1	40.7	48.1	1.52	5.20	3.8
106	26.5	3.545	296.7	64.4	238.2	1.46	4.90	11.5
107	24.1	2.022	202.4	20.0	41.8	3.51	5.20	7.6
108	14.2	4.110	261.7	58.9	197.7	0.91	5.20	9.2
109	30.7	3.065	407.6	51.4	28.6	2.55	4.70	6.1
110	28.3	3.496	471.3	63.4	188.6	0.42	5.10	7.6
111	24.6	3.034	450.6	62.8	374.2	1.34	5.20	5.9
112	12.4	2.562	214.3	50.9	21.6	1.12	5.00	0.0
113	21.8	3.151	383.8	66.6	88.0	0.44	4.90	0.0
114	18.7	3.131	273.8	57.6	208.5	1.40	5.00	3.7
115	22.5	3.795	360.4	77.8	78.1	0.64	5.20	5.9
116	12.4	2.954	777.4	66.0	250.7	6.97	5.10	7.4
117	333.2	2.310	3109.1	24.3	134.6	26.39	4.50	33.4
118	83.0	2.093	617.4	41.6	226.2	19.00	4.50	13.4
119	32.0	2.980	429.1	74.1	81.0	3.97	5.30	30.0
120	412.9	5.286	2883.3	77.2	478.8	39.53	4.50	94.9
121	473.2	2.310	657.9	185.3	204.8	22.92	4.50	7.4
122	140.4	0.890	471.2	120.5	344.3	31.98	4.50	0.0
123	159.7	1.309	392.3	193.2	1941.2	50.58	4.50	3.7
124	54.9	0.601	189.3	250.4	178.2	44.16	4.50	14.8
125	23.4	2.799	519.9	78.7	244.6	0.87	4.80	0.0
127	314.9	1.067	3085.4	21.1	87.2	17.03	4.50	18.5
128	151.3	1.401	1025.1	111.6	77.2	25.95	4.50	8.9
129	141.7	2.490	499.4	165.4	143.7	14.14	4.50	13.4
130	28.3	3.681	672.4	83.1	71.6	0.23	6.50	3.7
131	42.1	3.974	613.2	112.2	57.7	0.17	6.50	0.0
132	35.9	4.722	883.2	108.3	81.6	0.10	7.20	0.0
133	28.6	3.555	617.4	73.0	61.2	0.02	7.30	0.0
134	24.2	2.802	468.4	50.7	52.7	0.01	7.40	0.0
136	43.0	5.366	1448.6	155.0	71.9	0.18	7.10	0.0
137	28.3	3.826	664.7	72.5	75.3	0.05	7.50	0.0
138	30.5	3.882	711.0	82.2	69.4	0.10	7.20	0.0
139	33.9	4.402	548.6	95.2	16.7	0.05	7.30	3.9
140	26.0	3.533	597.1	81.8	33.3	0.02	7.40	6.3
141	25.4	3.561	597.1	82.7	78.3	0.01	7.60	0.0
142	32.2	3.477	570.7	67.0	98.0	0.04	7.50	0.0
143	27.3	3.626	354.0	70.9	66.9	0.07	6.20	0.0
144	30.2	4.277	607.7	83.4	81.3	0.05	6.90	0.0
145	26.2	3.403	602.4	95.6	78.3	0.31	7.30	3.9
146	27.4	3.505	618.2	77.7	77.1	0.13	7.30	0.0
147	10.9	3.607	158.5	44.7	24.5	0.26	6.60	27.5
148	20.2	3.161	549.5	51.9	104.4	0.05	5.80	0.0
149	17.9	3.189	496.7	47.5	140.6	0.01	5.90	0.0
150	27.5	3.691	649.9	83.3	82.1	0.01	6.20	0.0

ANALYTICAL RESULTS FOR SOIL AND TILL SAMPLES									
NUMBER	PPM CO	PPM CU	% FE	PPM MN	PPM NI	PPM ZN	% CARBON	PH	PPM MO
73-RL-151	31.6	376.8	3.951	760.9	100.6	212.9	0.01	6.20	0.0
152	33.4	369.6	4.137	739.0	79.7	136.5	0.09	7.00	6.3
153	45.4	2662.4	4.072	819.0	81.6	162.7	0.20	5.90	3.9
154	33.2	370.5	3.775	686.9	93.7	97.0	0.16	6.70	3.0
155	35.2	637.9	3.291	554.8	63.0	110.4	0.13	5.70	4.0
74-RL-1017	14.7	223.7	2.569	219.3	45.1	57.8	0.0	5.20	1.8
1019	18.3	86.6	3.376	389.4	58.9	51.4	0.39	4.80	1.8
1019	15.9	138.9	2.716	227.8	44.2	61.0	1.38	5.10	2.9
1020	17.7	216.5	3.303	366.7	54.1	55.9	0.03	5.20	5.4
1021	54.7	2058.8	3.429	424.9	93.6	118.8	2.41	4.90	1.9
1022	22.0	603.4	2.876	293.3	69.4	65.7	0.29	5.20	0.0
1023	8.6	3194.7	0.525	58.4	10.4	14.1	23.60	4.00	0.0
1024	0.0	2307.3	1.659	65.8	9.5	20.2	18.63	3.90	0.0
1025	13.5	415.3	1.843	180.5	46.3	47.3	1.46	3.90	0.0
1026	8.9	2307.3	1.604	150.4	21.7	28.2	15.68	4.60	7.6
1027	14.0	1405.7	1.567	159.2	22.4	35.5	5.07	4.50	0.0
1028	25.5	2484.7	3.576	477.6	83.3	180.6	2.95	5.90	10.6
1029	19.1	930.0	3.134	424.9	73.0	85.4	0.57	5.80	4.6
1030	29.8	2200.8	3.134	522.7	53.7	114.2	3.35	5.60	10.6
1031	39.7	8341.6	3.429	377.8	75.2	164.1	11.64	5.60	14.2
1032	32.8	3230.2	4.350	383.5	69.2	136.6	2.15	5.70	12.1
1054	69.8	5634.4	0.344	1337.3	50.9	63.0	31.38	4.90	0.0
1055	414.3	8406.9	0.695	2872.3	75.5	277.8	17.38	4.80	6.2
1056	81.2	7780.9	1.999	178.9	57.0	135.8	20.18	4.80	0.0
1057	152.0	24594.7	1.560	395.5	159.0	4687.5	28.33	7.00	4.9
1058	270.6	14846.3	2.803	404.9	197.1	1111.1	28.09	4.60	2.1
1059	266.0	16456.1	2.877	508.5	335.9	3472.2	27.94	4.60	6.7
1060	75.6	5795.4	3.998	361.6	132.0	951.4	7.68	4.70	2.4
1061	283.8	5545.0	0.902	527.4	35.4	177.1	17.46	4.70	0.6
1062	336.5	18334.3	1.048	52.7	177.3	1614.6	19.60	4.60	9.7
1063	482.2	22806.0	1.487	64.0	215.1	1180.6	21.81	4.30	3.9
1064	170.0	12342.1	0.878	49.0	93.3	536.5	21.28	4.60	3.9
1065	1777.0	3928.0	7.392	20735.6	17.0	21.8	28.56	4.60	60.8
1067	32.1	384.1	3.173	358.7	67.4	99.0	11.07	4.70	4.2
1068	18.4	2164.8	1.262	93.4	21.2	50.9	7.92	4.70	51.2
1069	18.2	303.8	3.055	306.4	56.9	71.1	0.95	4.70	3.4
1070	21.5	230.4	3.101	306.4	62.4	80.1	0.59	4.60	0.0
1071	0.0	5586.5	0.559	84.1	17.1	18.6	18.85	4.30	0.0
1072	26.3	4189.9	0.523	84.1	73.4	214.3	25.61	4.60	15.7
1073	22.5	439.9	2.091	224.2	58.6	150.5	2.80	4.40	3.4
1074	18.9	6284.8	1.127	112.1	25.5	28.7	20.96	4.30	10.5
1075	860.1	9165.3	2.055	242.8	92.7	223.0	27.94	4.50	29.4
1076	70.6	1169.7	3.353	343.7	91.9	294.1	3.59	4.10	14.7
1077	17.2	5761.0	0.469	93.4	23.0	31.5	18.47	4.50	10.5
1078	69.3	9950.9	0.883	65.4	62.7	264.8	24.99	4.30	18.9
1079	27.3	642.4	2.632	283.9	72.1	135.9	1.72	4.80	6.3
1080	34.5	5848.3	1.352	112.1	45.3	92.3	16.22	4.50	0.0
1081	43.2	10038.2	0.721	74.7	57.6	155.1	43.03	4.60	23.1
1082	23.2	708.8	3.101	291.4	87.5	182.6	2.43	4.50	2.1
1083	11.6	7245.0	0.667	93.4	24.8	46.5	23.05	4.50	5.2

ANALYTICAL RESULTS FOR SOIL AND TILL SAMPLES										
NUMBER	PPM CD	PPM CU	% FE	PPM MN	PPM NI	PPM ZN	% CARBON	PH	PPM MO	
74-RL-1084	67.0	9252.6	1.217	112.1	91.4	597.2	29.65	4.30	18.8	
1085	106.6	3928.0	3.038	242.8	125.9	504.9	16.30	4.50	18.9	
1086	30.3	230.4	3.606	418.4	84.4	117.1	0.74	5.00	4.2	
1087	19.7	8164.2	1.206	37.3	24.1	32.6	34.11	4.70	22.5	
1088	171.8	14196.6	1.522	168.0	118.4	562.4	41.44	4.30	19.8	
1089	74.1	3833.6	2.645	410.7	100.1	235.6	21.87	4.90	7.2	
1090	35.1	276.9	3.898	392.1	77.8	113.3	0.98	5.00	3.6	
1091	10.4	2174.2	4.037	56.0	19.2	28.0	13.65	5.30	0.0	
1092	271.0	8607.9	0.125	149.4	72.6	283.4	16.73	4.30	16.2	
1093	152.9	17038.3	0.724	242.7	97.8	321.3	23.13	4.30	0.0	
1094	164.4	23072.7	0.436	270.7	125.1	576.6	31.96	4.10	7.2	
1095	122.5	17748.2	0.432	532.1	139.3	535.4	39.40	4.00	19.8	
1096	287.2	13754.9	0.947	634.8	162.1	550.7	42.60	4.50	73.7	
1097	49.4	692.2	3.638	380.9	75.4	100.2	1.26	4.40	1.8	
1098	31.7	9761.5	1.318	261.4	38.9	37.6	26.52	5.00	10.8	
1099	78.4	7986.7	0.835	158.7	60.9	71.2	34.88	4.50	31.5	
1100	114.8	16860.8	0.464	140.0	65.0	83.7	44.02	4.50	25.2	
1101	266.3	17925.7	0.538	149.4	39.5	118.6	38.61	4.40	18.0	
1102	240.7	15086.0	0.191	457.4	61.6	60.6	42.00	4.80	16.2	
1103	267.2	5750.4	1.856	429.4	127.6	196.4	30.89	4.70	34.2	
1104	95.2	3194.7	4.455	328.6	72.9	210.9	3.95	3.70	42.4	
1105	34.7	575.0	3.564	373.4	75.6	85.7	1.65	5.10	22.5	
1106	30.6	3594.0	3.248	326.7	52.8	36.7	25.10	5.00	40.5	
1107	49.7	7720.5	2.784	242.7	58.1	174.6	15.57	4.80	34.2	
1108	27.2	3959.3	1.820	248.3	56.2	154.4	0.0	0.0	9.9	
1110	23.5	4810.2	2.558	650.2	57.6	141.3	18.28	5.40	23.1	
1111	67.8	5152.5	3.605	197.0	65.5	244.6	22.91	4.40	45.5	
1112	23.7	4013.6	2.335	208.9	51.8	135.7	5.56	4.80	13.9	
1113	33.6	2820.3	2.953	232.5	54.8	65.4	8.29	4.50	16.5	
1114	25.5	1355.9	3.845	551.7	59.7	192.9	7.41	5.50	19.2	
1115	17.2	943.7	3.021	244.3	56.5	158.4	5.36	5.70	12.6	
1116	69.1	16678.0	0.670	69.0	38.1	89.6	22.32	4.50	18.2	
1117	112.3	12881.4	2.249	216.7	70.6	182.6	10.94	7.00	24.8	
1118	118.0	23864.4	3.949	246.3	76.5	245.3	16.73	4.70	12.4	
1119	28.5	7159.3	0.645	90.6	27.8	73.0	10.94	5.00	7.2	
1120	398.3	4718.6	0.251	2206.9	50.6	120.6	4.89	4.90	29.1	
1121	17.2	5916.9	0.532	69.0	22.4	55.1	16.22	5.00	26.5	
1122	12.4	5857.6	0.378	47.3	17.5	117.1	10.00	4.60	24.8	
1123	11.6	3362.7	1.133	118.2	23.9	82.7	8.29	4.80	9.3	
1124	13.9	9003.4	0.618	63.1	37.1	67.5	9.58	4.70	23.8	
1125	15.1	5694.9	0.625	51.2	26.1	63.4	10.04	4.80	16.5	
1126	23.6	4772.9	0.474	31.5	27.6	74.4	13.05	4.80	19.8	
1127	18.3	7484.7	0.405	31.5	27.2	58.6	10.45	4.90	13.9	
1128	7.6	4000.0	0.755	14.8	10.2	14.8	36.69	4.20	18.2	
1129	0.0	5423.7	0.326	9.9	13.4	31.0	31.92	4.70	18.2	
1130	12.4	1773.6	0.842	63.7	24.5	66.1	6.96	4.30	5.0	
1131	14.9	2331.0	1.369	87.6	29.7	59.8	7.88	4.30	9.3	
1132	23.1	4155.2	1.635	71.6	46.9	161.7	9.19	4.80	18.2	
1133	41.1	4763.3	1.962	119.4	63.1	142.0	5.55	5.00	13.9	
1134	6.4	4307.2	1.093	69.7	17.7	32.7	33.49	4.20	16.6	

ANALYTICAL RESULTS FOR SOIL AND TILL SAMPLES										
NUMBER	PPM CO	PPM CU	% FE	PPM MN	PPM NI	PPM ZN	% CARBON	PH	PPM MO	
74-RI-1135	9.9	1621.5	1.103	55.7	19.2	36.6	8.81	4.40	4.0	
1135	23.4	1624.2	3.106	199.0	55.1	84.4	2.73	5.00	5.0	
1166	17.4	311.2	5.036	413.3	41.0	86.8	0.10	5.00	7.5	
1167	25.2	311.2	3.437	609.2	59.0	119.0	0.10	7.30	0.0	
1168	23.2	165.6	3.642	650.5	72.7	72.1	0.27	6.70	2.7	
1169	31.5	140.5	3.680	541.5	101.9	110.6	0.10	7.30	5.1	
1170	47.4	502.0	3.332	511.4	62.7	70.0	0.10	4.20	3.4	
1171	57.4	562.2	4.068	714.5	73.1	87.5	0.10	4.00	0.0	
1172	190.6	1129.4	3.680	1316.1	63.9	81.9	0.10	4.20	4.1	
1173	28.8	165.6	4.068	534.0	74.3	87.5	0.10	7.00	0.0	
1174	25.4	441.7	4.145	440.0	75.2	80.5	0.10	4.60	0.0	
1175	31.7	140.5	3.603	902.5	90.3	73.5	0.10	7.30	0.0	
1176	37.3	1607.5	4.094	469.1	81.3	96.2	0.10	5.30	3.3	
1177	41.9	160.8	3.776	382.5	102.0	89.3	0.24	7.40	5.0	
1178	32.1	477.2	4.094	707.6	107.2	96.2	0.10	7.30	0.0	
1179	35.0	713.3	4.452	429.3	97.4	106.5	0.24	6.10	2.7	
1180	40.5	1281.0	4.651	485.0	95.9	140.9	0.10	5.70	0.0	
1181	23.1	1355.4	3.697	298.1	61.1	94.2	0.20	5.90	3.3	
1182	19.0	2411.3	3.180	246.5	57.2	70.1	0.61	5.00	15.9	
1183	47.5	1155.4	4.055	735.4	71.9	143.0	0.20	6.00	2.7	
1184	23.3	221.0	3.776	548.5	57.2	77.7	0.47	7.40	4.0	
1185	21.3	135.6	3.180	270.3	44.6	50.9	0.10	5.90	6.0	
1186	21.2	241.1	3.180	270.3	49.6	63.2	0.59	5.00	7.3	
1187	23.3	733.4	3.776	699.6	60.2	164.9	0.43	6.30	33.9	
1188	28.6	130.6	4.253	644.0	72.1	71.5	0.10	7.40	4.0	
1189	21.6	1105.2	3.975	349.8	53.4	152.6	0.30	6.60	31.5	
1190	30.6	130.6	3.816	667.8	88.5	63.2	0.10	7.60	0.0	
1191	29.2	1205.7	3.657	314.0	61.7	137.5	1.18	4.80	27.2	
1192	55.3	5128.7	4.850	397.5	23.5	116.8	0.10	6.30	106.2	
1193	27.2	612.9	4.452	524.7	63.0	85.9	0.10	6.00	7.3	
1194	28.1	160.8	4.293	604.2	70.6	70.1	0.10	7.50	3.3	
1195	30.1	120.6	4.532	663.9	76.5	63.7	0.10	7.50	2.7	
1196	30.0	110.5	4.452	644.0	85.1	63.2	0.10	7.70	0.0	
1197	22.1	105.8	3.269	287.3	53.0	54.7	0.53	6.60	2.6	
1198	26.1	126.1	3.678	573.4	63.2	68.0	0.10	7.50	0.0	
1199	19.7	110.2	3.188	233.6	49.0	55.3	0.10	4.90	0.0	
1200	21.2	112.2	3.842	544.8	59.8	73.3	0.10	7.30	3.3	
1201	24.3	158.9	3.342	582.2	74.7	72.0	0.10	7.50	3.3	
1202	25.0	120.7	4.209	541.1	65.6	84.0	0.10	7.40	3.9	

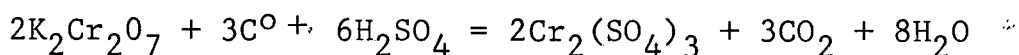
ANALYTICAL RESULTS FOR DISSOLVED METAL, ORGANIC					CARBON, SULPHATE CONTENTS AND PH IN BOG WATER SAMPLES				
NUMBER	PPM CU	PPM CARBON	PPM FE	PPM MN	PPM ZN	PH	PPMSO <sub>4</sub>	PPM CA	
74-RL-1207	0.0	1.500	0.153	0.0	0.028	7.000	0.0	27.000	
1208	0.075	2.000	0.0	0.0	0.020	5.500	0.0	6.000	
1209	0.042	3.000	0.0	0.0	0.011	5.800	0.0	6.000	
1210	0.021	3.000	0.0	0.0	0.014	5.500	0.0	5.000	
1211	0.042	0.0	0.061	0.0	0.0	5.500	23.000	6.000	
1212	0.0	5.000	0.0	0.041	0.0	5.800	0.0	9.000	
1213	0.117	0.500	0.0	0.0	0.0	5.800	0.0	8.000	
1215	0.271	1.500	0.0	0.0	0.0	6.000	0.0	8.000	
1223	0.0	0.0	0.0	0.0	0.0	5.800	37.000	24.000	
1224	0.229	0.0	0.0	0.0	0.0	6.500	40.000	22.000	
1225	0.062	1.000	0.092	0.0	0.0	6.400	0.0	9.000	
1226	0.042	1.000	0.074	0.0	0.0	0.0	0.0	6.000	
1227	0.466	4.000	0.0	0.062	0.014	5.600	0.0	14.000	
1228	0.591	2.000	0.0	0.041	0.023	7.300	0.0	14.000	
1229	0.117	3.500	0.0	0.0	0.009	0.0	0.0	0.0	
1230	0.250	0.0	0.0	0.0	0.020	6.800	0.0	24.000	
1231	0.021	1.000	0.0	0.0	0.0	7.200	20.000	119.000	
1232	0.0	0.500	0.0	0.0	0.054	6.800	120.000	125.000	
1233	0.133	2.500	0.0	0.0	0.011	0.0	0.0	34.000	
1234	0.033	3.000	0.0	0.0	0.062	6.800	0.0	27.000	
1275	0.117	2.000	0.0	0.041	0.006	7.000	0.0	42.000	
1277	0.075	3.000	0.0	0.0	0.006	7.000	35.000	22.000	
1279	0.050	3.000	0.0	0.0	0.006	6.000	37.000	58.000	
1280	0.021	0.500	0.0	0.0	0.0	0.0	40.000	0.0	
1262	0.042	3.000	0.0	0.0	0.0	7.000	0.0	21.000	
1283	0.0	1.500	0.0	0.0	0.0	7.500	0.0	52.000	
1285	0.062	3.000	0.0	0.0	0.0	7.000	0.0	27.000	
1287	0.175	2.000	0.0	0.0	0.0	7.000	40.000	21.000	
1289	0.146	3.500	0.042	0.0	0.020	5.500	0.0	8.000	
1290	0.125	2.000	0.061	0.0	0.010	5.800	0.0	16.000	
1290	0.0	0.117	2.500	0.061	0.0	5.000	0.0	30.000	
1292	0.175	2.000	0.0	0.028	0.034	5.500	0.0	21.000	
1293	0.241	2.000	0.0	0.043	0.034	5.500	0.0	21.000	
1294	0.158	1.500	0.0	0.0	0.031	5.800	0.0	16.000	
1295	0.146	0.0	0.0	0.0	0.054	5.500	0.0	28.000	
1311	0.021	1.000	0.061	0.0	0.0	7.000	0.0	56.000	
1312	0.0	0.500	0.0	0.0	0.0	7.000	20.000	26.000	
1314	0.658	0.0	0.0	0.034	0.030	5.000	65.000	23.000	
1315	0.699	0.0	0.0	0.043	0.028	4.500	75.000	23.000	
1316	0.749	0.500	0.0	0.043	0.030	4.000	75.000	23.000	
1317	0.708	0.0	0.0	0.051	0.037	5.200	80.000	29.000	
1318	0.062	2.000	0.0	0.0	0.025	6.000	18.000	6.000	
1320	0.395	0.500	0.0	0.034	0.039	4.000	50.000	16.000	
1321	0.283	2.000	0.276	0.043	0.025	0.0	0.0	13.000	
1322	0.104	2.000	0.0	0.0	0.069	5.000	0.0	6.000	
1323	0.146	0.500	0.0	0.023	0.022	5.500	0.0	8.000	
1324	0.146	3.000	0.0	0.0	0.020	4.000	0.0	7.000	
1325	0.208	2.500	0.092	0.0	0.051	5.000	0.0	12.000	

ANALYTICAL RESULTS FOR DISSOLVED METAL, ORGANIC CARBON, SULPHATE CONTENTS AND PH IN BUG WATER SAMPLES									
NUMBER	PPM CU	PPM CARBON	PPM FE	PPM MN	PPM ZN	PH	PPM SO <sub>4</sub>	PPM CA	
1326	0.200	2.000	0.061	0.0	0.021	7.000	0.0	19.000	
1328	0.021	1.000	0.0	0.0	0.028	6.000	0.0	25.000	
1329	0.241	0.0	0.0	0.0	0.015	6.800	0.0	24.000	
1330	0.042	0.0	0.0	0.0	0.0	0.0	0.0	24.000	
1414	0.0	1.000	0.061	0.0	0.010	0.0	0.0	84.000	
1416	0.0	1.000	0.0	0.0	0.010	0.0	0.0	69.000	
1418	0.0	0.0	0.0	0.0	0.0	0.0	0.0	60.000	
1420	0.0	0.0	0.123	0.0	0.010	7.000	0.0	56.000	
1427	0.021	9.500	0.0	0.204	0.015	6.000	45.000	25.000	
1428	0.0	9.000	0.110	0.136	0.010	7.500	40.000	25.000	
1429	0.050	16.000	0.172	0.074	0.022	7.000	27.000	11.000	
1439	0.400	2.000	0.398	0.043	0.015	6.000	60.000	18.000	
1442	0.050	4.000	2.228	0.051	0.0	6.200	62.000	23.000	
1443	0.052	3.500	0.441	0.059	0.0	6.000	62.000	25.000	
1444	1.061	4.000	0.061	0.043	0.039	0.0	65.000	25.000	
1491	0.062	9.000	0.0	0.0	0.077	0.0	0.0	2.000	
1492	0.0	9.000	0.0	0.165	0.0	4.000	27.000	16.000	
1493	0.632	7.000	0.0	0.057	0.015	4.500	0.0	0.0	
1494	0.375	4.500	0.135	0.062	0.010	0.0	0.0	17.000	
1495	0.241	1.500	0.123	0.0	0.0	5.800	0.0	19.000	
1495	0.187	0.0	0.0	0.0	0.047	5.800	0.0	0.0	
1497	0.200	0.0	0.061	0.0	0.049	0.0	0.0	0.0	
1507	0.0	12.000	0.092	0.071	0.0	4.800	30.000	28.000	
1508	0.649	5.000	0.061	0.062	0.010	0.0	40.000	13.000	
1509	0.042	5.500	0.123	0.176	0.010	6.500	37.000	20.000	
1511	0.0	7.500	0.0	0.0	0.0	0.0	0.0	35.000	
73-RL- 69	0.189		0.067		0.012	7.2	37.000		
72	0.058		0.075		0.006	6.8	20.000		
234	0.018		0.006		0.006	7.2	20.000		

## APPENDIX B

## B-1 ORGANIC CARBON BY WET OXIDATION

The method used for determination of organic carbon has been slightly modified from that described in the Royal School Mines Geochemical Prospecting Research Center, technical communication number 32. This technique, originally derived by Schollenberger (1927), is based on quantitative oxidation of carbon to carbon dioxide using a potassium dichromate-sulphuric acid solution by the following reaction.



Details of the procedure are outlined below.

- 1 Weigh 300 mg of the minus 80 mesh fraction of the sample into a 250 ml Erlenmeyer flask. The sample weight used for determinations must be decreased to 50 mg if organic carbon contents are greater than 40%.
- 2 Add 10 ml of 0.4 N potassium dichromate solution and 10 ml of concentrated sulphuric acid to the flask and mix the contents.
- 3 Heat the flask over a low flame for 25 seconds.
- 4 Cool the flask and add 100 ml of 5% sodium fluoride solution.
- 5 Add three drops of diphenylamine indicator to the flask.
- 6 Titrate the contents of the flask with 0.2 N ferrous ammonium sulphate and record the volume ( x cc) necessary for the colour to change from blue to green.
- 7 Carry out a blank titration following steps 2 to 6 and record the volume of ferrous ammonium sulphate ( y cc ) necessary for the colour change.

Percent organic carbon is calculated by the following relation-

ship.

$$\%C = \text{Vol. } K_2Cr_2O_7 \left(1 - \frac{y}{x}\right) \times \text{normality } K_2Cr_2O_7 \times 0.003 \times \frac{100}{\text{sample weight}}$$

Organic carbon values are multiplied by a correction factor of 1.3 to compensate for the fraction of carbon in the sample resistant to oxidation by the potassium dichromate.

#### Reagents.

Diphenylamine indicator: Dissolve 500 mg of diphenylamine in 100 ml of concentrated sulphuric acid and carefully add the mixture to 20 ml of water.

0.4 N potassium dichromate solution: Dissolve 19.6147 g potassium dichromate ( $K_2Cr_2O_7$ ), ANALAR grade, in distilled water, add 20 ml concentrated sulphuric acid, and make the solution up to 1 l.

#### B-2 ORGANIC CARBON BY LECO TOTAL CARBON ANALYSER.

Detailed operating instructions for the Leco Analyser are provided in the instrument manual. Essential components of the analyser are an induction furnace in which a small, fire-clay crucible can be loaded. The furnace and crucible are attached by a gas tight seal to a system consisting of an absorption vessel containing potassium hydroxide solution and a gas burette. 0.25 g of sample (minus 80 mesh fraction) are mixed with 2 scoops of iron accelerator and 1 scoop of tin accelerator in a clean crucible. Oxygen is passed through the system at a flow rate of 1.5 litres/minute and the sample ignited with the crucible attached to the system.

The carbon dioxide produced is absorbed in the potassium hydroxide solution and the volume decrease measured by balancing the two columns of the gas burette. Percent organic carbon is

indicated directly by graduations of the burette based on a one gram sample weight. Carbon content in the sample may require corrections for temperature and pressure which affect carbon dioxide volume measurements and for sample weights smaller than one gram. The Leco Analyser will measure both organic carbon and carbonates present in the sample. Since the peat samples analysed by this method were from a relatively acid environment it was assumed that carbonate content was negligible by comparison to organic matter content.

### B-3 SULPHATE IN WATER

The method for sulphate in water is given in Royal School of Mines Geochemical Prospecting Research Center, Technical Communication Number 27 and is based on the reaction between sulphate ions and barium chloride which precipitates barium sulphate. Sulphate content is measured by the intensity of the barium sulphate turbidity. Stages of the procedure are shown below:

1. Place 20 ml of filtered water in an 18 x 180 mm test tube calibrated at 20 and 25 ml.
2. Add 5 ml of acid-salt solution from a polythene wash-bottle
3. Add 250 mg of barium chloride crystals (dihydrate, Analar) using a scoop.
4. Shake for 30 seconds
5. Compare the turbidity produced with the standard series against a dark background (e.g. a matt black surface)
6. Calculate sulphate concentration from the relationship  
$$\text{PPM Sulphate} = \text{mg of matching standard} \times 50$$

Preparation of standards

1 To 12 test tubes (18 x 180 mm, calibrated at 20 and 25 ml) add respectively 0, 0.05, 0.1, 0.2, 0.3, 0.4, 0.5, 0.75, 1.0, 1.25, 1.5, 2.0 mg of sulphate.

2 Add 1 ml of gum acacia solution. (This may be omitted if determinations are made within several hours of preparing the standards.)

3 Dilute to 20 ml with water.

4 Add 5 ml of acid-salt solution.

5 Add 250 mg of barium chloride crystals.

6 Cork the tubes and shake for about 30 seconds to dissolve the crystals.

#### Reagents

Acid-salt solution: dissolve 240 g of sodium chloride ('ANALAR') in 900 ml of water, add 20 ml of concentrated hydrochloric acid (sp. gr 1.18, 'ANALAR') and dilute to 1 l with water.

Barium chloride: dihydrate, 'ANALAR'

Standard sulphate solution: dissolve 907 mg of potassium sulphate in water and dilute to 1 l to give a solution containing 0.5 mg of  $\text{SO}_4^{2-}$  / ml.

#### B-4 BIQUINOLINE EXTRACTABLE COPPER IN WATER

The procedure for biquinoline extractable copper in water, based on the method for copper in soils and sediments described by Stanton (1966), is outlined below.

1 Calibrate 18 x 180 mm test tubes at 20 ml volume.

2 Add 1 ml of buffer solution to 20 ml filtered water sample in the test tube.

3 Add 1 ml of 2-2 biquinoline to each tube.

4 Stopper each tube with a PVC bung and shake for 30 seconds.

5 Compare the colour developed with a standard series.

Preparation of standards (0 to 100 ppb copper)

To eight calibrated tubes add the following volumes of 1 ppm copper standard

No. ml 1 ppm standard	0	0.1	0.2	0.4	0.8	1.2	1.6	2.0
Copper in ppb	0	5	10	20	40	60	80	100

Make up the volume to 20 ml with distilled water and repeat stages 1 through 4.

Reagents

Buffer solution: dissolve 200 g of sodium acetate (tri-hydrate), 100 g potassium sodium tartrate (tetra-hydrate) and 20 g of ascorbic acid (all 'ANALAR' grade) in distilled water and dilute to 1 l. Extract with 0.01% dithizone solution until the buffer solution is free of copper and then remove the excess dithizone by extraction with carbon tetrachloride. The buffer solution should be at pH  $6.0 \pm 0.15$ .

0.01% dithizone solution: dissolve 40 mg of solid reagent in 400 ml of carbon tetrachloride and store in a vacuum flask.

0.02% 2-2 -biquinoline solution: dissolve 100 mg in iso-amyl alcohol by warming gently and dilute to 500 ml with iso-amyl alcohol.

Standard copper solution: 100 ppm copper; dissolve 200 mg of cupric sulphate (penta-hydrate) in 0.5 M hydrochloric acid and dilute to 500 ml with this strength of acid. Dilute this standard for 1 ppm copper with 0.5 M HCl.

Notes

1 All tubes and stoppers should be washed with 50% HCl, with water and finally with buffer/biquinoline before use.

2 Samples with more than 100 ppb copper may be analysed by diluting the original sample.

#### B-5 DETERMINATION OF SULPHATE IN SOIL BY HI REDUCTION AND BISMUTH COLORIMETRY

Sulphate-sulphur in soil is reduced to hydrogen sulphide using a hydriodic acid-hypophosphorous acid-formic acid mixture in a modified Johnson-Nishita apparatus (Tabatabai and Bremner 1970) and the hydrogen sulphide generated is carried by a nitrogen gas stream into a solution of sodium hydroxide. Bismuth nitrate is added to this solution and the concentration of precipitated bismuth sulphide measured by spectrophotometry (Kowalenko and Lowe 1972). The procedure outlined below is taken from an unpublished laboratory manual used in the Department of Soil Science, UBC.

##### Procedure

- 1 Pipette 20 ml of 1 N NaOH into a 22 x 200 mm test tube and attach to the distillation apparatus so that the delivery tube reaches almost to the bottom of the test tube (see sketch).
- 2 Adjust the nitrogen gas flow to roughly 8 bubbles/second.
- 3 Moisten the groundglass joint of the digestion flask, add the weighed sample and 4.2 ml of the reducing mixture from an automatic pipette. Sample weights of 10 to 100 mg may be used depending on the range of sulphate in the sample.
- 4 Attach the digestion flask to the condensor and digest for 20 minutes. (1 hour digestion time may be used for sulphate rich samples) at a Mark 3 setting on a LABCON heater or 70 on a Ful-Kontrol heater.
- 5 Remove the test tube after 20 minutes (or 1 hour), add 10

ml of the bismuth reagent and mix immediately on a "minishaker".

6 Read adsorbance at 400 nm on a Bausch and Lomb Spectronic 20 spectrophotometer against a blank obtained by mixing 20 ml of NaOH and 10 ml of bismuth reagent.

7 Standardize the apparatus before analysing unknown samples using a series of sulphate standards ranging from 10 to 100 ppm sulphate. The range can be increased to 200 ppm by blanking the spectrophotometer against a 40 ppm sulphate standard.

### Reagents

Reducing Mixture: Mix 200 ml hydriodic acid (47% with preservative), 50 ml hypophosphorous acid (50%) and 100 ml formic acid in a flask. Bubble nitrogen slowly through the solution and heat to 100°C; maintain this temperature for 10 minutes. Continue nitrogen flow while the solution cools. Store tightly stoppered. (Caution: highly corrosive).

Nitrogen purification solution: 10 g  $\text{HgCl}_2$  in 200 ml of 2%  $\text{KMnO}_4$ .

1 N NaOH: 4 g of solid NaOH ('ANALAR grade') in 1 l of distilled water.

Bismuth Reagent: Heat 3.4 g of 'ANALAR' grade bismuth nitrate ( $\text{Bi}(\text{NO}_3)_3 \cdot 5\text{H}_2\text{O}$ ) in 230 ml glacial acetic acid until dissolved. Filter if necessary (Whatman #50). Cool. Add 30 g gelatin dissolved by warming in about 500 ml water. Dilute solution to 1 l. Reagent is stable indefinitely.

Standard Sulphate: 1000 ppm S: 2.717 g  $\text{K}_2\text{SO}_4$  in 500 ml distilled water. Prepare working standards by diluting 1000 ppm standard with water.

Apparatus:

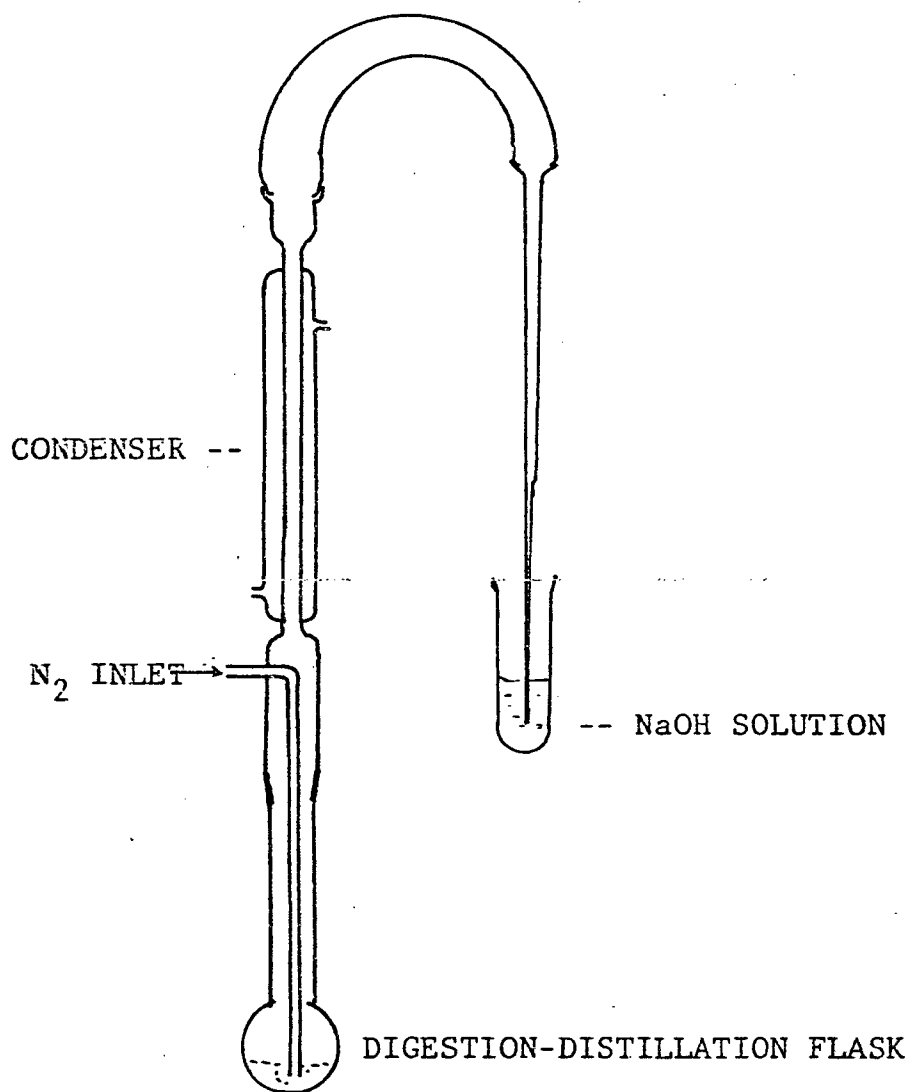
Johnson-Nishita digestion distillation apparatus with the following modification (Tabatabai and Bremner 1970).

- (a) Long-necked digestion flask with ground glass (T) socket.
- (b) Condenser with Nitrogen inlet and delivery tube.
- (c) Gas washing bulb omitted
- (d) Capillary tubes for nitrogen flow control (Kowalenko and Lowe 1972).

Notes:

- (a) Branch nitrogen lines for each unit from a common Reservoir flask through multi-holed stopper. Insert 30 cm of capillary glass tubing into each line to maintain uniform and balanced gas flow to each unit.
- (b) Condition apparatus prior to days run by running a standard solution through (standardize hydrogen sulphide adsorption by glassware).
- (c) Spectronic 20 spectrophotometer requires no optical filter at this wavelength.

Modified Johnson-Nishita apparatus used for determination of HI-reducibel sulphur (not drawn to scale).



### Appendix C

Probability graphs for metals, organic carbon and pH in soils and till.

Fig. C-1:

LOG PROBABILITY PLOT OF 96 COBALT VALUES IN THE TILL

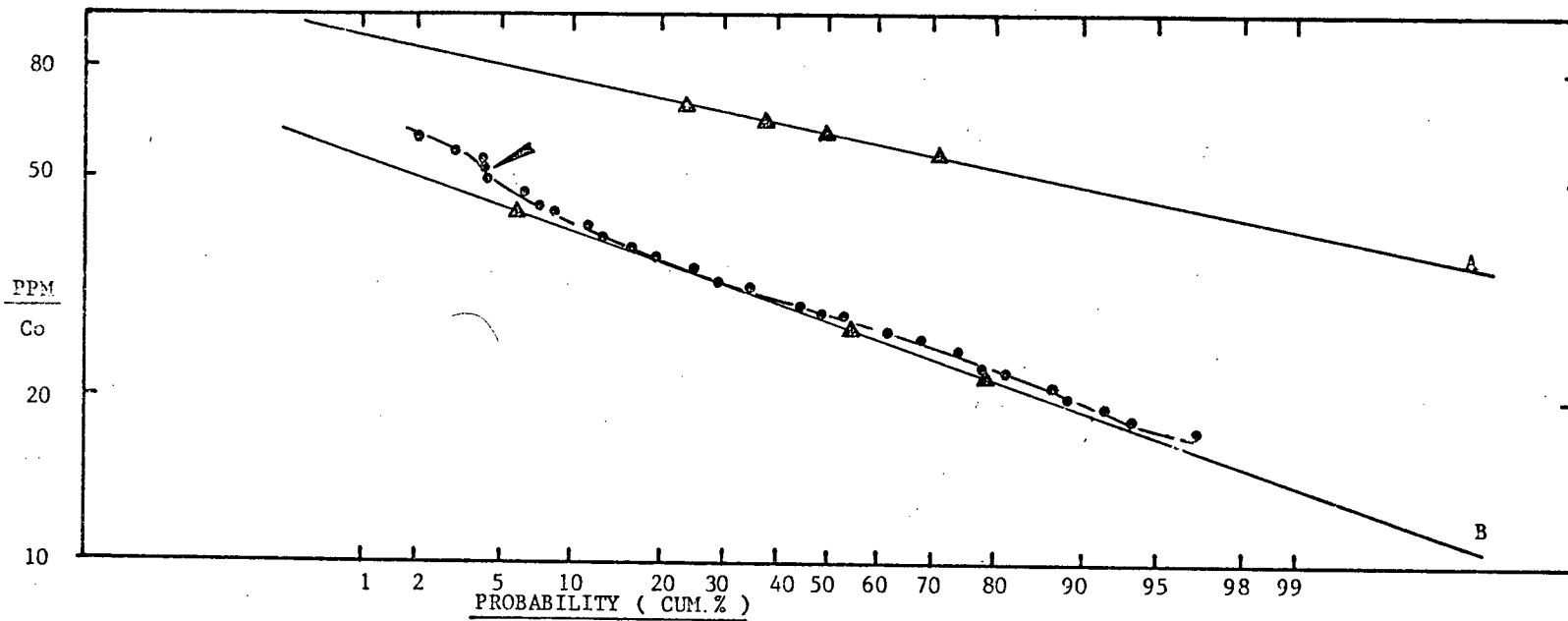


FIG. C-2:

LOG PROBABILITY PLOT OF 88 COBALT VALUES IN SOILS

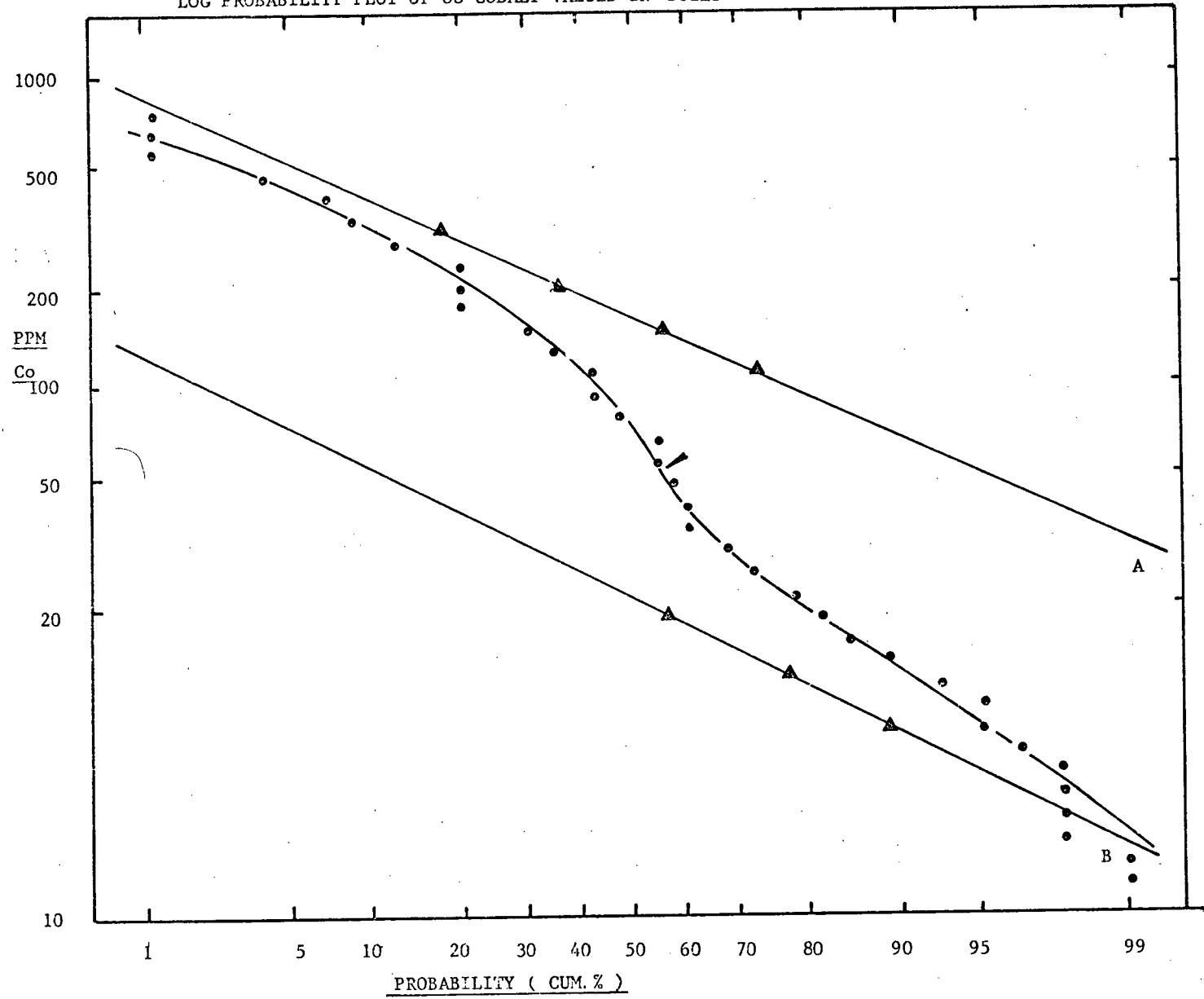


FIG. C-3: LOG PROBABILITY PLOT OF 96 COPPER VALUES IN THE TILL

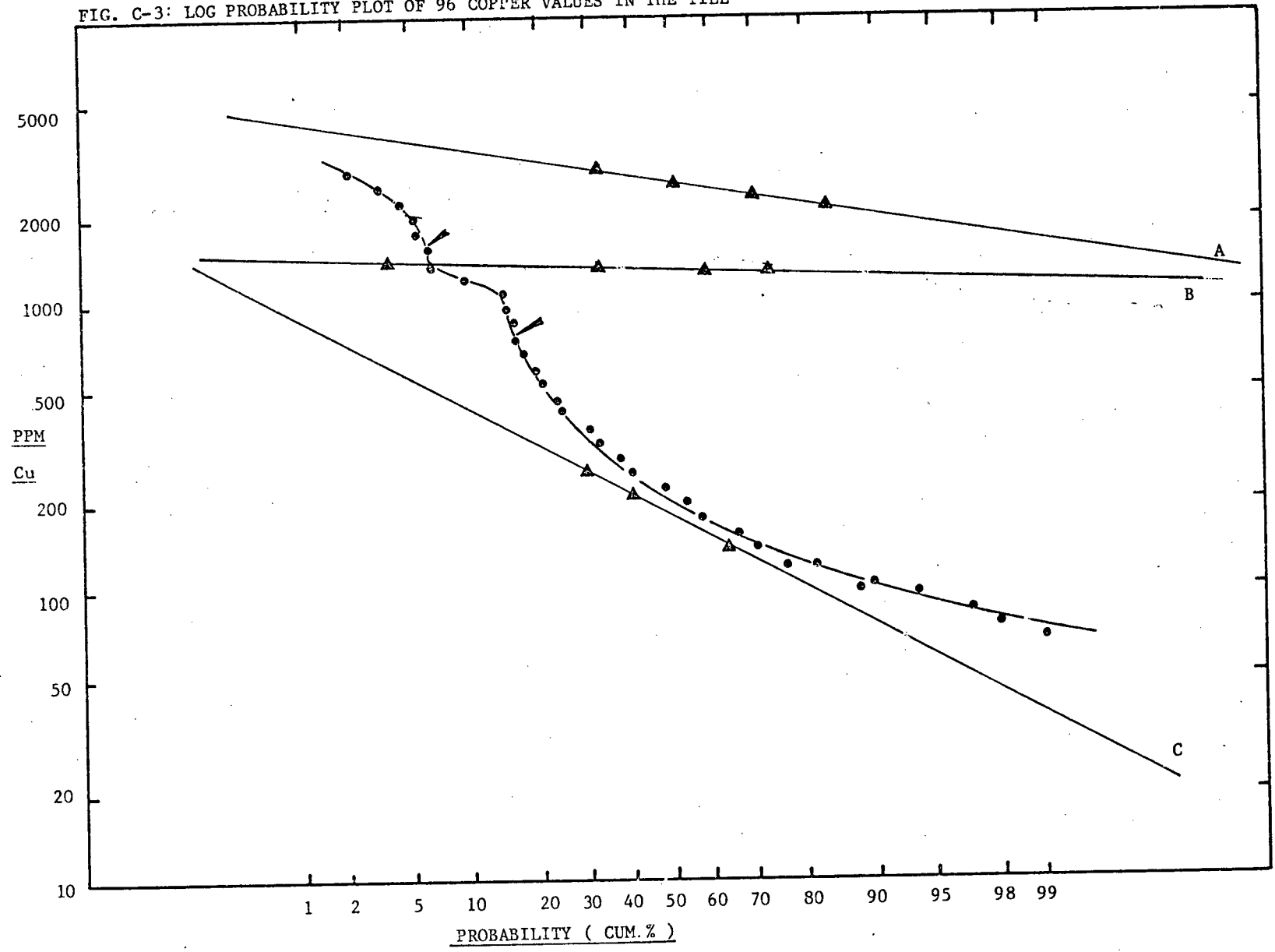


FIG. C-4: LOG PROBABILITY PLOT OF 90 COPPER VALUES IN SOILS

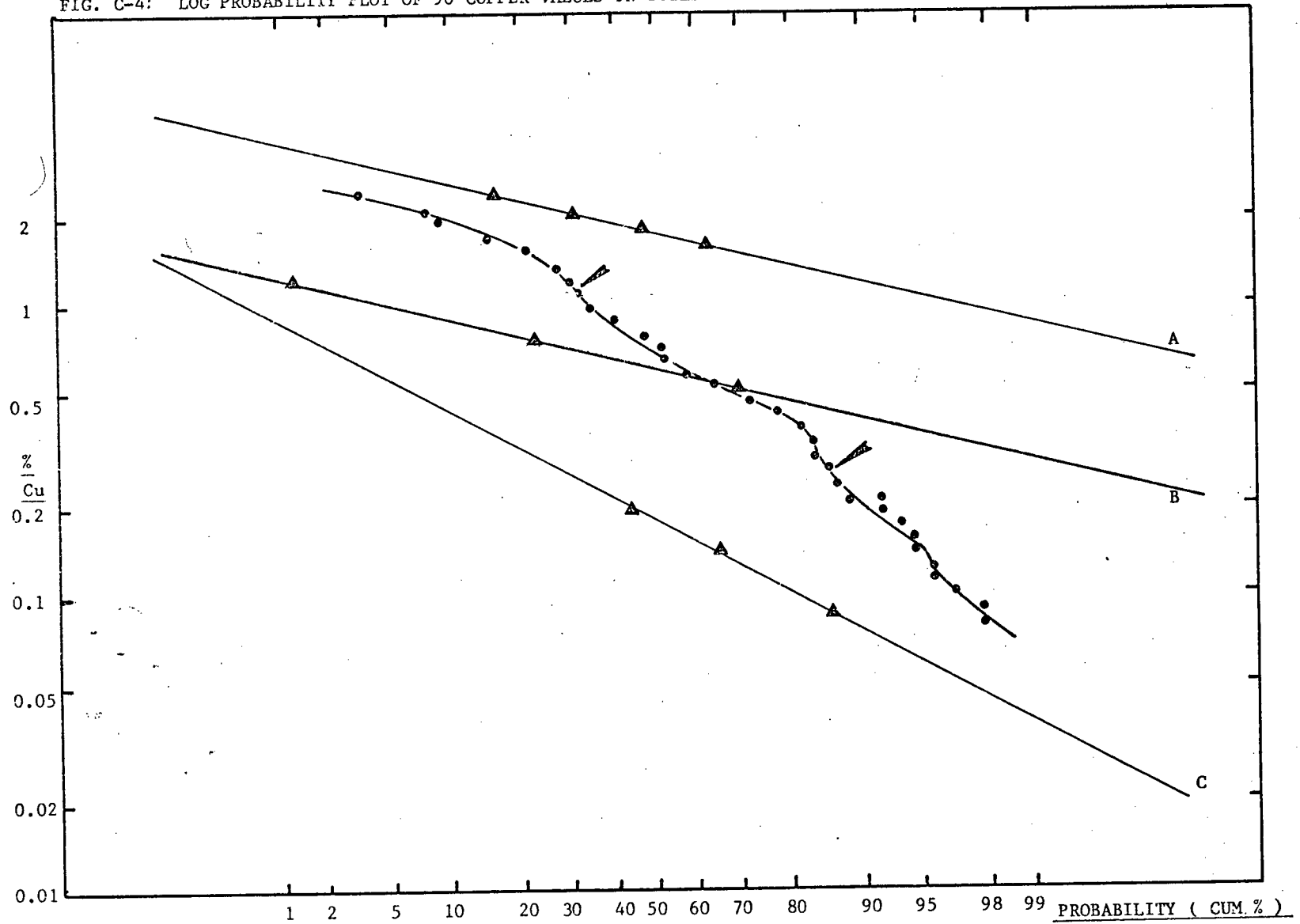


FIG. C-5: ARITHMETIC PLOT OF 96 IRON VALUES IN THE TILL

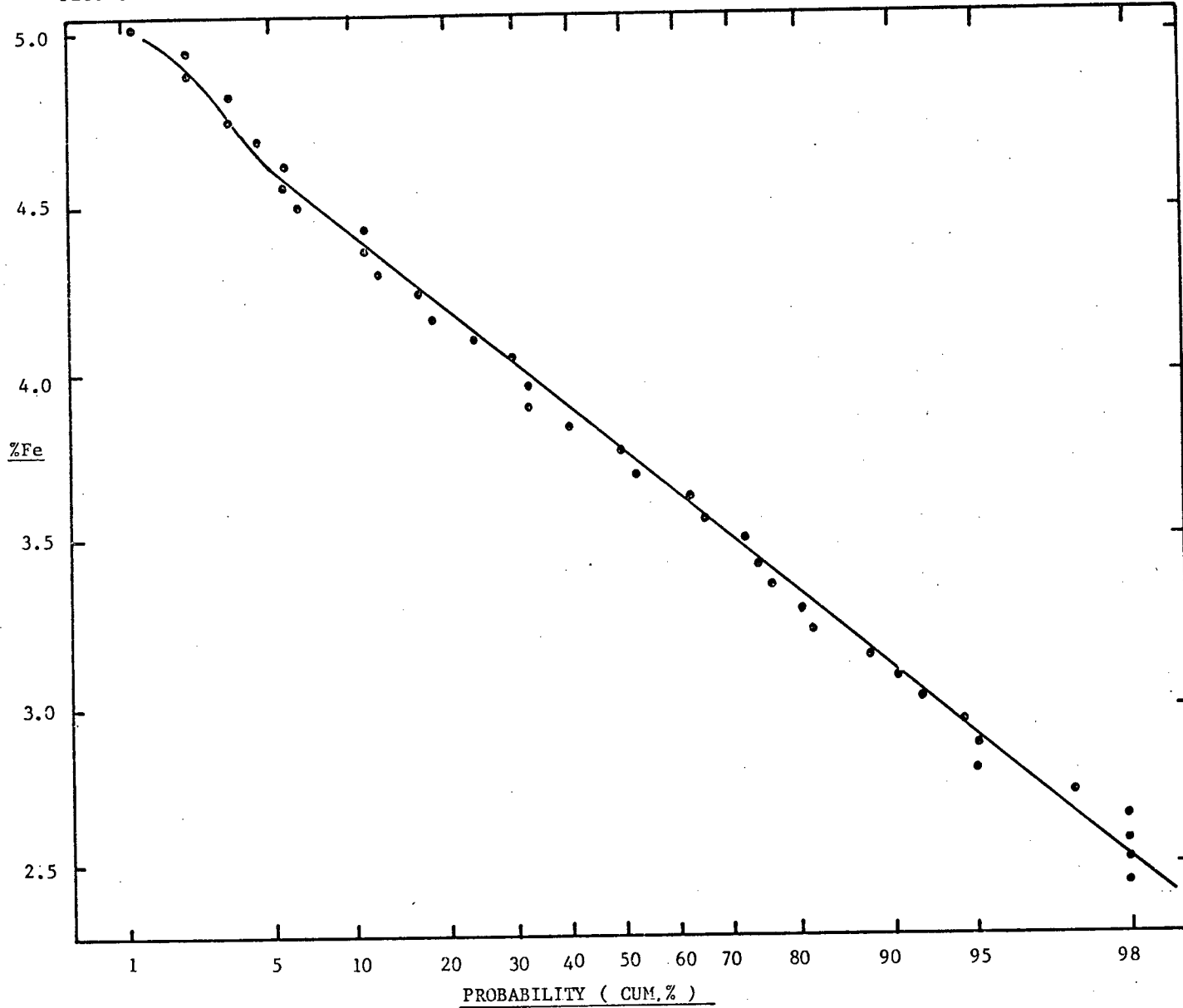


FIG. C-6: LOG PROBABILITY PLOT OF 88 IRON VALUES IN SOILS

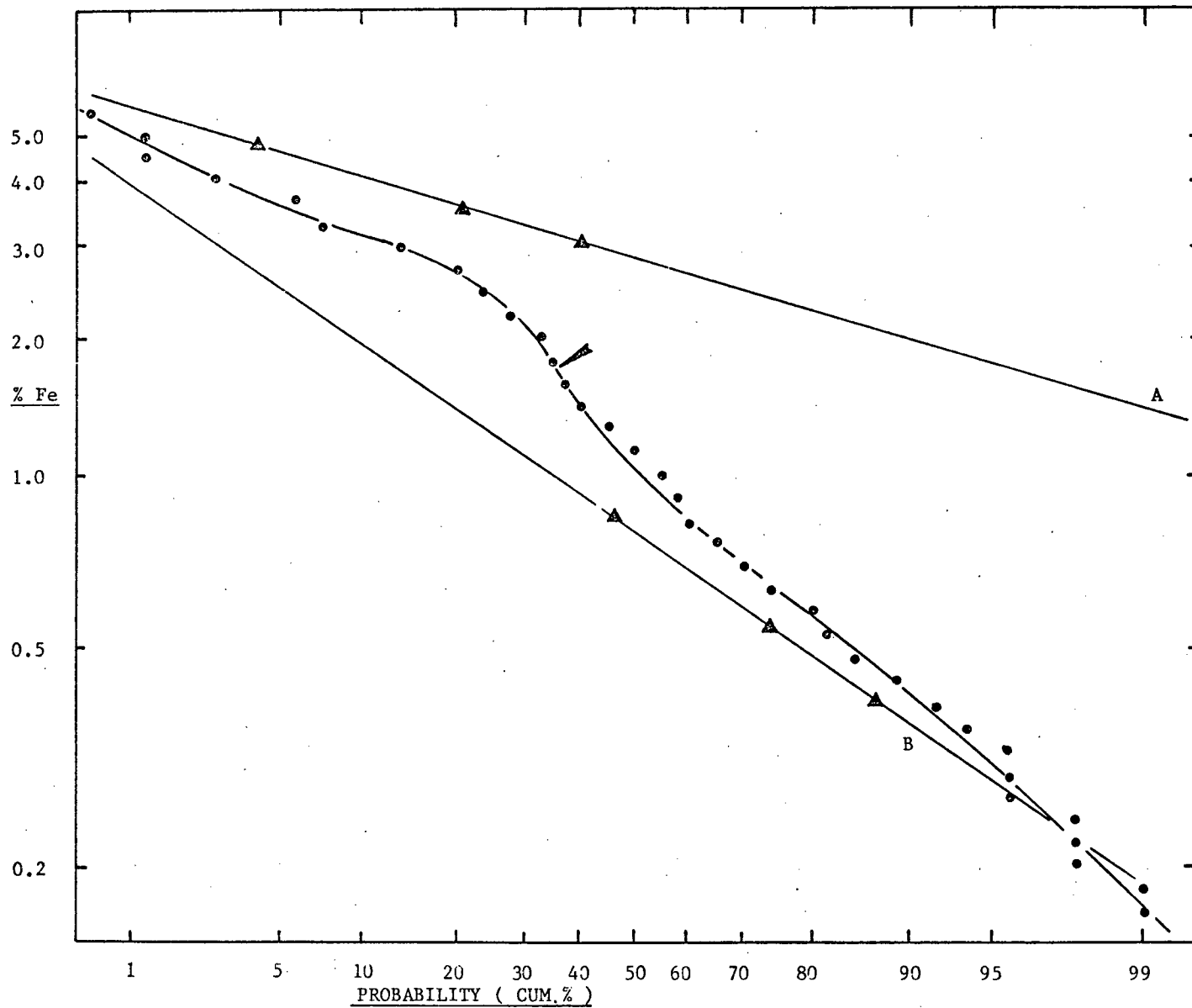


FIG. C-7: LOG PROBABILITY PLOT OF 96 MANGANESE VALUES IN THE TILL

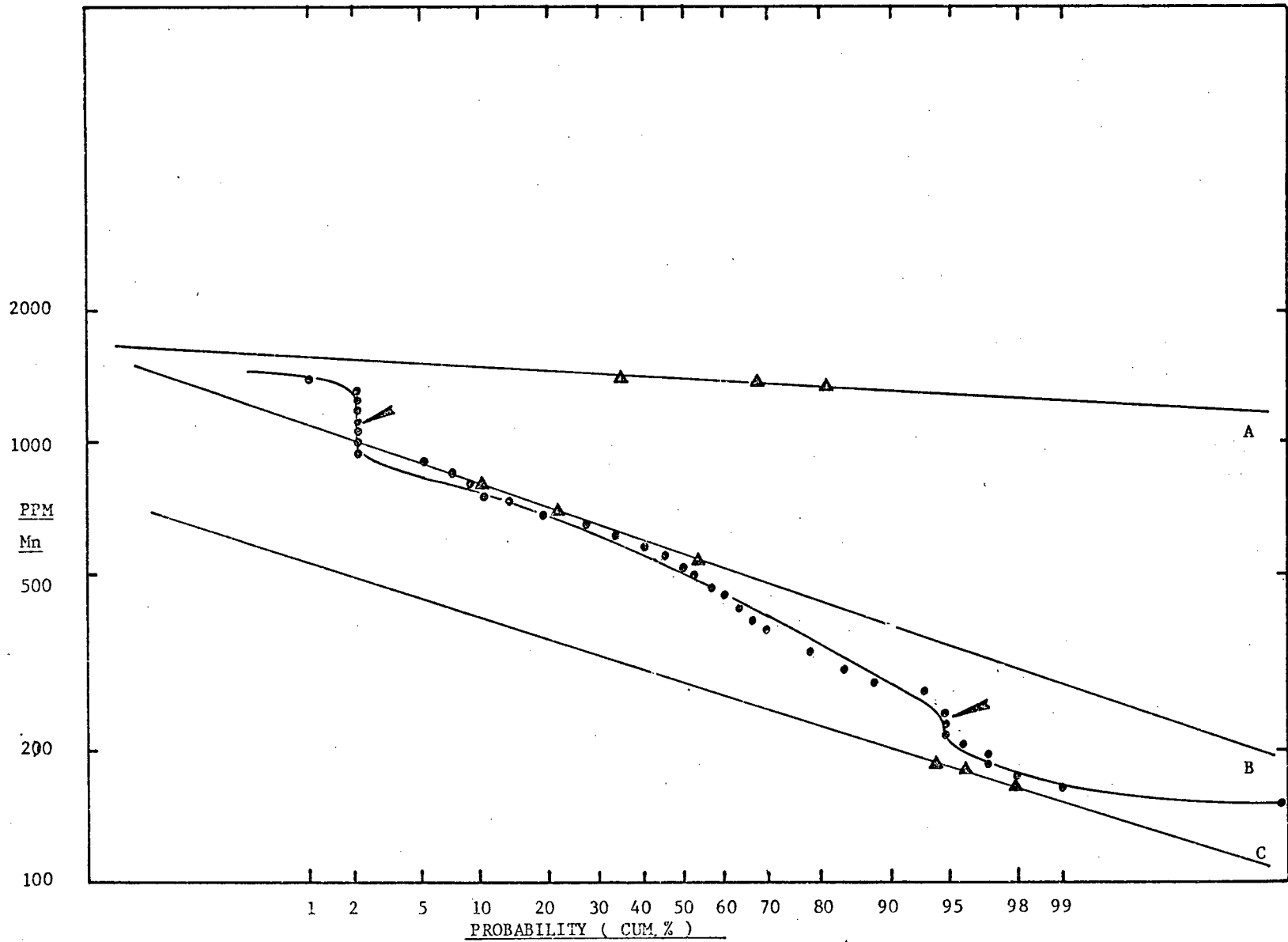


FIG. C-8: LOG PROBABILITY PLOT OF 88 MANGANESE VALUES IN SOILS

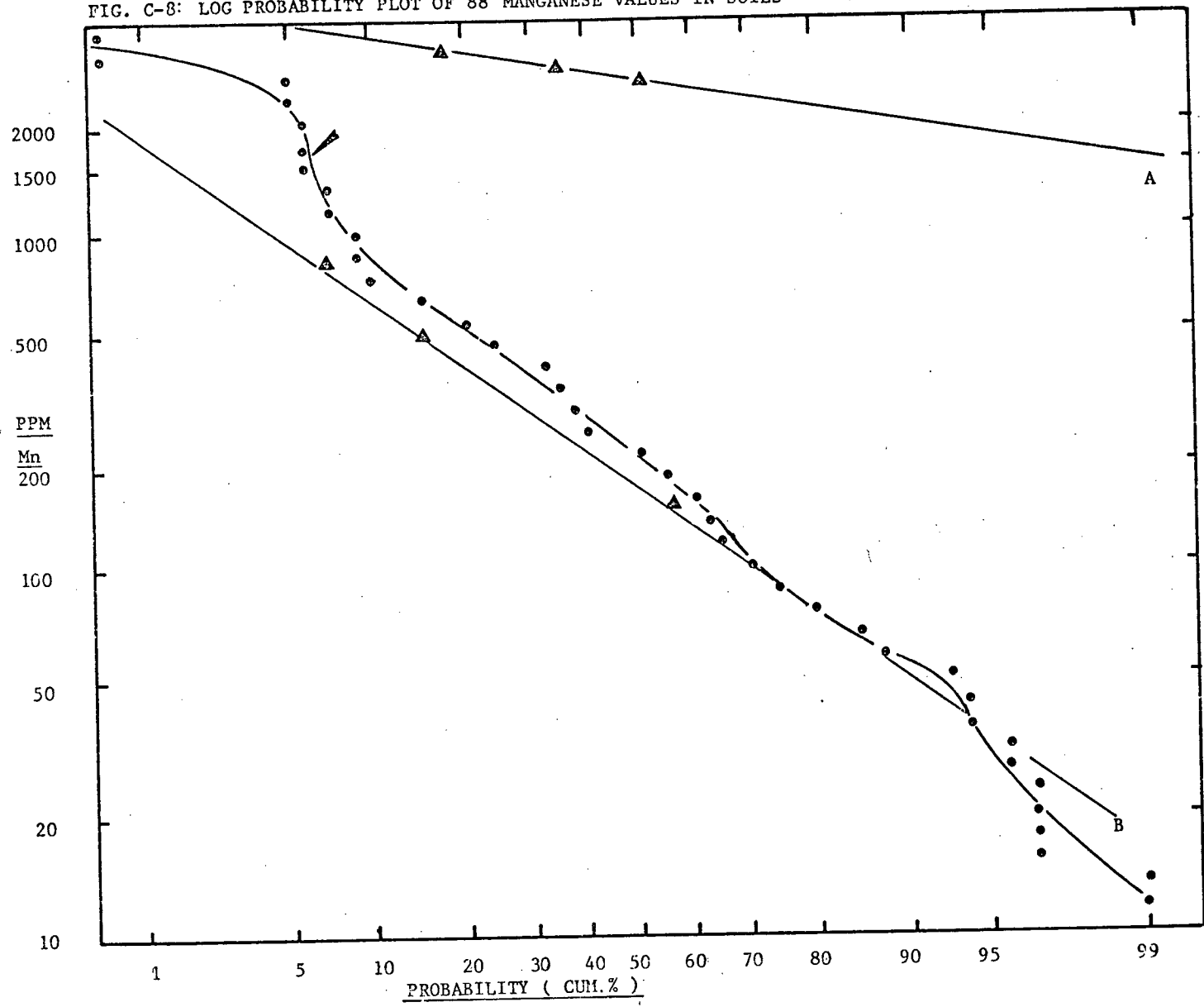


FIG. C-9: LOG PROBABILITY PLOT OF 96 MOLYBDENUM VALUES IN THE TILL

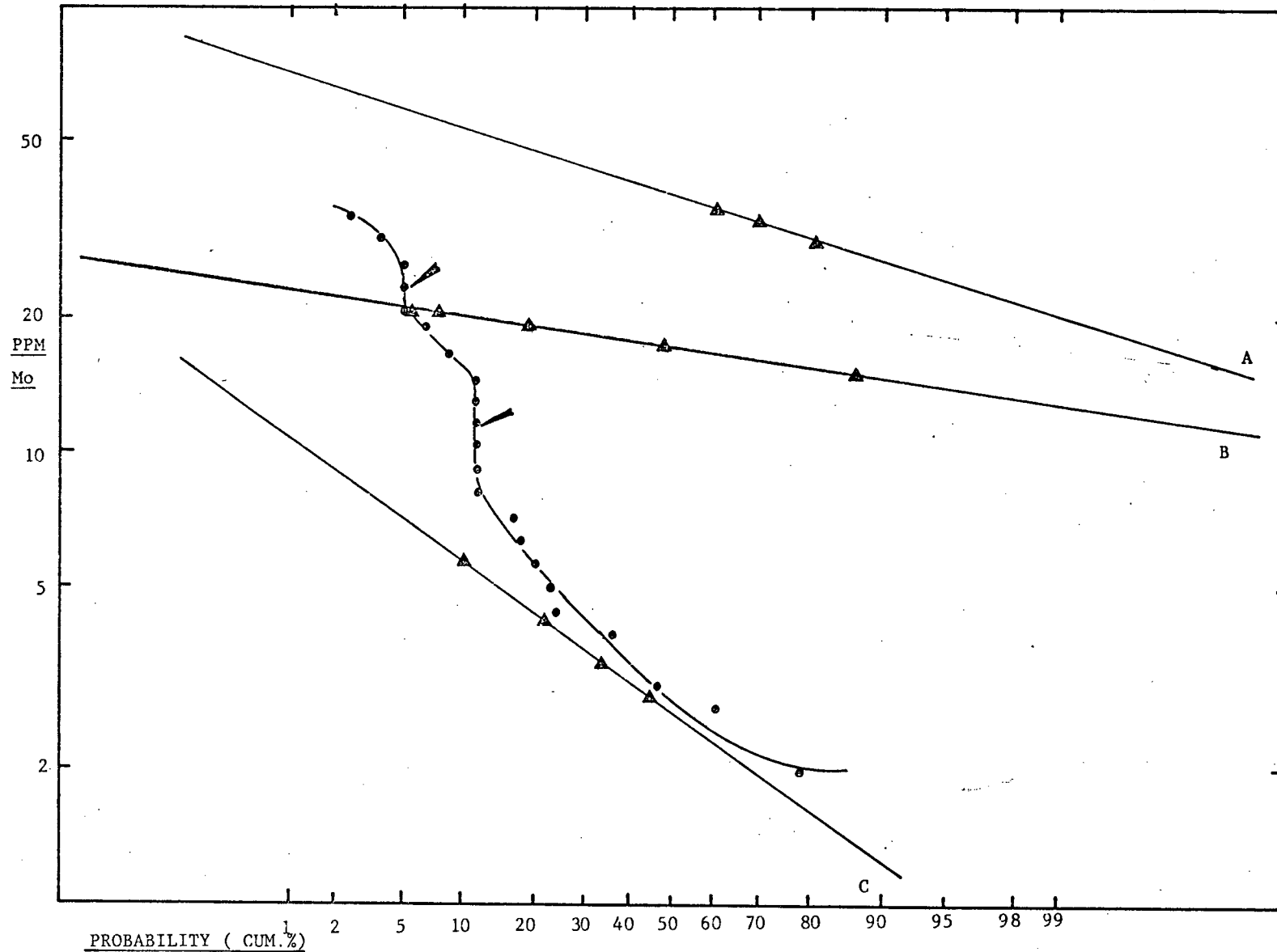


FIG. C-10: LOG PROBABILITY PLOT OF 80 MOLYBDENUM VALUES IN SOILS.

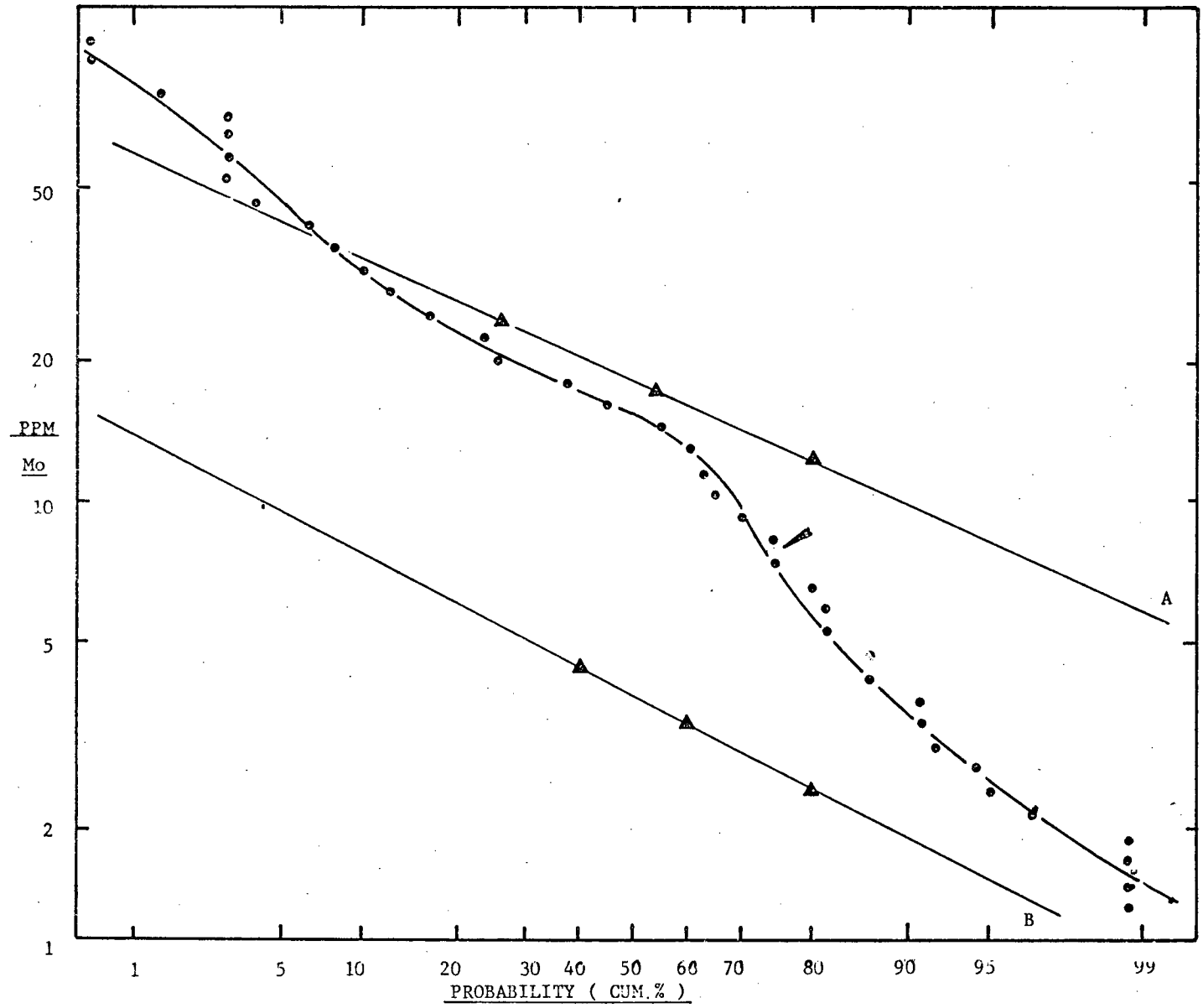


FIG. C-11: LOG PROBABILITY PLOT OF 96 NICKEL VALUES IN THE TILL

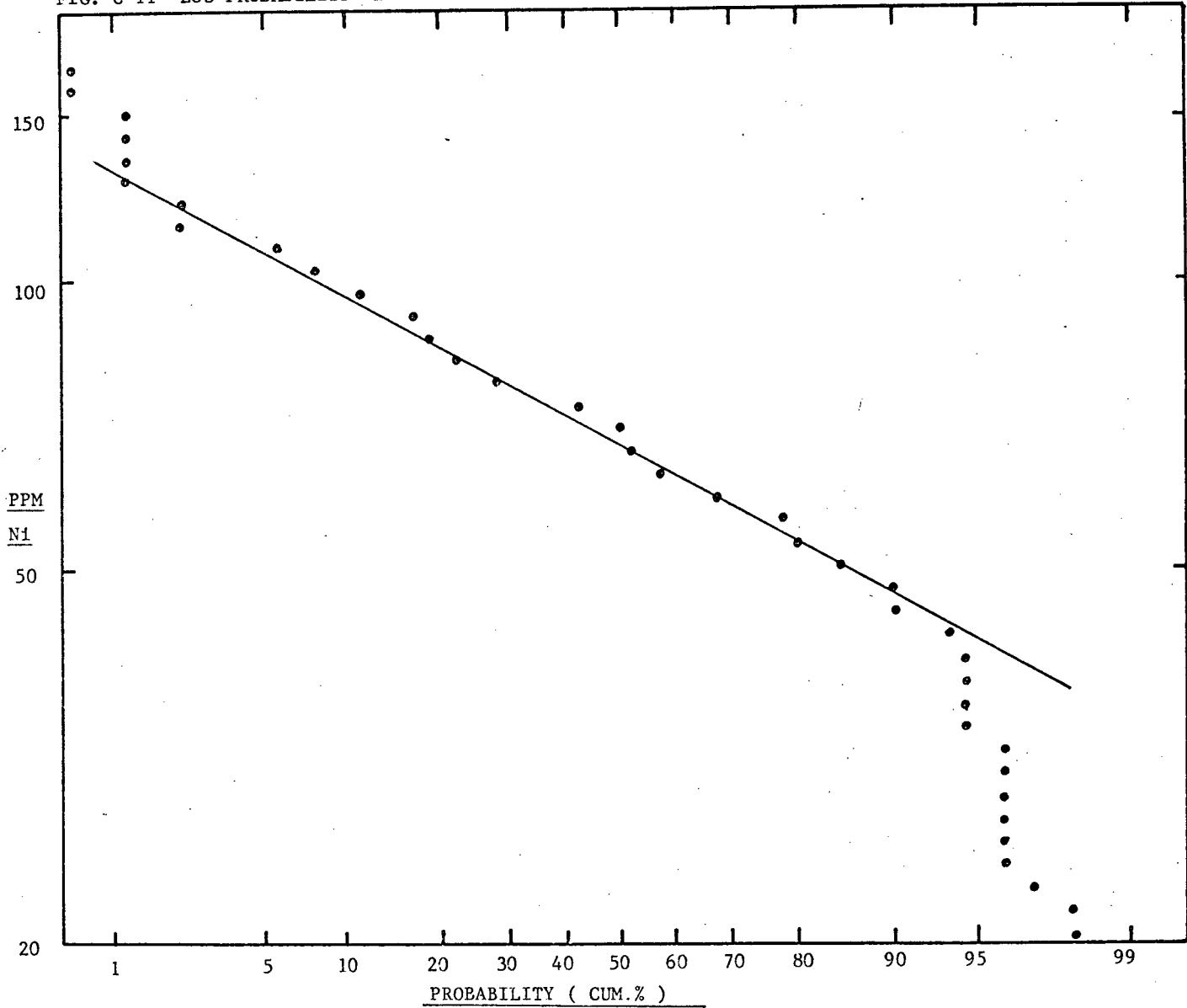


FIG. C-12: LOG PROBABILITY PLOT OF 90 NICKEL VALUES IN SOILS

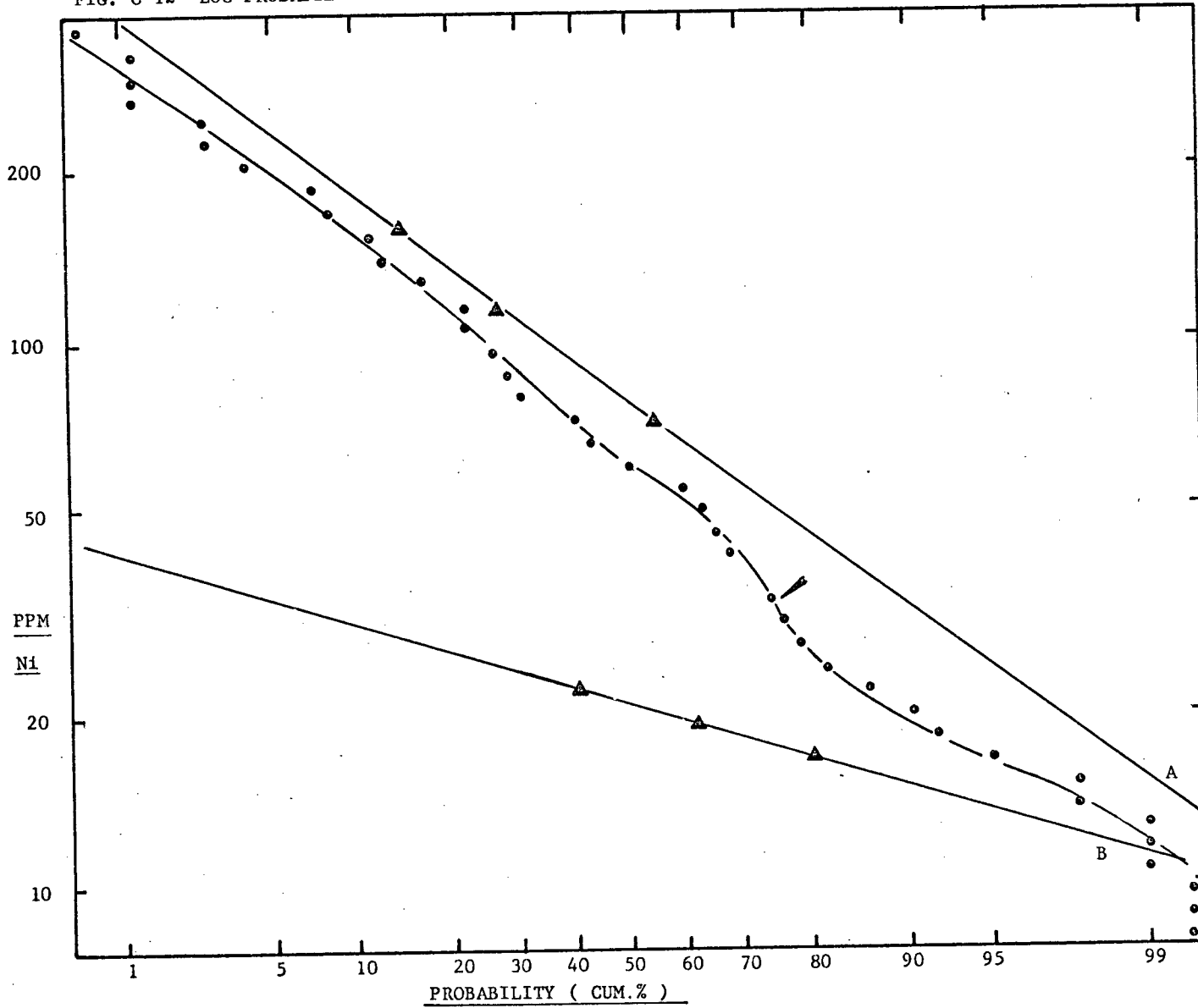


FIG. C-13: LOG PROBABILITY PLOT OF 96 ZINC VALUES IN THE TILL

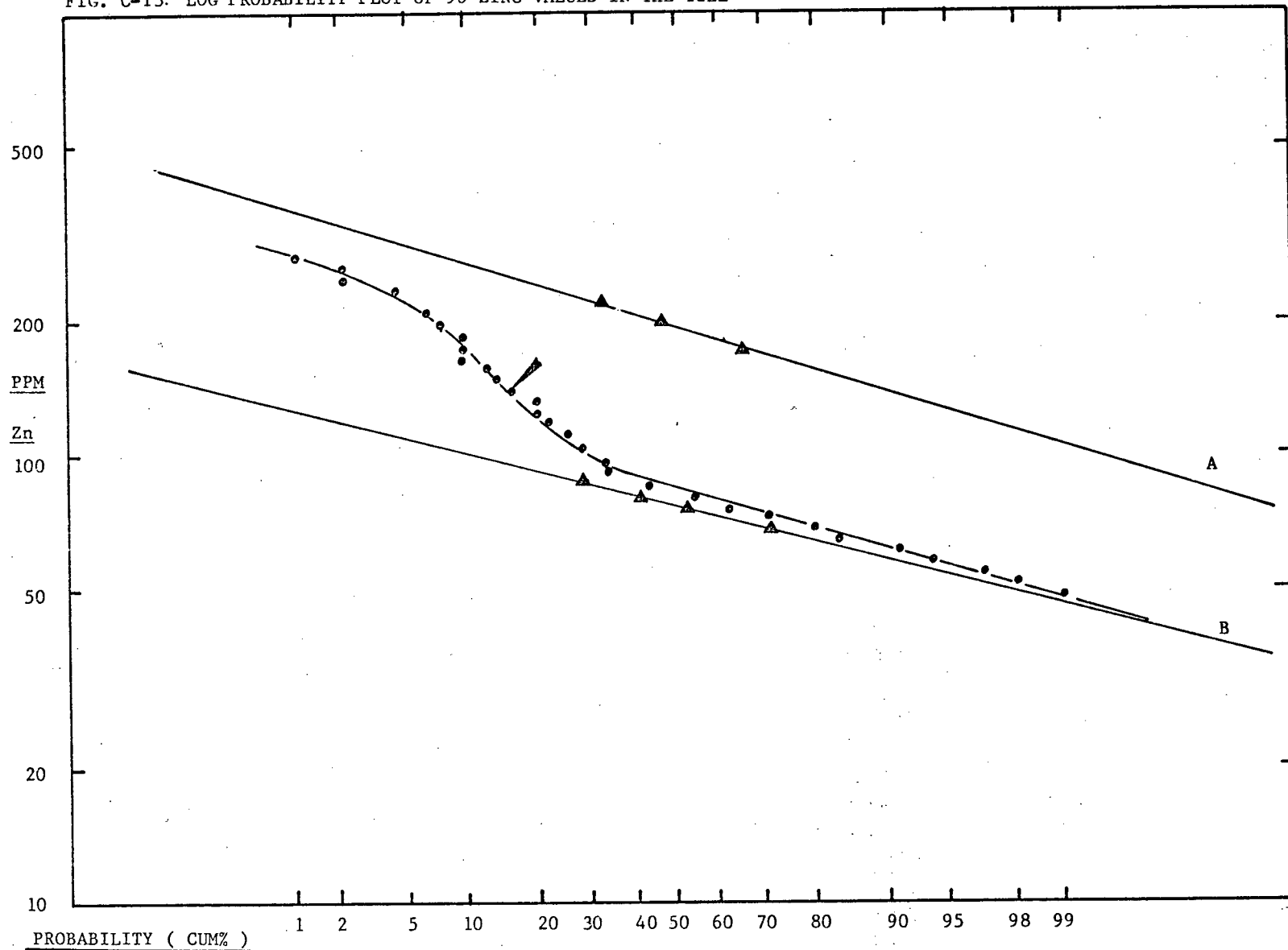


FIG. C-14: LOG PROBABILITY PLOT OF 90 ZINC VALUES IN SOILS

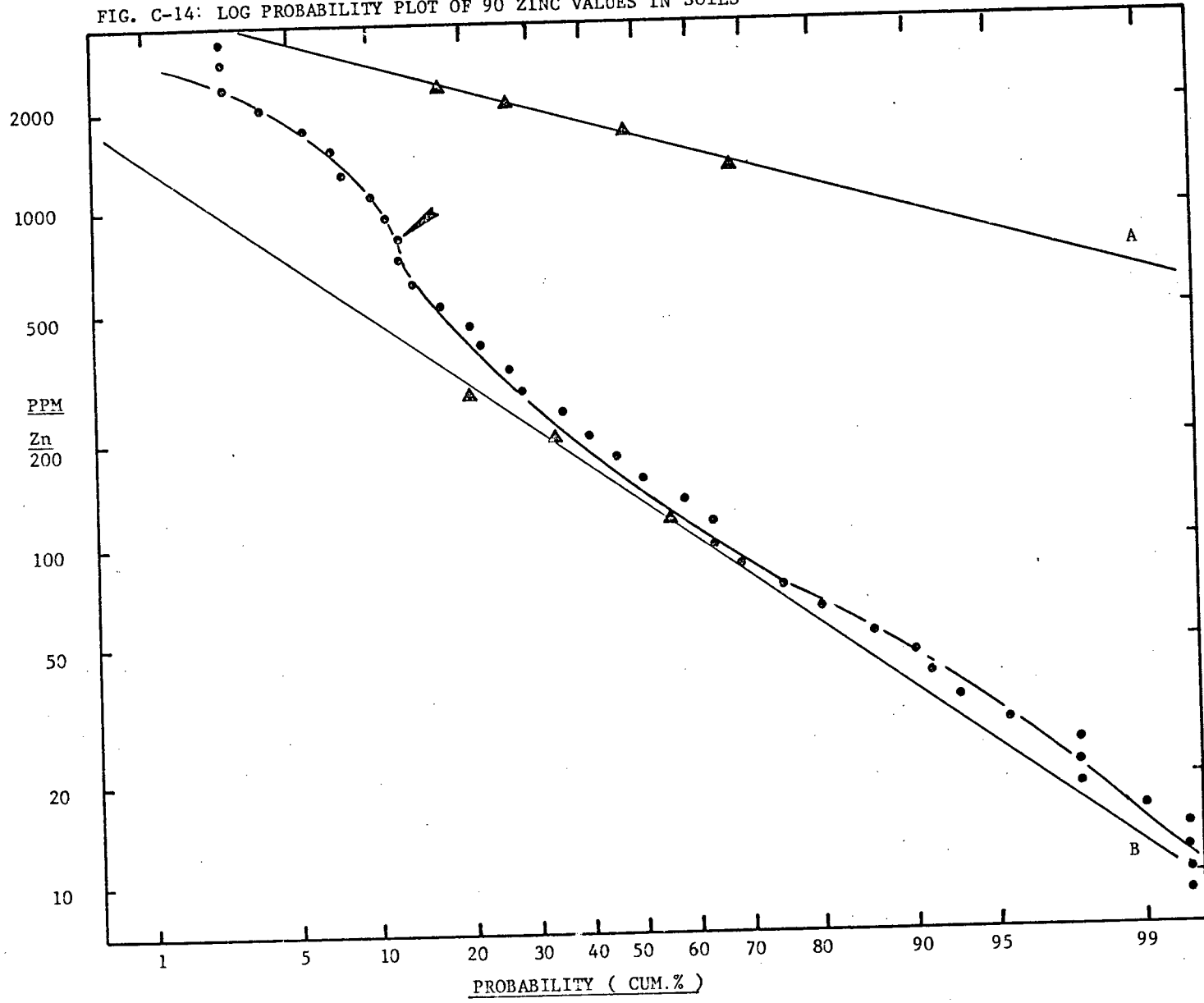


FIG. C-15: LOG PROBABILITY PLOT OF ORGANIC CARBON VALUES IN THE TILL

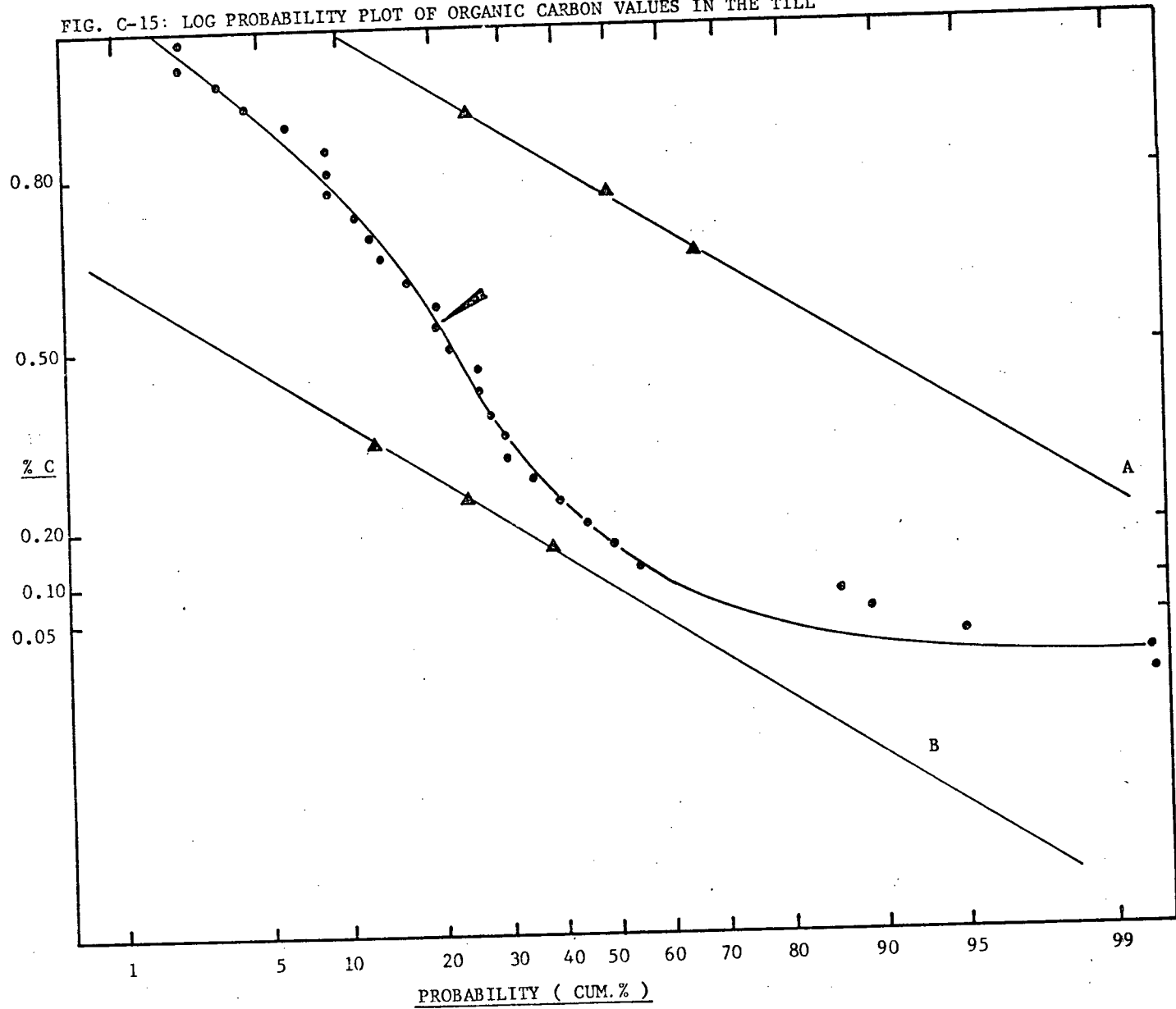


FIG. C-16: ARITHMETIC PROBABILITY PLOT OF 90 ORGANIC CARBON VALUES IN SOILS

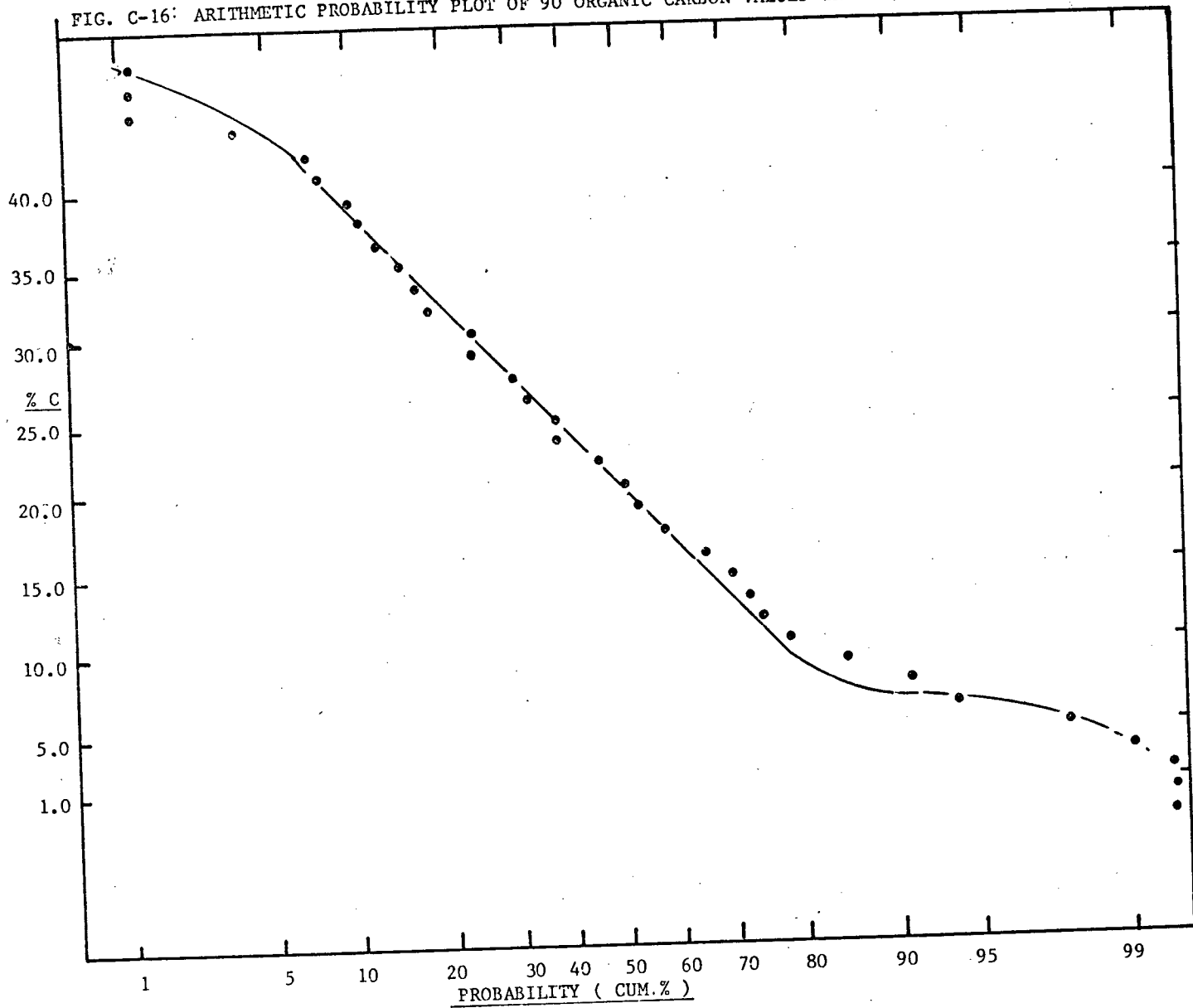


FIG. C-17: ARITHMETIC PROBABILITY PLOT OF 96 pH VALUES IN THE TILL

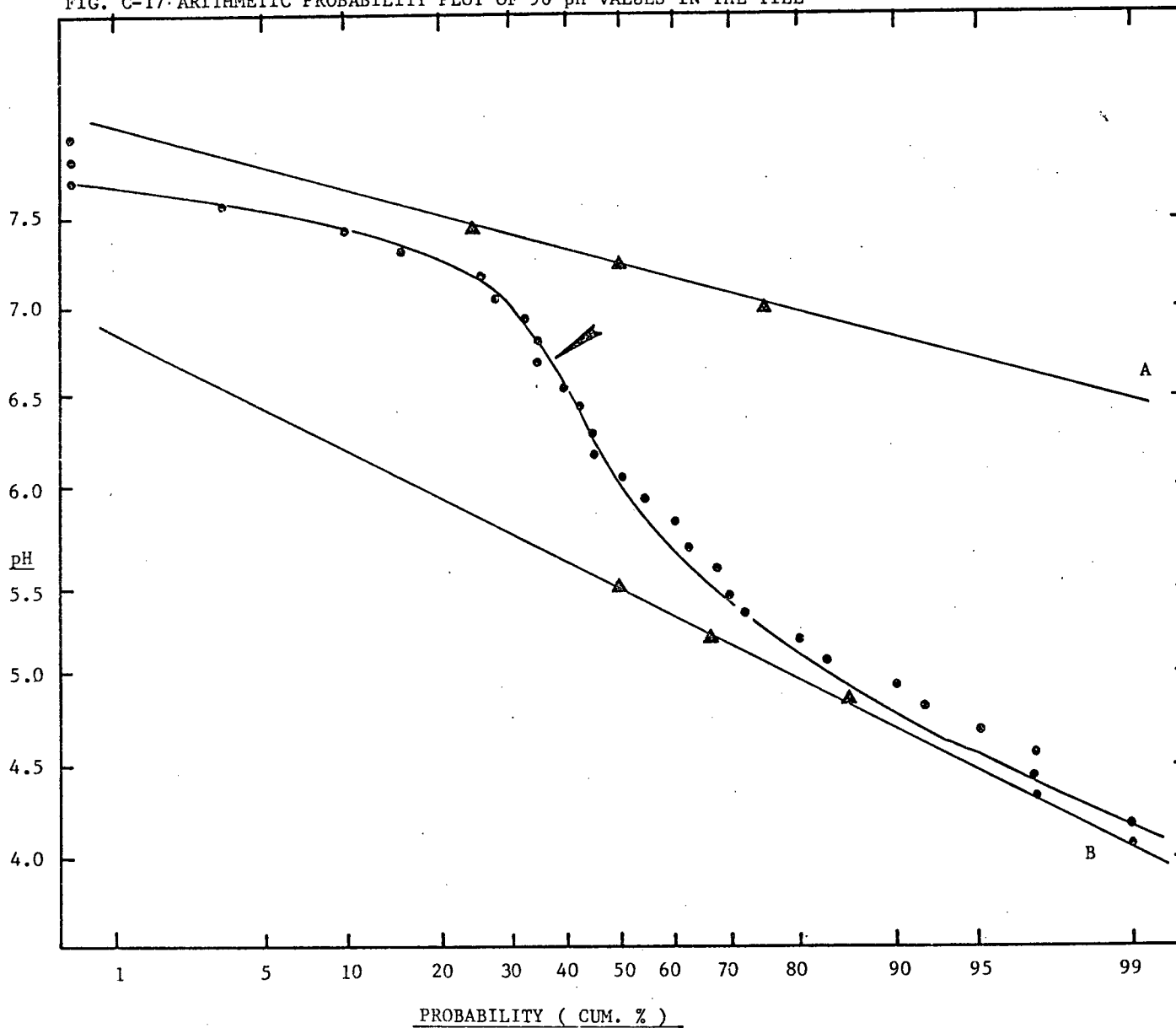
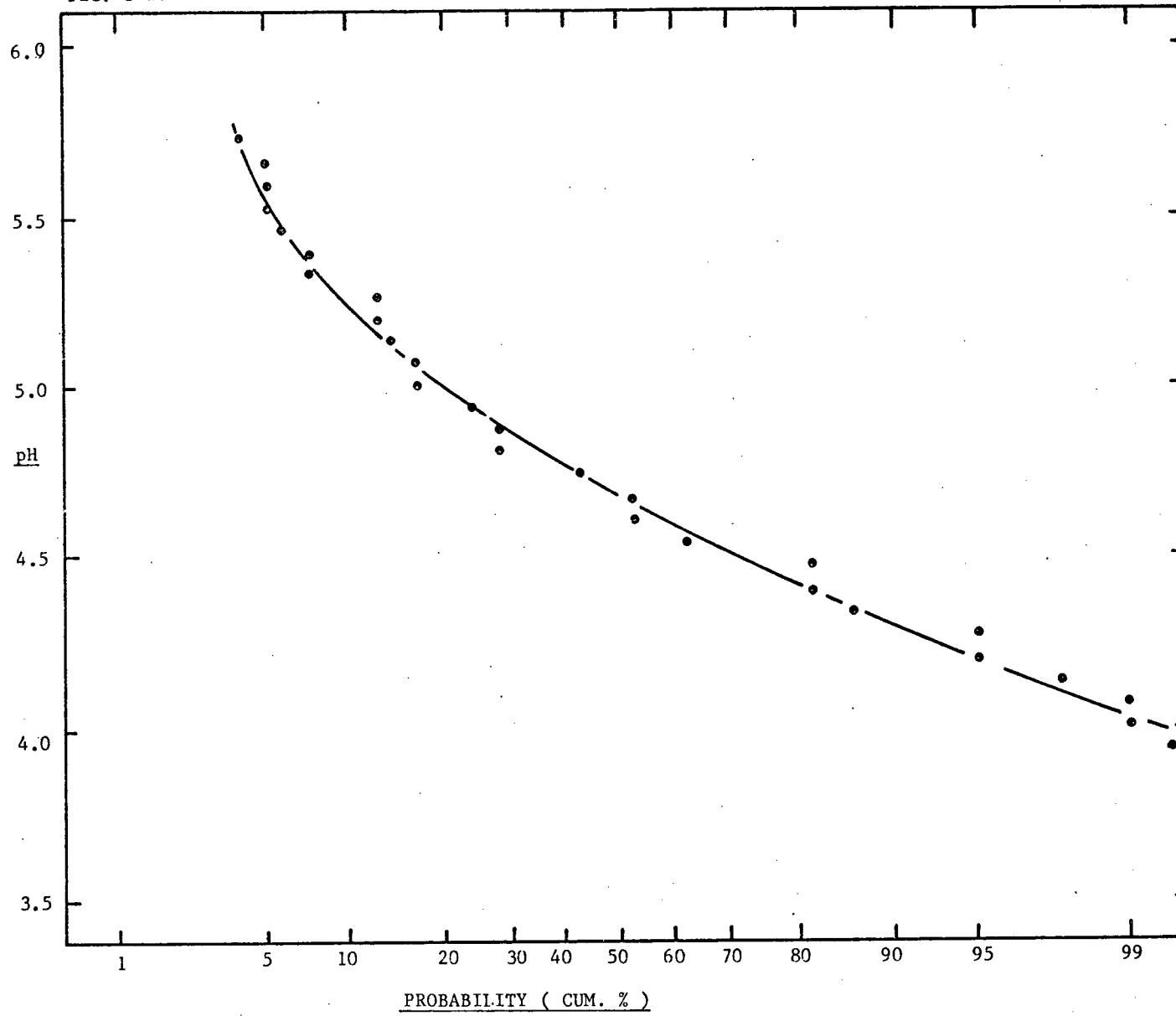


FIG. C-18. ARITHMETIC PROBABILITY PLOT OF 90 pH VALUES IN SOILS.



#### Appendix D

Example of DIAG program output for water sample 74-RL-1429 and distribution of aqueous species in water samples 74-RL-1428, 1439, 1442, 1443 and 1444.

\*\*\*\*\* DATA ECHO \*\*\*\*\*

DISTRIBUTION OF SPECIES FOR WATER SAMPLE 72-PL-1429  
AT A SULPHATE CONC OF 10<sup>-4</sup> Molal

TEMPERATURE (KELVIN) OF THIS RUN IS ..... 298.15  
PRESSURE (BARS) OF THIS RUN IS ..... 1.00

MAXIMUM NUMBER OF STEPS IS ..... 1  
NUMBER OF STEPS BETWEEN EACH PRINT CUT IS ... 0

ION CHOSEN FOR ELECTRICAL BALANCE IS ..... CA<sup>++</sup>  
MOLES OF SOLVENT H<sub>2</sub>O IN SYSTEM IS ..... 55.508250

\*\*\*\*\* INITIAL SOLUTION CONSTRAINTS \*\*\*\*\*

0.27500000E-03 MOLALITY	CA <sup>++</sup>	CA(1)	(AQUEOUS SPECIES)
0.33600000E-06 MOLALITY	ZN <sup>++</sup>	ZN(1)	(AQUEOUS SPECIES)
0.13500000E-05 MOLALITY	MN <sup>++</sup>	MN(1)	(AQUEOUS SPECIES)
0.78500000E-06 MOLALITY	CU <sup>++</sup>	CU(1)	(AQUEOUS SPECIES)
0.30800000E-05 MOLALITY	FE <sup>++</sup>	FE(1)	(AQUEOUS SPECIES)
0.20000000E-03 MOLALITY	HCO <sub>3</sub> <sup>-</sup>	H(1)C(1)C(3)	(AQUEOUS SPECIES)
-0.60000000E+01 LOG ACT.	H <sup>+</sup>	H(1)	(AQUEOUS SPECIES)
0.28100000E-03 MOLALITY	SO <sub>4</sub> <sup>--</sup>	S(1)C(4)	(AQUEOUS SPECIES)
-0.66500000E+02 LOG ACT.	OXYGEN GAS	O(2)	(GAS)

\*\*\*\*\*

DISTRIBUTION OF SPECIES FOR WATER SAMPLE 73-RL-1429  
AT A SULPHATE CONC OF 10-4 Molal

DISTRIBUTION OF SPECIES CALLED AT STEP C

ACLEOLS SPECIES

SPECIES	MOLALITY	LOG MOL	ACTIVITY	LOG ACT	ACT CCEF	LG ACT C	GRAMS/KGM H2O	PPM	LOG PPM
Ca++	0.29770E-02	-3.526	C.25602E-03	-3.592	0.85955E+00	-0.066	0.11932E-01	11.931	1.077
FE++	0.29342E-05	-5.533	0.25234E-05	-5.598	0.85955E+00	-0.066	0.16386E-03	0.164	-0.786
FE+++	0.54910E-20	-20.260	C.35512E-20	-20.403	0.71959E+00	-0.143	0.30665E-18	C.000	-15.513
MA++	0.13500E-05	-5.870	C.11610E-05	-5.925	0.85955E+00	-0.066	0.74166E-04	0.074	-1.130
ZN++	0.19881E-06	-6.705	0.16926E-06	-6.771	0.85955E+00	-0.066	0.12866E-04	0.013	-1.891
CU+	0.78497E-06	-6.105	C.75489E-06	-6.122	0.56158E+00	-0.017	0.49877E-04	0.050	-1.302
CU++	0.26972E-10	-10.571	C.22111E-10	-10.636	0.85955E+00	-0.066	C.17075E-08	C.000	-5.768
S--	0.34850E-17	-17.458	0.29322E-17	-17.524	0.85861E+00	-0.066	C.11174E-15	C.000	-12.952
SO4--	0.27085E-03	-3.567	0.23217E-03	-3.634	C.65720E+00	-0.067	0.26018E-01	26.017	1.415
CO3--	0.34106E-08	-8.467	0.29260E-08	-8.534	0.85751E+00	-0.067	0.20467E-06	0.000	-3.689
OH-	0.10690E-07	-7.571	C.10285E-07	-7.688	0.56209E+00	-0.017	0.18181E-06	0.000	-3.740
H+	0.10371E-05	-5.984	C.10000E-05	-6.000	C.56419E+00	-0.016	0.10454E-05	0.001	-2.981
H2O	0.55508E+02	1.744	0.99999E+00	-0.000	C.18015E-01	-1.744	C.10000E+04	955548.016	6.800
G2(AQ)	0.33881E-69	-69.470	C.33881E-69	-69.470	C.10000E+01	0.0	0.10842E-67	C.000	-64.565
CaCO3	0.93825E-09	-9.028	0.93854E-09	-9.028	C.10003E+01	C.000	0.93908E-07	0.000	-4.027
CASO4	0.55865E-05	-5.001	0.99996E-05	-5.000	C.10003E+01	C.000	0.13556E-02	1.360	0.133
ZNSO4	0.13919E-06	-6.856	C.13923E-06	-6.856	C.10003E+01	C.000	0.22469E-04	0.022	-1.648
HSO4-	0.22957E-07	-7.639	0.22091E-07	-7.656	0.56229E+00	-0.017	0.22284E-05	0.002	-2.652
HS-	0.23535E-09	-9.628	C.22647E-09	-9.645	0.56209E+00	-0.017	C.77849E-08	C.000	-5.109
H2S	0.23444E-08	-8.630	C.23452E-08	-8.630	C.10003E+01	C.000	0.79897E-07	0.000	-4.097
HCO3-	0.64590E-04	-4.190	0.62167E-04	-4.206	0.56249E+00	-0.017	0.39411E-02	3.941	0.596
H2CO3	0.12541E-03	-3.866	C.13545E-03	-3.868	0.10003E+01	C.000	0.83986E-02	8.398	C.524
FE(OH)+	0.14582E-06	-6.836	C.14033E-06	-6.852	C.56229E+00	-0.017	0.10624E-04	0.011	-1.974

IONIC STRENGTH = 0.117936E-02

ELECTRICAL BALANCE = -0.269791E-13

GASES

NAME	LOG K	ACTIVITY	LOG ACTIVITY
OXYGEN GAS	0.0	0.31623E-66	-66.50000
CARBON DIOXIDE	-7.83540	0.42557E-02	-2.37103
STEAM	1.50517	0.21248E-01	-1.50518
SULFUR GAS	192.34951	0.76229E-24	-24.11188
HYDROGEN SULFIDE	125.01049	C.22663E-07	-7.64469
HYDROGEN GAS	41.66022	C.38884E-08	-8.41023
METHANE	135.90718	C.76979E-13	-13.11363

THE LOG K FOR BORNITE HAS BEEN EXCEEDED AT STEP C  
LOG K = 499.735987E LOG C = 549.1842661

THE LOG K FOR CHALCOCITE HAS BEEN EXCEEDED AT STEP C

LOG K = 134.471587C LOG C = 153.3434279

THE LOG K FOR CHALCOPYRITE HAS BEEN EXCEEDED AT STEP C  
LOG K = 231.2013686 LOG C = 242.4974102

THE LOG K FOR COVELLITE HAS BEEN EXCEEDED AT STEP 0  
LOG K = 110.1634839 LOG C = 118.7296209

THE LOG K FOR CUPRITE HAS BEEN EXCEEDED AT STEP C  
LOG K = 34.3191369 LOG C = 35.9776141

THE LOG K FOR NATIVE COPPER HAS BEEN EXCEEDED AT STEP 0  
LOG K = 30.1820197 LOG C = 34.6138071

THE LOG K FOR PYRITE HAS BEEN EXCEEDED AT STEP C  
LOG K = 205.8617660 LOG C = 207.8836032

THE LOG K FOR SPHALERITE HAS BEEN EXCEEDED AT STEP 0  
LOG K = 120.4642586 LOG C = 122.5943556

MINERALS	LOG K	LOG C
ALABANDITE	122.589	123.4306369
ANHYDRITE	-4.144	-7.2259194
ARAGONITE	1.968	-1.7981672
AZURITE	9.161	-16.3214529
BERNITE	499.740	549.1842661
BROCHANTITE	14.733	-10.1789763
CALCITE	1.803	-1.7681672
CHALCANTHITE	-2.536	-14.2704098
CUSO4	2.990	-14.2703791
CU2SO4	34.816	20.3434279
FESO4	1.118	-9.2322107
IRON	55.480	39.6519755
NATIVE SULFUR	89.226	84.1158128
CHALCOCCITE	134.472	153.3434279
CHALCOPYRITE	231.201	242.4974102
COVELLITE	110.163	118.7296209
CUPRITE	34.319	35.9776141
FERRIC OXIDE	11.318	6.4019755
GRAPHITE	61.476	56.2935660
HEMATITE	-19.957	-20.4460489
LIME	32.707	8.4082668
MAGNETITE	-11.807	-14.0440734
MALACHITE	5.946	-7.4788260

MANGANOSITE	17.921	6.0648231
MELANTERITE	-4.614	-9.2322537
NATIVE COPPER	20.182	34.6138071
PYRITE	205.862	207.8826032
PYRRHOTITE	127.051	123.7677892
RHODOCHROSITE	-0.207	-4.1416109
SIDERITE	-2.400	-3.8044585
SMITHSONITE	-0.626	-4.9778922
SPHALERITE	120.464	122.5943556
TENORITE	7.667	1.3629071
KURTZITE	122.763	122.5943556

GASES

NAME	LOG K	ACTIVITY	LOG ACTIVITY
OXYGEN GAS	0.0	0.31623E-66	-66.50000
CARBON DIOXIDE	-7.83540	0.42557E-02	-2.37103
STEAM	1.50517	0.31248E-01	-1.50518
SULFUR GAS	192.34551	0.76229E-24	-24.11788
HYDROGEN SULFIDE	125.01049	0.22663E-07	-7.64469
HYDROGEN GAS	41.66022	0.38884E-08	-8.41023
METHANE	125.90718	0.76975E-13	-13.11363
EXECUTION TERMINATED	10:26:43 T=1.193	RC=C	\$.64

!SIGNOFF

\*\*\*\*\* DATA ECHO \*\*\*\*\*

DISTRIBUTION OF SPECIES FOR WATERS SAMPLE 74-RL-1428  
AT SULPHATE CONC OF 10<sup>-4</sup> Molal

TEMPERATURE (KELVIN) OF THIS RUN IS ..... 298.15  
PRESSURE (BARS) OF THIS RUN IS ..... 1.00

MAXIMUM NUMBER OF STEPS IS ..... 1  
NUMBER OF STEPS BETWEEN EACH PRINT OUT IS ... 0

ION CHOSEN FOR ELECTRICAL BALANCE IS ..... CA<sup>++</sup>  
MOLES OF SOLVENT H<sub>2</sub>O IN SYSTEM IS ..... 55.508250

\*\*\*\*\* INITIAL SOLUTION CONSTRAINTS \*\*\*\*\*

0.15700000E-06 MOLALITY	CU <sup>++</sup>	CU(1)	(AQUEOUS SPECIES)
0.19700000E-05 MOLALITY	FE <sup>++</sup>	FE(1)	(AQUEOUS SPECIES)
0.24800000E-05 MOLALITY	MN <sup>++</sup>	MN(1)	(AQUEOUS SPECIES)
0.15300000E-06 MOLALITY	ZN <sup>++</sup>	ZN(1)	(AQUEOUS SPECIES)
0.62500000E-03 MOLALITY	CA <sup>++</sup>	CA(1)	(AQUEOUS SPECIES)
0.20000000E-03 MOLALITY	HCO <sub>3</sub> <sup>-</sup>	H(1)C(1)O(3)	(AQUEOUS SPECIES)
-0.75000000E+01 LOG ACT.	H <sup>+</sup>	H(1)	(AQUEOUS SPECIES)
0.41600000E-03 MOLALITY	SO <sub>4</sub> <sup>--</sup>	S(1)O(4)	(AQUEOUS SPECIES)
-0.66500000E+02 LOG ACT.	OXYGEN GAS	O(2)	(GAS)

\*\*\*\*\*

DISTRIBUTION OF SPECIES FOR WATERS SAMPLE 74-RL-1428  
AT SULPHATE CONC OF 10<sup>-4</sup>Molal

DISTRIBUTION OF SPECIES CALLED AT STEP 0

AQUEOUS SPECIES

SPECIES	MOLALITY	LOG MOL	ACTIVITY	LOG ACT	ACT COEF	LG ACT C	GRAMS/KGM H2O	PPM	LOG PPM
CA++	0.40405E-03	-3.315	0.40179E-03	-3.396	0.83006E+00	-0.081	0.19401E-01	19.399	1.288
FE++	0.77835E-06	-6.109	0.64609E-06	-6.190	0.83006E+00	-0.081	0.43469E-04	0.043	-1.362
FE+++	0.47894E-22	-22.320	0.31992E-22	-22.495	0.66798E+00	-0.175	0.26747E-20	0.000	-17.573
MN++	0.24800E-05	-5.606	0.20535E-05	-5.686	0.83006E+00	-0.081	0.13625E-03	0.136	-0.866
ZN++	0.78202E-07	-7.107	0.64912E-07	-7.138	0.83006E+00	-0.081	0.51121E-05	0.005	-2.291
CU+	0.15700E-06	-6.804	0.14954E-06	-6.825	0.95250E+00	-0.021	0.99758E-05	0.010	-2.001
CU++	0.17442E-12	-12.758	0.14673E-12	-12.839	0.83006E+00	-0.081	0.11082E-10	0.000	-7.955
S--	0.50646E-17	-17.295	0.41936E-17	-17.377	0.82802E+00	-0.082	0.16239E-15	0.000	-12.789
SO4--	0.39396E-03	-3.405	0.32538E-03	-3.488	0.82592E+00	-0.083	0.37845E-01	37.842	1.578
CO3--	0.32141E-06	-6.493	0.26590E-06	-6.575	0.82698E+00	-0.083	0.19288E-04	0.019	-1.715
OH-	0.34123E-06	-6.467	0.32524E-06	-6.438	0.95313E+00	-0.021	0.58035E-05	0.006	-2.236
H+	0.23068E-07	-7.481	0.31623E-07	-7.500	0.95631E+00	-0.019	0.33331E-07	0.003	-4.477
H2O	0.55303E+02	1.744	0.92298E+00	-0.000	0.18015E-01	-1.744	0.10000E+04	999927.250	6.000
O2(AQ)	0.33881E-69	-69.470	0.33881E-69	-69.470	0.10000E+01	0.0	0.10842E-67	0.000	-64.965
CACO3	0.13374E-06	-6.874	0.13380E-06	-6.874	0.10005E+01	0.000	0.13386E-04	0.013	-1.873
CAS34	0.21961E-04	-4.658	0.21972E-04	-4.658	0.10005E+01	0.000	0.29898E-02	2.990	0.476
ZNSO4	0.74796E-07	-7.126	0.74835E-07	-7.126	0.10005E+01	0.000	0.12075E-04	0.012	-1.918
HSO4-	0.10269E-08	-8.988	0.97906E-09	-9.009	0.95344E+00	-0.021	0.99678E-07	0.000	-4.001
HS-	0.10530E-10	-10.978	0.10017E-10	-10.998	0.95313E+00	-0.021	0.34824E-09	0.000	-6.458
H2S	0.32850E-11	-11.483	0.32867E-11	-11.483	0.10005E+01	0.000	0.11195E-09	0.000	-6.951
HCO3-	0.18725E-03	-3.728	0.17858E-03	-3.748	0.95374E+00	-0.021	0.11425E-01	11.424	1.058
H2CO3	0.12298E-04	-4.910	0.12304E-04	-4.910	0.10005E+01	0.000	0.76280E-03	0.753	-0.118
FE(OH)+	0.11916E-05	-5.924	0.11362E-05	-5.945	0.95344E+00	-0.021	0.86816E-04	0.037	-1.061

IONIC STRENGTH = 0.189783E-02

ELECTRICAL BALANCE = 0.505744E-13

GASES  
-----

NAME	LOG K	ACTIVITY	LOG ACTIVITY
OXYGEN GAS	0.0	0.31623E-66	-66.50000
CARBON DIOXIDE	-7.93540	0.33659E-03	-3.41275
STEAM	1.50517	0.31248E-01	-1.50518
SULFUR GAS	192.34951	0.14973E-29	-29.82470
HYDROGEN SULFIDE	125.01049	0.31762E-10	-10.49810
HYDROGEN GAS	41.66022	0.38884E-08	-8.41023
METHANE	135.90718	0.69928E-14	-14.15535

THE LOG K FOR BORNITE HAS BEEN EXCEEDED AT STEP 0  
LOG K = 499.7399878 LOG Q = 544.1633237

THE LOG K FOR CHALCOCITE HAS BEEN EXCEEDED AT STEP 0

\*\*\*\*\* DATA ECHO \*\*\*\*\*

DISTRIBUTION OF SPECIES FOR WATER SAMPLE 74-RL-1439  
AT SULPHATE CONC OF  $10^{-4}$  Molal

TEMPERATURE (KELVIN) OF THIS RUN IS ..... 298.15  
PRESSURE (PASC) OF THIS RUN IS ..... 1.00

MAXIMUM NUMBER OF STEPS IS ..... 1  
NUMBER OF STEPS BETWEEN EACH PRINT CUT IS ... 0

ION CHOSEN FOR ELECTRICAL BALANCE IS ..... CA<sup>++</sup>  
MOLES OF SOLVENT H<sub>2</sub>O IN SYSTEM IS ..... 55.508250

\*\*\*\*\* INITIAL SOLUTION CONSTRAINTS \*\*\*\*\*

0.7830000E-05 MOLALITY	CU <sup>++</sup>	CU(1)	(AQUEOUS SPECIES)
0.7120000E-05 MOLALITY	FE <sup>++</sup>	FE(1)	(AQUEOUS SPECIES)
0.7830000E-06 MOLALITY	MN <sup>++</sup>	MN(1)	(AQUEOUS SPECIES)
0.3360000E-06 MOLALITY	ZN <sup>++</sup>	ZN(1)	(AQUEOUS SPECIES)
0.4500000E-03 MOLALITY	CA <sup>++</sup>	CA(1)	(AQUEOUS SPECIES)
0.2000000E-03 MOLALITY	HCCO <sub>3</sub> <sup>-</sup>	H(1)C(1)O(3)	(AQUEOUS SPECIES)
-0.6000000E+01 LOG ACT.	H <sup>+</sup>	H(1)	(AQUEOUS SPECIES)
0.6240000E-03 MOLALITY	SO <sub>4</sub> <sup>--</sup>	S(1)O(4)	(AQUEOUS SPECIES)
-0.6650000E+02 LOG ACT.	OXYGEN GAS	O(2)	(GAS)

\*\*\*\*\*

DISTRIBUTION OF SPECIES FOR WATER SAMPLE 74-RL-1439  
AT SULPHATE CONC OF 10-4 Molal

DISTRIBUTION OF SPECIES CALLED AT STEP 0

AQUEOUS SPECIES

SPECIES	MOLALITY	LOG MOL	ACTIVITY	LOG ACT	ACT CCEF	LOG ACT C	GRAMS/KGM H2O	PPM	LOG PPM
CA++	0.60533E-03	-3.218	0.45031E-03	-3.310	0.80958E+00	-0.092	0.24262E-01	24.255	1.385
FE++	0.67968E-05	-5.168	0.55053E-05	-5.259	0.80958E+00	-0.092	0.37958E-03	0.380	-0.421
FE+++	0.13578E-19	-19.867	0.86205E-20	-20.064	0.63467E+00	-0.197	0.75831E-18	0.000	-15.120
MN++	0.78300E-06	-6.106	0.63421E-06	-6.198	0.80958E+00	-0.092	0.43016E-04	0.043	-1.266
ZN++	0.14297E-06	-6.845	0.11580E-06	-6.936	0.80958E+00	-0.092	0.53457E-05	0.009	-2.029
CU+	0.78297E-05	-5.106	0.74078E-05	-5.130	0.94612E+00	-0.024	0.49750E-03	0.497	-0.303
CU++	0.27959E-09	-9.553	0.22679E-09	-9.644	0.80958E+00	-0.092	0.17791E-07	0.000	-4.750
S--	0.75148E-17	-17.124	0.60676E-17	-17.217	0.86742E+00	-0.093	0.24056E-15	0.000	-12.618
SO4--	0.58499E-03	-3.233	0.47079E-03	-3.327	0.80479E+00	-0.094	0.56195E-01	56.189	1.750
CO3--	0.36123E-08	-8.442	0.29120E-08	-8.536	0.80612E+00	-0.094	0.21677E-06	0.000	-3.664
OH-	0.10861E-07	-7.964	0.10285E-07	-7.988	0.94652E+00	-0.024	0.18472E-06	0.000	-3.734
H+	0.10516E-05	-5.978	0.10000E-05	-6.000	0.95057E+00	-0.022	0.10599E-05	0.001	-2.975
H2O	0.55508E+02	1.744	0.58957E+00	-0.000	0.18015E-01	-1.744	0.10000E+04	999500.946	6.000
O2(AQ)	0.33881E-69	-69.470	0.33881E-69	-69.470	0.10000E+01	0.0	0.10842E-67	0.000	-64.565
CaCO3	0.17976E-08	-8.748	0.17888E-08	-8.747	0.10000E+01	0.000	0.17892E-06	0.000	-3.747
CaSO4	0.38769E-04	-4.412	0.38794E-04	-4.411	0.10000E+01	0.000	0.52781E-02	5.278	0.722
ZnSO4	0.19303E-06	-6.714	0.19316E-06	-6.714	0.10000E+01	0.000	0.31162E-04	0.031	-1.506
H2SO4	0.47288E-07	-7.325	0.44796E-07	-7.349	0.54732E+00	-0.024	0.45902E-05	0.005	-2.238
HS-	0.48457E-09	-9.314	0.45223E-09	-9.336	0.54652E+00	-0.024	0.16039E-07	0.000	-4.755
H2S	0.47524E-08	-8.323	0.47555E-08	-8.323	0.10000E+01	0.000	0.16196E-06	0.000	-3.791
HCO3-	0.65283E-04	-4.185	0.61869E-04	-4.209	0.94771E+00	-0.023	0.39834E-02	3.983	0.600
H2CO3	0.13471E-03	-3.871	0.13480E-03	-3.870	0.10000E+01	0.000	0.83555E-02	8.355	0.922
Fe(OH)+	0.32317E-06	-6.491	0.30615E-06	-6.514	0.94732E+00	-0.024	0.23544E-04	0.024	-1.628

IONIC STRENGTH = 0.243337E-02

ELECTRICAL BALANCE = -0.761622E-13

GASES

NAME	LOG K	ACTIVITY	LOG ACTIVITY
OXYGEN GAS	0.0	0.31623E-66	-66.50000
CARBON DIOXIDE	-7.83540	0.42352E-02	-2.37311
STEAM	1.50517	0.31248E-01	-1.50518
SULFUR GAS	192.34951	0.31345E-23	-23.50383
HYDROGEN SULFIDE	125.01049	0.45955E-07	-7.33766
HYDROGEN GAS	41.66022	0.38884E-08	-8.41022
METHANE	135.95718	0.76609E-13	-13.11572

THE LOG K FOR BORNITE HAS BEEN EXCEEDED AT STEP 0  
LOG K = 499.7399878 LOG Q = 555.7101822

THE LOG K FOR CHALCOCITE HAS BEEN EXCEEDED AT STEP 0

\*\*\*\*\* DATA ECHO \*\*\*\*\*

DISTRIBUTION OF SPECIES IN WATER SAMPLE 74-RL-1442  
AT A SULPHATE CONC OF  $10^{-4}$  Molal

TEMPERATURE (KELVIN) OF THIS RUN IS ..... 298.15  
PRESSURE (BARS) OF THIS RUN IS ..... 1.00

MAXIMUM NUMBER OF STEPS IS ..... 1  
NUMBER OF STEPS BETWEEN EACH PRINT OUT IS .... 0

ION CHOSEN FOR ELECTRICAL BALANCE IS ..... CA<sup>++</sup>  
MOLES OF SOLVENT H<sub>2</sub>O IN SYSTEM IS ..... 55.508250

\*\*\*\*\* INITIAL SOLUTION CONSTRAINTS \*\*\*\*\*

0.78500000E-05 MOLALITY	CU <sup>++</sup>	CU(1)	(AQUEOUS SPECIES)
0.41700000E-04 MOLALITY	FE <sup>++</sup>	FE(1)	(AQUEOUS SPECIES)
0.92800000E-06 MOLALITY	MN <sup>++</sup>	MN(1)	(AQUEOUS SPECIES)
0.15300000E-06 MOLALITY	ZN <sup>++</sup>	ZN(1)	(AQUEOUS SPECIES)
0.57500000E-03 MOLALITY	CA <sup>++</sup>	CA(1)	(AQUEOUS SPECIES)
0.20000000E-03 MOLALITY	HCO <sub>3</sub> <sup>-</sup>	H(1)C(1)O(3)	(AQUEOUS SPECIES)
0.64500000E-03 MOLALITY	SO <sub>4</sub> <sup>--</sup>	S(1)O(4)	(AQUEOUS SPECIES)
-0.60000000E+01 LOG ACT.	H <sup>+</sup>	H(1)	(AQUEOUS SPECIES)
-0.66500000E+02 LOG ACT.	OXYGEN GAS	O(2)	(GAS)

\*\*\*\*\*

DISTRIBUTION OF SPECIES IN WATER SAMPLE 74-RL-1442  
AT A SULPHATE CONC OF 13-4 Molal

DISTRIBUTION OF SPECIES CALLED AT STEP 0

AQUEOUS SPECIES

SPECIES	MOLALITY	LOG MOL	ACTIVITY	LOG ACT	ACT COEF	LG ACT C	GRAMS/KGM H2O	PPM	LOG PPM
CA++	0.59286E-03	-3.225	0.48087E-03	-3.318	0.80728E+00	-0.093	0.23874E-01	23.872	1.373
FE++	0.39812E-04	-4.400	0.32139E-04	-4.493	0.80728E+00	-0.093	0.22234E-02	2.223	0.347
FE+++	0.79817E-19	-19.098	0.59326E-19	-19.298	0.63052E+00	-0.200	0.44575E-17	0.000	-14.351
MN++	0.92300E-06	-6.032	0.74916E-06	-6.125	0.80728E+00	-0.093	0.50982E-04	0.051	-1.233
ZN++	0.64063E-07	-7.193	0.51717E-07	-7.286	0.80728E+00	-0.093	0.41878E-05	0.004	-2.378
CU+	0.76497E-06	-6.105	0.74199E-06	-6.130	0.94525E+00	-0.024	0.49877E-04	0.050	-1.302
CU++	0.23135E-10	-10.551	0.22216E-10	-10.644	0.80728E+00	-0.093	0.17879E-08	0.000	-5.743
S--	0.77192E-17	-17.109	0.62396E-17	-17.203	0.80465E+00	-0.094	0.24943E-15	0.000	-12.603
SO4--	0.60563E-03	-3.218	0.48569E-03	-3.314	0.80195E+00	-0.096	0.58178E-01	58.172	1.765
CO3--	0.38240E-08	-8.441	0.29112E-08	-8.536	0.80331E+00	-0.095	0.21747E-06	0.000	-3.663
OH-	0.10371E-07	-7.964	0.10285E-07	-7.988	0.94609E+00	-0.024	0.18489E-06	0.000	-3.733
H+	0.10224E-05	-5.978	0.10000E-05	-6.000	0.95025E+00	-0.022	0.10607E-05	0.001	-2.974
H2O	0.55535E+02	1.744	0.99997E+00	-0.000	0.18915E-01	-1.744	0.10000E+04	99997.742	6.000
CL(AQ)	0.35381E-09	-9.470	0.33881E-09	-9.470	0.10000E+01	0.0	0.10842E-07	0.000	-64.965
CAC03	0.17527E-08	-8.756	0.17539E-08	-8.756	0.10007E+01	0.000	0.17543E-06	0.000	-3.756
CAS04	0.39224E-04	-4.406	0.39251E-04	-4.406	0.10007E+01	0.000	0.53401E-02	5.340	0.728
ZNS04	0.65737E-07	-7.051	0.38997E-07	-7.051	0.10007E+01	0.000	0.14357E-04	0.014	-1.843
HS04-	0.48326E-07	-7.311	0.46214E-07	-7.335	0.94649E+00	-0.024	0.47396E-05	0.005	-2.324
HS-	0.50976E-09	-9.300	0.47376E-09	-9.324	0.94608E+00	-0.024	0.16561E-07	0.000	-4.791
H2S	0.49326E-08	-8.310	0.49359E-08	-8.309	0.10007E+01	0.000	0.16708E-06	0.000	-3.777
HCO3-	0.65322E-04	-4.185	0.61853E-04	-4.209	0.94689E+00	-0.024	0.39858E-02	3.985	0.600
H2CO3	0.13467E-03	-3.871	0.13476E-03	-3.870	0.10007E+01	0.000	0.83531E-02	8.352	0.922
FE(OH)+	0.18883E-05	-5.724	0.17872E-05	-5.748	0.94649E+00	-0.024	0.13757E-03	0.138	-0.862

IONIC STRENGTH = 0.291875E-02

ELECTRICAL BALANCE = -0.284082E-13

GASES

NAME	LOG K	ACTIVITY	LOG ACTIVITY
OXYGEN GAS	0.0	0.31623E-06	-66.50000
CARBON DIOXIDE	-7.83540	0.42342E-02	-2.37323
STEAM	1.50517	0.31248E-01	-1.50518
SULFUR GAS	192.34951	0.33360E-23	-23.47677
HYDROGEN SULFIDE	125.01049	0.47409E-07	-7.32414
HYDROGEN GAS	41.66022	0.38883E-08	-8.41023
METHANE	139.90718	0.76588E-13	-13.11584

THE LOG K FOR BORNITE HAS BEEN EXCEEDED AT STEP 0  
LOG K = 499.7349878 LOG Q = 551.5340862

THE LOG K FOR CHALCOCITE HAS BEEN EXCEEDED AT STEP 0

\*\*\*\*\* DATA ECHO \*\*\*\*\*

DISTRIBUTION OF SPECIES IN WATER SAMPLE 74-RL-1443  
at a sulphate conc of  $10^{-4}$  Molal

TEMPERATURE (KELVIN) OF THIS RUN IS ..... 298.15  
PRESSURE (BARS) OF THIS RUN IS ..... 1.00

MAXIMUM NUMBER OF STEPS IS ..... 1  
NUMBER OF STEPS BETWEEN EACH PRINT OUT IS ... 0

ION CHOSEN FOR ELECTRICAL BALANCE IS ..... CA++  
MOLES OF SOLVENT H<sub>2</sub>O IN SYSTEM IS ..... 55.508250

\*\*\*\*\* INITIAL SOLUTION CONSTRAINTS \*\*\*\*\*

0.14100000E-05 MOLALITY	CU++	CU(1)	(AQUEOUS SPECIES)
0.78500000E-05 MOLALITY	FE++	FE(1)	(AQUEOUS SPECIES)
0.18200000E-05 MOLALITY	MN++	MN(1)	(AQUEOUS SPECIES)
0.15300000E-06 MOLALITY	ZN++	ZN(1)	(AQUEOUS SPECIES)
0.62500000E-03 MOLALITY	CA++	CA(1)	(AQUEOUS SPECIES)
0.64500000E-03 MOLALITY	SO4--	S(1)O(4)	(AQUEOUS SPECIES)
0.20000000E-03 MOLALITY	HCO3-	H(1)C(1)O(3)	(AQUEOUS SPECIES)
-0.62000000E+01 LOG ACT.	H+	H(1)	(AQUEOUS SPECIES)
-0.66500000E+02 LOG ACT.	OXYGEN GAS	O(2)	(GAS)

\*\*\*\*\*

DISTRIBUTION OF SPECIES IN WATER SAMPLE 74-RL-1443  
 SAMPLE # 1443

DISTRIBUTION OF SPECIES CALLED AT STEP 0

AQUEOUS SPECIES

SPECIES	MCLALITY	LOG MOL	ACTIVITY	LOG ACT	ACT CCF	LG ACT C	GRAMS/KGM H2C	PPM	LOG PPM
CA++	0.62622E-03	-3.196	0.51315E-03	-3.290	0.80656E+00	-0.093	0.25500E-01	25.497	1.406
FE++	0.73015E-05	-5.137	0.58891E-05	-5.230	0.80656E+00	-0.093	0.40777E-03	0.408	-0.390
FE+++	0.92451E-20	-20.034	0.58184E-20	-20.235	0.62935E+00	-0.201	0.51631E-18	0.000	-15.287
MN++	0.18200E-05	-5.740	0.14679E-05	-5.833	0.80656E+00	-0.093	0.99987E-04	0.100	-1.000
ZN++	0.64281E-07	-7.192	0.51846E-07	-7.285	0.80656E+00	-0.093	0.42020E-05	0.004	-2.377
CU+	0.14100E-05	-5.851	0.13324E-05	-5.875	0.94501E+00	-0.025	0.89589E-04	0.090	-1.048
CU++	0.31911E-10	-10.496	0.25738E-10	-10.589	0.80656E+00	-0.093	0.20276E-08	0.000	-5.693
S--	0.77481E-17	-17.111	0.62288E-17	-17.206	0.80391E+00	-0.095	0.24844E-15	0.000	-12.605
SO4--	0.60323E-03	-3.220	0.48330E-03	-3.316	0.80118E+00	-0.096	0.57947E-01	57.941	1.763
CO3--	0.76492E-08	-8.116	0.61389E-08	-8.212	0.80256E+00	-0.096	0.45902E-06	0.000	-3.338
OH-	0.17234E-07	-7.764	0.16300E-07	-7.788	0.94589E+00	-0.024	0.29310E-06	0.000	-3.533
H+	0.66413E-06	-6.178	0.63096E-06	-6.200	0.55005E+00	-0.022	0.66942E-06	0.001	-3.174
H2O	0.55508E+02	1.744	0.99997E+00	-0.000	0.18015E-01	-1.744	0.10000E+04	999897.916	6.000
O2(AQ)	0.33881E-69	-69.470	0.33881E-69	-69.470	0.10000E+01	0.0	0.10842E-67	0.000	-64.965
CACO3	0.36441E-08	-8.404	0.36468E-08	-8.404	0.10007E+01	0.000	0.39476E-06	0.000	-3.404
CASO4	0.41652E-04	-4.380	0.41680E-04	-4.380	0.10007E+01	0.000	0.56705E-02	5.670	0.754
ZNSO4	0.88719E-07	-7.052	0.88780E-07	-7.052	0.10007E+01	0.000	0.14322E-04	0.014	-1.844
H2SO4	0.30663E-07	-7.513	0.29015E-07	-7.537	0.54626E+00	-0.024	0.29764E-05	0.003	-2.526
HS-	0.31448E-09	-9.502	0.29745E-09	-9.527	0.94589E+00	-0.024	0.10400E-07	0.000	-4.983
H2S	0.19421E-08	-8.712	0.19435E-08	-8.711	0.10007E+01	0.000	0.66188E-07	0.000	-4.179
HCO3-	0.86932E-04	-4.061	0.82296E-04	-4.085	0.54667E+00	-0.024	0.53044E-02	5.304	0.725
H2CO3	0.11205E-03	-3.947	0.11313E-03	-3.946	0.10007E+01	0.000	0.70124E-02	7.012	0.846
Fe(OH)+	0.54851E-06	-6.261	0.51903E-06	-6.285	0.54626E+00	-0.024	0.59961E-04	0.040	-1.398

IONIC STRENGTH = 0.254210E-C2

ELECTRICAL BALANCE = -0.493916E-13

GASES

-----

NAME	LOG K	ACTIVITY	LOG ACTIVITY
OXYGEN GAS	0.0	0.31623E-66	-66.50000
CARBON DIOXIDE	-7.83540	0.35546E-02	-2.44921
STEAM	1.50517	0.31248E-01	-1.50518
SULFUR GAS	192.34951	0.52353E-24	-24.28106
HYDROGEN SULFIDE	125.01049	0.18781E-07	-7.72628
HYDROGEN GAS	41.66022	0.38883E-08	-8.41023
METHANE	135.90718	0.64296E-13	-13.19182

THE LOG K FOR BORATE HAS BEEN EXCEEDED AT STEP 0  
 LOG K = 499.7299878 LOG Q = 551.8597575

THE LOG K FOR CHALCOITE HAS BEEN EXCEEDED AT STEP 0

\*\*\*\*\* DATA ECHO \*\*\*\*\*

DISTRIBUTION OF SPECIES IN WATER SAMPLE 74-RL-1444  
AT A SULPHATE CONC OF 10-4 Molal

TEMPERATURE (KELVIN) OF THIS RUN IS ..... 298.15  
PRESSURE (BARS) OF THIS RUN IS ..... 1.00

MAXIMUM NUMBER OF STEPS IS ..... 1  
NUMBER OF STEPS BETWEEN EACH PRINT CUT IS ... 0

ION CHOSEN FOR ELECTRICAL BALANCE IS ..... CA++  
MOLES OF SOLVENT H2O IN SYSTEM IS ..... 55.508250

\*\*\*\*\* INITIAL SOLUTION CONSTRAINTS \*\*\*\*\*

0.1460000E-04 MOLALITY	CU++	CU(1)	(AQUEOUS SPECIES)
0.1090000E-05 MOLALITY	FE++	FE(1)	(AQUEOUS SPECIES)
0.7830000E-06 MOLALITY	MN++	MN(1)	(AQUEOUS SPECIES)
0.5970000E-06 MOLALITY	ZN++	ZN(1)	(AQUEOUS SPECIES)
0.6250000E-03 MOLALITY	CA++	CA(1)	(AQUEOUS SPECIES)
0.2000000E-03 MOLALITY	HCO3-	H(1)C(1)O(3)	(AQUEOUS SPECIES)
-0.6200000E+01 LOG ACT.	H+	H(1)	(AQUEOUS SPECIES)
0.6760000E-03 MOLALITY	SO4--	S(1)O(4)	(AQUEOUS SPECIES)
-0.6650000E+02 LOG ACT.	OXYGEN GAS	O(2)	(GAS)

\*\*\*\*\*

DISTRIBUTION OF SPECIES IN WATER SAMPLE 74-PL-1444  
AT A SULPHATE CONC OF 10-4 Molal

DISTRIBUTION OF SPECIES CALLED AT STEP 0

AQUEOUS SPECIES

SPECIES	MOLALITY	LOG MOL	ACTIVITY	LOG ACT	ACT CCEF	LOG ACT C	GRAMS/KGM H2O	PPM	LOG PPM
CA++	0.66229E-03	-3.178	0.52295E-03	-3.273	0.80344E+00	-0.095	0.26589E-01	26.586	1.425
FE++	0.10140E-05	-5.994	0.81472E-06	-6.089	0.80344E+00	-0.095	0.56631E-04	0.057	-1.247
FE+++	0.12893E-20	-20.890	0.80493E-21	-21.094	0.62434E+00	-0.205	0.72001E-19	0.000	-16.143
MN++	0.78300E-06	-6.106	0.62909E-06	-6.201	0.80344E+00	-0.095	0.43016E-04	0.043	-1.366
ZN++	0.24556E-06	-6.610	0.19729E-06	-6.705	0.80344E+00	-0.095	0.16052E-04	0.016	-1.795
CU+	0.16600E-04	-4.780	0.15670E-04	-4.805	0.94400E+00	-0.025	0.10547E-02	1.055	0.023
CU++	0.37674E-09	-9.424	0.20265E-09	-9.515	0.80344E+00	-0.095	0.23928E-07	0.000	-4.621
S--	0.80934E-17	-17.092	0.64844E-17	-17.188	0.80077E+00	-0.097	0.25967E-15	0.000	-12.586
SO4--	0.63058E-03	-3.200	0.50313E-03	-3.298	0.79789E+00	-0.098	0.60574E-01	60.568	1.782
CO3--	0.76770E-08	-8.115	0.61363E-08	-8.212	0.75920E+00	-0.097	0.46069E-06	0.000	-3.337
OH-	0.17252E-07	-7.763	0.16300E-07	-7.788	0.94487E+00	-0.025	0.29340E-06	0.000	-3.533
H+	0.66471E-06	-6.177	0.63096E-06	-6.200	0.94922E+00	-0.023	0.67001E-06	0.001	-3.174
H2O	0.55509E+02	1.744	0.99997E+00	-0.000	0.16015E-01	-1.744	0.10000E+04	999893.163	6.000
O2(AO)	0.33881E-69	-69.470	0.33881E-69	-69.470	0.10000E+01	0.0	0.10842E-67	0.000	-64.965
CaCO3	0.40947E-08	-8.388	0.40977E-08	-8.387	0.10000E+01	0.000	0.40984E-06	0.000	-3.287
CASO4	0.45036E-04	-4.346	0.45068E-04	-4.346	0.10000E+01	0.000	0.61313E-02	6.131	0.788
ZNSO4	0.35144E-06	-6.454	0.35169E-06	-6.454	0.10000E+01	0.000	0.56734E-04	0.057	-1.246
MSO4-	0.31954E-07	-7.495	0.30206E-07	-7.520	0.94529E+00	-0.024	0.31018E-05	0.003	-2.508
HS-	0.22772E-09	-9.484	0.20266E-09	-9.509	0.94487E+00	-0.025	0.10839E-07	0.000	-4.965
H2S	0.20218E-08	-8.694	0.20232E-08	-8.694	0.10000E+01	0.000	0.68902E-07	0.000	-4.162
HCO3-	0.86933E-04	-4.061	0.82261E-04	-4.085	0.94571E+00	-0.024	0.53075E-02	5.307	0.725
H2CO3	0.11301E-03	-3.947	0.11309E-03	-3.947	0.10000E+01	0.000	0.70092E-02	7.008	0.846
FE(OH)+	0.75940E-07	-7.119	0.71809E-07	-7.144	0.94529E+00	-0.024	0.55341E-05	0.006	-2.257

IONIC STRENGTH = 0.264422E-02

ELECTRICAL BALANCE = -0.665814E-13

GASES

-----

NAME	LOG K	ACTIVITY	LOG ACTIVITY
OXYGEN GAS	0.0	0.31523E-66	-66.50000
CARBON DIOXIDE	-7.83540	0.35531E-02	-2.44936
STEAM	1.50517	0.31247E-01	-1.50519
SULFUR GAS	192.34951	0.56738E-24	-24.24612
HYDROGEN SULFIDE	125.01049	0.19552E-07	-7.70881
HYDROGEN GAS	41.66022	0.38883E-06	-8.41024
METHANE	135.90718	0.64268E-13	-13.15200

THE LOG K FOR PERHITE HAS BEEN EXCEEDED AT STEP 0  
LOG K = 499.7399878 LOG C = 556.4226980

THE LOG K FOR CHALCOHITE HAS BEEN EXCEEDED AT STEP 0